Volcanic architecture of the Deccan Traps, western Maharashtra, India: an integrated chemostratigraphic and paleomagnetic study

Thesis

Volcanic architecture of the Deccan Traps, Western Maharashtra, India: an integrated chemostratigraphic and palaeomagnetic study

A thesis presented for the degree of Doctor of Philosophy

By

Anne E Jay

M.Sci. (Hons)
University College London, United Kingdom

Department of Earth Sciences
The Open University

May 2005

THIS THESIS CONTAINS A CD WHICH
WE ARE NOT PERMITTED TO COPY

PLEASE CONTACT THE UNIVERSITY
IF YOU WISH TO SEE THIS MATERIAL

Volume 2 restricted access

Abstract

Detailed volcanostratigraphic logs of seven traverses up the lava sequence in the Western Ghats, Deccan Traps, India, are presented. The main study area, the Mahabaleshwar Plateau, was chosen because the lavas were emplaced around the time of the Cretaceous-Tertiary Boundary and because there is access to exposed lavas on three of its four sides, permitting investigation of the volcanic architecture in 3-D. Besides characteristics of the lava units, the logs include integrated geochemical and palaeomagnetic samples. The lava pile is dominated by pāhoehoe sheet lobes and smaller lobes and toes. It can be divided into flow-fields, the products of one eruption, by the occurrence of weathering horizons. Palaeomagnetic results demonstrate that the chron 29R/29N reversal boundary horizon occurs in all four of the traverses around the Plateau and nearby Khumbarli Ghat. The elevation of the reversal horizon on each traverse varies between 897-945 m and 982 m, a value greater than that predicted by the small regional dip. Statistical analysis of geochemical data from samples taken between the reversal horizon and the base of the Mahabaleshwar Formation do not show any apparent correlation around the Mahabaleshwar Plateau, indicating that individual sheet lobes are less than 20 km wide. Determining the lateral extent of flow-fields is not possible using this method but from the occurrence of a similar number of flow-fields in three traverses of similar length round the Plateau, it is probable that most flow fields are at least as wide as the Mahabaleshwar Plateau (more than 20 km). Comparing the thickness of the lava pile between the base of the Mahabaleshwar Formation, the palaeomagnetic reversal horizon and the laterite cap, shows that as much as 95 m of topography occurred on the surface of the active Deccan lavas over a distance of approximately 20 km. The volcanic architecture is controlled by the morphology of small sheet lobes, large sheet lobes, and, on a larger scale, flow-fields. These observations, and the varying number of individual sheet lobes making up flow-fields, demonstrates that the structure of the Deccan lava province at the level of eruptive units is extremely complex.

To be young
and in love
and in Mahabaleshwar
and in season
is heaven itself.

From: ***The Wonderland of Mahabaleshwar*** **by Dilip Sarda B.Arcg. G.D. Arch**

Frontispiece

The view looking north along the Western Ghats from Elphinstone Point, The Mahabaleshwar Plateau, western Maharashtra

Acknowledgements

So many people have helped me with this project, so if I forget any of them I am sorry. I would first like to thank my supervisors, Mike Widdowson, Steve Self and Steve Blake. without them I'd have found India much harder, never had a Valentines day meal in the Hotel Leela where the chef 'went wrong', been totally stuck with my end of thesis panic and I'd have commas all over the place. There are so many other things that they have done for me during my time at the OU that I can't write them all down.

I would also like to thank my examiners Professor Peter Hooper and Dr. David Rothery for their very useful comments and suggestions on how to improve my thesis and for not making my viva too scary.

Some of the best conclusions of this work would not have been possible with out the palaeomagnetic data, so I must thank Conall MacNiocail and Will Turner for carrying out so much of the analysis, and patiently teaching me the intricacies of palaeomagnetism.

To Sam Sethna and family, I am completely indebted to him for getting the rock drill and GPS into India, again my work would not have been possible without him.

Chotumiya Eshak Patel, I have to thank him so much, for his excellent driving, for always looking after us, solving so many problems, always being able to find water for us when we were drilling, and most of all for his endless patience especially on the monkey day at Varandah Ghat. He is also very good at pumping water and his wife makes a great biryani.

Thanks to Rich Single for his help with GoCad, which was fruitless, but fun.

John Watson, what a star, I'm not sure how many XRF analyses he had to run for me, but it was a lot and again, I couldn't have done this without him.

John Holbrook, well he is the most important person as he has control of all the money, thanks for always finding me the funds I needed and to Liz for being lovely and putting up with John!

Ray Brown for his help with my statistics, I have never been able to do stats before, but with your computer wizardry, I got some great data.

Alan Hobbs and all the staff at the NERC geophysical equipment pool thanks for the GPS, I am never attempting to import GPS into India again.

The Dina hotel and its entire staff who were so kind to us and always managed to find us some garum pani and fresh lime soda (or beer), all that is needed at the end of a long day tramping the Western Ghats.

And a special thanks to my lunch buddies, Andrew, Martin, Axel and Elske, lunch would have been so much duller, (but quicker) without you. You have made MK and OU life great and I have learnt so much from you, thanks so much you are great friends.

A Special thanks to Andrew Ball for helping me to format my thesis and to rescue it when it all when hay-wire.

Thanks to Jenny Cripps and Charlie Pearce for letting me moan at them about the Deccan.

Thanks to everyone in my year especially Jason and Luke and my office mates, Kirti and Elske who put up with years of my moaning about my housemates, until I moved out and then I moaned about my thesis! And to Wes and Charlotte, you have been great this last few months when I have been so stressed, I hope your work goes well.

To all the post-grads and members of the Earth Sciences Dept., Dick Brandon and Craig who kept my computer alive and Carina, Dougal Jerram, the OU and New Bradwell women's cricket club, Yoseph Araya and there must be so many others, thank you all.

Everyone on VDG especially Ashea without whom, we'd never get anything done
To all my friends at UCL and HMSG who supported me during my degree and schooling without whom, I'd have never got this far.

To David Jones, who inspired my love of geology by saying, 'it's ok, sometimes during A levels you can get a bit stressed. If that happens just go to my cupboard, get out the Noddy puzzles and go to the back and do them.' That was my kinda work, so I took A level geology and have never looked back. He also told me 'after doing this course (A level geology) you will never look at the world in the same way again.' He was so right.

To my Uncle Robert, who gave me my first taste of geology by having a gravel driveway full of *Gryphaea.*

To Matt, who has been there through thick and thin and really put up with my temper and gives great cuddles.

And finally to my family, my daddy for his support, his trilobite song and for planting in me an inquisitive mind and answering so many of my questions, I hope I can do the same, but only about geology, I'll leave the physics to someone else! My mum for just being there and I got what few useful brain cells I have from her to! And to Tom you're a great brother and you are my best friend. And granny, I definitely don't study mud any more. Thanks to you all for putting up with me.

Table of Contents

List of Figures

List of Tables

Chapter 1
Introduction

1.1 Objectives of thesis

Flood basalt provinces consist of large volumes (~10^6 km^3) of lava emplaced over short (1-10 Ma) periods of geological time. They are the surface expressions of major events in the mantle and affect Earth's lithospheric composition, structure and surface environment. The Deccan Volcanic Province (DVP), also known as the Deccan Traps, in India is one of the largest continental flood basalt provinces on Earth. It is also one of the most interesting as the lavas were erupted over the Cretaceous/Tertiary boundary (KTB), ~65 Ma (Cande and Kent, 1995), which is defined by one of the largest mass extinctions in geological time with up to 40% of genera extinguished (Sepkoski, 1996). There is intense debate regarding the involvement of the DVP volcanism in this mass extinction event. Obviously large volumes of lava were produced in a, geologically speaking, very short period of time; these would have released large volumes of gas, and possibly ash, into the atmosphere. However, the likely effect of this on the regional and global atmosphere and on the climate, flora and fauna, is not yet known.

The main objective of this work is to improve the understanding of the volcanic architecture and, hence, the 3-dimensional structure of a key area of a flood basalt province using the Mahabaleshwar Plateau of the DVP (Figure 1.1), as an example. In addition, this work has arguably produced the first integrated study of the DVP, combining detailed field observations of the physical volcanology with geochemical and palaeomagnetic data.

The methods used to carry out this work are three-fold. Detailed volcanological logging was conducted up the four roads that ascend the Mahabaleshwar Plateau in order to provide a 3-dimensional view of the lava units occurring in this area. Further logging

was carried out 60 km south of the Mahabaleshwar Plateau to compare the characteristics of units that are at the same stratigraphical level but, possibly, more distal to source in order to observe how or if the flow units change as they progress. Logging was also carried out 125 km to the north, to study the volcanic architecture of older units. This work provides an integrated study of units from eight of the twelve formations in the Main Deccan Province (MDP; Figure 1.2).

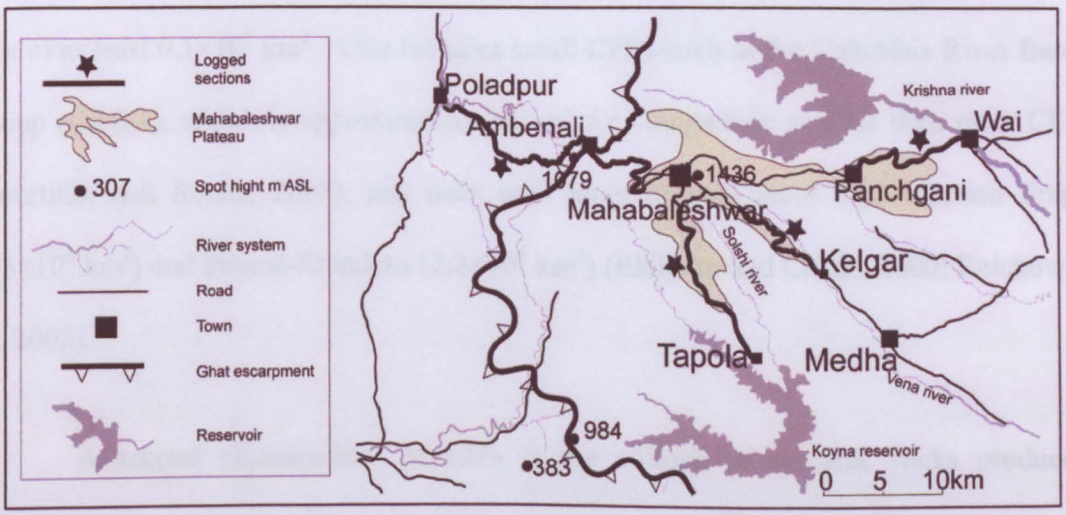

Figure 1.1 The traverses studied up the Mahabaleshwar Plateau

In order to integrate this work with previous chemostratigraphic data, samples were taken of almost every lobe along the sections studied. These were analysed for major and trace elements to allow the chemostratigraphy and the volcanology to be integrated. To correlate the units across the Mahabaleshwar Plateau and the surrounding region, palaeomagnetic samples were also taken of almost every lobe to provide an isochronous horizon along which to correlate the sections. These three data sets were collected in unison with high precision static GPS in order to constrain location positions and elevations at a level of accuracy never achieved before in the DVP.

The remainder of this chapter outlines the character, origin and impact of large igneous provinces (LIPs) and continental flood basalt provinces (CFBs) (Section 1.2), the specific setting of the DVP (Section 1.3), and the structure of the thesis (Section 1.4).

1.2 Large Igneous Provinces (LIPs)

1.2.1 Characteristics of LIPs

LIPS are predominantly formed of tholeiitic basalt with early alkaline and picritic volcanism and later, sometimes in CFBs, silicic volcanism. The classification of a group of igneous rocks as a LIP is highly dependent on its actual, or assumed, original size. Coffin and Eldholm (2001) define the minimum size of a LIP as originally covering an area of at least 0.1×10^6 km^2. This includes small CFBs such as the Columbia River Basalt Group (CRBG), which is approximately an order of magnitude smaller than most CFBs (Courtillot and Renne, 2003), and ones with large original areas e.g., Siberian Traps, (2.3×10^6 km^2) and Paraná-Etendeka (2.3×10^6 km^2) (Eldholm and Coffin, 2000; Reichow et al., 2002).

A second characteristic of LIPs is the volume of volcanic rocks produced. Estimating the erupted volume of even a moderately intact LIP can be difficult, but increasingly accurate dating, modelling and stratigraphic correlation is improving this (Ernst et al., 2005). Such work has resulted in the doubling of the recognized size of the Siberian Traps from 1×10^6 km^3 (Fedorenko et al., 1996) to 2.3×10^6 km^3 (e.g., Reichow et al., 2002). The total intruded and underplated basaltic material, however, leads to a large uncertainty in the total volumes of material forming a LIP (White and McKenzie, 1989), especially in CFBs where it is difficult to distinguish the intrusive and underplated components from the host basement rocks, using seismic studies. In oceanic LIPs however, the volume can be estimated from seismic studies if the original crustal thickness is known (Ernst et al., 2005).

A third characteristic of LIPs is their rapid emplacement, usually within 10 Myr, with the majority of the lava being erupted within a period of about 1 Myr (Ernst et al.,

2005). This is of interest as it may be a matter of considerable importance to environmental aspects of volcanism. The time-averaged LIP emplacement rate, assuming a typical duration of one million years for the bulk of the lavas to be emplaced, is estimated to be of the order of 1-2 km^3 yr^{-1} (Courtillot and Renne, 2003), equivalent to ~ 32-64 m^3 s^{-1}. This is considerably higher than time averaged rates determined for Hawai'i ~0.1 km^3 yr^{-1} (~3-4 m^3 s^{-1}; Swanson, 1972), Iceland 0.04 km^3 y^{-1} (Swanson et al., 1975) or the Columbia River 0.17 km^3 y^{-1} (based on a volume of 220,500 km^3 and a 1.3 Ma duration for the main phase (Camp and Ross, 2003)). Such rates are, naturally, less than eruption rates observed at Laki, Iceland 1783-1784 (~15 km^3 yr^{-1}), the only modern analogue for a modern flood basalt event (Thordarson and Self, 1993). The reason for the apparently modest emplacement rate of LIPs is that the 1-2 km^3 yr^{-1} is the time averaged rate throughout the whole LIP formation period, however, the volcanism probably took place in a series of massive eruptions followed by long periods of quiescence (Widdowson et al., 1997). These eruptions might have lava effusion rates in the order of tens of km^3 y^{-1} based on the Laki example. The hiatuses are inferred from the numerous soil (or bole) horizons that are seen in between flow fields in CFBs. These attest to extensive periods of inactivity, and can be corroborated by modern day volcanoes on which periods of dormancy are more extensive than periods of activity. However, after the acme of a LIP formation, magmatism may continue at a much reduced rate for tens of millions of years to form hotspot or seamount chains (Ernst et al., 2005) which represent the plume tail.

LIPs are extensive areas of, predominantly, mafic volcanic and plutonic rocks, formed by the most voluminous and short-lived basaltic volcanism on Earth (Figure 1.3) (Eldholm and Coffin, 2000). LIPs can be subdivided into four categories:

Continental flood basalt provinces (CFBs): composite accumulations of horizontal or sub-horizontal flows, erupted in rapid succession over large areas of continental lithosphere, primarily by fissure eruptions.

Oceanic plateaus: Broad, largely flat topped features isolated from continents, generally rising >2000 m above the adjacent deep ocean basin. The extrusive cover may be subaerial or submarine.

Oceanic basin flood basalt: Extensive submarine flow and sill units overlying older oceanic crust formed by sea-floor spreading. A sediment sequence pre-dating the flood basalt may separate the two igneous units.

Volcanic passive continental margin: Outer margin continental margin covered by thick extrusive complexes constructed during continental break-up and initial sea-floor spreading. Commonly recognised by wedges of seaward dipping reflectors in seismic records.

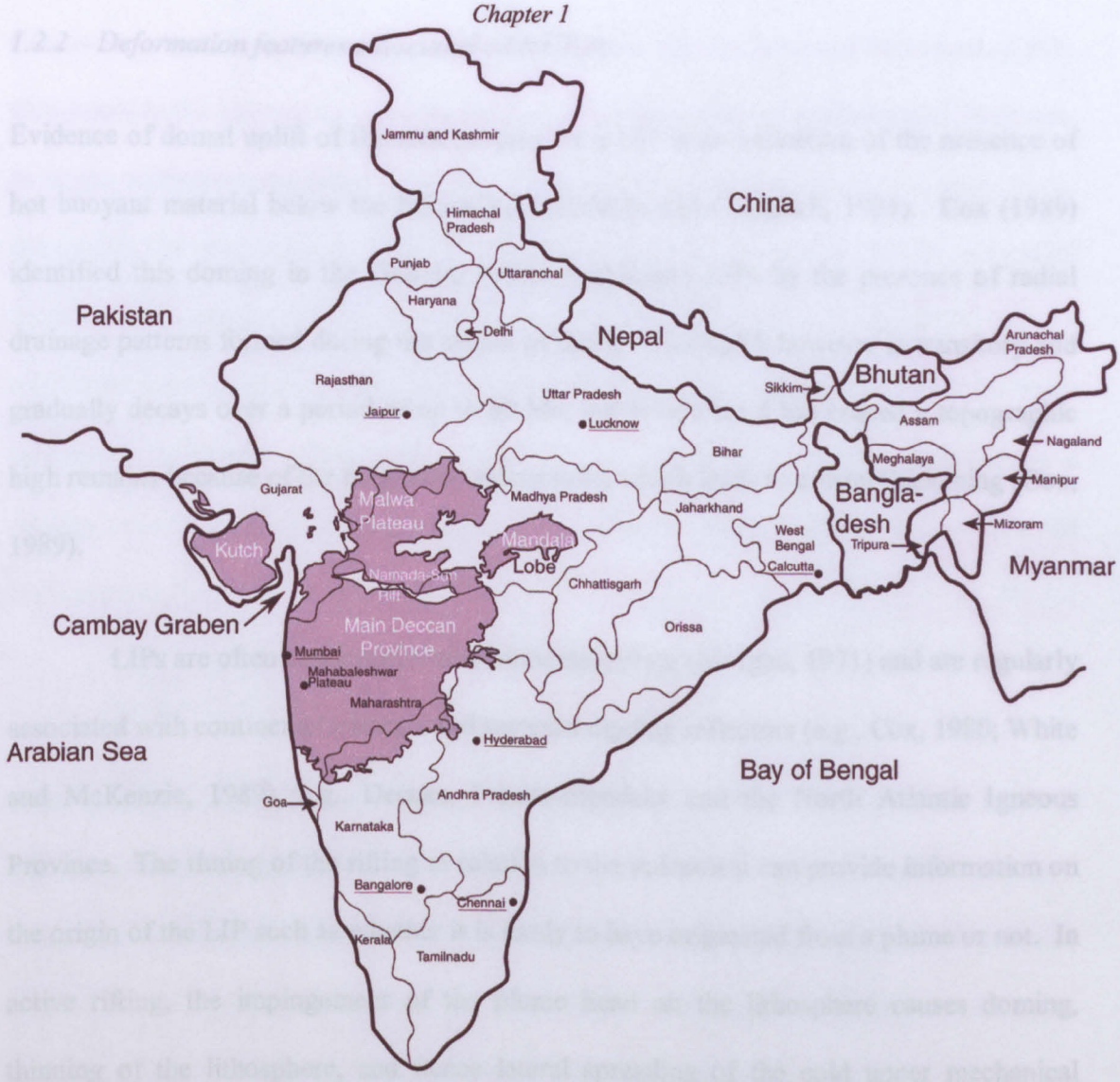

Figure 1.2. India with its states and main cities, showing the extent of the DVP.

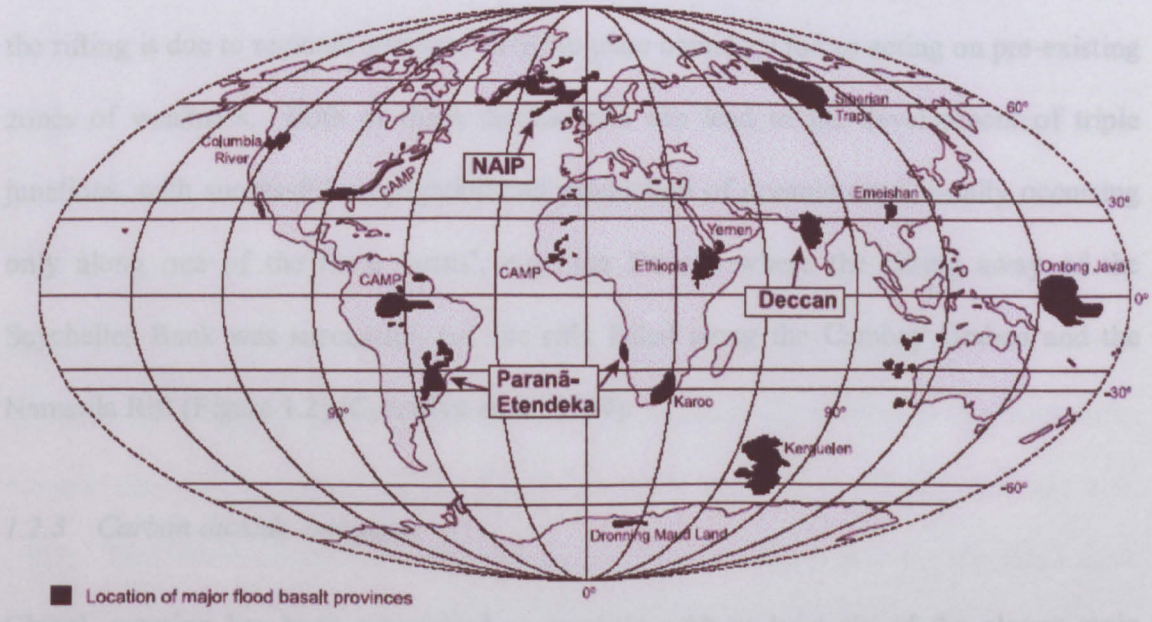

Figure 1.3. The location of LIPs worldwide (from Jerram and Widdowson, (2005)

1.2.2 *Deformation features associated with CFBs*

Evidence of domal uplift of the area covered by a LIP is an indication of the presence of hot buoyant material below the lithosphere (Griffiths and Campbell, 1991). Cox (1989) identified this doming in the Deccan, Paraná and Karoo LIPs by the presence of radial drainage patterns formed during the period of uplift. This uplift however is transitory and gradually decays over a period of up to 60 Ma, but even after it has ceased a topographic high remains because of the magmatic underplating which leads to crustal thickening (Cox, 1989).

LIPs are often connected with continental rifting (Morgan, 1971) and are regularly associated with continental margins and seaward dipping reflectors (e.g., Cox, 1980; White and McKenzie, 1989), e.g., Deccan, Parana-Etendeka and the North Atlantic Igneous Province. The timing of the rifting in relation to the volcanism can provide information on the origin of the LIP such as whether it is likely to have originated from a plume or not. In active rifting, the impingement of the plume head on the lithosphere causes doming, thinning of the lithosphere, and hence lateral spreading of the cold upper mechanical lithosphere which leads to tensional failure (Courtillot et al., 1999). In the passive model the rifting is due to regional stresses related to plate boundary forces acting on pre-existing zones of weakness. Both of these mechanisms can lead to the development of triple junctions, with successful propagation and production of oceanic crust usually occurring only along one of the three 'arms', e.g., the Deccan where the rifting away of the Seychelles Bank was successful, but the rifts failed along the Cambay Graben and the Namarda Rift (Figure 1.2) (Courtillot et al., 1999).

1.2.3 *Carbon dioxide emissions*

Global warming has been recognised to coincide with at least six of the eleven main Mesozoic and Cainozoic LIPs (Wignall, 2001). From this Wignall (2001) proposes that

CO_2 is the most likely cause of any mass extinction associated with LIPs. Atmospheric CO_2 levels in the Cretaceous were higher than the present day and at KTB times they were twice the current concentration, but this level is approximately three times less than during the middle Cretaceous (Berner, 2001). Caldeira and Rampino (1990a; 1990b) ran global models which suggest that the increase in atmospheric CO_2 caused by the DVP, and the related increase in global temperatures, is too small to have generated the KTB mass extinction. $\delta^{18}O$ data support this conclusion (Stott and Kennet, 1990) and suggest a cooling prior to the KTB and that no warming occurred during Chron 29R (in which the KTB occurs).

1.2.4 Sulphur dioxide emission

Other gases as well as CO_2 are released during flood basalt eruptions. S, Cl, and F are all emitted in significant quantities. Thordarson and Self (1996) used data from the Roza flow in the CRB to gauge the effect of large eruptive events during flood basalt province formation. The gases released can form two layers within the atmosphere. The upper layer is formed in the upper troposphere and stratosphere as material and gas are transported there by the eruption column, material is only injected into the stratosphere if the eruption column is high enough or the tropopause low. Gas is also released into the lower troposphere by degassing of the flow itself (Thordarson and Self, 1996). The gases that enter the stratosphere are typically a direct input from the eruption column at the vent; these are converted to sulphuric acid aerosols, which can remain in the stratosphere for up to a few years. If global dispersal occurs, the aerosol cloud leads to increased backscatter and absorption of solar radiation and produces a darkened sky similar to that seen on an overcast day and causes global cooling by as much as 5-15° C (Thordarson and Self, 1996). Thordarson and Self (1996) predict that with continued eruption of the Roza flow, the 'volcanic winter' produced by such an eruption could have lasted for ten years or more. Whether these effects would have been enough to severely alter the Earth's climate and

flora and fauna is uncertain. The gases released by the degassing of the flow itself remain in the lower troposphere where they also convert into aerosols, and are transported by local weather systems over considerable distances. The Laki 1783-1784 eruption was documented as producing a dry fog which choked most of Europe and northern Asia for five months, and damaged and scorched the earth and vegetation; many people and livestock were killed (Thordarson and Hoskuldsson, 2002; Grattan and Durand, 2003). This damage occurred only for one season, as the residence time of these aerosols in the troposphere is only a few months; it was then washed out by rain. If the eruption had lasted for decades, as is inferred for a flood basalt event (Thordarson and Self, 1998) the local and regional flora and fauna could have been even more severely affected.

1.2.5 Mechanisms for the formation of LIPs

LIPs are caused by anomalously high volumes of melt. The process by which this melt is produced, however, has long been a source of debate. Mantle plumes are one theory; they are thought to form from instabilities at a thermal boundary layer, either at the core-mantle boundary or at the shallower upper-lower mantle boundary. Plumes are zones of abnormally hot mantle material which rise with a bulbous plume head and much narrower plume tail (Richards and Duncan, 1988). Once the plume head encounters the base of the lithosphere it causes lithospheric doming and spreads out (to a diameter of 1000-2000 km). The centre of the plume contains the hottest material and hence the active volcanism is concentrated above this area. As the plume head cools and spreads, the volume of melt produced decreases. The plume tail, however, is still hot and continues to rise through the mantle. If the plate is still in motion, its surface expression is a ridge or chain of extinct volcanoes terminating in the current active spot.

White and McKenzie (1989) suggest that the mantle plume arrives beneath unbroken lithosphere which causes doming, followed by continental lithospheric rifting

across the hottest part of the plume head. This produces large volumes of decompression melting. Part of this melt erupts to form the LIP, the remainder is underplated or intruded into the thinned continental crust. White and McKenzie (1995) suggest that the 100-200° C increase in temperature caused by the arrival of the plume is not enough to produce the volumes of material which occur in a LIP, and they suggest some degree of lithospheric thinning must occur as well.

However, Campbell (1998) and Courtillot et al. (1999), amongst others, have proposed that in the majority of cases volcanism precedes rifting and so White and McKenzie's model cannot be applied. White and McKenzie (1989; 1995), however, demonstrated that the volumes of lava in a LIP are too great to have been formed solely by the arrival of an anomalously hot mass at the base of the lithosphere. In order to produce the volumes of melt required without decompression from rifting, Campbell (1998) suggests that the plume head contains some eclogite as this tends to melt first. Other workers (e.g., King and Anderson, 1995) suggest that plumes do not exist at all. However, with the advent of better seismic tomography pipe-like columns of low seismic velocity thought to be plume tails have been imaged within the mantle below some volcanic hotspots (e.g., Pilidou et al., 2004),. Even so, some LIPs do not show evidence of volcanism before rifting (Ernst et al., 2005) and other theories have been put forward for their formation. One of these theories is edge-driven convection, which is proposed by, amongst others, King and Anderson (1995). King and Anderson (1995) propose that thermal variations between hotter, old, thick, continental cratonic lithosphere and cooler, young, thin oceanic lithosphere forces material to flow from beneath the thicker towards the thinner lithosphere, allowing melt to rise through cracks in the lithosphere. Jones et al. (2002) and Ingle and Coffin (2004) suggest a very different mechanism. They both propose the cause of some LIPs as due to the massive decompression melting caused by the impact of a bolide with the Earth.

1.3 The Deccan continental flood basalt province

1.3.1 Location and extent

The DVP or Deccan Traps cover approximately a quarter of peninsular India, encompassing much of Maharashtra, Madhya Pradesh, southern Gujarat and northern Karnataka States (Figure 1.2). The current outcrop area is estimated to be 500,000 km^2 but the original area is still a matter of debate. Estimates of the original area vary from 1,500,000 km^2 (Krishnan, 1956) to at least 1,800,000 km^2 (Todal and Eldholm, 1999), while some put it as high as 2,600,000 km^2 (Khadkikar et al., 1999). M. Widdowson (pers. com., 2004) estimates the original volume at 750,000 km^3. Much of this variation in area and volume estimates is due to the relatively unknown area of the DVP that was rifted away as the Cambay rift system propagated south and the Seychelles-Mascarene Plateau and part of the DVP moved west. Further problems are caused by the difficulty in estimating the volume that has been eroded from the periphery and northern parts, and a paucity of published data on the continental shelf off the west coast of India.

The DVP can be divided into four sub-regions. The MDP is the largest area, and is found to the south of the Namarda-Son rift valley (Figure 1.2). North of this is the Malwa Plateau and to the north east is the Mandala Lobe. The fourth area is found in Gujarat and is often referred to as Kutch. This is separated from the rest of the DVP by the north-south oriented Cambay graben (Mahoney, 1988).

1.3.2 Topography

Much of the DVP exists as an elevated, relatively flat, plateau (the Maharashtra Plateau), that is on average 550 m asl. Towards the western margin, c.50-100 km inland of the coast, there is an escarpment known as the Western Ghats (ghat means descent in Hindi), or Sahyadri, in the local Marathi language. The Western Ghat Escarpment is thought to be

formed by progressive scarp recession: it is not a fault scarp (Widdowson, 1997). 'Great Escarpments', like the Western Ghats, are common along continental rifted margins, e.g., the Karoo of southeast Africa and the Serra do Mar of eastern South America (Widdowson, 1997). The process by which these escarpments become uplifted has been under debate. The proposed processes are: rift-related mechanism of crustal thinning, magmatic underplating, transient thermal effects and secondary convective effects associated with extension and flexural unloading (see Widdowson, 1997 and references therein). Once uplifted, the rifted margin, i.e., the Western Ghats, underwent scarp recession and the Western Ghat escarpment developed. The formation of the Ghat scarp has led to the development of the Konkan coastal plain. As scarp recession advances inland, eastwards, it consumes the headwaters of eastward flowing rivers and has led to truncated valleys with misfit streams (Widdowson, 1997).

1.3.3 Climate

The present-day climate of the DVP is monsoonal with much of the rain falling on the Western Ghat escarpment. Mahabaleshwar is situated right on the edge of the escarpment, and receives almost 600 cm of rain in the months of June-September, whereas neighbouring Panchgani, only 15 km further inland receives only a little over 200 cm. The elevation of the Mahabaleshwar Plateau (c.1100-1200m) provides a much cooler and fresher climate than the hot, humid, coastal, Konkan Plain. The inland Maharashtra Plateau has moderate to low rainfall, and high summer temperatures. The high rainfall on the escarpment has led to dense tropical forest along the Western Ghats, but inland this gives way to semi-arid grassland.

1.3.4 Historical background

Much of the Western Ghats area has been important in the history of India. Many Marathi hill forts took advantage of the steep cliffs of the Western Ghats and are found over-

looking the Konkan plain. The forts date from pre-Colonial times. One of the most famous names associated with some of these forts is the infamous Shivaji (1630-1680), who ruled over a large area of the Marathi lands (what is now Maharashtra) during the Mogul occupation. Later, during the Raj, the British escaped the stifling heat of the Konkan plain and Mumbai, and took refuge in 'hill stations' in the Western Ghats. Government officials from Bombay retired to the cool of Mahabaleshwar, or Malcolmpeth as it was known for a time, during the summer months before the wet monsoon started. But the cool of the Western Ghats was not for the officialdom alone. Soldiers who were considered to have had too much heat were sent to Deolali (19°56'55"N 73° 50'08"E near Nasik), or Doolally as it became known.

1.3.5 Tectonic History

The origin of the DVP is closely related to the geological history of India as it rifted from Pangaea and became an island. During the Late to Middle Jurassic (160 Ma, Figure 1.4), India and Madagascar lay between about 25 and 45 degrees south and began to separate from what is now Africa with the opening of the Mozambique channel (Golonka and Bocharova, 2000).

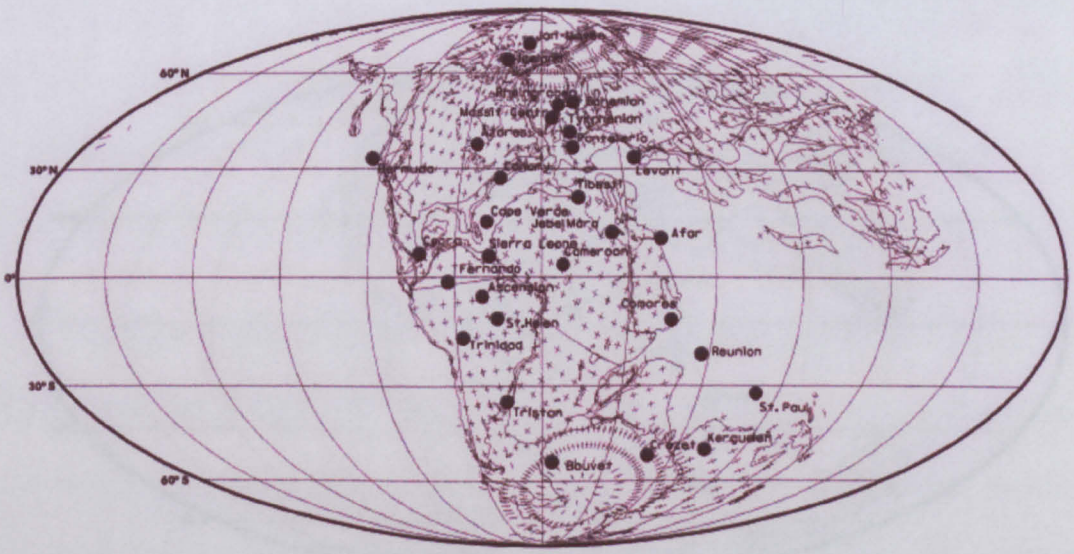

Figure 1.4. Late to Middle Jurassic (160 Ma) continental arrangement and position of major Pangean hotspots. (Glasby and Kunzendorf, 1996)

By the Early Cretaceous (120 Ma, Figure 1.5), they had separated completely by drifting southwards and lay between approximately 32 and 60° S. By the Late to Middle Cretaceous (Figure 1.5), India and Madagascar had drifted north and began to separate from each other at approximately 88-84 Ma; India lay across the 30° S line of latitude (Golonka and Bocharova, 2000). This rifting from Madagascar led to the first volcanic activity to be related to "Greater India" during this part of its history. Dykes found in southwest India are of both Deccan and India-Madagascan rifting ages (Storey et al., 1995). By the Late Cretaceous-earliest Palaeogene (65 Ma; Figure 1.6), India was moving northwards towards Asia at a rate of approximately 14 cm per year (Klootwijk and Peirce, 1979). "Greater India" contains a series of Precambrian structural features which reactivated during the Cretaceous (Biswas, 1987) when the western part of the island is thought to have encountered the arrival of the proto-Reunion Plume, forcing its way through the lithosphere. Towards the end of the DVP volcanism, rifting occurred along the Narmada and Cambay rifts. The rifting of the Seychelles-Mascarene block or microplate, along the western coast of India represents, the successful rift of one arm along the triple junction. As India continued to move northwards, the trace of the Reunion Plume produced the Chagos-Laccadive Ridge. Its current location is the island of Reunion itself.

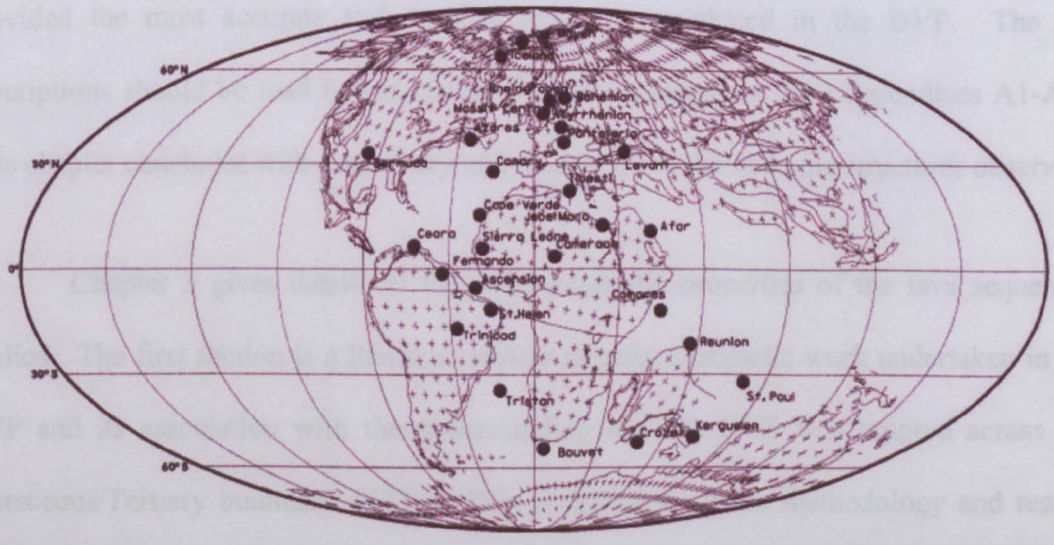

Figure 1.5. Late Cretaceous (90 Ma) continental arrangement and position of major Pangaean hotspots. (From Glasby and Kunzendorf, 1996)

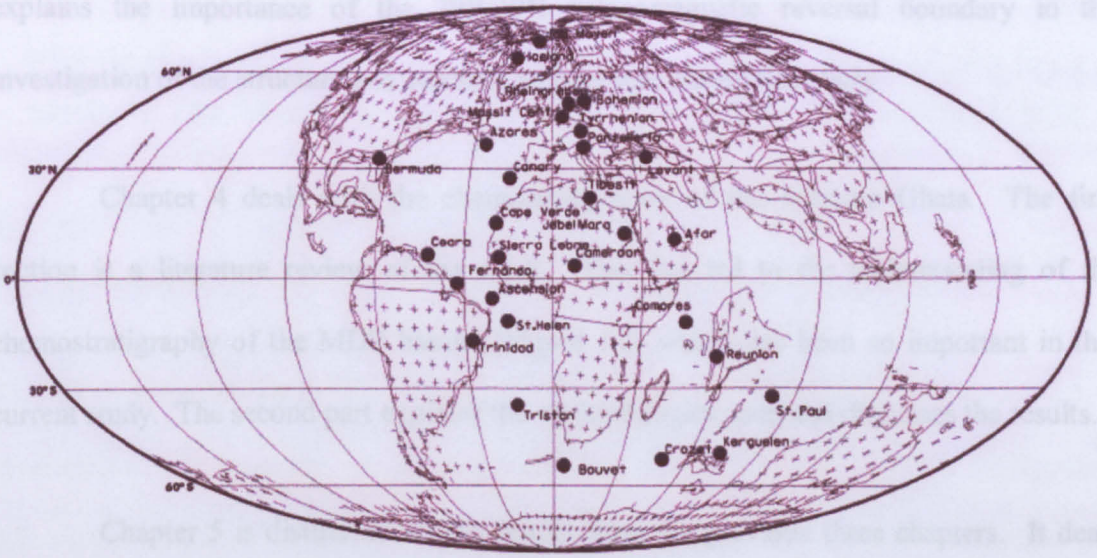

Figure 1.6. Late Cretaceous Early Palaeogene (65 Ma) continental arrangement and position of major Pangaean hotspots; this map also shows the position of "Greater India" at the time of the DVP formation (From Glasby and Kunzendorf, 1996)

1.4 Outline of present work

Chapter 2 describes the physical characteristics and volcanic stratigraphy of the Western Ghats. An overview of the nomenclature and the theory of lava inflation is given followed by a literature review of the volcanology of continental flood basalt provinces and more specifically that of the DVP itself. The second part of the chapter provides detailed descriptions of the seven sections that were logged up the Western Ghat Escarpment. The elevation data for these traverses were acquired using high precision static GPS which has provided the most accurate and detailed logs ever produced in the DVP. The log descriptions should be read in association with the appropriate log (Appendices A1-A7). This chapter concludes with a summary and discussion of the volcanic structures observed.

Chapter 3 gives details of the palaeomagnetic properties of the lava sequences studied. The first section is a literature review of palaeomagnetic work undertaken in the DVP and its association with the understanding that the DVP was erupted across the Cretaceous/Tertiary boundary (KTB). This is followed by the methodology and results from palaeomagnetic work on the seven traverses described in Chapter 2. The discussion

explains the importance of the 29R/29N palaeomagnetic reversal boundary in the investigation of the structure and volcanic architecture during this study.

Chapter 4 deals with the chemostratigraphy of the Western Ghats. The first section is a literature review of the work. This has led to the understanding of the chemostratigraphy of the MDP basalts (Figure 1.2) which has been so important in this current study. The second part explains the methodologies used and discusses the results.

Chapter 5 is distillation of the results from the previous three chapters. It deals with stratigraphic correlations which lead to the understanding of the volcanic structure and architecture of the areas studied. It looks at short, medium and long range correlations and demonstrates that topography developed on the active surface of the DVP and that the individual sheet lobes have limited lateral extent. The final part of this chapter explains that the 3-dimensional structure of the study area is complex and that the volcanic architecture is the same when dealing with small lobes, only decimetres thick and thick, sheet lobes, tens of metres thick.

Chapter 6 investigates the similarity and differences between the chemostratigraphy and the volcanic architecture of the DVP and the lavas of the island of Hawai'i. To provide a comparison between the DVP and a currently active plume associated volcano.

Chapter 2
Physical characteristics and volcanic stratigraphy of the lava units in the Western Ghats, Deccan Volcanic Province, India

2.1 Introduction

This chapter has two parts. The first part of this chapter, up to and including Section 2.5, is predominately a literature review and aims to inform the reader of the background information required to carry out the volcanostraigraphic logging and understand the features observed. It firstly provides a brief introduction to the previous work which has been carried out on the Deccan Volcanic Province (DVP). Then, most importantly, the nomenclature used during this study is introduced and explains the theory of inflation and features associated with it, using observations made in Hawai'i by previous workers and myself. The theory of inflation is then applied to continental flood basalt provinces (CFB) using the Columbia River Basalt Province (CRBG) as an example, this is in order to demonstrate that the theory of inflation is applicable to CFBs. The final section of the first part of this chapter describes the previously published literature on the volcanology of the DVP, which has mostly described only small-scale features associated with the lava emplacement and does not acknowledge inflation as the mechanism of emplacement of the thick sheet lobes in the DVP. This current study investigates small and large scale features over a considerable area and incorporates it precisely and accurately into the established chemostratigraphy and palaeomagnetic stratigraphy. I thus unravel the method of emplacement of the majority of the units observed.

The second part of the chapter (Sections 2.6-2.9) presents new data starting with the description of the seven volcanologically logged sections completed during two field seasons in India. Each individual log description is divided into its geochemical formations (Section 2.6) and is then arbitrarily sub-divided into sections based on

elevation, and where possible, upon any significant changes observed in the volcanological characteristics, petrography and weathering horizons. After the log descriptions, the volcanological features are described and then further discussed in terms of their origin and implications of this for CFB formation.

2.1.1 Overview-Volcanology and the DVP

Despite a long history of study in DVP (e.g., Wadia, 1937; West, 1959), most recently concentrating upon the geochemical stratigraphy (e.g., Cox and Hawkesworth, 1985; Beane et al., 1986; Devey and Lightfoot, 1986; Vandamme et al., 1991), the morphology of the lavas is only beginning to be discussed in detail in the literature (e.g., Sharma and Vaddadi, 1996; Keszthelyi et al., 1999; Khadri et al., 1999; Duraiswami et al., 2002). Some of the first volcanological work in the DVP was undertaken by Walker (1972), who studied a number of locations around the DVP and developed the idea of simple and compound flows to describe the two different flow morphologies that he observed. More recent work on CFBs by Self et al. (1997) has challenged the validity of these two categories when applied to whole assemblages of sheet lobes and related lava bodies produced by a single flood basalt eruption or a series of eruptions. Nevertheless, the recently published articles regarding the physical characteristics of lavas within the western DVP north of Pune (Figure 2.1) (e.g., Sharma and Vaddadi, 1996; Thorat, 1996; Duraiswami et al., 2001; Duraiswami et al., 2002), and on the type and origin of the lava units seen there (Bondre et al., 2004), have all used the obsolete terminology of 'simple' and 'compound flows'. A critical re-evaluation of lava morphology in the DVP is therefore needed and is an aim of this thesis.

Much of the work in this thesis has involved studying the Wai Sub-group (Table 2.1. The sub-groups and formations of the MDP (after Cox and Hawkesworth, 1985; Beane et al., 1986; Devey and Lightfoot, 1986)), which is the most voluminous sub-group

of the DVP and is thought to make up approximately half of the total erupted volume, ~ 750×10^3 to 1×10^6 km^3 of lava (Widdowson et al., 2000). From a combination of palaeomagnetic data and $^{40}Ar/^{39}Ar$ age dates, it is thought likely that the Wai Sub-group was erupted across the Cretaceous-Tertiary boundary or KTB (M. Widdowson, pers. comm., 2005) and, as such, it is important that the volcanological characteristics of the lavas are understood in order to better assess the environmental impact of DVP volcanism.

Sub-Group	Formation
Wai	Desur
	Panhala
	Mahabaleshwar
	Ambenali
	Poladpur
Lonavala	Bushe
	Khandala
Kalsubai	Bhimashankar
	Thakurwadi
	Neral
	Igatpuri
	Jawhar

Table 2.1. The sub-groups and formations of the MDP (after Cox and Hawkesworth, 1985; Beane et al., 1986; Devey and Lightfoot, 1986)

Lithostratigraphy				Geochemical stratigraphy			
Super Group	Group	Sub-Group	Formation	Group	Sub-group	Formation	
DECCAN TRAPS	NORTHERN SAHYADRI	Mahabaleshwar	Mahabaleshwar M4	DECCAN BASALTS	Wai	Desur	
						Panhala	
						Mahabaleshwar	
						Ambenali	
						Poladpur	
		Diveghat	Purandargad				
			Diveghat		Lonavala	Bushe	
			Karla			Khandala	
		Lonavala	Indrayani M3		Kalsubai	Bhimashankar	Upper
						Thakurwadi	Middle
		Kalsubai	Upper Ratangad M2				Lower
			Lower Ratangad M1			Neral	
			Salher			Igatpuri	
						Jawar	

Table 2.2. Godbole et al.'s (1996) classification of the lithostratigraphy of the DVP compared to the widely used geochemical stratigraphy. Note that M1-4 are megacryst-bearing (also referred to as giant plagioclase basalts (GPB)) marker horizons (from Godbole et al., 1996).

The current generally accepted stratigraphy of the MDP is based upon trace element abundances and elemental ratios of the basaltic lavas of the Western Ghats (Cox and Hawkesworth, 1985; Beane et al., 1986; Devey and Lightfoot, 1986). This geochemically-based stratigraphy (chemostratigraphy) divides the volcanic pile into three sub-groups and twelve formations (Table 2.2 (right)) (Beane et al., 1986). A lithostratigraphic classification (Table 2.2 (left)) has also been published (Godbole et al., 1996) based on the lavas around the western DVP region between ~21°30'N to 16°30'S, but its reliability across the whole of the DVP, or within the wider outcrop along the Western DVP, is highly questionable since such an approach would assume and require the lateral continuity and persistence of the 'marker horizons'.

2.2 Nomenclature used in this study

2.2.1 Division of the units

To evaluate the volcanostratigraphic architecture, the three categories of lava body adopted by Self et al. (1997), *flow-field*, *lava flow* and *flow lobe* are used in this study, and summarised here. A *flow-field* is the aggregate product of a single eruption or vent and is built up of one or, usually, more lava flows. For this work, we have used flow-field to describe the lava unit or units that occur between two weathering horizons, marked by red soils, or boles, assuming that sufficient time would elapse between eruptions to permit at least minor weathering to occur. Surfaces showing demonstrable erosion without weathering would also be used to divide the lava pile into flow-fields, but are rare in the tropical environment into which the Deccan lavas were erupted at ~ 30°S (Courtillot et al., 1986).

A *lava flow* is defined as the product of a 'single outpouring of lava' (Bates and Jackson, 1987). A new lava flow is typically formed after a short pause in effusion.

However, it is entirely possible for an eruption to form two or more lava flows simultaneously.

The term *flow lobe* is used to describe an individual unit of lava which is bounded top, bottom and sides by a glassy rind or selvage. It must be remembered that when observed in a traverse, a single flow lobe can be a lava flow and can also be a flow field if it is bounded top and bottom by a red bole. In continental flood basalt provinces (CFBs), flow lobes can vary in size from 10^{-1} m (also called toes) to 10^{3} m in width, and 10^{-1} to 10^{2} m in thickness. Where a single flow lobe is a large-scale feature, i.e., wider than an outcrop (10^{2} to 10^{3} m), as is common in CFBs, then the term *sheet flow lobe* (shortened to sheet lobe) is used. The term *unit* is used in a generic sense to describe a body of lava, either a single or multiple sheet lobes without any connotation of its origin, character or size, and is often used if it is not possible to determine the type of lava body observed due to a lack of exposure.

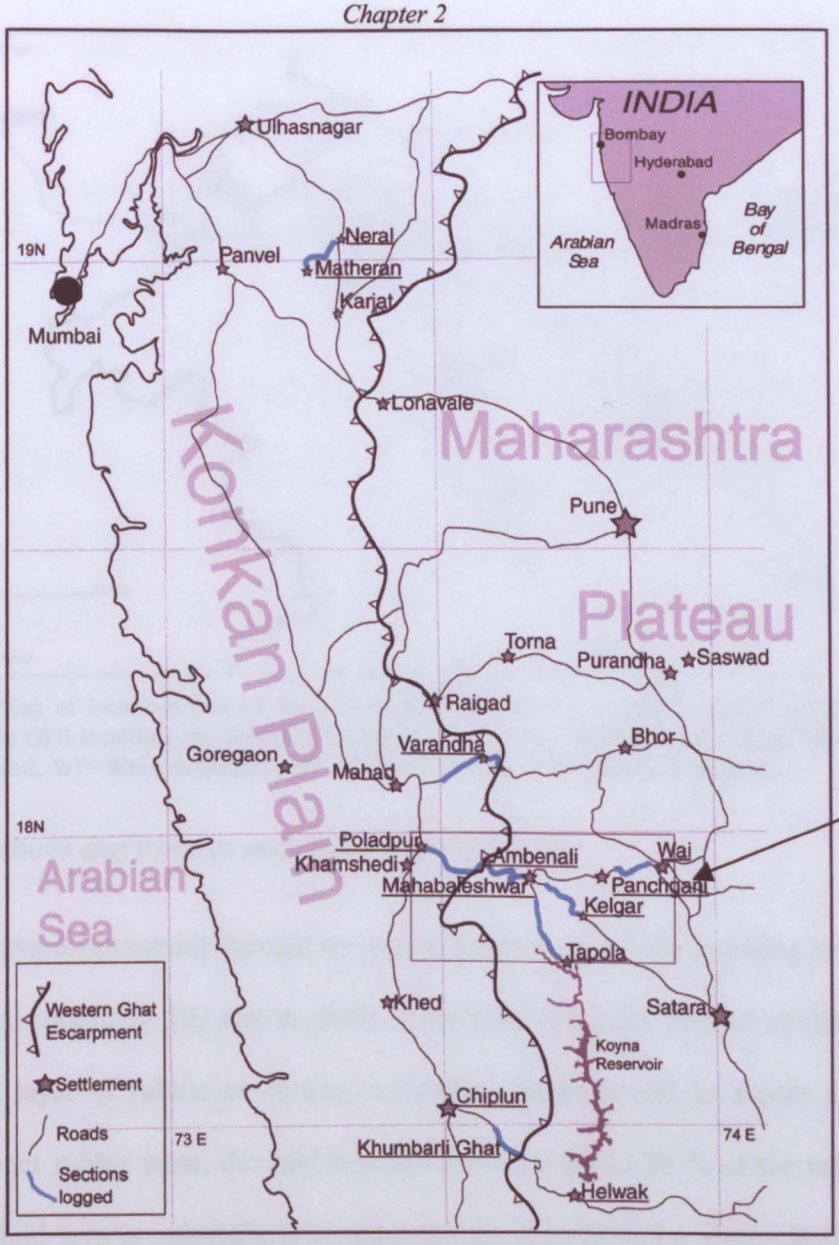

Figure 2.1. Map of field area in Western Ghats of DVP. Roads along which the logging traverses were conducted are highlighted in bold and blue, towns related to logged sections underlined. Inset locates this region within India.

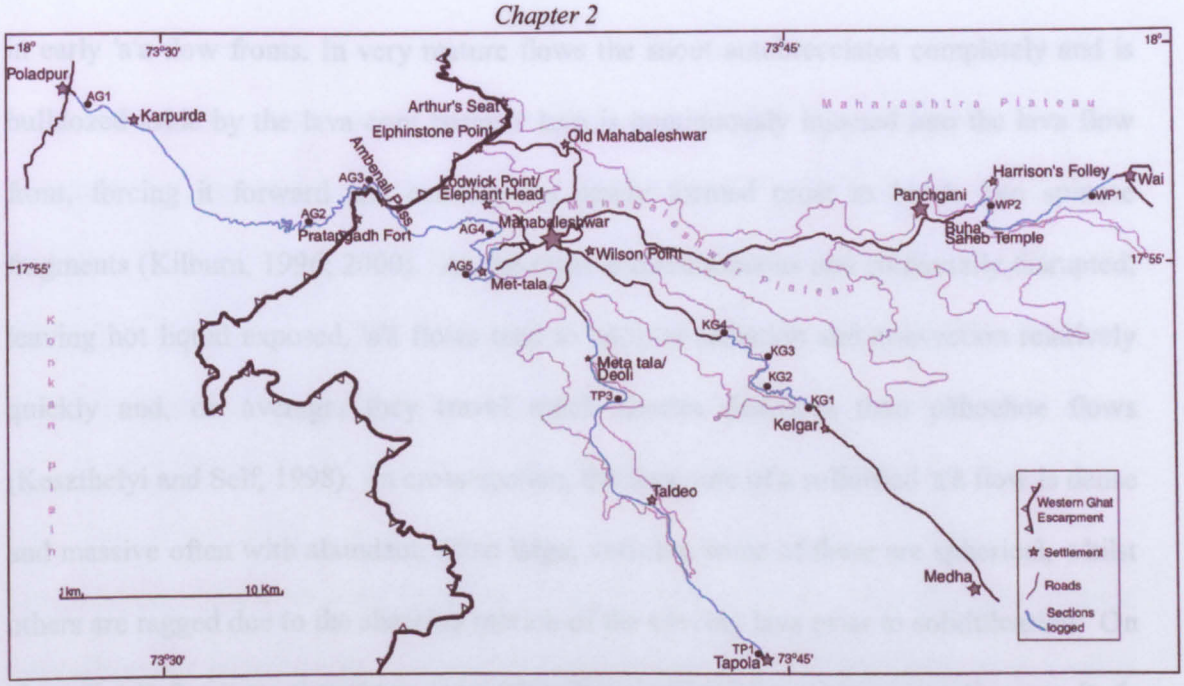

Figure 2.2. Map of locations around the Mahabaleshwar Plateau. Logged sections are in blue. High precision Static GPS locations are designated according to traverse: AG=Ambenali Ghat, TP=Tapola Road, KG=Kelgar Road, WP=Wai-Panchgani Road. Koyna Reservoir is not shown on this map.

2.2.2 Structures and features associated with lava fields

'A'ā. 'A'ā lava is commonly formed by channelised flows and the resulting lava unit is up to a few (exceptionally 10) metres thick. Internally the units consist of three parts: an upper thick layer of rubble or clinker, a middle, massive solid lava core and a lower, usually thinner rubble zone, the rubble zones can form up to 80 % of the unit thickness. When the fluid lava is erupted and contacts the air it cools and a visco-elastic - partially solid crust forms. The characteristic 'a'ā 'rubble surface' is thought to form because of the more viscous nature of the lava compared to pāhoehoe due to a number of related reasons (e.g., Cashman et al., 1999) such as eruption temperature, amount of degassing, amount of groundmass crystals, silica content, degree of polymerization, (also possibly eruption rate and ground slope; Kilburn, 1996; Francis, 1993). Due to the higher viscosity and yield strength, the partially solidified upper crust cannot deform with the flowing liquid lava beneath so it tears and forms the clinker-like-rubble as the lava moves. The tearing produces spinose edges to the rubble particles, like in the tearing of solidifying toffee. The rubble at the flow front is pulled around the snout and under the front as it moves forward

in early 'a'a flow fronts. In very mature flows the snout autobrecciates completely and is bulldozed aside by the lava core because lava is continuously injected into the lava flow front, forcing it forward and causing the newly formed crust to break into spinose fragments (Kilburn, 1996; 2000). As the crust is discontinuous and continually disrupted, leaving hot liquid exposed, 'a'ā flows tend to cool by radiation and convection relatively quickly and, on average, they travel much shorter distances than pāhoehoe flows (Keszthelyi and Self, 1998). In cross-section, the lava core of a solidified 'a'ā flow is dense and massive often with abundant, often large, vesicles, some of these are spherical, whilst others are ragged due to the shearing motion of the moving lava prior to solidification. On Hawai'i, 'a'ā flows are thought to form when lava is erupted at a higher eruption rate (> 5-10 m^3 s^{-1}) than when pāhoehoe flows (< 5- 10m^3 s^{-1}) are formed (Rowland and Walker, 1990; Francis, 1993).

Pāhoehoe. There are many divisions of pāhoehoe, usually relating to the surface morphology, and/ or vesicle type and distribution. The most well known of the many different surface structures is 'ropy pāhoehoe', formed when the newly created surface crust wrinkles up due to flowing lava beneath it. All pāhoehoe lavas have a continuous surface and are highly vesicular, at least in the upper sections (Rowland and Walker, 1990). 'Shelly' pāhoehoe forms when large vesicles occur beneath the cooled, vesicular, thin pāhoehoe surface. Descriptions of two further types of pāhoehoe, P and S-type pāhoehoe (after Walker, 1989), can be found in the glossary. Extensive, flat sheet flow lobes of inflated pāhoehoe form when the lava flows over low-gradient to flat surfaces; however, over uneven or steeper surfaces, hummocky pāhoehoe usually forms. Pāhoehoe flows are formed by lower eruption rates, grow by inflation (Section 2.3.1) with the liquid lava insulated under a crust and they are less viscous than 'a'ā (Rowland and Walker, 1990), again based on observations in Hawai'i. Pāhoehoe flows may form in CFBs under considerably higher eruption rates than have been recorded in historic flows on Hawai'i.

Tumuli (single tumulus). Tumuli are mounds, or whale-back ridges, 1 to 10 m high which are split by axial, or more-or-less radial, gaping clefts. Tumuli form when inflation occurs in a restricted area, and are generated when the lava crust is pushed up by increased lava pressure. Lava may ooze out of the tumuli to form separate lobes and toes and or drain away if the obstruction causing the restriction is removed or overcome (Self et al., 1998). They are formed in hummocky pāhoehoe fields, on shallow slopes, produced by the tilting up of lava crust without any crustal shortening (Walker, 1991).

Lava rise pits. These are common in hummocky pāhoehoe fields. They are depressions in the surface of a pāhoehoe sheet lobe or between groups of lobes, with steep, often vertical or overhanging sides. The floor of the lava rise pit has pāhoehoe surface features. They form when the movement of lava within a flow is restricted, thus causing uneven inflation. In an area where no or little lava is being injected, inflation will slow or stop; by contrast, the surrounding crust, which has a plentiful supply of lava injected beneath it, will continue to rise. Lava rise pits have no connections with lava tube systems and hence must not be confused with sky lights which form from the collapsed roof of a lava tube. The identification on the walls of lava rise pits of horizontal banding, probably indicative of the gradual inflation of the surrounding material (Walker, 1991), will distinguish them from sky-lights.

Hummocky pāhoehoe. This type of lava has a surface dominated by discrete tumuli and lava rise pits. In active hummocky pāhoehoe flows the pathways of lava through the various lobes are discrete and often terminate before the flow front. If the fluid lava within the flow does not extend across the whole flow inflation cannot take place in all areas simultaneously, and lava rise pits will form in the non-, or less-inflated parts. If an individual lava pathway terminates before the flow front, the build-up of lava breaks the overlying crust and a tumulus will result by pushing up the crust. If the blockage is

removed or bypassed, the liquid lava may drain out and leave an empty tumulus, and possibly an empty lava tube. A sheet lobe, with its continuous liquid lava core, can develop into hummocky pāhoehoe if it is active long enough for parts of it to freeze shut. This process leads to irregularities in the crustal thickness and concentrates the flowing lava into narrow pathways which may then become blocked (Self et al., 1998).

Rubbly pāhoehoe. The surface of rubbly pāhoehoe lava is entirely covered with loose blocks of broken pāhoehoe lava crust, which are often piled into metre-sized mounds forming elongated and sinuous ridges along the margins of individual lobes or in front of obstacles (Keszthelyi, 2000). The largest blocks are commonly 20-50 cm thick and 1-2 m wide and can have basal scraper marks and or glassy protrusions similar to gas-blister walls. Filling the interstitial spaces are smaller fragments of slabs, fragments of toes and some denser blocks up to 20 cm thick. The smallest fragments, cm-sized rubble, show evidence of deformation by plastic tearing (Guilbaud et al., in press).

Segregation features. Horizontal vesicular sheets (HVS) and vesicle cylinders (VC) are 1-10 cm wide horizontal or vertical sheets and cylinders seen in section in sheet lobes, recognised by their unusually high concentration of vesicles that form in the core of a lava flow. Once inflation has ceased and the molten lava core begins to solidify, the lava crystallises and the differentiated residual melt starts to collect. This material is less dense than the surrounding (partially crystallised/liquid) lava so rises towards the upper crust in vesicle cylinders. When this material reaches the solid base of the upper crustal zone, it can rise no further so spreads out to form a horizontal vesicle sheet (HVS) (Self et al., 1997). Geochemical analysis of this material shows a more evolved (higher) silica and incompatible trace element content (Goff, 1996).

Break-out lobes. These are small pāhoehoe lobes up to 1 m thick, but usually thinner. They form during inflation of a sheet lobe when some of the liquid lava core is pushed out

of a fracture in the upper crust due to an influx of lava at higher pressure. They are most probably formed when the sheet lobe was relatively thin and young, when the upper crust is not overly thickened. Once a sheet lobe is frozen, the lava which has formed break-out lobes is generally older than the majority of the lava which forms the core, this is because as inflation progresses new lava is continually pushed into the sheet lobe. As break-out lobes occur on the upper surface of an inflated sheet lobe they can be subjected weathering and therefore are found below red boles.

Precursor lobes (Figure 2.25 & Figure 2.33). These are small pāhoehoe lobes that occur above boles and below the main inflated sheet lobes of a flow field. They are thought to be lobes which are emplaced before the main influx of lava occurs and, as such, are generally smaller than break-out lobes as they probably do not have such a large supply of lava.

2.3 Inflation and sheet flow lobes

2.3.1 Inflation

The idea that lava units thickened by inflation was first touched on by Wentworth and Macdonald (1953), who described 'pressure plateaus'. This name was applied to the more-or-less flat-topped portion of a flow-field that was uplifted by the injection of lava beneath the surface crust. In his paper describing the origin of tumuli, lava rises and lava-rise pits, Walker (1991) also recognised the internal injection of lava as an input mechanism. Walker identified that tumuli grow by the injection of liquid lava, and proposed that the crust of the sheet lobe 'floats' on large bodies of fluid lava. The theory of inflation *sensu stricto* (an extension of Walker's ideas) was proposed by Hon et al. (1994) following a series of observations carried out upon active lava flows on Kilauea, Hawai'i. The sheet flow lobes were observed to start as small lobes or toes 20-30 cm thick, with the upper surface cooling almost immediately to form a brittle crust. Beneath this chilled surface

crust is a visco-elastic layer which acts like a balloon, and retains the incoming lava. Thus the toe or lobe begins to inflate (Figure 2.3). However, if the pressure becomes too high the lava will burst through the flow front and form new toes. Within a given area, the toes grow, thicken into lobes and coalesce, and the liquid lava cores of each flow lobe can thus become joined forming a single sheet lobe. The hydrostatic pressure within this single sheet flow lobe is evenly distributed and the influx of more lava results in the uniform uplift of the solidifying crust. The initial uplift rate is rapid, for instance, 1 m in 1-2 hours (Hon et al., 1994), but as the flow front increases in area, breakouts continue, the crust thickens, and the rate of inflation decreases.

During flow inflation the lava is typically fed to the flow front through the whole sheet flow lobe. As time progresses cooling and solidification occurs along the margins, which are exposed to the atmosphere. This limits the area within the sheet lobe that the lava can flow through. These pathways may become lava tubes which transport the lava to the active flow front with little loss of heat (Peterson and Swanson, 1974; Kauahikaua et al., 1998). In large, rapidly emplaced sheet lobes of CFB dimensions which are emplaced onto flat surfaces, it is thought that the whole sheet may conduct the lava, and that a discrete 'tube' may not actually develop due to a sustained rate of lava input (Self et al., 1998). By contrast, slower discontinuous emplacement over rough and steeper surfaces produces "hummocky" flows with many discreet tumuli (Self et al., 1998).

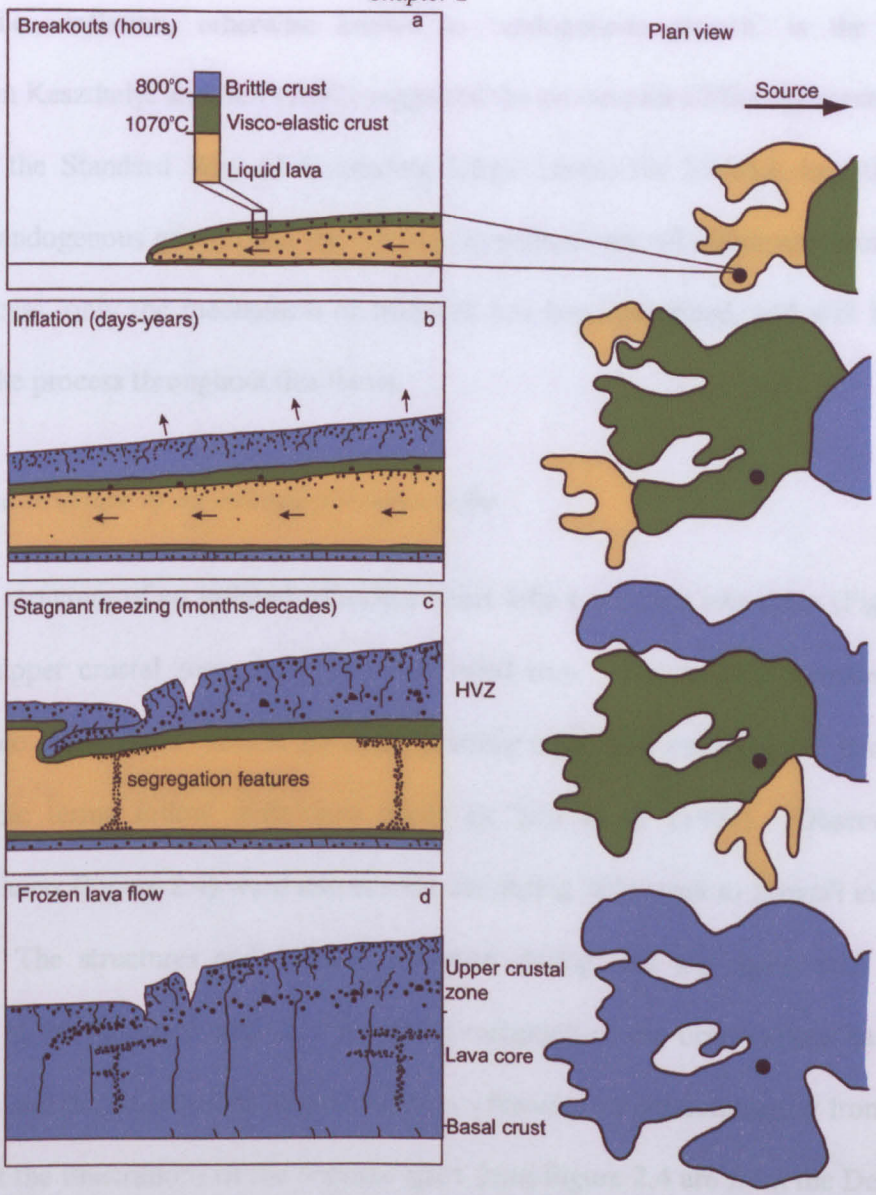

Figure 2.3 Schematic cross section and plan of emplacement of a generic inflating pāhoehoe flow lobe. Vertical scale varies from 1-5 m for Hawaiian lobes to 50-60+ m for CFB sheet lobes, horizontal scale varies from 100s m to 10s km, for area shown. a) Flow arrives as a small, slow-moving lobe of molten lava held inside a stretchable, chilled visco-elastic skin with brittle crust on top. Bubbles are initially trapped in both the upper and basal crusts. b) Continued injection of lava into the lobe results in inflation, (lifting up of the upper crust) and new breakouts. During inflation bubbles rising from the fluid core become trapped in the visco-elastic mush at the base of the upper crustal zone, forming horizontal vesicular zones (HVZ). The growth of the lower crust, in which pipe vesicles develop, is much slower. Relatively rapid cooling and motion during inflation results in irregular jointing in the upper crustal zone. c) After stagnation, diapirs of vesicular residuum form vertical cylinders and horizontal sheets (segregation features) within the crystallising core. Slow cooling of the stationary liquid core forms more regular joints. d) Emplacement history of the lobe is preserved in the vesicle distribution and jointing pattern of frozen lava. (After Self et al., 1996; Self et al., 1998).

The application of the inflation model to the interpretation of CFBs was first attempted by Self et al. (1996), who employed the idea to describe the emplacement of the basalts of the CRBG. The mechanism of emplacement of lavas in CFBs is currently understood to be the same as for smaller pāhoehoe eruptions such as those on Hawaii and

Iceland, i.e., inflation, otherwise known as 'endogenous growth' is the dominant mechanism Keszthelyi and Self (1997) suggested the process for CFB emplacement should be called the Standard Way of Emplacing Large Lavas; the SWELL hypothesis. As inflation, endogenous growth and the SWELL hypothesis are all effectively names for the same process, only the mechanism of inflation has been described, and will be used to describe the process throughout this thesis.

2.3.2 The structure of an inflated pāhoehoe lobe

The basic structure of an inflated pāhoehoe sheet lobe is divided into three (Figs. 2.3 and 2.4), the upper crustal zone, lava core, and basal zone. The internal structures can be divided into three types: vesicle patterns, jointing style, and petrographic texture. The petrographic terms follow definitions given by Self et al. (1997). Observations on pāhoehoe lavas (Figure 2.4) were also carried out during field work to Hawai'i in the spring of 2002. The structures and features observed during that trip agree with the terms described in the literature, and so a detailed description of the observations has not been made here and the descriptions of pāhoehoe lava features are predominantly from literature review but the illustrations of the features apart from Figure 2.4 are from the Deccan lavas in the study area.

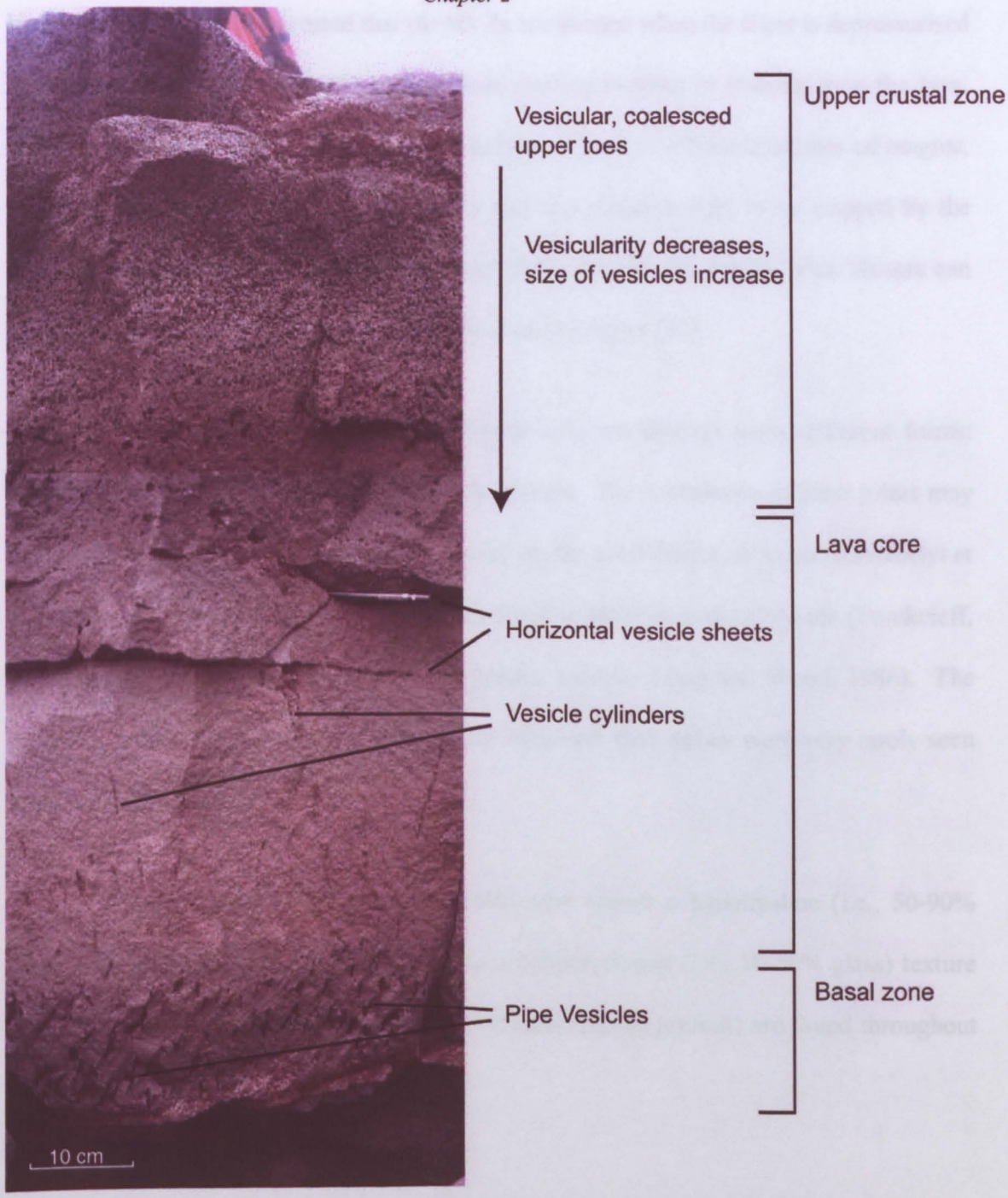

Figure 2.4. Inflated pāhoehoe sheet flow lobe approximately 1 m thick and 10s m long at Kalapana, Hawai'i, showing features associated with growth by inflation and division into an upper crustal zone, lava flow core, and basal zone. Horizontal line towards the base of the upper crustal zone is a photographic join.

The upper crustal zone (abbreviated to upper crust) typically comprises 40-50% of the total flow-lobe thickness (Figure 2.4). It has a high vesicularity, but the vesicularity decreases down into the flow whereas the vesicle size increases (Cashman and Kauahikaua, 1997). The vesicles are often arranged into layers of similar size bubbles, this forms so-called horizontal vesicular zones (HVZs). The origin of HVZs is still uncertain;

Hon et al. (1994) have suggested that the HVZs are formed when the sheet is depressurised by a sudden, large outbreak at the flow front causing bubbles to exsolve from the lava. Another suggestion is that the layering of bubbles is due to different batches of magma, with varying volatile content. The bubbles rise and coalesce only to be stopped by the downward migrating, solidifying upper crust (Keszthelyi et al., 1999). Gas blisters can also be found in the lower portions of the upper crust (Figure 2.5).

The jointing in the upper crust (Figure 2.6) can take on many different forms: hackly and curvilinear being some of the commonest. The complexity of these joints may be due to the constant stress and strain imposed on the crust during inflation (Keszthelyi et al., 1999). Keszthelyi et al. (1999) avoid the terms entablature and colonnade (Tomkeieff, 1940) as they are associated with specific genetic models (Long and Wood, 1986). The terms are avoided in this work as well, as the structures they define were very rarely seen in the field area studied.

The petrography of the upper crustal zone shows a hypohyaline (i.e., 50-90% glass) cm-thick glassy rind, which grades to a hypocrystaline (i.e., 10-50% glass) texture through the whole depth of the upper crust. Phenocrysts (if present) are found throughout the upper crustal zone.

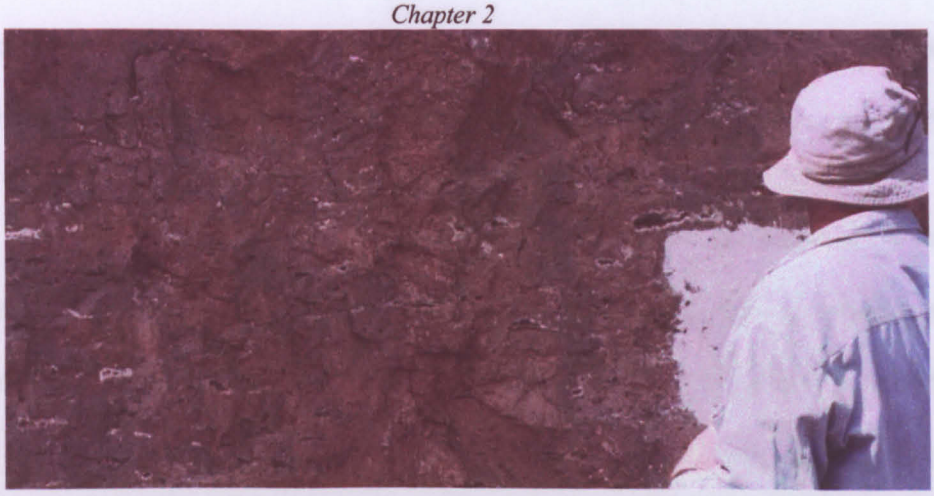

Figure 2.5. Small gas blisters in the lower upper crust, viewed in a sheet lobe on Khumbarli Ghat, in the Ambenali Formation (334 m asl). Note that some are partially, and some fully infilled with secondary minerals. Lat. long. 17°25'28.9"N 73°40'18.5"E .

Figure 2.6. Upper crustal prismatic joints, at the level of the hammer head, in a small ~2 m thick sheet flow. The base and core of the overlying flow is also visible; Co, core; BZ, Basal zone; UC, upper crust. This exposure is at ~ 575 m asl in the Ambenali Formation. White patch is a painted-on road side marking. Lat. long. 17°56'06"N 73° 33.5'3.7" E) (Photo by S. Self.)

The lava core (Figure 2.7) characteristically makes up 40-60% of the total sheet lobe thickness. Typically its vesicularity is low. Sparse mega-vesicles are sometimes found at the top of the lava core. The occurrence of segregation features, such as vesicle cylinders (Goff, 1996) and HVSs are also a diagnostic tool for identifying the core of a sheet lobe. The jointing is usually more regular than in the upper crust and can form proper columns. If water cooling occurs, hackly and fan joints may form. The core is holocrystalline (90-

100% crystals) and the crystals are typically fine-to medium grained, sometimes with phenocrysts (in the DVP of plagioclase feldspar and olivine) (Keszthelyi et al., 1999).

The basal zone (Figure 2.4) is usually 10% or less of the whole sheet flow lobe thickness. The vesicularity is moderate, dominated by stretched vesicles although sometimes pipe vesicles are prominent. Jointing is often poorly developed. The basal zone is hypohaline and the outer rind is a quenched glassy chill margin (Keszthelyi et al., 1999).

2.3.3 Structure of a CFB inflated pāhoehoe sheet lobe

The features observed in a sheet flow lobe tens of metres thick from the CRBG appear to be very similar to those seen in metre-scale Hawaiian lobes (Thordarson and Self, 1998). Sheet flow lobes can be divided into an upper crust, lava core and basal zone (Figure 2.7). Often, due to the highly vesicular nature of the upper crust, it can be more susceptible to alteration and weathering (Figure 2.8). The core is generally poorly vesicular (Figure 2.9) but the vesicularity increases towards the core/ upper crust boundary where large mega-vesicles and bell-jar vesicles can be observed. Segregation features can also be seen (Figure 2.10). The cores of large sheet lobes are often jointed. The joints can be crude and poorly developed, or well-developed columnar joints with a variety of widths. Joints which are formed due to water interaction with the cooling flow produce a variety of different jointing patterns: fan columnar joints, secondary sets of joints perpendicular to the main jointing, or joints which are obviously wavy. These can be collectively termed as hackly joints (Lyle, 2000) see Figure 2.11.

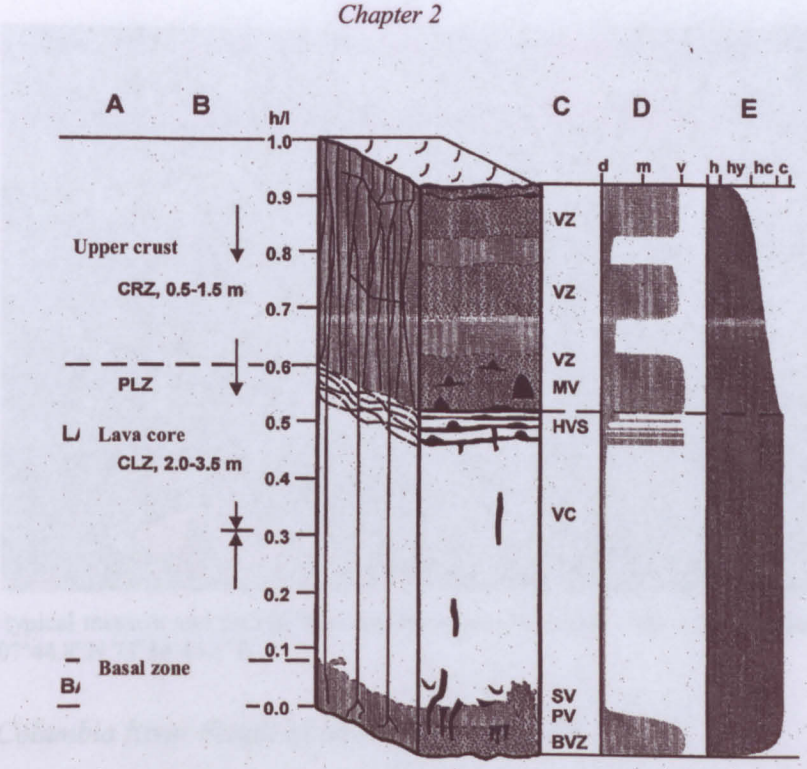

Figure 2.7. Composite graphic log illustrating the characteristic structures of a Roza sheet lobe from the CRBG. Left side of column, A), shows characteristic three-part division of sheet lobes; B), displays type of jointing; C), type of vesicles; D), vesiculation (d=dense, m=moderate, v=vesicular); E), degree of crystallinity. h/l is the normalised height above base of sheet lobe; VC, vesicle cylinder; MV, mega-vesicles; HVS, horizontal vesicular sheet; SV, segregation vesicle; PV, pipe vesicles; BVZ, basal vesicular zone; CRZ, crustal zone; PLZ, platy zone; CLZ columnar zone. (From Thordarson and Self, 1998).

Figure 2.8. Contact of two lava flows in the Ambenali Formation on Varandah Ghat (elevation 472 m; Appendix A5). Red bole (B; 15 cm thick) containing clasts of lower lava occurs between the two flows. Well-developed HVZ in upper crustal zone of lower flow is accentuated by its amygdaloidal nature. Note that upper flow has very thin basal zone (BZ) and (at top of photo) base of non-vesicular core (Co) with crude columnar joints (CJ). Hammer for scale is 36 cm long. White patches in this and future Figs. are painted-on road side markers. Lat. long. unavailable (Photo by S. Self)

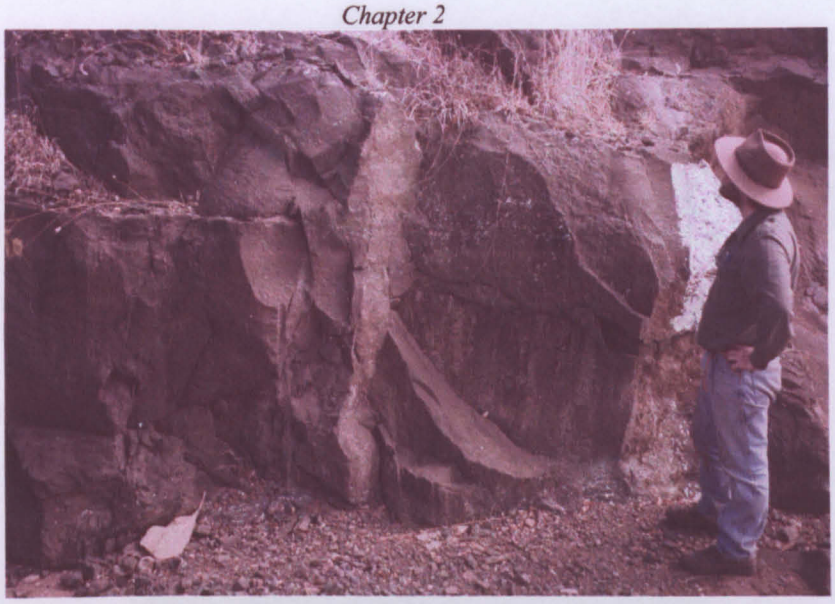

Figure 2.9. A typical massive and poorly vesicular lava core, Varandah Ghat, Bushe Formation 117 m asl. Lat. Long. 18°07'44.8"N 73°34'44.2"E

2.3.4 The Columbia River Basalt as an example of a CFB

The CFB which has been studied most extensively and intensively is the CRB. Comprehensive investigations into the geochemistry, palaeomagnetism and, brief, physical volcanology have all been undertaken (Reidel and Hooper, 1989). As such, it is perhaps the best known example of a CFB, and so is described here, briefly, to demonstrate that the theory of inflation has successfully been applied to a CFB and so can reasonably be applied to the DVP. The CRBG has also been used on occasion during this study, in comparison to the DVP, when features are noted to be different.

Figure 2.10. Vesicle cylinders with filled vesicles (some amygdaloidal), viewed in a sheet lobe core on Varandah Ghat, at 217 m asl in the lower sheet lobe with unusual geochemistry, which can not be assigned to a formation, but close to the Poladpur Ambenali Formation boundary. Small markings on card=1cm. ~Lat. long.18°07'29.3"N 73°35'17.4"E (Photo by S. Self)

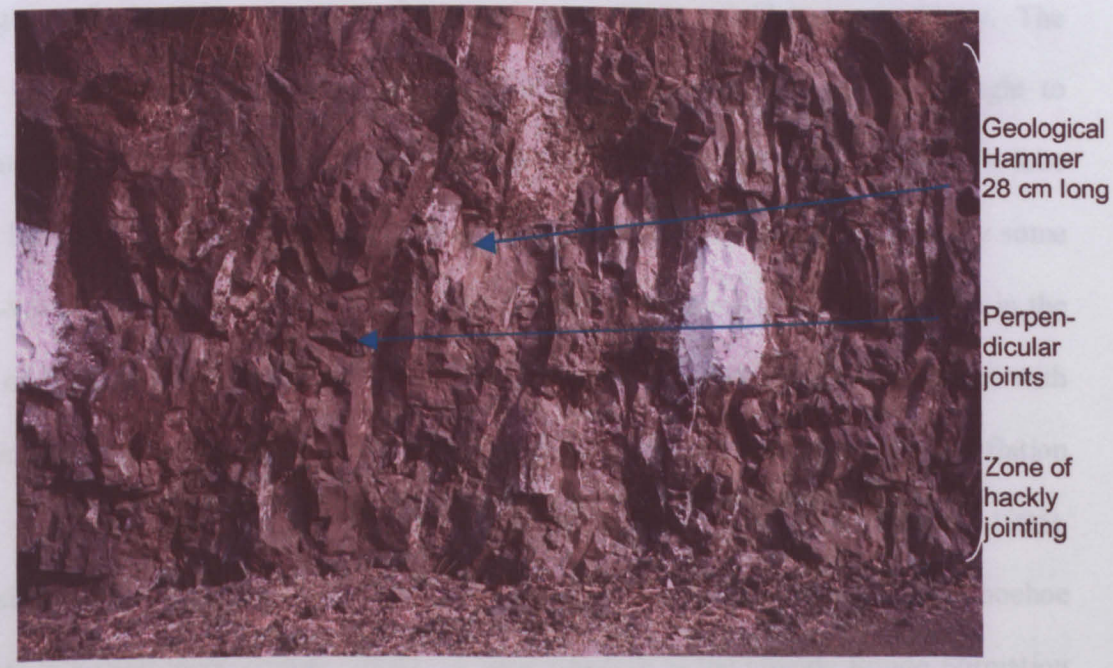

Figure 2.11. Hackly jointing in a lava core, on Khumbarli Ghat at 465 m asl in Ambenali Formation. Scale, geological hammers 28 cm. Lat. long. unavailable.

The majority of data collected on the CRBG have been based around work carried out in the 1980s by various research groups. Much of the work was funded by the U.S. Department of Energy in order to asses the suitability of the CRBG lava flows as a site for high-level nuclear waste storage. Consequently, a number of cores were drilled through the lava pile, which gives a unique view into otherwise impenetrable parts of the CRBG succession. Much of this work has been published in a Geological Society of America Special Paper (Reidel and Hooper, 1989). Subsequent work on the CRBG has shown that the lava units in the CRBG are built up of inflated pāhoehoe sheet lobes which form lava flows and flow-fields (Self et al., 1996). The sheet lobes have long been known to be pāhoehoe in nature from the field observation of their internal features (e.g., Reidel and Tolan, 1992) but it took longer to connect their internal features with their mode of formation, i.e., inflation.

The CRBG flow lobes commonly vary in size from 0.3 to 30 m thick and show vesicular, glassy crusts sometimes with surface pāhoehoe ropes intact. These glassy selvages grade down into the HVZ of the upper crust, which has higher crystallinity. The basal crusts are also glassy and vesicular, often displaying pipe vesicles, thought to indicate emplacement of degassed lava onto a low gradient (Walker, 1987). The flow lobe cores have a much lower vesicularity than the upper and basal crust but do display some mega-vesicles towards their top, and many sheet lobes contain segregation features in the form of HVS and vesicle cylinders (Self et al., 1996). Further features associated with inflation are also found on the upper surfaces of many sheet lobes; tumuli, lava inflation clefts and lava rise pits are also common (Self et al., 1991; Thordarson, 1995). Occasionally flow tops are clinkery in nature but these are thought to be rubbly pāhoehoe and not 'a'ā (Self, pers. comm., 2004). A vent structure in the Grande Ronde Formation shows possible spatter from Hawai'i-style fire fountaining, shelly pāhoehoe, and a lava

pond (Reidel and Tolan, 1992). Very few further vents have been noted around the CRBG (Thordarson and Self, 1998).

2.4 Previous and current volcanological theories on CFBs

2.4.1 Mode of eruption

It has already been cited (Section 1.2.1) that CFB provinces are the product of large volume out-pourings of (mainly) tholeiitic basaltic magma (Cox, 1980), and that these great volumes of lava are most likely to have been derived from vents or vent systems of considerable size. What form these vents took, either fissures or central vents, is, however, a matter for debate. Fissure eruptions and central vents are both regularly associated with basaltic eruptions, but determining which type commonly supplied the lavas comprising CFBs is difficult. In general, fissure eruptions are more common than central-vent sources (Macdonald, 1972), and occur when magma-filled dykes encounter the surface (Francis, 1993), especially where an area is under extension (e.g., Laki, Iceland, and Kilauea, Hawai'i). There is a sequence in evolution of eruptive style of fissures: the earliest eruption occurs along the whole length of the fissure, forming a 'curtain of fire' many kilometres long, but as the volcanism persists, parts of the dyke can become blocked or enlarged and the activity becomes concentrated at a few points along the fissure; it is at these locations that cones rapidly develop (Francis, 1993 pg. 117).

Central vents or summit eruptions produce material from a single point, which may be made up of a number of closely spaced vents (e.g., Mount Etna, Sicily, and Mount Fuji, Japan). Instead of being fed by a dyke breaching the surface their source is a single conduit which usually directly taps a magma chamber (Francis, 1993). Some authors have suggested that CFBs emanate from central vents (e.g., Agashe and Gupte, 1972), but the majority consider that fissure eruptions are the most likely source (e.g. Walker, 2000).

Modern analogues to CFB eruptions are, perhaps, the Icelandic fissure eruptions such as Laki (1783-84). This was fed by a 25-km-long fissure and produced a flow-field of approximately 15 km^3 of lava. In contrast with most historic lava eruptions, which are <1 km^3 (Self et al., 1998), this is a large volume of lava, but compared to a typical CFB eruption the volume erupted by Laki is at least an order of magnitude smaller.

Locating vents in CFBs has proved to be difficult, I think this is probably because each eruption comes from a different fissure, and thus the lavas formed by each subsequent eruption covers those of the previous ones. The exception is the feeder system and cones supplying the Roza Member of the CRBG (Swanson et al., 1975; Thordarson and Self, 1996; Thordarson and Self, 1998). Subsequent erosion of the upper sheet lobes in a province may rarely reveal vent systems but more commonly feeder dykes are uncovered which either turn into sheet lobes, or are not associated with any surface lobes but have a similar chemistry to observed formations and are thus assumed to be their feeders.

CFBs are also often associated with continental rifting e.g., the Ethiopian Traps, Deccan Traps and the Paraná-Etendeka Province (Courtillot et al., 1998; Jerram and Widdowson, 2005 in press). This may lead to the original vent systems being rifted away from their lava flows, or else being down-faulted and subsequently covered by water or sediment. To date, no vent complexes have been found in the DVP, but dykes, indicative of feeders for volcanic centres, are common along the Konkan Plain to the north of, and around Mumbai and in the Narmada region (Figure 1.2). The majority of the southern region of the DVP, around Mahabaleshwar (Mahabaleshwar) and further south, has no exposure of dykes. The exception is a single dyke which has previously been identified in the area studied during this work, close to the town of Mahad was carried out by Devey (1982) concluded that the dyke fed lavas in the Poladpur Formation. DVP dykes have also been identified beyond the extent of the DVP lavas themselves, in Goa. Widdowson et al.

(2000) presented $^{40}Ar/^{39}Ar$ dates on a series of dykes which where found to post-date the DVP (they have an age of 62.8 $\pm$ 0.2 Ma), yet have a geochemical signature similar to the basaltic lavas forming the Ambenali and Mahabaleshwar Formations They suggested this evidence indicates that Deccan type magmatism continued for a longer time after the KTB than is generally acknowledged.

2.5 Previous and current theories on the volcanology of the Deccan Volcanic Province

2.5.1 Simple and compound flows

As mentioned in Section 2.1, one of the first modern studies on the volcanology of the DVP was carried out by George Walker (1972) and this work was revised in 1999 (Walker, 1999). Using the Deccan as an example, (Walker, 1972) developed a basaltic flow classification of compound and simple flows. Walker (1972) defines compound flows as "those lavas which are divisible into flow-units, commonly have shield-like form, and are thought to develop when the rate of extrusion is low" and simple flows as "lavas which are not divisible into flow units; are thought to develop when the rate of extrusion is relatively high". Walker (1999) suggested that compound flows are formed near to the source of eruption and by implication, become simple flows further from source. Compound flows are made up of a series of small lobes, each surrounded by a glassy selvage and can vary in size from 10 cm to occasionally 10-15 m. The flows themselves (formed of many individual lobes) can be a few hundred metres thick, e.g., Trimbak Hill, (~19°55'N 73°31'E, 30 km west of Nasik, Figure 2.12) is formed of a 150 m thick compound flow (Walker, 1972). The compound flows were thought to be separated from each other by red boles, sedimentary intertrappean beds, or pyroclastic material indicating a pause in lava emplacement, or a much thicker simple lava flow (Deshmukh, 1988). However, Walker (1972) did admit that his 'simple' and 'compound' classification may not be applicable to modern basaltic lavas. He suspected that the terms would be useful in describing outcrops

of limited size (due to dissection of a CFB) but that, in actual fact, if a simple flow was seen in its entirety it would actually be compound in nature. Even so, much of the subsequent DVP volcanological literature has been built upon the descriptions and divisions in Walker's (1972) paper and so his terms have dominated the literature.

Deshmukh (1988) identified a geographical distinction in the occurrence of Walker's (1972) simple and compound two-fold division of lava flows. In the older, north western area of the MDP, the volcanism is dominated by compound flows (i.e., small (10^{-1} m-10 m) inflated pāhoehoe lobes). In the remaining areas of the DVP, the Mandala lobe, Kutch and the Malwa Plateau (Figure 1.2) are dominated by simple flows (i.e., thick (~20 m) inflated pāhoehoe sheet lobes; Figure 2.9). The thick, simple flows to the south and east of the MDP are demonstrably younger than the thinner units which form compound flows to the north. From this it is commonly believed by many workers on the DVP that the source vents of the DVP must have occurred in the area which is dominated by compound flows (Figure 2.12).

The results of this thesis agree with Walker's (1972) idea that all simple flows are in fact compound in nature. The terms 'compound' and 'simple' are therefore avoided during this work. Instead the terms, flow-field, lava-flow and flow-lobe (Section 2.2.1. Self et al., 1997) are preferred. It is hoped that this work will help pave the way for the abandonment of the terms 'simple' and 'compound' flows.

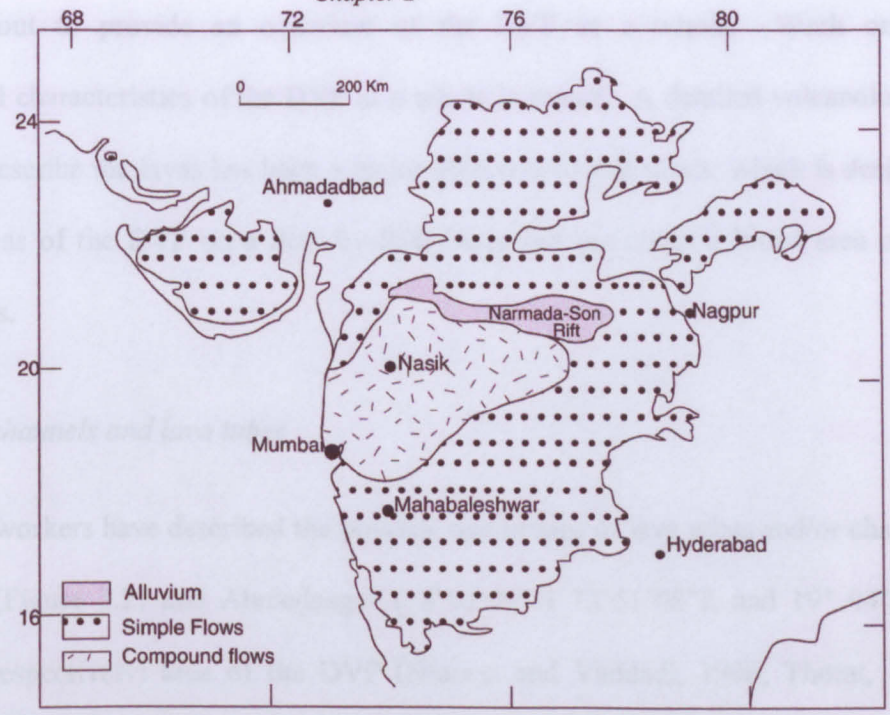

Figure 2.12. Map of the Deccan volcanic province indicating the areas dominated by so-called simple and compound flows (after Deshmukh, 1988).

One of the first attempts at a stratigraphy not based solely on geochemistry was proposed by Godbole et al. (1996), as given in Table 2.2. This study was based in the western DVP, encompassing the whole length of the Western Ghats to the western Narmada-Son Rift and was based upon the attempted correlation of various megacryst-bearing sheet lobes in adjacent lava piles and the occurrence of simple and compound flows throughout the exposed lava pile. Although Godbole et al. (1996) noted the complexities of creating a volcanological stratigraphy, due to erosion, regional dip, topography and the lateral pinching out of flows, they still claimed to have created a reliable stratigraphy over the DVP (Table 2.2). However, the hierarchy of their divisions is often inconsistent. For example, their megacryst horizons 1-4 sometimes mark a formation boundary, and sometimes a sub-group boundary. No information is given about where the 'type sections' for these divisions occur, and it seems questionable whether the authors are certain that they are observing the same megacryst horizons throughout the DVP or even over the smaller region of the Western Ghats Escarpment. Godbole et al. (1996), does not attempt to identify the products of single eruptive events largely because much of the work

was carried out to provide an overview of the DVP as a whole. Work on the volcanological characteristics of the DVP as a whole is scarce. A detailed volcanological approach to describe the lavas has been a major objective of this thesis, which is designed to look at areas of the DVP on a flow-by-flow basis and yet cover a broad area of the Western Ghats.

2.5.2 Lava channels and lava tubes

A number of workers have described the possible occurrence of lava tubes and/or channels in the Pune (Figure 2.2) and Ahmednagar (18°03'09"N 73°51'08"E and 19° 04'36"N 74°47'05"E respectively) area of the DVP (Sharma and Vaddadi, 1996; Thorat, 1996; Misra, 2002), but the descriptions and arguments outlining the identification of these features is often unclear. Crucially, these papers fail to mention inflation as a means of forming flows and, as such, only mention the possibility of tubes forming due to the roofing-over of leveed lava channels, rather than as part of the internal structure of an inflated pāhoehoe sheet lobe, or flow-field, where levees would be absent. Frequently the tubes and channels mentioned appear to be too wide (30-60 m) to be the feeders for relatively small flow lobes (5-10 m thick, Sharma and Vaddadi, 1996) and there is no evidence for vents nearby which the lava channels could be proximal to, before supplying inflating sheet lobes further away.

If a flow-field was erupted onto a level, or very low-angle, surface any lava tubes would have remained filled after the eruption ceased and the lava solidified (Peterson and Swanson, 1974). If this is the case, it can be almost impossible to identify ancient 'lava tubes' in older basalt lava flow sections. However, if the flow-fields are on a steeper angled surface the lava tends to drain from them when the supply of lava ceases (Peterson and Swanson, 1974) thus preserving an empty or partially filled tube (Figure 2.13).

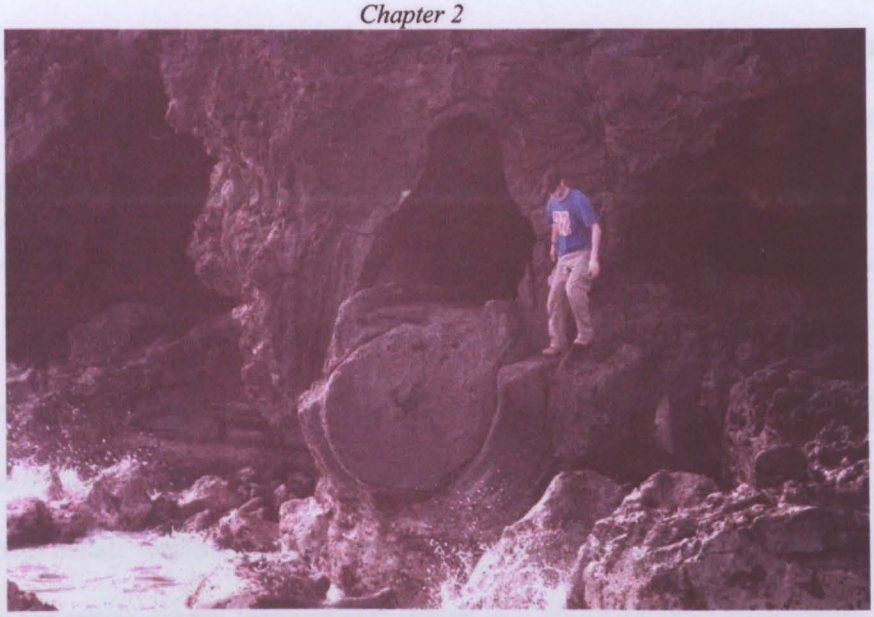

Figure 2.13. Photograph of a partially drained lava tube within a pāhoehoe flow-field on the Big Island, Hawai'i, taken during fieldwork in 2002. No tubes were identified during fieldwork in the DVP, possibly because the original angle of depositional dip on the DVP, in general, was too shallow and the tubes did not drain. Alternatively, there was little or no tube development. Lat. long. unavailable

2.5.3 Weathering horizons

Flow tops which underwent weathering during a hiatus in volcanic activity commonly occur in the upper section of the DVP, particularly in the Wai Sub-group, but less so in the older lavas, such as those of Matheran Ghat. These weathering horizons are usually red in colour, but occasionally green-grey material is found, which may be the result of local penecontemporaneous oxidation. The term commonly used in the DVP for these weathering horizons is 'boles'. Boles should not be confused with laterites, as they have markedly different physical and chemical characteristics.

Laterites typically display pisolitic or vermiform textures (Widdowson et al., 1997) and a well-defined division or layering due to the presence of a water table during their formation. A complete laterite profile is approximately 10-20 m thick. Boles on the other hand are much softer, more friable and thinner, with a maximum thickness of ~2 m. although are more usually 10 cm to 1 m. Widdowson et al. (1997) describe a laterite as a 'super-bole' and states that a bole is formed contemporaneously with the eruption of the CFB, whereas a laterite horizon is a weathering horizon, the development of which

continues uninterrupted after all the eruptions have ceased. Widdowson et al., (1997) divide the types of boles that are found in the DVP into two types. The first, and probably most common, are termed 'saprolitic' boles (a saprolite being totally decomposed material formed from the chemical weathering of a rock). In the lavas I studied, saprolitic boles are the whole weathering profile down through the upper surface of a sheet lobe. The upper section consists of a portion of fine grained clay or silty material, the saprolite, which gradually grades down through an apparently rubbly section into fresh basalt. The process by which the basalt weathers causes small semi-round masses (or clasts) of fresh basalt (similar to the much larger 'corestones' which are found in the spheroidally weathered cores of sheet lobes) to remain below the upper, fine grained saprolite. These are surrounded by soft red clay or silt material, called in this thesis saprolitic material, which gives the impression of a rubbly flow top (Figure 2.14) but which is actually formed by the progressive weathering of the basalt (Figure 2.15) (M. Gerard and E. Frisch, 2003). The bole material can retain relics of its original structure, such as amygdales, vesicles or pseudomorphed phenocrysts (Widdowson et al., 1997). The length of time taken for these to form is unsure but may form from weathering of an exposed flow top over tens, hundreds or thousands of years. The pure saprolite section of a bole is not present on all boles.

The second bole type, named as 'cherty boles' by Widdowson et al. (1997), contains abundant glass shards and crystal fragments; these boles are often brittle. They are thought to form from a weathered blanket of pyroclastic material, and their brittle nature may indicate original welding of the pyroclastic material. A second characteristic is that they appear to rest directly upon relatively fresh basalt and have no or little progressive weathering profiles beneath them (Widdowson et al., 1997).

Figure 2.14. The 'green' bole on Ambenali Ghat at 1090 m asl in the Transitional, Mahabaleshwar - Ambenali formation, showing ~10 cm of saprolite on top of what appears to be a rubbly flow top, but is in fact the weathering profile (see Figure 2.15 below). Lat. long. 17°55'00.0"N 73°37'32.9"E.

Figure 2.15. The 'green' bole on Ambenali Ghat having been 'cleaned' of all modern weathering, showing a transition from a dark saprolite at the top, through the weathering profile (1-6) to solid but altered basalt at the base; length of extended tape 2 m. 1) Compacted yet friable, fine-grained grey green material, 2) less compacted with a few basalt clasts grey green material, 3) phantom basalt clasts up to 30 cm surrounded by a clay matrix, whole section dark grey in colour, 4) sharp colour boundary between this section and section 3 caused by secondary alteration, contains clasts between 5 & 15 cm, some of which cross the colour transition between section 3 and 4; light olive brown, 5) diffuse transition between 4 & 5, sub-rounded to sub-angular altered basaltic clasts between 1-10 cm, matrix is yellowish brown in colour, 6) altered basalt dark brown in colour. Lat. long. 17°55'00.0"N 73°37'32.9"E

The chemical differences between laterites and boles are marked. Laterites show a significant enrichment in aluminium and iron and a depletion in silica, on average: Al_2O_3 37%, Fe_2O_3 52% and SiO_2 7% compared to bole averages of: Al_2O_3 17%, Fe_2O_3 18% and SiO_2 53% (Widdowson et al., 1997). There is also an important difference in chemistry and isotopic signature between saprolitic boles and cherty boles. An example of a cherty

bole from Widdowson et al. (1997) has a SiO_2 composition of almost 68%, much higher than that of the original basaltic flow below it. These cherty boles are thought to form from explosive eruptions where the magma chemistry is more evolved. Compare this to a saprolitic bole, SiO_2 48% which has the same silica content as the basaltic average.

2.5.4 Previous work on DVP inflation features and theories on their origin

Small scale features

Recent work has been carried out in the DVP investigating the small-scale volcanological features of the DVP. Tumuli have been described (Figure 2.16) in the Pune (Figure 2.2) and Dhule (20°54'07"N 74°46'15"E) areas of the Western Ghats by Duraiswami et al. (2001; 2002). Tumuli are associated with inflated hummocky pāhoehoe flow-fields in Hawai'i and, as those described in the DVP are similar, it is assumed that tumuli described by Duraiswami et al. (2001; 2002) form hummocky pāhoehoe flow-fields as well. The tumuli described by Duraiswami et al. (2001, 2002) are found in an area that is dominated by small inflated pāhoehoe lobes (also termed compound pāhoehoe in Duraiswami et al. (2001, 2002)) and are described in conjunction with other inflation-induced features such as squeeze ups, and vertical and horizontal grooves, relating to tumuli formation (Duraiswami et al., 2002).

Evidence of flow inflation

Although the possibility of applying the theory of inflation to the DVP was considered by Keszthelyi et al. (1999), Bondre et al. (2000) were the first to undertake field investigations into inflation features in the DVP, such as HVS, HVZ, and pipe vesicles. Further work involved a more detailed study of the lava units, features seen and their interpretation (Bondre et al., 2004). Bondre et al. (2004) looked at the basalts in two different areas of the DVP (Figure 2.12), defined in Deshmukh (1988).

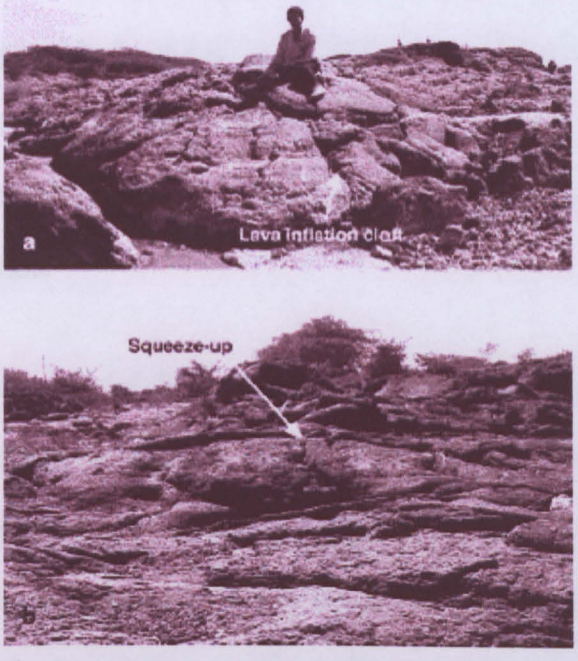

Figure 2.16. Small-scale tumuli near Daunde (18°26'05"N 74°33'37"E) in the Thakurvadi Formation; a) shows a small tumulus on the end of a flow lobe about 8 m across; b) shows a very low profile tumulus, about 10 m in length with a squeeze up between a single axial cleft. (From Duraiswami et al., 2001)

In the compound flow zone, described by Deshmukh (1988); (Figure 2.12), Bondre et al. (2004) confirm much of the previous work concerning the volcanic structures and characteristics of the lavas and conclude that the units were formed by inflation, as they contain all of the 'classic' indicators: a three fold division of the lobe into basal crust, core and upper crustal zone (Section 2.3.2) and features such as HVS, HVZ, pipe vesicles, surface rope structures and tumuli (Section 2.2.2). The authors suggest that the great size and length of these flow-fields is achieved by interconnecting and overlapping lobes which form an anastomosing system rather than by well-defined tubes. The thicker flows (referred to as 'simple' flows in much of the published literature) in the remainder of the DVP have previously been described as 'a'ā flows (Godbole et al., 1996; Raja Rao et al., 1999), yet Bondre et al. (2004) disagree with this because the lava units do not have flow-bottom breccias, entrained clinker or ragged vesicles (Section 2.2.2). Bondre et al. (2004) reject the theory proposed by Shaw and Swanson (1970) that the lava was emplaced as turbulent sheets. They also dismiss inflation as a method of formation, citing rubbly flow

tops and a lack of features consistent with inflation. The only method offered for the formation of such thick flows is ponding in depressions of pre-eruptive topography, but it was noted that it is impossible for this to occur higher up in the sequence, due to the entire pre-eruptive topography having been covered by earlier lava. The features observed during my fieldwork in the DVP show, indeed, that the lava units are sheet lobes formed by the process of inflation.

Despite the majority of the previously published DVP literature claiming that there is a lack of evidence for inflation being the mode of emplacement for the thicker units in the DVP, during this study many inflation related features were observed. This work aims at demonstrating categorically that the majority of the sheet lobes encountered during the field work for this study are inflated pāhoehoe. The next section describes all the field observations made, which demonstrate this fact.

2.6 Volcanostratigraphic logs constructed along road sections of the Western Ghats

A considerable portion of the field effort of this thesis work was directed towards producing detailed volcanological logs of classic Ghats sections. These logs aim to convey key features of the lava which aid in determining flow type due to the presence of internal and surface volcanological features, such as smooth to ropey surfaces, jointing, tumuli, HVS and HVZ. The descriptions with the logs do not aim to describe everything seen along the section; they should be read in conjunction with the individual log (Appendices A1-A7,) that the text describes.

Sections on the logs are divided into 'good exposure', 'poor exposure' and 'no exposure'. The zones covered by the latter two are indicated by faint dashed lines with either P/E or N/E between them. Poor exposure (P/E) is defined as a section along which ither the rock is highly weathered and in which it is therefore difficult to identify the

volcanological features, or an area where there are small sporadic outcrops, which are too small to log individually or combine into a meaningful interpretation. No exposure (N/E) is a section where no rock is exposed at all, and in which it is not possible to identify any original features.

Traverse	Length of road logged km	Vertical height of section, m	Elevation at which traverse commences and terminates, m	Formations encountered	No. thick sheet lobes or groups of small lobes	% of Good Exposure	% of Poor Exposure	% of No Exposure
1) Ambenali Ghat	~36	1235	21-1256	Bushe, Poladpur, Ambenali, Mahabaleshwar	~52	47	23	30
2) Tapola Road	15	563	687-1250	Ambenali, Mahabaleshwar	~18	45	23	32
3) Kelgar Road	~8	455	770-1225	Ambenali, Mahabaleshwar	~27	86	6	8
4) Wai-Panchgani Road	~9	450	769-1220	Ambenali, Mahabaleshwar	~20	73	27	0.1
7) Varandah Ghat	~15	572	10-582	Bushe, Poladpur, Ambenali,	~16	60	9	31
5) Khumbarli Ghat	~10	580	120-700	Ambenali, Mahabaleshwar	~28	54	40	6
6) Matheran Ghat	~16	632	50-682	Neral, Thakurvadi, Bhimashanka, Khandala	~34	68	7	25

Table 2.3. Information on each traverse logged during this study. For a map of the traverses see, Figure 2.1 and Figure 2.2

In order to try to better constrain the elevations during logging and to rule out barometric altimeter drift and calibration variations, a Static GPS survey was undertaken (Appendix D1 for methods). Due to the large number of flow boundaries encountered during field work, each one could not be surveyed, so measurements were taken at key, easily identifiable locations on the four traverses around the Mahabaleshwar Plateau (Figure 2.2; e.g. gps-X1,2,3... Appendices D2). This GPS survey provided a hitherto unattainable degree of precision and accuracy (in both the x, y and z) regarding formation boundary and palaeomagnetic reversal horizon elevation for the Mahabaleshwar Plateau. This gave accurate tie-point elevations to which the key locations on the logs could be anchored, and the remaining sections were either stretched or compressed to accommodate these fixed locations.

The traverses may be summarised as follows (Figure 2.2 and Figure 2.1 for the locations):

1) Road section from Poladpur bridge, (17° 58' 40.5"N - 73° 28' 14.8"E) 22 km WNW of Mahabaleshwar town, to the final exposure below the Mahabaleshwar Plateau.
2) Road section from the first exposure after the village of Tapola (17° 45' 56.2"N - 73° 44' 24.9"E north Koyna Reservoir) 16 km SSE of Mahabaleshwar town, to the final exposure below the Mahabaleshwar Plateau.
3) Road section from the village of Kelgar (17° 51' 50.4"N - 73° 45' 28.5"E) 15 km SE of Mahabaleshwar town, to the final exposure (17° 53' 21.6"N - 73° 43' 32.4"E), 7 km SE of Mahabaleshwar town.
4) Road section, from the first exposure after Panchgani (17° 56' 05.4"N - 73° 49' 0.8"E), to 2 km W of Wai (17° 56' 29.22"N - 73° 52' 08.7"E).
5) The road section from the first exposure along Varandah Ghat 15 km E of Mahad (Figure 2.1), 18° 05' 56.2N - 73° 30' 56.1"E) to the Ghat crest (18° 07' 43.5"N - 73° 36' 26.7"E), 4 km SE of Varandah.
6) Road section from, 7 km SE of Chiplun (Figure 2.1, 17° 25' 55.3"N - 73° 39' 12.1"E) to 100 m short of the ghat crest (17° 23' 45.5"N - 73° 40' 08.2"E), 15 km NW of Helwak.
7) Road section from the first exposure after Neral (Figure 2.1, 19° 01' 04.2N" - 73° 18' 54.0"E) to the last exposure, on the metalled road, before Matheran (Figure 2.1, 19° 00' 06.3"N - 73° 17' 02.7"E).

Chemostratigraphy (Table 2.1) is the only currently effective method of dividing the DVP lava succession and is discussed in detail in Chapter 4. It is used in this section to provide a framework in which the new volcanological detail may be described. Samples, mainly in the form of palaeomagnetic drill cores, were taken from almost every sheet lobe encountered. X-Ray fluorescence (XRF) analysis (Appendix C) was also undertaken so that each sheet lobe could be assigned to a formation using the four criteria (Table 4.4) laid

down in Devey and Lightfoot (1986). This has provided two new key advances. First, it is now possible to test if there is any volcanological change coinciding with change in chemistry, and second, it is possible to identify the exact flow tops and flow base which mark the formation boundaries. The basalts studied in this work were found to lie within the Wai Sub-group and the Bushe, Neral, Thakurvadi, Bhimashankar and Khandala Formations (Table 4.4 and Table 2.3), although in some cases a formation could not be assigned uniquely. This is especially the case for the upper parts of the four Mahabaleshwar Plateau traverses which have a geochemical signature that appears to be a mixture between Mahabaleshwar and Ambenali Formation chemotypes and also pure Ambenali Formation. This is further discussed in Chapter 4.

The logs are presented in segments divided on three criteria; the formation (chemotype), flow-fields, and elevation. Each elevation segment described, which is based on variable exposures, does not cross a formation or suspected flow field boundary, but may contain more than one flow-field. Each log is colour-coded to indicate the chemostratigraphic formations. The location of the samples collected and the high precision GPS data are also marked.

Four logged sections ascend the Mahabaleshwar Plateau (Figure 2.2) on the west, south, south-east and eastern sides of the Plateau. Only the westerly, Ambenali Ghat, ascends the full height of the Western Ghats Escarpment ~ 20 to 1400 m. The remaining three climb from the elevation of the Maharashtra Plateau (~600 m) up the slopes of the Mahabaleshwar Plateau, but terminate (at ~ 1200 m) before the summit (~1400 m) due to poor exposure and lateritization of the lavas. Thus the topmost 150-200 m is unexposed (Widdowson and Cox, 1996).

The mineralogy of the basalts is briefly discussed in this section, and it must be noted that the percentage values given for various mineral types is the percentage by volume.

2.6.1 *Ambenali Ghat,*

- *Log Appendix A1*
- *Geochemical data Appendix C2*
- *Palaeomagnetic data appendix B2*
- *Static GPS data Appendix D2*

The section starts at 20 m above sea level (asl), 1 km east of Poladpur (Figure 2.2., 17°58'40.5"N - 73°28'14.8"E), and the highest exposure is observed at 1253 m (17°56'27.9"N 73°38'08.3'E). The highest point on the Mahabaleshwar Plateau is Wilson Point (1436 m), thus between 160 and 200 m (this variation is due to the uncertainty in the precise position of the anticline in relation to the final logged point and the unreliability of the regional dip over small areas (Section 4.6.1)) is unexposed or covered with thick laterite (Widdowson, 1990).

Bushe Formation succession

Elev. 20-37 m asl

The section starts adjacent to a bridge over a Savitri River tributary at their confluence, and close to the town of Poladpur. Here gps-AG1, the first static GPS reading was taken in order to ensure more accurate elevations for this and future work. The exposure is approximately 6 m thick and consists of pāhoehoe lobes 10 cm-2 m thick; it is part of a typical multi-lobe pāhoehoe flow-field. Small break-out lobes occur on top of some of the sheet flow lobes (Figure 2.17, Figure 2.18); ropey flow tops and pipe vesicles are also common, although there are no visible tumuli. Palaeoflow direction from ropey flow tops is ~240°, but this is an unreliable indication of flow direction (pg. 134), but does correspond to the slightly more reliable palaeodirections taken on Varandah Ghat (pg. 103). The basalt is aphyric but not glassy. These basalts have a reversed magnetic polarity which places them in chron 29R. The geochemical characteristics obtained during this study (Appendix C1), and by Devey and Lightfoot (1986), suggest that these flow lobes

belong to the Bushe Formation, but they have some Poladpur Formation characteristics. The top of this exposure (at road level) shows a slightly thicker and more extensive sheet lobe, minimum 4 m thick, with an unexposed top, but it has pipe vesicles at the base. This flow-field would be considered to be a typical compound pāhoehoe flow in the Bushe Formation, using Walker's (1972) terminology.

Figure 2.17. Pāhoehoe ropes on upper surface of a small Bushe Formation pāhoehoe lobe, possibly a break-out from the top of a thin sheet flow lobe, at the bridge near Poladpur. Lat. long. 17°58'40.5"N 71°28'14.8"E

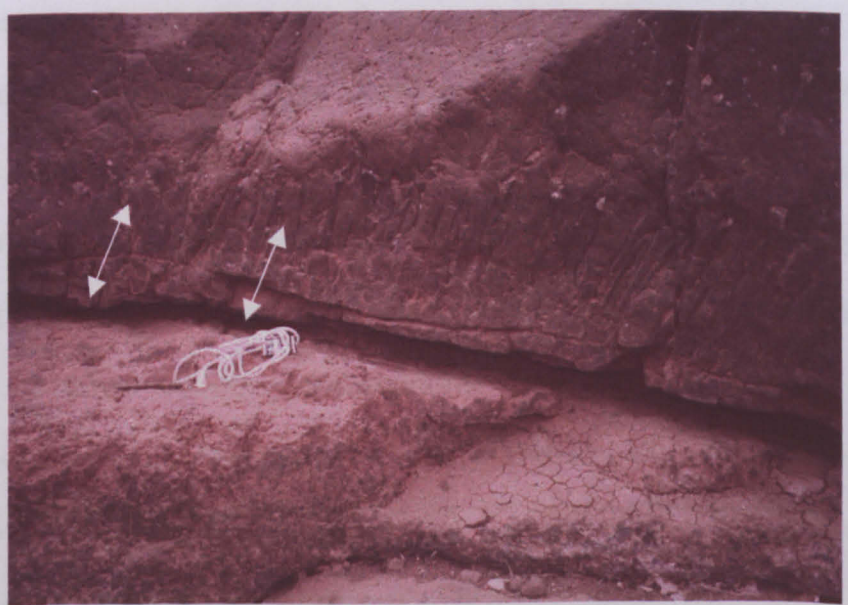

Figure 2.18. A lobe 30 cm thick below the bridge near Poladpur, showing well developed inclined pipe vesicles. Scale indicated by hand lens. Lat. long. 17°58'40.5"N 71°28'14.8"E

Poladpur Formation succession

Elev. 60-82 m asl

The next exposure consists of three partially exposed units at 62, 68 and 80-82 m. Each one is part of the core of separate sheet flow lobes. All contain plagioclase crystals no bigger than 5 mm; the upper unit has 5 mm plagioclase glomerocrysts and weathered pyroxene crystals. The middle unit occurs in the dry stream valley at Karpurda village (Figure 2.2, lat. long. 17°58'29.9"N 73°28'55.6"E) and contains sub-horizontal columnar joints, possibly indicative of water cooling. It is not possible to tell if these three exposures are part of the same flow-field (i.e., multiple eruptive units form the same eruption; Section 2.2.1) or if they are parts of separate eruptions, or one sheet flow lobe, but the former is thought to be the most probable. The geochemistry places these outcrops in the Poladpur Formation and this agrees with previous work (Devey and Lightfoot, 1986). Accordingly, the Bushe-Poladpur Formation boundary must therefore lie between 35 and 62 m; the boundary is positioned at 50 m in this section according to Devey and Lightfoot (1986).

Elev. 82-252 m asl

Between 82 and 252 m the flows are poorly exposed. It is not possible to determine the number of sheet flow lobes or their average thickness. Each exposure, especially a prominent one at 150-156 m, appears to be part of a sheet lobe core, displaying typical characteristics of wide columnar joints, HVS and vesicle cylinders up to 10 cm thick. Plagioclase glomerocrysts and plagioclase laths are seen in some of the outcrops. Other lavas are aphyric and their overall coarseness is variable as well. These observations lead to the conclusion that they are probably from different sheet flow lobes and possibly different flow-fields. All the outcrops show characteristics which suggest a continuation of the sequence of Poladpur Formation pāhoehoe sheet flow lobes below.

Elev. 252-277 m asl

Exposure improves above 252 m, where a group of aphyric sheet lobes, is visible. They have HVZs in the upper crustal zone, HVSs and vesicle cylinders in the core, and columnar joints with small prismatic joints perpendicular to the main set, which may indicate water-induced cooling. These units make up the top two of a flow-field whose upper boundary is at ~277 m and is marked by a HVZ. The actual contact is poorly exposed and is not marked by a bole, but can be assumed due to a marked change in petrography across the boundary from aphyric basalt to basalt with 1-2 cm blocky plagioclase with some laths, and possibly, altered pyroxene.

Elev. 277-333 m asl

From 277-299 m there is a single 20 m thick pāhoehoe sheet flow lobe with HVZ at the top and a poorly exposed bole. Using the terminology of Walker (1972) this would be described as a simple flow, (i.e., one flow lobe constituting a single flow-field). This unit has many of the features typical of sheet lobes in the DVP. The core contains straight and hackly columnar joints, vesicle cylinders and mega-vesicles at the core-upper crust boundary. Although the flow top is poorly exposed it appears to be typical with hackly joints, a HVZ, and is topped by a 10 cm-thick saprolite i.e., bole at 298 m. The sheet flow lobe above is thin, only 8 m thick. Its core is not exposed but the upper part of the upper crust is, where it is topped by a 30-cm-thick bole which contains a few basaltic clasts.

Another thin flow-field, the majority of which is not exposed, is seen from 299-306 m. The final exposure in the Poladpur Formation is an approximately 25 m thick section of a sheet flow lobe, showing characteristic features, although the upper section of the upper crustal zone is obscured by a section of poor exposure.

Ambenali Formation succession

Elev. 333-367 m asl

Above the obscured flow top at 333 m is a group of lava units 34 m thick, which may form a flow-field as it is topped by a pockety red bole at 367 m. This may be a continuation of the flow-field which started at the 307 m asl bole, but it is impossible to tell because the section from 333-367 m was not sampled so it is not possible to determine the geochemistry and assign a formation. The flow core terminating at 333 m is thus the uppermost proven exposure of the Poladpur Formation in this traverse. Thus it can be assumed that the Poladpur-Ambenali Formation boundary occurs in this section and so these are either the first sheet flow lobes in the Ambenali Formation or the final sheet lobes in the Poladpur Formation. The flow-field is probably formed of three to four superimposed sheet flow lobes. Each of the exposures here contains plagioclase, although the morphology and percentage of the crystals varies. Weathered and altered pyroxenes 1-2 mm are seen in all the outcrops.

Elev. 367-429 m asl

A 30 m thick sheet lobe starts at 367 m. Its flow top is not visible but the HVZ in the upper crust is recognisable. The lava contains 5% of 5 mm plagioclase glomerocrysts. This is overlain by another 30 m thick sheet flow lobe, with 10% of 5-10 mm plagioclase crystals. The unit is poorly exposed, but it has a recognisable HVZ in the upper crust and is topped by a thin red horizon within modern soil at 429 m. These two sheet flow lobes form one flow-field as they are bounded top and bottom by red boles and geochemical analysis reveals that they are indisputably in the Ambenali Formation (Appendix C1).

Elev. 429-461 m asl

Continuing up through the Ambenali Formation, the next flow from 429-461 m is a single sheet flow lobe and flow-field totalling 33 m thick. It is poorly exposed, but

displays occasional columnar jointing in the core and its upper crust has a HVZ. The basalt contains 3-4% of 5 mm plagioclase and pyroxene glomerocrysts.

Elev. 461-497 m asl

At 461-497 m, there is one or two sheet flow lobes forming a flow-field. The exposure is poor but some typical lava core features are visible in the lower section, which contains 5-10% of 1 cm plagioclase glomerocrysts. The flow-field is capped by an undulating reddened flow top with red saprolite material in the depressions. Amygdales up to 10 cm are visible below the bole, and were presumably part of a HVZ.

Elev. 497-556m asl

The following 56 m, from 497-556 m, are formed by three sheet flow lobes which, each form a flow-field as they are bounded by reddened flow tops and boles with red saprolite upper horizons. The lower two boles undulate, probably due to break-out lobes on the top of the main sheet flow lobe. The bole at 530 m is 1 m thick and rubbly with a 15 cm saprolite. It is exposed on a sharp bend in the road so is easy to locate; this was chosen as GPS site gps-AG2. The flow top at 553 m, however, is only reddened and does not show any saprolite. The lower two sheet lobes have poorly exposed cores but it is possible to determine the crystal content; the lowest flow contains 1-2% of 6 mm plagioclase glomerocrysts. The middle flow lobe has up to 5% of 7 mm diameter plagioclase glomerocrysts. The upper of the three is well exposed and shows blocky plagioclase crystals up to 1 cm. A possible vesicle cylinder was observed as were highly vesicular, brecciated, amygdaloidal masses of lava in too poor a state of preservation to be able to interpret an origin.

Elev. 553-612 m asl

Immediately above the reddened flow top at 553 m is a series of amygdaloidal, 1-2 m thick precursor, basal lobes all welded together. Above this is an 18 m thick sheet

flow lobe with another vesicular amygdaloidal mass, otherwise the core is featureless. This sheet lobe passes up into a series of centimetre to 10 m thick pāhoehoe lobes that are welded together without passing through any obvious boundary at 573 m (Figure 2.19). The small lobes show the typical features expected of thin, so-called compound lobes but they are part of a flow-field that also contains sheet lobes. Up to 586 m the lobes have a medium-grained groundmass with 4-5 mm glomerocrysts of plagioclase and weathered pyroxene crystals. Above this, to 612 m the exposure becomes poorer but the basalt persists in bearing plagioclase crystals, which have an acicular habit and are up to 3 mm long. The lava at the top of this sequence contains 35% blocky plagioclase (up to 1 cm long, therefore a GPB) in a poorly vesicular flow top capped by a 10-cm-thick saprolite at 612 m asl. This sheet lobe may be genetically linked to the next set of units, considering its high plagioclase content, but it is certainly the product of a different eruption, as there is a red bole between them.

Figure 2.19. A small vesicular lobe, 10 cm thick with a reddened outer selvage of altered glass. Part of a series of small lobes and toes observed between 570 and 580 m asl in Ambenali Ghat Formation. Lat. long. 17°56'05.9"N 73°33'53.7"E. Hammer 36 cm

Elev. 612-682 m asl

At 612 m, possibly the first of four 'giant plagioclase basalt' (GPB) sheet lobes is observed (Figure 2.20). They contain 25-30% of 1-2 cm plagioclase crystals in a fine-grained groundmass. These four sheet flow lobes are part of one flow-field. All four flow lobes show similar characteristics to the inflated sheet flow lobes lower down in the sequence. The fourth flow lobe is topped with an amygdaloidal flow top and break-out lobes, these are the cause of the undulatory nature of the pockety bole at 682 m. The saprolite within the pockets is up to 15 cm deep with a further 20 cm of red weathered material below this.

Figure 2.20. The first of four GPBs on Ambenali Ghat at ~620 m above sea level. The exposure is highly weathered but the plagioclase crystals can be seen as cream marks on the fresh surface. Lat. Long. not available. (Photo by S. Self)

Elev. 682-705 m asl

Above the 'pockety' red bole is a series of small precursor lobes containing 10% of 1 cm long plagioclase crystals. The main sheet lobe of this flow-field contains only 2% of 0.5-1 cm plagioclase, it is spheroidally weathered but some poorly visible columnar

joints are present. This indicates that there can be subtle changes in crystal content between lava units in the (presumed) same flow-field.

At 693 m the dense sheet lobe appears to terminate abruptly in a thick red cherty bole up to 70 cm thick. This is the famous 'Big Red Bole' which is so often seen in images of the DVP (Figure 2.21) and is the location of gps-AG3. It is visible at around road level for ~ 2 km, where it shows variations in thickness and relationship to the flow below, along its length. In some places it appears as if the vesicular flow top has been removed and the bole lies directly on the flow core, yet in others the saprolite grades down into weathering profile of the sheet flow lobe. The bole contains unidentified crystals (i.e., presumed to be from the GPB beneath) and what appears to be lithics up to 5 mm but the average is approximately 1-2 mm.

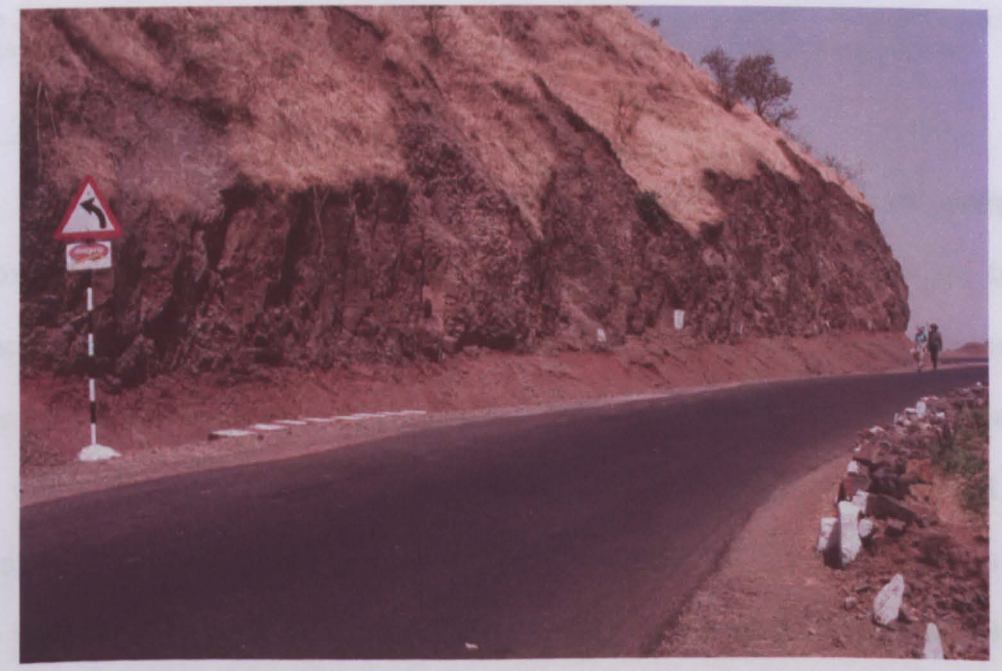

Figure 2.21. The 'Big Red Bole' on Ambenali Ghat. Up to 70 cm thick, the bole can be traced for ~2 km as the road has been cut into the cliff at bole level. Found in the Ambenali Formation at 693 m asl. Lat. long. 17°57'03.07"N 73°35'00.19"E. (Photo by S. Self)

Directly above the Big Red Bole, at 694 m, are a number of small vesicular lobes and toes, probably precursor lobes to the 11 m thick sheet lobe which terminates at 705 m, with a poorly exposed 10-cm-thick red bole (Figure 2.22).

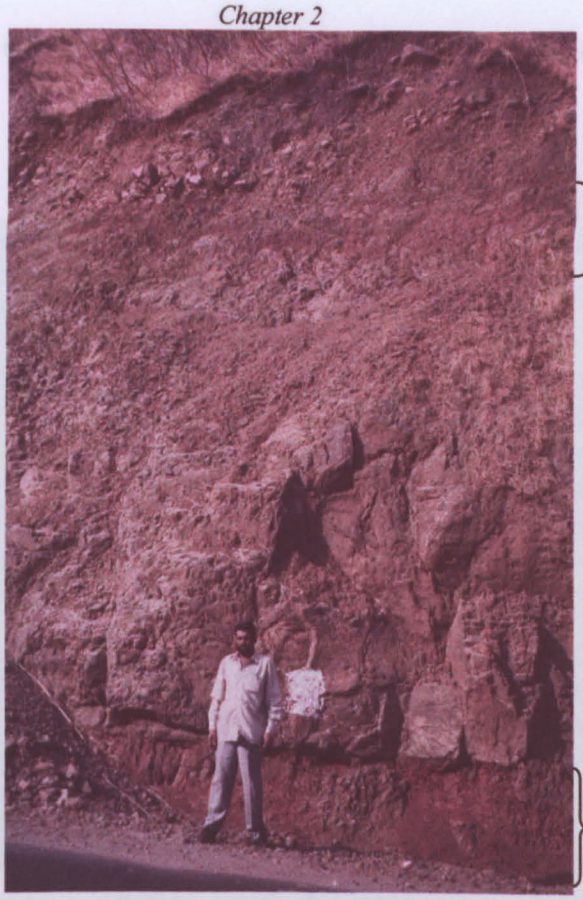

Figure 2.22 Lower red bole is the 'Big Red Bole' on Ambenali Ghat approximately 10 m above is a thinner less discreet red bole, indicating that the sheet lobe between is a single flow-field. Lat.long.unknown

Elev. 705-784 m asl

This 79 m thick flow-field is composed of aphyric basalt and comprises approximately four sheet flow lobes of varying thickness. Each contains the typical characteristics of a sheet flow lobe. At 778 m the basalt sequence is eroded out as the road enters the Koyna River valley at the location of Ambenali Pass. It then descends into the river valley where the exposure is poor. Once back at the height of Ambenali Pass, logging of the road cut is again possible and the assumption had to be made that this is the same flow-field, if not the same flow lobe. The flow-field terminates at a thin reddened flow contact at 784 m.

Elev. 784-922 m asl

Above the red contact is a series of small basal lobes 1-3 m long and ~2 m thick. They show stretched surface vesicles typical of those seen in the top of the upper glassy

selvage of the crust of small Hawaiian lobes, but no evidence of glassy lava remains (Figure 2.23).

Figure 2.23. Stretched vesicles on a flow top but the glass has been removed. At ~785 m asl in Ambenali Formation, on Ambenali Ghat. Arrows indicate vesicle elongation direction. Lat. long. 17°56'00.7"N 73°37'05.9"E

Above the lobes is a small section of aphyric flow core, the top of which is not exposed due to a 40 m section of no exposure. Immediately above this is a thin red flow top at 837 m; the weathered rock below contains scattered 1 cm plagioclase crystals. This section is probably one flow-field but the number of sheet flow lobes cannot be determined. Above this are two further flow-fields, both poorly exposed and composed of a poorly phyric lava. The first is topped by a hard 10 cm thick saprolite (at 879 m) and the second (at 922 m) by another 10 cm saprolite.

Elev. 922-934 m asl

From 922-965 m the exposure is poor but basalt with semi-horizontal columnar joints is visible at 925 m, although, due to poor exposure, the flow top of this sheet lobe is not observed.

Elev. 934-965 m asl

There is a change in geochemical lava type from Ambenali to Mahabaleshwar Formation at ~934 m, although the precise flow contact was not identified in the field due to poor exposure. At approximately 953 m an outcrop of basalt with 30% of 1 cm plagioclase was observed in a temporary roadside trench; it is not seen in normal exposure conditions. A thin red bole is exposed at 965 m (Figure 2.24); it is determined by this work to be at the palaeomagnetic reversal horizon 29R-29N. The high precision static GPS reading gps-AG4 was taken at this red bole.

Figure 2.24. Thin red bole which is thought to coincide with the palaeomagnetic reversal between 29R and 29N at 965 m asl, on Ambenali Ghat, Mahabaleshwar Formation; position of GPS AG4. The exposure is poor and the rock is highly altered. Lat. long. 17°55'41.6"N 73°37'45.0"E

Elev. 965-1020 m asl

The next flow-field is identified from 965-995 m. The units grade from basalt containing 8-10% small plagioclase crystals and some glomerocrysts in the lower part of the flow-field (where it is poorly exposed) to aphyric in the upper sheet flow lobes. The bole at 995 m is a thin red horizon, probably composed of rotten flow top glass. Above this flow-field (995-1020 m), is a single sheet flow lobe 25 m thick which contains 8-10%

small acicular plagioclase crystals and some glomerocrysts 5 mm across. This single unit is equivalent to one flow-field.

Elev. 1020-1024 m asl

A thin flow-field (1020-1024 m) is bounded top and bottom by undulating saprolitic boles which can be difficult to follow due to the winding road cutting. The lower bole has a 5 cm saprolite grading into a 60 cm thick weathering profile below. The flow-field is formed from a number of small, weathered, 0.5 to 2 m thick inflated pāhoehoe sheet flow lobes, although it is dominated by one 2-m-thick sheet flow lobe. It contains 15% of 1 cm plagioclase crystals.

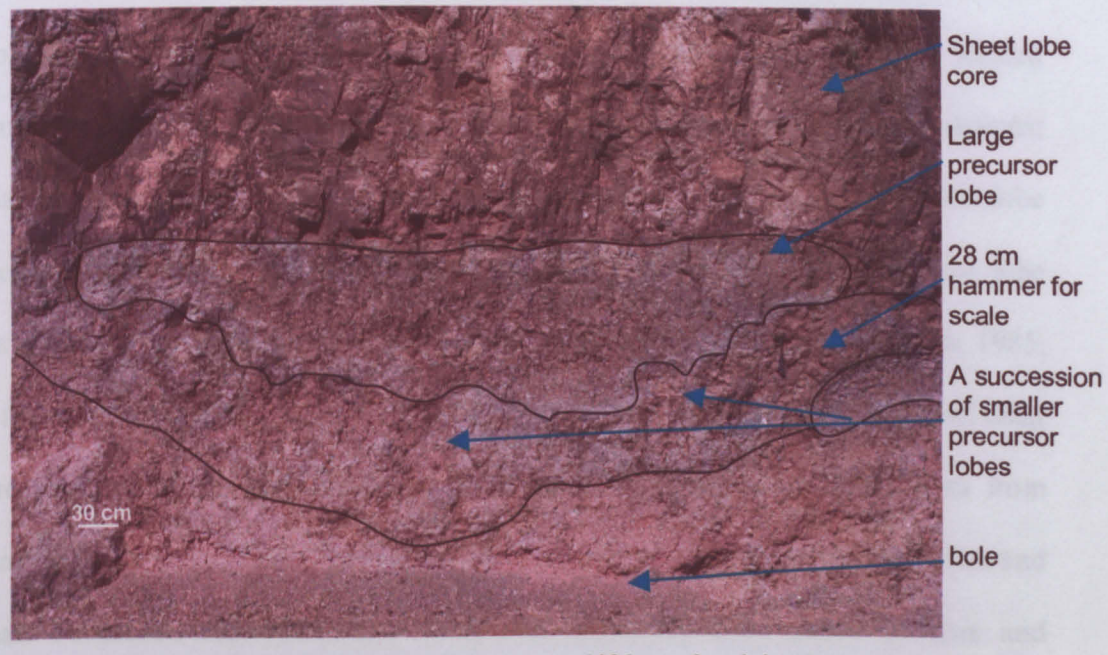

Figure 2.25. Precursor lobes between the bole that occurs at ~1024 m asl and the sheet lobe above. This picture is dominated by an ~ 1.5 m thick sheet lobe overlying a series of much smaller, decimetre sized lobes which lie on the bole. Lat. long. 17°55'28.7"N 73°37'27.9"E (Photo by S. Self)

Elev. 1024-1058 m asl

This flow-field from 1024-1058 m contains at least two sheet flow lobes and a number of precursor lobes above the bole at 1024 m (Figure 2.25). The lower flow lobe has a varying plagioclase content 6-7% of 1 cm laths at the base, but with decreasing amount and size towards the core. The core contains a large amygdaloidal mass, 5 m high

and 24 m long, although the base is not visible. The lava around it appears to show some chilled margins, and vesicles in the surrounding basalt appear to have risen parallel to its margin; its origin, like those reported below is unknown. Three metres above this, at 1045 m, is an undulating (by up to 5 m) flow contact. Lava in the thin flow-field above this contains 5% square plagioclase crystals. Basal lobes are present above the bole and the core of the sheet lobe contains hackly, water-cooled joints.

Mixed Ambenali/ Mahabaleshwar Formation chemotype succession

Elev. 1058-1090 m asl

A red bole at 1058 m shows 5 cm of soft saprolite, (Figure 2.26) with some vugs partially in-filled with zeolite, the weathering profile is ~ 2 m thick. Immediately above the bole at most locations is a highly vesicular zone, 0.2 m to 1.5 m thick, of precursor, or basal lobes; occasionally they have red-weathered glassy rinds. These lobes are welded into a massive 32 m thick sheet lobe above, which has two plagioclase crystal populations; big square crystals up to 7 mm and small needles up to 3 mm. This single sheet flow lobe is topped by a green-grey bole and so constitutes one flow-field and the sheet flow lobe marks a slight change in the geochemistry. In the literature (Cox and Hawkesworth, 1985; Devey and Lightfoot, 1986), the units exposed from here to the top of the Ambenali Ghat road are assigned to the Mahabaleshwar Formation, however, the trace elements from geochemical analysis indicate a mixture of Mahabaleshwar Formation characteristics and Ambenali Formation characteristics. This had previously been noted by Cox and Hawkesworth (1985) and Lightfoot (1985) but not explained or investigated (further comment on this is found in Section 4.3.5).

Figure 2.26. Red bole and progressive weathering profile into the upper crustal zone; note how the proportion of red material to grey basalt decreases down into the flow top. This is at 1059 m asl, at the boundary between the Mahabaleshwar Formation and the mixed Ambenali and Mahabaleshwar chemotype section. Lat. long. 17°55'09.6"N 73°37'39"E

Elev. 1090-1183 m asl

The green-grey bole (at 1090 m, AG5, Figure 2.14 and Figure 2.15) is seen on this traverse and possibly on the Wai-Panchgani road (Figure 2.7). It has a sandy texture and can be wet due to springs which occur along it. At road level, the total thickness of sandy textured saprolite is 30 cm, and a further 1.7 m of the weathering profile can be traced into the sheet flow below. If the bole is traced northwards, i.e., towards Ambenali village but above road level, it becomes thinner and red.

The sheet flow lobe above the green-grey bole is a bench-forming flow, of which only the lower 16 m are visible as the top has been eroded at this location. It contains 6% blocky plagioclase crystals which are up to 0.4 cm. This flow, which is prominent by the road can be traced in the cliff above the road for approximately 100 m towards the north,

again in the downhill direction. After this the prominent flow disappears and a tree-covered slope is observed; this may indicate of the lateral termination of the sheet lobe.

Figure 2.27. Rubbly altered grey-green flow-top, with undulose contact at 1089 m asl on Wai-Panchgani Road, possibly the same as the Green bole on Ambenali Ghat. The position of GPS position WP2 on the Wai-Panchgani road. Lat. long. 17°56'10.0"N 73°49'57.3"E (Photo by S. Self)

From 1106-1183 m there is no exposure due to a topographic bench on which Met-Tala village is situated (Figure 2.2).

Upper Ambenali Formation chemotype succession

Elev. 1183-1255 m asl

From 1183-1205 m the upper and lower portions of two sheet flow lobes are observed. The lower flow contains 10-15% plagioclase laths and the upper 5% 1-2 mm plagioclase crystals. There is no exposure from 1205-1252 m, at which a small 3-m-high exposure of weathered rock occurs with a coarse groundmass containing 8-10% plagioclase needles 1-2 mm long. This basalt has trace element characteristics of the Ambenali Formation, using Devey and Lightfoot (1986) criteria, which may be the Panhala Formation (Section 4.3.5).

2.6.2 *Tapola traverse*

- *Log Appendix A2,*
- *Geochemical data Appendix C3,*
- *Palaeomagnetic data appendix B3,*
- *Static GPS data Appendix D2*

Ambenali Formation succession

Elev. 690-757 m asl

The base of the Tapola road section starts at approximately 700 m, just north of the village of Tapola, on the shores of the Koyna Reservoir (Figure 2.1 and Figure 2.2). The top of the section is about 5 km to the south of Mahabaleshwar town. This section has not been studied before, consequently there is no published literature on the geochemistry or the volcanostratigraphy.

The first exposure starts at approximately 687 m. The rock here is highly spheroidally weathered with corestones of competent rock (Figure 2.28). The first well-exposed sheet flow lobe starts at ~700 m, however, a flow contact may have been missed between these two exposures due to poor outcrop quality. This sheet lobe is moderately fine-grained and aphyric displaying remnant columnar joints. The top of this flow, the location of static GPS point gps-TP1, is marked by a thin red bole at 708 m, which undulates by ~20 cm. This exposure is highly weathered and the bole is barely visible (Figure 2.29). The geochemistry indicates that this unit is in the Ambenali Formation.

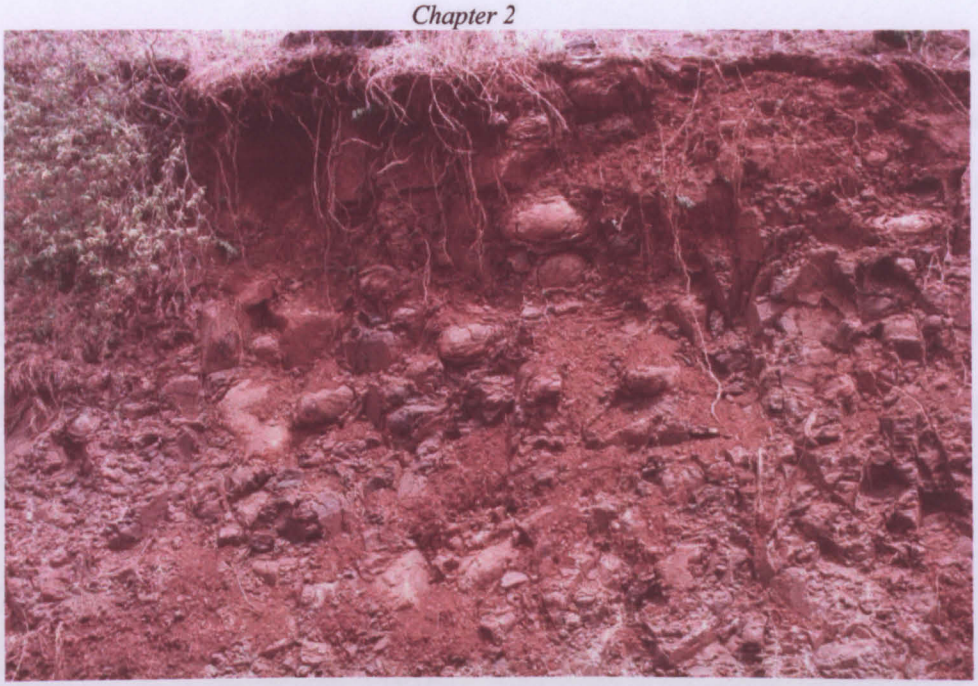

Figure 2.28. Spheroidally weathered basalt, typical of much of the poor exposure in this area of the DVP. Exposure near the base of the Tapola road section at ~ 705 m asl in the Ambenali Formation. Despite the highly weathered appearance of this exposure the basalt in the centre of the corestones is very fresh. Lat. long. 17°45'56.2"N 73°44'24.9"E (Photo by S. Self)

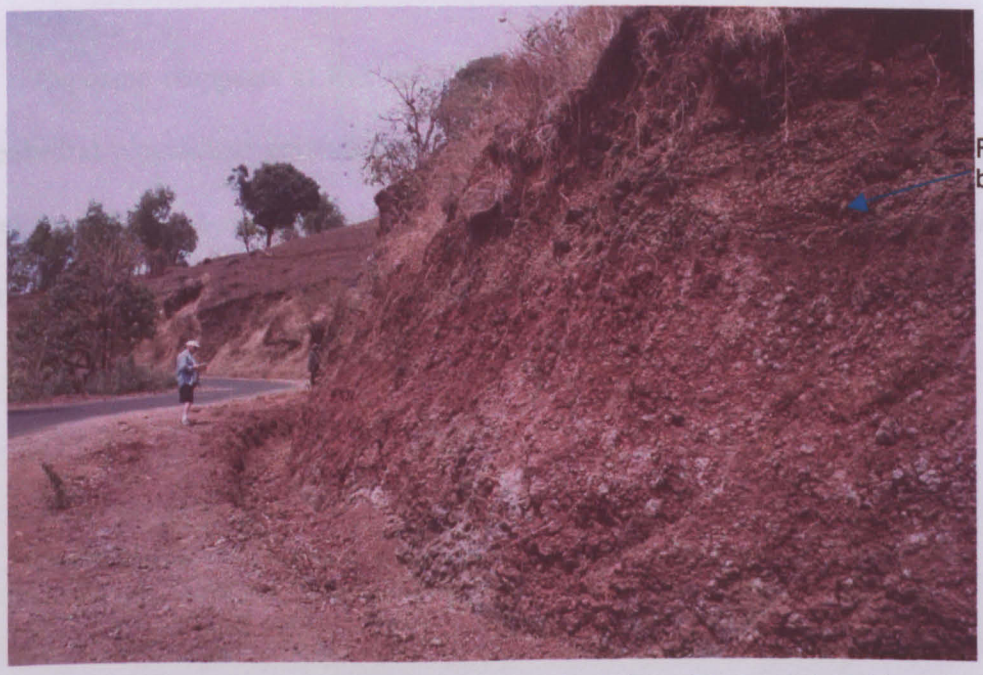

Figure 2.29. First exposure of a flow top in the Tapola section 708 m. The basalt is highly altered but the change in colour from red to brown clearly picks out the flow top; all other flow features are obscured. Position of gps-TP1 (Appendix D2), at elevation 708 m asl, in the Ambenali Formation. Lat. long. 17°46'06.6"N 73°44'20.1"E

The next two flows form the first identifiable flow-field in this section; the lower sheet flow lobe is again spheroidally weathered. Small 1 mm long plagioclase laths can be observed on fresh broken lava surfaces. The flow boundary at 732 m is poorly defined. The upper sheet flow lobe of this flow-field is weathered and displays 1-2% plagioclase

laths, 1-2 mm long. The bole material at the top of the flow-field (757 m) occurs in pockets, with loose material up to 40 cm deep occurring in places. The bulk of the bole material is fine grained but it has some clasts which appear different to the flow below; a few euhedral plagioclase megacrysts (up to 1 cm) and unaltered basaltic clasts (3-4 cm) are visible. This indicates that the bole may possibly be pyroclastic in origin, but not welded (therefore the term saprolite has not been used to describe the loose soil-like material). The top of this flow also marks the first regional bench in the traverse.

Elev. 757-830 m asl

The first 10 m of the next aphyric sheet flow lobe is visible before 45 m of no exposure occurs (767-812 m). A number of weathering horizons could be obscured here so it is impossible to identify the flow-fields in this part of the sequence.

Exposure reappears at 812 m in a sheet lobe core which is sparsely porphyritic with euhedral plagioclase crystals and pyroxene crystals up to 4 mm. The uppermost surface, at 830 m, shows signs of a ropey flow top with minor reddening, which is probably rotten glass. The weathering has not penetrated the flow top (Figure 2.30).

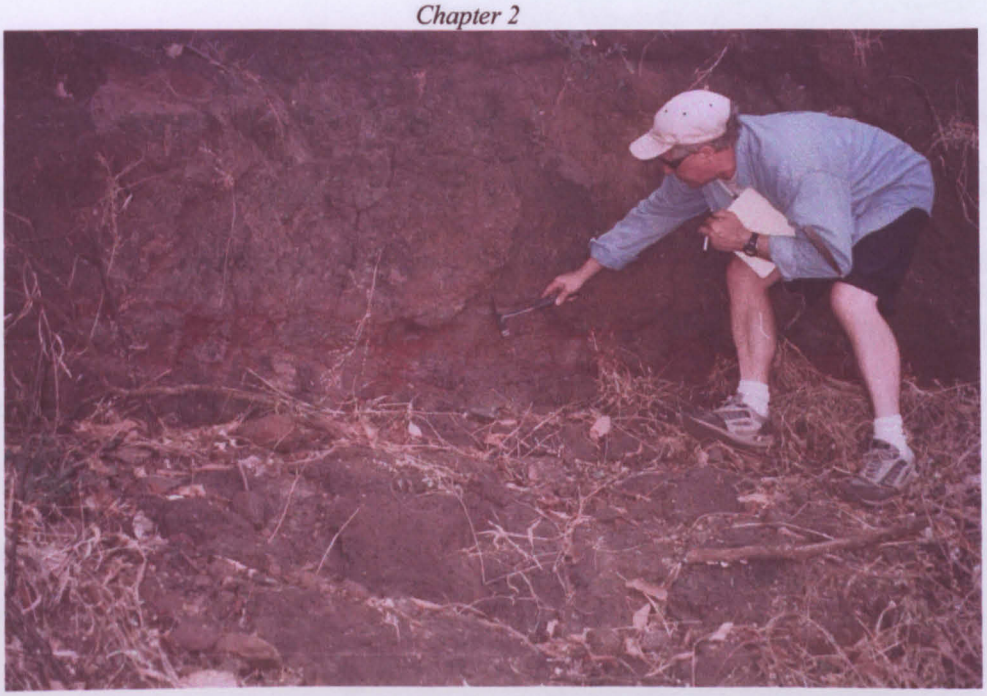

Figure 2.30. A slightly weathered flow top of an Ambenali Formation sheet flow lobe (Tapola road 830 m asl) showing some red clay material, but the majority of the flow top is intact and pāhoehoe ropes can be observed in places. The bole is between the locations of samples PMh14 and PMh15 in the log, Appendix A2. Hammer indicates this flow contact. Lat. long. ~17°47'32.5"N 73°42'54.9"E

Elev. 830-856 m asl

The next sheet flow lobe represents a single flow-field, which is the final Ambenali Formation unit. The basal lobes at 831 m have 10% plagioclase crystals 2-5 mm long. The top of the unit is marked by a 10 cm thick reddened horizon at 857 m.

Mahabaleshwar Formation succession

Elev. 856-957 m asl

The basal lobes of the flow-field above the bole at 857 m are of Mahabaleshwar Formation chemotype. This sheet lobe is terminated by 100 m of no exposure (869-957 m) forming the next prominent topographical bench. Within this section (between 897 m and 945 m) the palaeomagnetic polarity of the rock changes from reversed (29R) to normal (29N). It is assumed that the rocks in this zone of poor exposure are Mahabaleshwar Formation and this corresponds to the similar polarity change in the lower Mahabaleshwar Formation lavas on Ambenali Ghat.

Elev. 957-1005 m asl

Exposure reappears at 957 m in a massive sheet lobe core formed of basalt with a fine grained texture containing sparse plagioclase crystals up to 4 mm and glomerocrysts up to 1 cm. The concentration of crystals decreases up through the flow. The top of this sheet flow lobe is marked by a flow boundary at 989 m with no reddening, but the basalt is altered and soft. The sheet lobe above is 20 m thick it has 10%, 1 cm blocky plagioclase crystals and pipe vesicles at the base (Figure 2.31). The flow top of this 16-m-thick sheet lobe, at 1005 m, consists of a reddened 5-10 cm thick inconsistent bole and so marks the top of a flow-field.

Figure 2.31. Undulating flow boundary at 989 m asl in the Mahabaleshwar Formation on the Tapola road, marked by a geological hammer and line. No reddening is observed. The unit above shows a marked change in chemistry and is highly porphyritic, giving a white measly appearance to the soft altered rock. 28 cm geological hammer for scale. Approximate Lat. long. 17°65'09.8"N 73°37'32.2"E

Mixed Ambenali/Mahabaleshwar Formation chemotype succession

Elev. 1005-1141 m asl

Twenty metres of the next sheet flow lobe are exposed before another major bench marks an erosional horizon upon which Taldeo village is situated. The sheet lobe contains 5% 1-2 cm glomerocrysts and 5% smaller phenocrysts. This Taldeo bench forms a zone of no exposure from 1029-1123 m. The first notable feature above the bench is a

poorly exposed red horizon at 1125 m. At 1134-1141 m there is a well-exposed section of sheet lobe core at the Meta-tala bus stop/Deoli Junction (Figure 2.2). The flow core contains 8% plagioclase phenocrysts, ~0.5 cm long in a fine groundmass. As on Ambenali Ghat, there is a return to a mixed Ambenali-Mahabaleshwar Formation chemotype in these lavas at an elevation a little lower than on Ambenali Ghat.

Ambenali Formation chemotype succession

Elev. 1141-1243 m asl

The exposure becomes much poorer from here to the end of the section at 1243 m and it is difficult to place the outcropping basalts into flow-fields. The trace element chemistry suggests that the remainder of the exposed basalts have an Ambenali Formation chemotype, as seen in the upper units of Ambenali Ghat and again this is at a slightly lower elevation than on Ambenali Ghat. At 1165 m there is a small outcrop showing a weathered flow-top with a thin 1-2 cm purple bole (possibly the top of the flow-field whose base is at 1125 m), is probably weathered flow-top glass (the elevation of Static GPS location gps-TP3 and gps-TP2; the latter location was discarded due to poor satellite coverage); and above this is a small exposure of basalt with sub-horizontal joints. Another zone of no exposure between 1169 and 1175 m is followed by a moderately well-exposed sheet lobe core with 15% plagioclase glomerocrysts up to 4 mm.

The next exposure is also of a sheet lobe core with a possible flow top at 1205 m; it is separated from the one below by 4 m of poor exposure. These two sheet lobe core exposures are possibly from the same sheet flow or there may be an unexposed flow boundary between. The penultimate outcrop (between 1217 and 1221 m) is of basalt containing 10% plagioclase laths. The final exposure at road level is between 1228 and 1232 m and is probably the flow-top of the same unit. Above this is a thick sheet lobe core which forms a prominent cliff. Although it was not possible to sample this unit, it may be

the same unit as that which forms Elephant Head at Lodwick Point (Figure 2.2), although this is based solely on its similar appearance (from a distance) and approximate elevation.

2.6.3 Kelgar traverse

- *Log Appendix A3,*
- *Geochemical data Appendix C4*
- *Palaeomagnetic data appendix B4*
- *Static GPS data Appendix D2*

The Kelgar log was made along the Mahabaleshwar-Medha road. It starts near the village of Kelgar where the Mahabaleshwar Plateau Ghat section meets the Maharashtra Plateau (Figure 2.2) and levels out. The traverse starts at approximately 770 m and finishes at approximately 1225 m.

Ambenali Formation succession

Elev. 770-859 m asl

The lowest exposure is a poorly visible, vesicular flow top which contains 5% of 1 cm plagioclase crystals. It is topped at 771 m by a rubbly red bole with a 30 cm deep weathering profile, the first static GPS reading was taken on this traverse, (gps-KG1). This sheet flow lobe belongs to the Ambenali Formation. The bole contains 0.5-3 mm long plagioclase crystals. The base of the flow below has similar petrography. There is a zone of no exposure from 773-787 m.

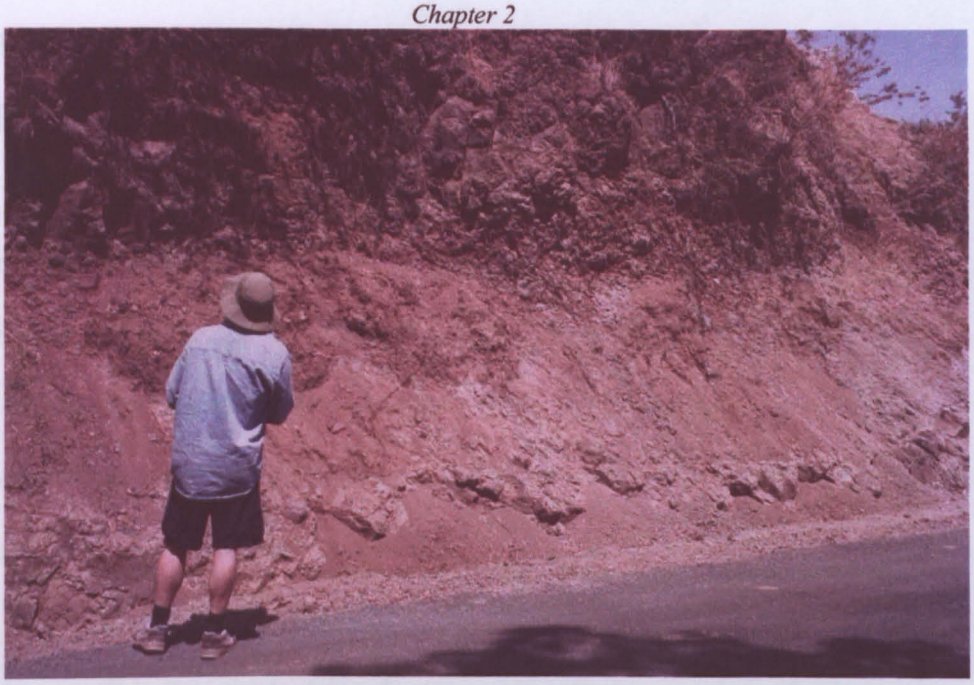

Figure 2.32. Undulating flow top at 813 m in the Ambenali Formation on the Kelgar road. The saprolite is thin, but lies on top of the weathering profile of the upper crustal zone. The bole overall, is friable and weathers easily, so it falls and covers a considerable amount of the flow top below. Lat. long. 17°51'56.1"N 73°45'09.0"E

Three more sheet flow lobes with visible flow boundaries at 793 m, 804 m and 813 m form the remainder of this flow-field. A possible tumulus occurs at the 804 m level boundary. All of these sheet flow lobes are poorly phyric with ~1% small plagioclase laths or glomerocrysts if present at all. The thin saprolite at 813 m is variable in thickness (~10 cm) but the weathering profile below it penetrates ~1.5 m into the upper crust (Figure 2.32). Above this bole are some thin pāhoehoe lobes overlain by another sheet flow lobe above, only 6 m thick. These form the base of the next flow-field, which is made up of three aphyric sheet flow lobes. The existence of the third of these aphyric lobes is dubious as its base is inferred at 843 m by a rubbly zone which is thought to indicate a flow top or a set of small lobes, but it may just be a continuation of the second lobe. The top of the flow-field is marked by a thin red horizon at 859 m. This is the final eruptive unit in the Ambenali Formation.

Elev. 859-933 m asl

The lowest sheet flow lobe in the next flow-field (the first unit in the Mahabaleshwar Formation) is poorly exposed and gives way to a zone of poor exposure from 864 to 885 m, inside which three small exposures of sheet lobe core are observed. Better exposure returns above, within a sheet flow lobe that contains ~5-7% 1 cm euhedral plagioclase laths and some glomerocrysts. The top of this sheet lobe, at 918 m, is marked by a slight decrease in phenocrysts compared to the core (now up to 3%), and a 5-6 m thick HVZ. There is no bole at the boundary, but there is a marked increase in plagioclase in the flow above. This 7-m-thick sheet flow lobe has 30% 1 cm square plagioclase crystals, making it a GPB. It is the final unit in this flow-field and ends at 933 m where it is topped by an impersistent red bole horizon which has ~3 m of topography.

Elev. 933-953 m asl

The next flow-field is 20 m thick and consists of only one sheet flow lobe and some break-out lobes. It is spheroidally weathered and is almost aphyric with only a few ~1 mm plagioclase crystals. There are a series of break-out lobes above this sheet lobe; which are highly vesicular and weathered. Above these lobes at 953 m is an undulating saprolite a few centimetres thick. This is the position of the static GPS location gps-KG2. These units are the final units within palaeomagnetic chron 29R.

Elev. 953-996 m asl

The first flow-field in chron 29N is ~31 m thick (953-978 m) and is poorly exposed. At 967 m there is a possible flow top or amalgamation of break-out lobes. The sheet flow lobe below these contains 10% glomerocrysts of acicular plagioclase up to 1 cm. Between 966 and 971 m is a well-developed HVZ which is particularly noticeable as it contains four obvious layers of vesicle-rich and vesicle-poor basalt. The flow-field is

terminated by a laterally impersistent bole. A red bole of saprolite is found in the dips of the undulating flow top with a wavelength of approximately 40 cm and height of ~15 cm. It is not possible to be sure that these sections of sheet flow lobes are only one flow-field but it is probable, as the thickness (~45 m) is similar to that of other flow-fields in this area of the DVP. The actual number of sheet flow lobes in this flow-field is difficult to determine, but it is at least two.

The next flow-field is composed of only one 18-m-thick sheet flow lobe. It contains 2% plagioclase crystals up to 1 cm long with scattered glomerocrysts. The red horizon at the top of this unit, at 996 m, is very thin.

Elev. 996-1032 m asl

The subsequent four flow-fields, from 996 m-1090 m, are all only one sheet flow lobe thick. The lowest of the four (996-1018 m) is course grained, it has only a few plagioclase crystals, up to 3 m at the base, but this increases to 5% of 1-cm-sized plagioclase crystals at the top. The upper crust is very weathered and rubbly. It is difficult to see structures, so it is not possible to determine if there are surface break-out lobes or just a HVZ. The red saprolite is only 5-10 cm thick and the red weathering continues down into the flow top to an undetermined depth.

The second flow (1018-1032 m) contains 5% acicular plagioclase crystals up to 1 cm long and is topped by a thin red bole. This sheet flow lobe is the final pure Mahabaleshwar Formation chemotype unit in this traverse.

Mixed Ambenali/Mahabaleshwar Formation succession

Elev. 1032-1092 m asl

The next flow-field is thin, 1032-1043 m. The lowest units are a series of 1-m-thick break-out lobes with red weathered selvages. The lava has a similar petrography to

the unit below but has an unknown chemotype as it was not sampled. The upper 6 m is dominated by a series of lobes that form a highly vesicular dome-shaped zone 100 m long. It is possible that there is a tumulus-like feature here as well. The bole rises up and over this lobate mass. The saprolite is 10-20 cm thick but the weathering horizon below is deep (Figure 2.33) and some of the clasts within the weathering horizon which appear to be part of a HVZ are not horizontal. This is either due to their having been some movement in the upper zone rotating some of the clasts or that the bole is formed from break-out lobes which often have non-horizontal vesicles in their upper crust. The third static GPS reading was taken here, gps-KG3.

The final unit in this set of four is preceded by small discontinuous precursor lobes (Figure 2.33), but the main sheet lobe above these is about 50 m thick. It is a GPB which, contains sparse large plagioclase laths 1-2 cm long and glomerocrysts ~1 cm in size. This flow-field is terminated by a red bole with up to 50 cm of saprolite (at 1092 m), but deep weathering has produced a rubbly flow top, 2 m deep.

Above this bole at 1092 m is the final exposed sheet lobe in the mixed Ambenali/ Mahabaleshwar Formation succession. This sheet lobe has sporadic precursor lobes below it, but the sheet lobe itself contains 10-15% plagioclase laths which are 1-2 cm long; 1-cm-sized glomerocrysts are also observed. There is no exposure between 1103-1117 m although this is probably mixed Ambenali/Mahabaleshwar Formation chemotype as well.

Figure 2.33. A saprolitic bole at 1043 m asl in the mixed Ambenali/Mahabaleshwar Formation chemotype zone on the Kelgar Road, with its extensive, deep weathering profile. The HVS of some clasts in the bole are not horizontal. This is either due to some movement occurring within the bole or that the HVS is part of a small breakout lobe. Note also the thin precursor lobes immediately above the bole. KG3 was taken at this location. Lat. long. 17°37'50"N 73°44'28.9"E

Upper Ambenali Formation chemotype succession

Elev. 1092-1230 m asl

At 1117 m there is a poorly-defined and poorly visible bole. The next flow-field is also poorly exposed and remains so until 1142 m. The number of sheet flow lobes is difficult to determine, but it appears to be one continuous unit until ~1148 m. This sheet lobe contains 15% plagioclase up to 0.5 cm long, glomerocrysts of plagioclase and pyroxene up to 1 cm across are also seen. This section from 1117 to 1142 m is not well exposed and not sampled, however a sample was taken of the tumuli at 1150 m, and this is of Ambenali Formation chemotype and so it is assumed that the poorly exposed lava from 1117-1142 m is also Ambenali Formation chemotype.

Between 1148 and 1157 m there are two sets of what appear to be tumuli (Section 2.2.2). There is dense lava with highly vesicular sections between (Figure 2.34). The basalt is highly porphyritic with 15% plagioclase and very amygdaloidal. The top of this flow-field is at 1167 m and is marked by a thin red bole

Figure 2.34. A series of probable tumuli on the Kelgar Road at 1148-1150 m asl in the Mahabaleshwar Formation. Note the highly vesicular weathered material surrounding a much more solid lava core. Lat. long. 17°52'46.6"N 73°44'18.9"E

The penultimate flow-field is probably also a single sheet lobe but from 1181-1190 m it is poorly exposed. It contains 1-2% plagioclase needles up to 1 cm long and 0.2 cm wide. The groundmass is fine and the rock fractures conchoidally. The geochemistry of the sampled, well exposed section of this flow-field indicates that the lava is of mixed Ambenali/Mahabaleshwar Formation chemotype. The top of this flow-field is marked by a very thin red horizon, probably rotted flow top glass. On top of this is a sheet lobe containing a round hole over 50 cm deep and 5-6 cm diameter, possibly a mould of a fallen tree, left after it burnt as lava surrounded it (Figure 2.35). This sheet lobe contains 30% blocky plagioclase and glomerocrysts. The sheet lobe above this one is highly vesicular and amygdaloidal (Figure 2.36) with 5-10% needle-like plagioclase and glomerocrysts; this unit may be rubbly pāhoehoe. At the top is a low-angle linear feature (1217 m) exposed in the cliff face, which is perhaps a small fault or a fracture rather than a

flow boundary as it appears to cross another flow boundary. The third and final static GPS reading was taken at the height of the low angle fracture, gps-KG4. The final, uppermost flow observed forms the base of the highest bench and is highly altered by modern weathering. The Kelgar road traverse is capped by basaltic boulders in modern soil.

Figure 2.35. Possible tree/branch cast in a sheet flow lobe at 1200 m asl, on the Kelgar road. The hole is at least 60 cm deep and 6 cm in diameter. This sheet lobe is in basalt which is of Ambenali chemotype. Lat. long. 17°53'21.3"N 73°43'39.0"E

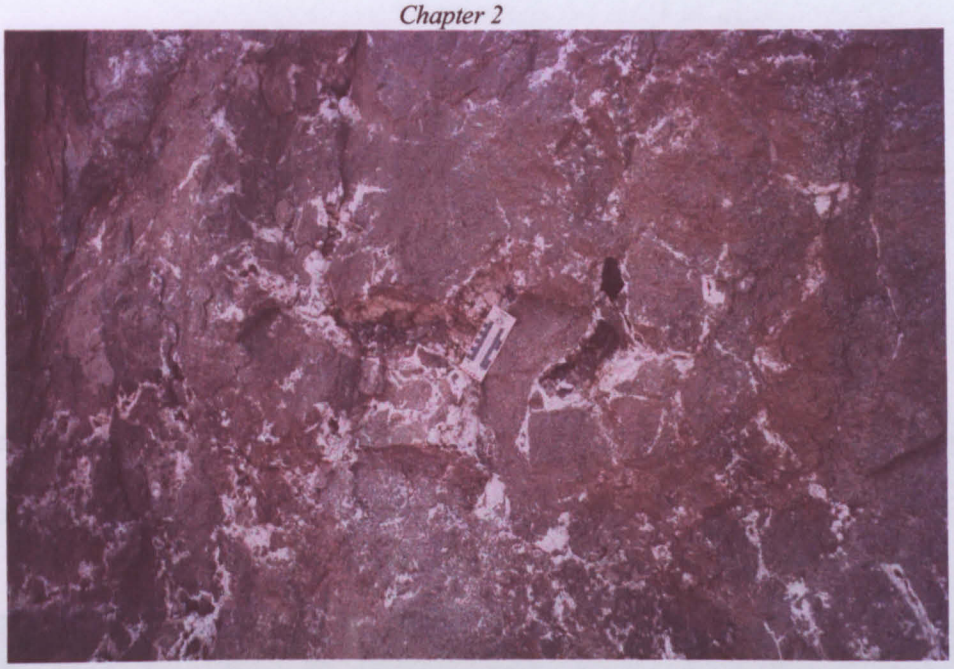

Figure 2.36. Blocky, rubbly, amygdaloidal sheet lobe top. At 1207 m asl on the Kelgar road, this basalt has Ambenali chemotype. Lat. long. 17°53'21.2"N 73°43'36.8"E

2.6.4 *Wai-Panchgani traverse*

- *Appendix A4,*
- *Geochemical data Appendix C5,*
- *Palaeomagnetic data appendix B5,*
- *Static GPS data Appendix D2*

The section starts at approximately 770 m asl and terminates below the laterite cap of the Panchgani Tableland (Figure 2.37) at 1130 m asl.

Figure 2.37. A view across Panchgani Tableland towards the south. The flat tops of the mesas are due to the laterite caps, which is the result of extreme weathering of the topmost lava flow. Rivers have dissected them forming individual mesas. Lat. long. 17°55.5'N 73°49.1'E (Photo by S. Self)

Ambenali Formation succession

Elev. 769-814 m asl

The first 70 m of this section is poorly exposed but shows a number of sheet flow lobes. There are probably three but there is an 8 m section from 775-785 m section of no exposure. The flow boundary at 785 m is rubbly and poorly exposed, it is within a flow-field the upper unit of which terminates in a thin red saprolitic bole (814 m), visible just

below the modern soil horizon, close to the 2 km to Wai road-stone. This flow is highly altered and appears to have been hydrothermally altered and zeolitised to temperatures as high as 500° C (M. Gerard, E. Frisch, 2003, pers. comm.). These units belong to the Ambenali Formation chemotype.

Elev. 814-822 m asl

The 7 m thick sheet flow lobe above, 814-822 m, is aphyric and perhaps unusually for such a thin flow again represents a flow-field formed of only one flow lobe. Its undulating flow top has been highly weathered to form a red saprolitic bole with a deep weathering profile that appears to have undergone some movement. The clasts vary in size with some up to 50 cm long. One clast appears to be a piece of HVZ with vesicles trending almost vertically, this may be due to the clasts having rotated 90° within this flow-top material (Figure 2.38), possibly due to some localised mechanical slumping that occurred whilst the flow top was exposed. A further explanation for this inclined clast is that the bole is formed from break-out lobes which can have HVZs which follow the curved shape of the lobe, and hence may be almost vertical in places (e.g. inclined vesicles in Figure 2.33). This bole is the location of GPS site gps-WP1. Directly above the bole lie a few small precursor lobes.

Figure 2.38. Undulating red flow-top at 822 m asl on the Wai-Panchgani road, in the Ambenali Formation. This is also the location of gpsWP1. There is no saprolite, i.e., a section of red clayey material without any large clasts, at the top of this weathering profile, but the whole profile is over 2 m deep and contains clasts with inclined HVZ. Lat. long. 17°56'29.3"N 73°51'44.02"E

Elev. 822-863 m asl

The section from 822-840 m designates the next flow-field which again contains one sheet flow lobe which is aphyric and has low vesicularity. The bole at the top of the flow-field is difficult to see due to modern weathering.

The next flow-field (840-863 m) is formed from one or two sheet flow lobes, which are again aphyric and have low vesicularity. The saprolite (863 m) is soft and forms in lenses above a 1.5-m-deep very rubbly, red weathering profile.

Elev. 863-915 m asl

Small lobes with reddened upper rinds are observed at 874 m mark the top of a 10 m thick sheet flow lobe with small white plagioclase phenocrysts. It is tentatively assigned as a flow-field due to its contrasting petrography with the lavas above and below.

The next two flow-fields are also formed from one sheet flow lobe each, and both are aphyric. The top of the lower flow at 892 m is marked by a 20-cm-thick saprolite with the upper part of the flow below rubbly and reddened. The top of the upper flow-field marks the last lava of the Ambenali Formation at 915 m, where a red bole is found next to a small, roadside shrine called Buha Saheb temple (Figure 2.2). The 20 cm saprolite has been baked and shows prismatic joints below a sharp contact with the sheet lobe above. The weathering profile descends into the flow top to a depth of 1.2 m.

Mahabaleshwar Formation succession

Elev. 915-982 m asl

The flow-field above the red bole is complex; it is approximately 53 m thick (from 915-968 m). The first thick sheet lobe contains 10% star-shaped plagioclases. It terminates at approximately 954 m, although neither the classic vesicular flow top nor any upper contact is observed. Above this thick sheet lobe is a series of smaller plagioclase-phyric, pāhoehoe lobes, the largest being 3-4 m thick and ~100 m long, forming a 5-m-thick sequence. From 960 to 968 m a single sheet lobe with a highly vesicular crust forms the final unit in this flow-field. A thin bole caps it at 968 m.

Above this bole and buried by sheet flow lobes is a tumulus structure, with a solid core and steep sides of vesicular lava. Above the tumulus is a 10 m sheet lobe containing glomerocrysts of plagioclase. The section from 968 to 982 m forms a slope where the lava is preferentially weathered back. This may be part of the undulating feature which can be seen along much of the length of the southern wall of the Krishna River valley (Figure 2.2)

from Harrison's Folly at the top of this traverse (Figure 2.2). The thin bole, at 982 m, with a red rubbly flow top below, marks the top of this flow-field and the palaeomagnetic reversal from 29R to 29N.

Elev. 982-1089 m asl

Two flow-fields that are, again, each formed from one sheet flow lobe, occur between 982-1049 m. The first is an aphyric sheet lobe with a fine grained groundmass. The upper is a poorly exposed GPB containing 25-30% 1.5 cm long plagioclase crystals. The saprolite between them is 5 cm thick with some reddened rubbly flow top below (Figure 2.39). The top of the upper flow-field at 1049 m is a thin red horizon, which is probably little more than rotten glass.

The next flow-field in the pile is 41 m thick, (1049-1089 m) and formed from one sheet flow lobe. It is a dark, fine-grained basalt with 2-3% plagioclase crystals. It is columnar jointed with some joint sets inclined up to 50° from the horizontal (Figure 2.40). Agate-filled mega-vesicles are also observed, the agate banding indicating a dip of no more than 0.5°E. The top of the flow, at 1089 m (Figure 2.37), is undulose (the static GPS location, gps-WP2). Below, the normal HVZ is replaced or masked by very soft pale grey rock which appears rubbly in places; it is probably highly weathered and may be weathered break-out lobes which for some reason have not oxidised to a red colour, although a small section at the top of the bole is coloured red. This soft material also appears to be invaded by fingers of denser lava. This could also be the equivalent of the green-grey bole seen at the same elevation on Ambenali Ghat.

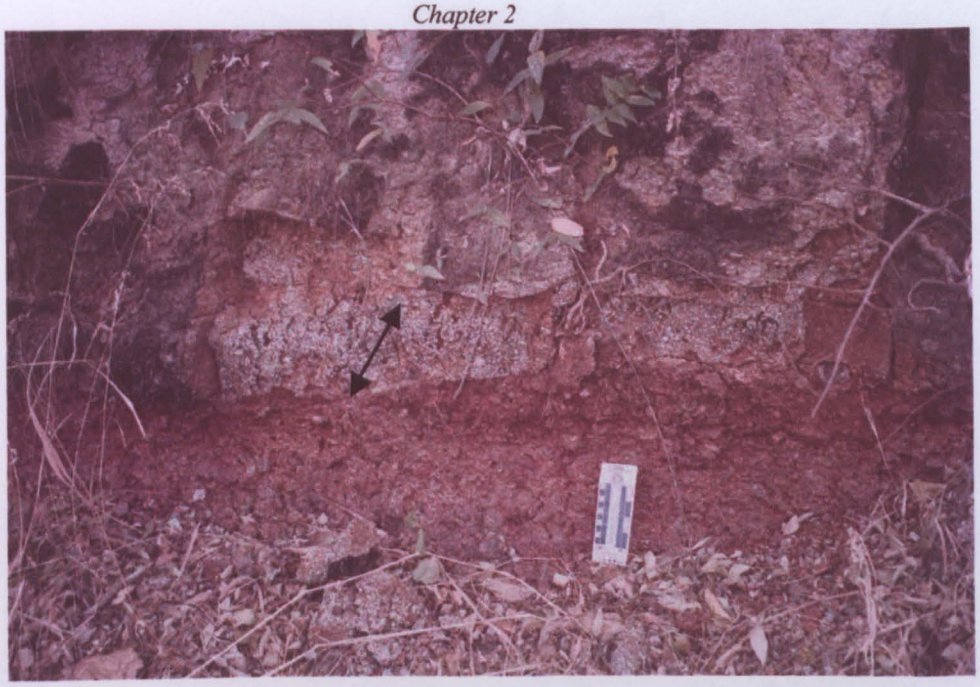

Figure 2.39. Flow top at 1007 m asl on the Wai-Panchgani road, Mahabaleshwar Formation. The lower flow only shows a bole. The basal zone of the upper, altered flow displays inclined pipe vesicles (see arrow). Lat. long. unavailable

Mixed Ambenali/Mahabaleshwar Formation succession

Elev. 1089-1165 m asl

The flow-field which starts at 1089 m asl is at least one sheet flow lobe, possibly two, but the upper 10 m is poorly exposed. This sheet lobe marks the beginning of a sequence of flows, which have a mixed Ambenali-Mahabaleshwar chemical signature. The well-exposed section of lava contains 10% plagioclase glomerocrysts. The top of this flow-field is marked by a poorly visible, thin red horizon at 1141 m; the poor exposure continues to 1162 m where it improves to show a red bole at 1165.

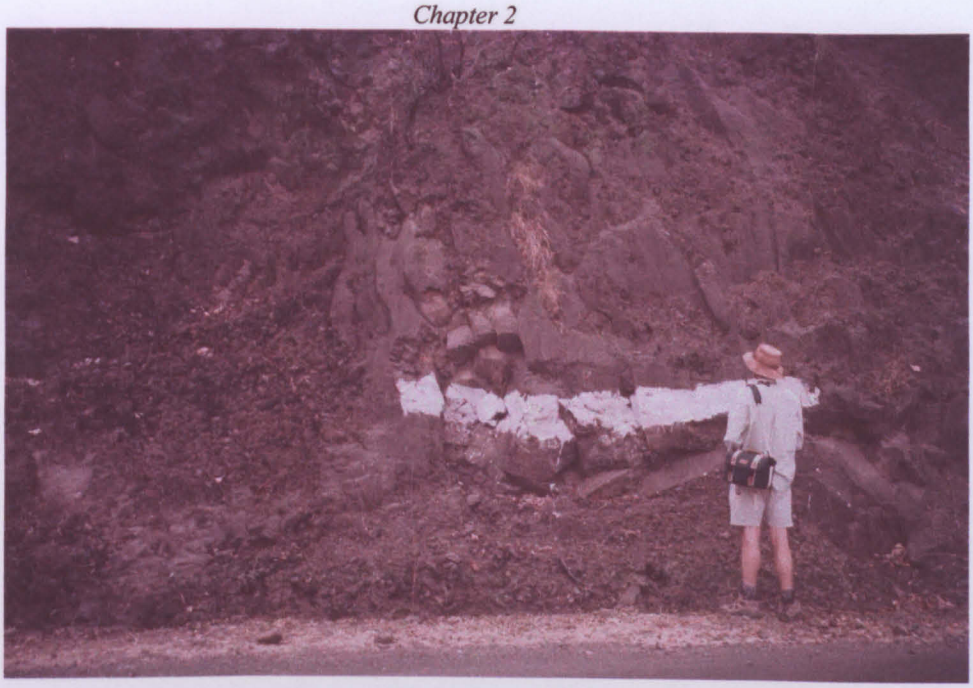

Figure 2.40. Narrow inclined, columnar joints at 1067 m asl on the Wai-Panchgani road in the Mahabaleshwar Formation. Lat. long. 17°56'05.4"N 73°49'10.8"E

Upper Ambenali Formation chemotype succession

Elev. 1165-1220 m asl

Below the undulating red saprolitic bole at 1165 m is a soft, grey, highly weathered and zeolitised rock. This bole is thin and does not penetrate more than a few 10s of centimetres into what appears to be a rubbly flow top below.

The penultimate flow-field in this traverse is 43 m thick, from 1165-1208 m and is formed from one or possibly two sheet flow lobes. There are 1-2 m thick amygdaloidal basal lobes at 1165 m. The lower part of the flow has 5% small blocky plagioclase crystals but the percentage increases to 10% in the fanned columnar jointed zone of the flow core (Figure 2.41). At 1200 m there is a possible flow contact but it is poorly exposed. From a distance there appears to be a hummocky feature at this elevation but it does not outcrop at road level. The sheet flow lobe at the top of the flow-field contains 2-3% plagioclase but is poorly exposed; the top of the flow-field is marked by a thin bole. The final flow-field and sheet flow lobe in this traverse ends at 1220 m where it has been eroded and is now covered with modern soils.

Figure 2.41. Fanned columnar joints on the Wai-Panchgani traverse at ~1190 m asl, perhaps indicating water cooling (Lyle, 2000). This basalt is of upper Ambenali Formation chemotype. Lat. long. 17°56'05.4"N 73°49'10.8"E

2.6.5 *Varandah Ghat*

- *Appendix A5,*
- *Geochemical data Appendix C6,*
- *Palaeomagnetic data appendix B6,*
- *Static GPS data Appendix D2,*

This traverse is along the western section of the Varandah-Bhor road, from the Konkan Plain to the top of the Varandah Ghat section at a small collection of roadside stalls (Figure 2.2). The heights on this log were all collected using a barometric altimeter and hand-held GPS and so are not corrected to the static GPS used on the Mahabaleshwar Plateau traverses. The traverse starts at an altitude of 10 m asl and finishes at 620 m asl.

Bushe Formation succession

Elev. 10-18 m asl

This first outcrop is in the Bushe Formation and observed at 10 m asl in the river bed of the Kalnadu river, a tributary of the Savitri river. The exposure appears to be hummocky pāhoehoe and consists of a series of small sheet flow lobes, on average 2-3 m thick and possibly up to 100 m long. The upper crust of these lobes is brecciated, but the core is solid (Figure 2.42). The brecciated clasts are surrounded by an orange-brown clay like material. It is possible that this is due to the fact that these sheet flow lobes were emplaced into shallow water. Sub-vertical joint sets, not seen in the other lava sequences in the region cut the area. The groundmass of the basalt is very fine, but it possesses 10% crystals of blocky plagioclase and plagioclase/ mafic glomerocrysts.

Figure 2.42. Brecciated flow top in the lowest exposure of Varandah Ghat at ~26 m asl. In the Bushe Formation, on the banks of the Kalnadu river. The average sheet lobe thickness here is 1-4 m and not all are brecciated. Lat. long. 18°05'56.2"N 73°30'56.1"E (Photo by S. Self)

Elev. 18-115 m asl

No exposures are observed from 18-62 m, although it can be assumed that there is probably at least one flow boundary in this zone. The outcrop above this is part of a sheet lobe core and a section of the upper crust. This unit is much thicker than those seen below, as the outcrop itself is 16 m thick and the sheet lobe must exceed this. The petrography has changed as well, this unit contains a few plagioclase and mafic minerals, possibly weathered pyroxene. The top of this exposure is 68 m asl and marks a 12 m thick zone of no exposure in which the flow top of the flow below must reside as the next exposed section of sheet flow lobe is also a core. Again the rock is almost aphyric, with a coarse groundmass but it contains some dark spots, which may be weathered pyroxene. A highly vesicular upper crust is observed (105-108 m), but not an actual flow top as the exposure becomes a 7 m high, highly weathered cliff in which details are difficult to discern. Loose boulders from the spheroidally weathered cliff have a medium grained groundmass with plagioclase glomerocrysts ~5 mm.

Elev. 115-231 m asl

From 115-176 m there is a series of aphyric lobes and toes with a medium grained groundmass. The size varies from 15 cm to 6 m although the topmost complete unit is thicker. Poor or no exposure dominates from 176-207 m. The upper exposure of poorly exposed basalt (202-207 m) contains <1% of 2 mm plagioclase laths in a coarse groundmass. Between 207 and 215 m, a spheroidally weathered core grades into a poorly exposed convex flow top, probably indicating a relatively small sheet flow lobe. Samples from this section show that these are the final units of typical Bushe Formation chemotype.

The next sheet lobe contains multiple sets of HVS and vesicle cylinders at 217 m, (Figure 2.10), and also contains 2-3% blocky plagioclase crystals 5-8 mm long, in a medium-grained groundmass. This unit should be in the Bushe Formation according to elevation data from Devey (1982), but the geochemical signature does not fit with the Devey and Lightfoot (1986) formation criteria. The top of this outcrop terminates at 224 m with 7 m of poor exposure.

Poladpur Formation succession

Elev. 231-383 m asl

The first exposure of Poladpur Formation on Varandah Ghat is at 231 m asl and the lava is similar to the exposure between 217 and 225 m. The next 55 m are predominately poor or no exposure. A grey-green weathering horizon was observed at 267 m which appears to be the base of a poorly exposed 8 m thick sheet flow lobe which has a lobate upper surface at 275 m. Three metres of good exposure show a section of basaltic sheet flow lobe which contains 4-5% plagioclase/pyroxene glomerocrysts up to 6 mm long and some individual plagioclase crystals. From 294-297 m is a highly vesicular zone, and immediately above this is a dense, dark grey, aphyric sheet lobe core, with a coarse grained groundmass. This unit may be the lateral equivalent of the thick, large

sheet flow lobe that can be seen across the valley. There is no exposure from 310-383 m, as there is a bench on which Macheri village sits (~ lat. long. 18°07'28.8"N 73°35'17.4"E).

Elev. 383-470 m asl

Small, 50 cm to 2 m thick P-type pāhoehoe lobes, some of which have fine ropes on the upper surface are observed from 383-399 m. All of the lobes appear to be aphyric with a mid-grey medium grained groundmass. There is no exposure between 399 m and 417 m.

From 417-470 m, 53 m of a thick sheet flow lobe is observed (the base is not visible). This unit has a well-developed colonnade and entablature, with the transition between the two jointing styles forming an obvious shelf. This is the only unit where these two types of jointing were observed. This unit is large and competent and is visible in the cliffs of the surrounding area. The groundmass is dark and fine with <1% clear plagioclase up to 4 mm long. This is the final sheet flow lobe in the Poladpur Formation.

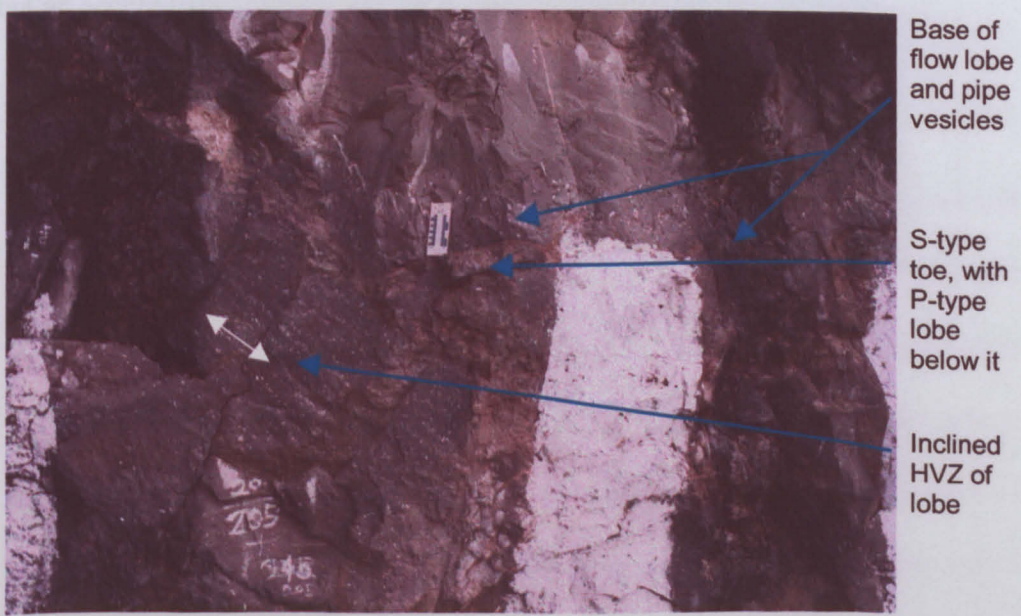

Figure 2.43. Lobes of various sizes some showing HVZs, pipe vesicles and an S-type pāhoehoe toe (Glossary of terms). The orientation and direction of inclination of the HVZ is marked by a white arrow. Varandah Ghat, 470-474 m asl, in the Ambenali Formation. Lat. long. unavailable

Elev. 470-532 m asl

At 470 m asl there is 5 m of small, aphyric, P-type pāhoehoe lobes, some only 10s of centimetres thick and a few metres long. The upper surface of these units is reddened with a thin saprolite in pockets up to 10 cm thick (Figure 2.43). This is the first red horizon seen in this traverse. The subsequent sheet flow lobe and flow-field is 35 m thick (475-510 m). The base is aphyric, but the plagioclase content increases up the unit from 2-3% in the centre to 3-6% clear white plagioclase crystals in the hackly jointed zone towards the top of the core. The flow top is slightly reddened with a thin discontinuous red weathering horizon.

Precursor lobes containing 1% plagioclase form the base of this flow-field. The main sheet flow lobe is 19 m thick 513-532 m and is aphyric. The HVS observed in this unit is wavy and the vesicle cylinders feeding it, thin. The flow top is well preserved, but 2-3 cm thick red ashy material has collected in pockets, this may not be a true weathering horizon, but an accumulation of ash, soil or saprolite (Figure 2.44).

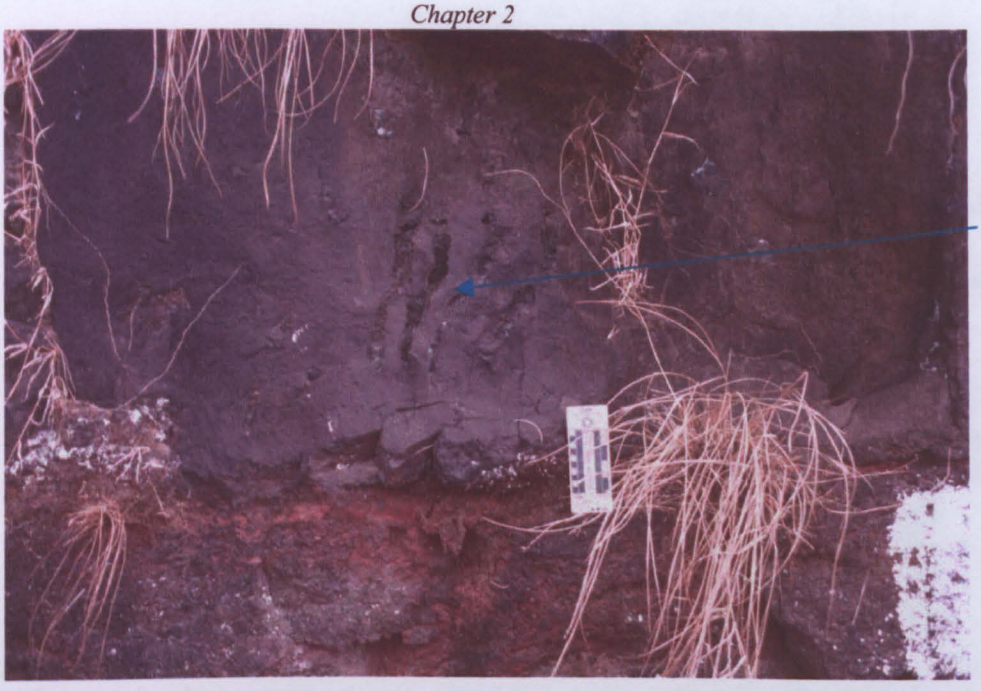

Figure 2.44. 'Pockety' bole at 533 m asl on Varandah Ghat, Ambenali Formation. Large (~20 cm long by 3 cm wide) pipe-like vesicles are observed in the sheet lobe above. Note however that the basal zone of the lobe and the rest of the lobe itself is poorly vesicular. Lat. long. unavailable (Photo by S. Self)

Elev. 532-610 m asl

The penultimate thick sheet flow lobe at road level in this section is 28 m thick, and almost aphyric except for a few small plagioclase crystals in a coarse groundmass. Fanned columnar joints towards the top suggest some water cooling. This sheet flow lobe and flow-field is topped at 560 m by an unusual bole (Figure 2.45). It is grey green, 1 m thick, contains no unaltered basalt or relic lava features and contains thin veins of a white secondary mineral, which may have in-filled cracks formed by the baking of the soil-like material by the sheet lobe above (it is very unclear as to which type of bole this is (Section 2.5.3) and as such the fine bole material is not described as a saprolite). This is the final sheet lobe sampled which is of typical Ambenali Formation chemotype.

Figure 2.45. Thick brown bole at the pass (560 m asl) on Varandah Ghat, Ambenali Formation. Note the in-filled shrinkage cracks which resemble rootlets. There are no clasts in this bole and it appears to be resting directly on the flow top of the lobe below, although this is poorly exposed. Lat. long. 18°07'42.4"N 73°36'26.4"E

A few small basal lobes are observed above this grey bole and on top of these is a 22-m-thick aphyric, medium-grained sheet flow lobe, which has an anomalous geochemical signature, in that it cannot be assigned to a DVP geochemical formation, it is assumed to be an unusual chemotype within the Ambenali Formation. Above this 22 m thick sheet lobe, on the underside of the basal crust above, striations or slikensides can be observed, probably caused by scraping as the lava moved over the solid flow beneath (Figure 2.46). This indicates that at this particular location the lava was flowing from the north west.

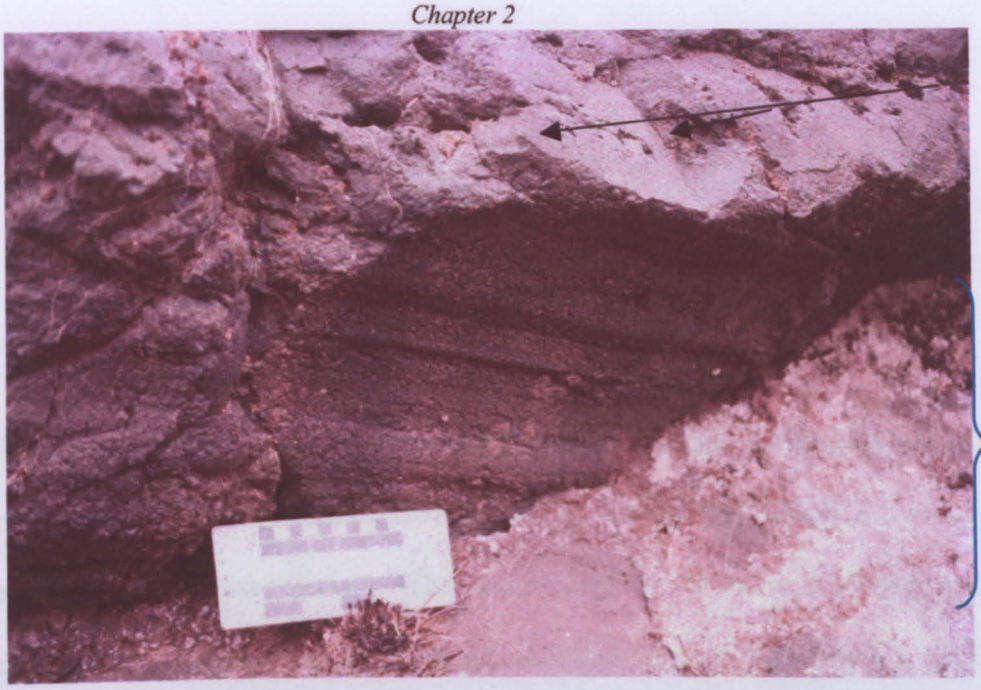

Figure 2.46. The top of Varandah Ghat, 582 m asl, in the Ambenali Formation, The lower unit visible in this figure is the sheet lobe above the thick green grey bole at 560 m asl. Scraper marks on the base of a sheet flow lobe formed whilst the lobe was being emplaced and the lava was liquid. Pipe vesicles are also visible in the base of this lobe and indicate the same palaeodirection as the scraper marks, i.e., that the flow direction was from the north west. Lat. long. similar to that of Figure 2.47 (Photo by S. Self)

No more sheet flow lobes can be observed at road level, although the exposed, but inaccessible basalt pile along the road is at least another 40 m thick. The top of the Maharashtra Plateau, however, is a further 100-200 m higher still.

2.6.6 *Khumbarli Ghat*

- *Appendix A6,*
- *Geochemical data Appendix C7,*
- *Palaeomagnetic data appendix B7,*
- *Static GPS data Appendix D2,*

Khumbarli Ghat is a road section that ascends the Western Ghat Escarpment from Chiplun (200 m, Figure 2.1), east towards Helwak (~600 m, Figure 2.1), which is located at the southern end of the Koyna reservoir. The section starts at 120 m asl and terminates at the ghat crest at a road check-point at 700 m asl. A series of three sheet lobes is seen in the cliff above the road, but was not accessed on this occasion. The heights for this log were taken using a barometric altimeter and hand held GPS and so are not corrected to the static GPS used on the Mahabaleshwar Plateau traverses.

Ambenali Formation succession

Elev. 120-178 m asl

The section starts at 120 m with a spheroidally weathered, massive, basalt unit which contains 1% of 0.5 cm plagioclase phenocrysts in a dark, medium grained groundmass. This unit falls geochemically into the Ambenali Formation. Small exposures at around 150 m indicate a slight change in petrography with 3% plagioclase crystals up to 1 cm, but with the same dark groundmass. This could be a continuation of the same sheet lobe, and probably the same flow-field, as there is a red bole at 167 m (Figure 2.47). The total thickness of reddened material is ~10 cm with the majority of the red weathering horizon containing numerous clasts, probably part of the flow top itself. Above the bole, the base of the next sheet flow lobe is vesiculated, this may be basal lobes but they are difficult to see. This flow-field contains at least one sheet flow lobe, but possibly more, if not, it is a 47 m thick sheet lobe. A benchmark with no height marked on it was observed at 178 m.

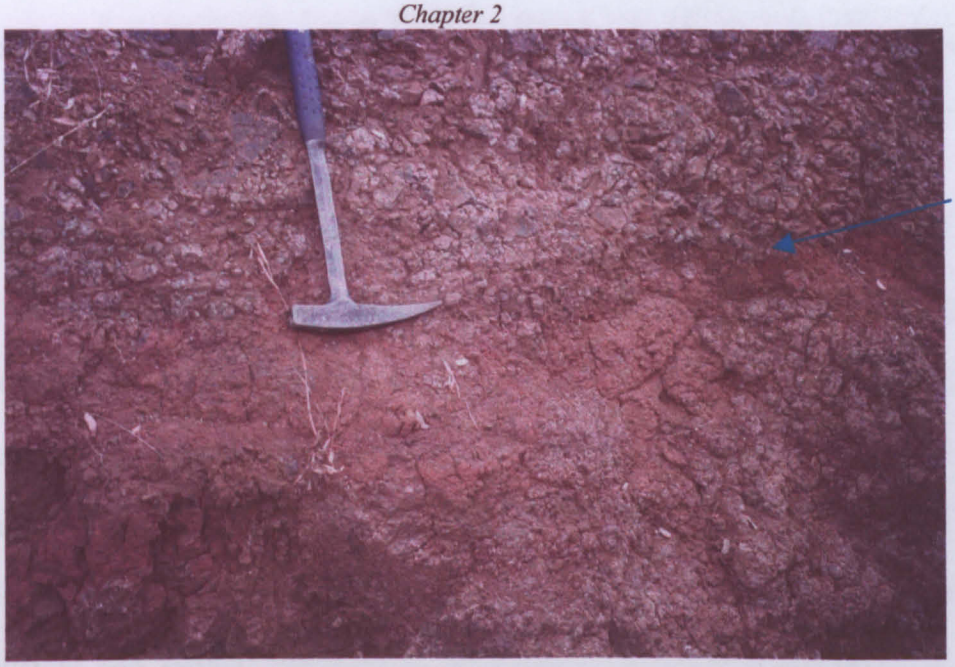

Figure 2.47. Slightly undulating red bole between two altered sheet lobes (168 m asl) Khumbarli Ghat in the Ambenali Formation. The saprolite is ~10 cm thick and grades down into the altered flow top. Lat. long. unavailable

Elev. 178-280 m asl

A 5-m-thick outcrop of solid, dark well-exposed basalt occurs between 179 and 184 m. It is the core of a sheet lobe which contains a few plagioclase needles up to 2 mm. Open, pipe-like vesicles are also seen, but not at the base of a sheet flow lobe, so they could be open vesicle cylinders which have been emptied of their volatile rich material. The road to Popoli (~lat. long. of road junction to Popoli 17°25'55.4"N 73°39'49.0"E) village leaves Khumbarli Ghat at ~192 m.

Colluvium covers much of the exposure up to 218 m. The next good exposure is only 10 m thick, observed between 218 and 228 m. This spheroidally weathered rock is pale grey on a fresh surface and moderately vesicular, with the vesicularity increasing up the exposure which contains 4-5% plagioclase in the form of glomerocrysts and laths. A small exposure at 236 m indicates that the basalt is the same as that observed below, but with a lower vesicularity. At 270 m a HVZ is observed but the contact with the sheet flow lobe above is not visible. The rock still has the same petrography as the outcrops below.

These exposures could still be the same sheet flow lobe, but it is unlikely. It is possible though that they all belong to the same flow-field

Elev. 280-326 m asl

At 280 and 290 m, the basalt has changed petrography; the plagioclase glomerocrysts are much fresher and the basalt is much darker and glassier. This may indicate a new flow-field, but no reddened horizons have been observed, and so these exposures may be part of the same sheet flow lobe. No flow top is observed until 326 m, this section could be a 65 m thick sheet flow lobe and/or flow-field. The flow top at 326 m is undulating and slightly reddened; it is underlain by a HVZ which has a higher plagioclase content than the outcrops below, (10%, of 2 mm glomerocrysts). This is significantly different to the outcrops observed below and could indicate a different sheet flow lobe.

Elev. 326-339 m asl

From 326-339 m the section contains a single inflated sheet flow lobe, possibly constituting a flow-field. It is very well exposed and contains 5-10% plagioclase in the form of laths and glomerocrysts and a few percent mafic minerals. The flow top has up to 50 cm of topography which may indicate the presence of break-out lobes. There is as much as 20 cm of friable, hard saprolite (Figure 2.48) on top of these which grades down into 1-1.5 m of red weathered flow top with less weathered vesicular, basaltic clasts.

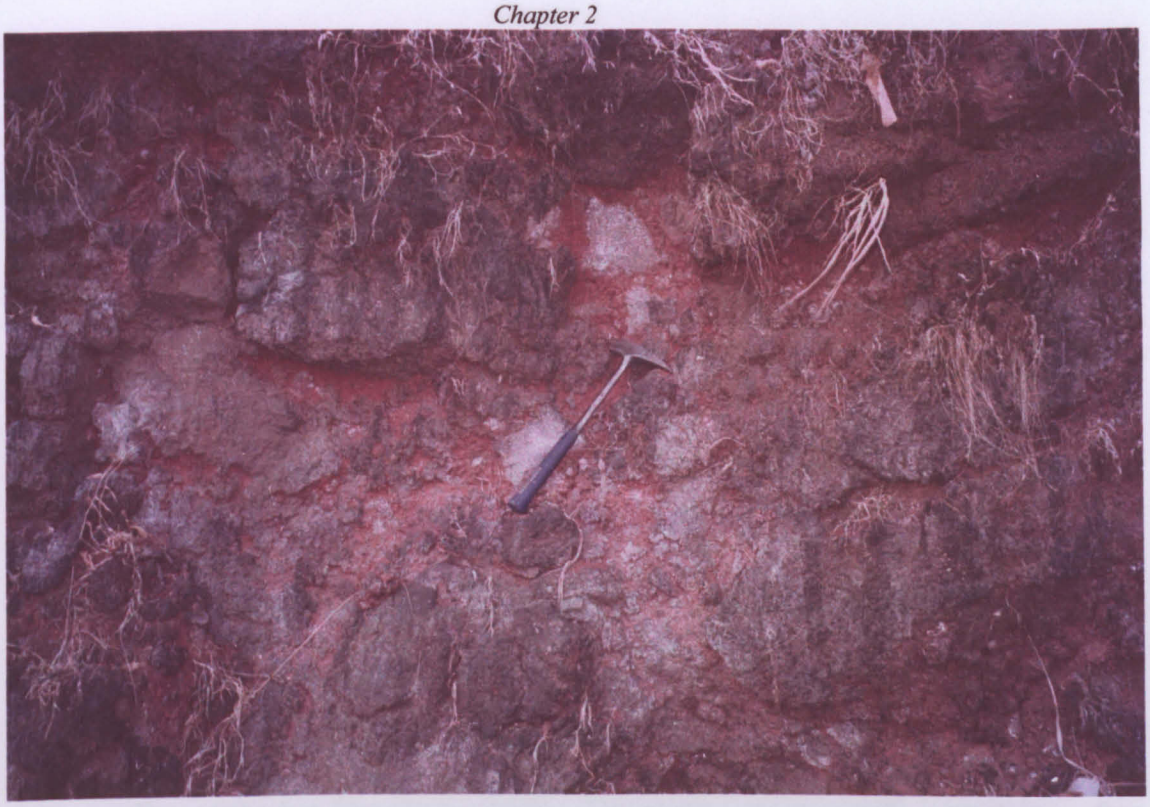

Figure 2.48. An undulating weathered flow top at 339 m asl on Khumbarli Ghat, in the Ambenali Formation, showing the typical weathering profile of saprolitic bole, however it is still possible to view the highly vesicular nature of the upper crust in the less weathered sections. Note how the semi horizontal cracks, in-filled with reddened material are parallel, probably indicating that these formed along highly vesicular horizons of the HVZ. Lat. long. 17°25'18.3"N 73°40'19.0"E

Elev. 339-459 m asl

Some areas immediately above the bole are highly vesicular, which may indicate the presence of precursor lobes. The core of this sheet lobe is poorly vesicular and contains only 1-3% plagioclase glomerocrysts. The top of this lobe is indicated by a highly amygdaloidal outcrop which may be a HVZ, but no actual flow boundary can be seen.

Six metres of flow core is visible from 355-361 m and the lava contains 2-3% of 3-4 mm plagioclase glomerocrysts. Poor to no exposure then dominates from 361-459 m. Eight metres of a sheet lobe core are observed between 398 and 406 m, containing <1% of 2-3 mm plagioclase glomerocrysts. Colluvium covers the subsequent areas of no exposure. At 442 m a thin red flow top is observed with 50 cm of its preceding vesicular and amygdaloidal flow top which contains 2% plagioclase crystals up to 1 cm across. This red flow top must indicate the top of a flow-field, but due to the limited exposure the identity

of the basal red bole is not definite, but it could be the same bole which is seen at 339 m. Poor exposure obscures much of the following 16 m of exposure but it can be seen that the groundmass of the basalt is very dark and fine with <1% of 1 cm plagioclase phenocrysts. An exposure further up shows a decrease in plagioclase size <1% of 1 mm plagioclase laths, perhaps indicating a different sheet flow lobe.

Elev. 459-479 m asl

Exposure from here (459 m) to the top of the pass (700 m) is excellent, with only a 16 m section of poor exposure (between 533 and 549 m). The visible section of the first sheet flow lobe (between 459 and 479 m) shows part of a core up to the flow top. Hackly joints and small secondary joints, perpendicular to the main joints (Figure 2.11), indicate water cooling of the hot lava (Lyle, 2000). The unit is poorly phyric, containing a few plagioclase laths ~1 mm long. Three vesicular masses were also observed. The first is approximately 3 m by 3 m (Figure 2.49) and the two further up are smaller, 1 m by 1 m. Both are highly vesicular and have radiating cooling joints, which suggests that they were cooler than the material they were entrained into. They appear to be what is sometimes referred to as war-bonnet structures (Viswanathan and Misra, 2002). The upper crust of this sheet flow lobe is unusual. The typical rounded bubbles arranged by size into horizons is absent here; instead the upper crust is dominated by irregular shaped vesicles, this is the most ʻaʻā-like unit that occurs in the field areas studied, but is probably a rubbly pāhoehoe lobe. The base of this flow lobe was obscured so it was not possible to see if rubble occurred at the base. The red bole at the top of this sheet flow lobe, and flow-field, is observed at 479 m. It is a reddened rubbly horizon 40 cm thick, indicating the depth to which weathering occurred.

Figure 2.49. A war-bonnet type structure. A highly vesicular mass in the centre of a sheet flow lobe, with cooling joints radiating from it. Khumbarli Ghat, ~472 m asl in the Ambenali Formation. Lat. long. Not available

Elev. 479-500 m asl

The subsequent flow-field comprises two sheet flow lobes. The first (479-491 m) sits upon the bole mentioned above yet, in places, it is welded to the sheet flow lobe below, which must be a local effect due to heating of the substrate. This unit is truly aphyric, dark and fine grained; occasional flow foliation is observed. Vesicular masses are again seen but the cooling joints are absent and the masses appear to have been partially 'digested'. This unit is welded to the flow above at 491 m, and there is no sign of reddening, suggesting that they are both part of the same flow-field. The next unit (491 to 500 m) is dark, aphyric and fine grained again with some flow foliation. The flow's crust indicates that this is spongy pāhoehoe and the 10 cm thick red bole above it undulates, possibly due to break-out lobes.

Elev. 500-572 m asl

A thin, aphyric sheet flow lobe with a maximum thickness of 5 m and length of 20 m, is the first unit observed in the next flow-field. This is surrounded by a much larger 15 m thick, aphyric sheet flow lobe, the flow top of which, at 519 m, undulates by 1-2 m, which is probably due to small break-out lobes. The sheet flow lobe above may have some precursor lobes below it, but what ever the case the two units above and below the boundary at 519 m are welded together. The unit above has a coarse-grained groundmass and contains 1-2% of 1-cm-long plagioclase crystals and sparse acicular plagioclase laths 3 mm long. Exposure is poor from 532-549 m. At approximately 540 m asl in the cliff on the opposite side of the valley is what looks like an angular disconformity in the sheet lobe, but this is not obvious in the road cuts. The final section of sheet flow lobe in this flow-field is 23 m thick and has the same petrography as the unit below the poor exposure. Within it, at 558 m, is a large mass consisting of moderately rounded basaltic clasts up to 3 m by 1 m which is partially matrix and partially clast supported. The matrix consists of a light ashy, sandy material. This may be sediment that has been washed into a rubbly flow top, but there appears to have been some movement of the clasts and the high degree of matrix material is unusual. Another interesting feature is a possible fault indicated by a stream bed at approximately 560 m asl, but the displacement, if any, must be relatively small. At the top of this flow-field (572 m), a saprolite and red weathering profile with a thickness varying from 10-75 cm occurs.

Elev. 572-605 m asl

The next 33-m-thick flow-field consists of a single sheet flow lobe. Again this unit contains flow foliation but it dips at 35°; the vesicles are aligned to this dip and the cooling joints cross them. The unit contains 2% plagioclase glomerocrysts which on average are 1 cm but occasionally up to 2 cm long, horizontal banded agate filled mega-vesicles are also observed which indicate that the basalt pile here has not undergone much

tectonism. The top of this unit (605 m) is marked by a reddened flow top which undulates by 2 m. There is no saprolite, but the red weathering profile is approximately 2 m deep. This sheet lobe is the final unit which has been recorded as having Ambenali Formation chemotype.

605-640 m asl

The next two flow-fields were not sampled and so it is impossible to place them in either the Ambenali or Mahabaleshwar Formations. Both are single sheet flow lobes, 35 m and 19 m thick respectively. The first sheet flow lobe has a medium-grained groundmass that contains 3-5% of 5 mm glomerocrysts, the concentration of which decreases up through the flow. Further masses are seen in this unit, however, they differ from those lower down the succession. Both are non-vesicular masses, the first at ~618 m asl appears to be slightly weathered and has cooling joints radiating from it, the second at 626 m is bigger, ~5 m across and is not weathered. At 630 m there is a zone of rubbly material, where vesicular and amygdaloidal basalt is surrounded by much denser rock; this does not appear to be part of the upper crust. In the upper crustal zone some of the clasts are spinose and appear to be welded together, typical of an 'a`ā flow, whereas in other parts the character is not rubbly but vuggy. Rubble-filled pipes, 2 m long and 2 cm wide were also observed in the upper crust. The flow top is variable; there is some slight reddening but no actual saprolite.

Mahabaleshwar Formation succession

Elev. 640-720 m asl

The sheet flow lobe above the unusual flow top at 640 m contains 5-10% of 1 cm long plagioclase glomerocrysts. This is the first unit to be positively identified as belonging to the Mahabaleshwar Formation chemotype. This unit is topped by a thin red bole, but again, no saprolite. As it is highly amygdaloidal and rubbly this may be flow top

breccia or part of the weathering profile. The red horizon may be the palaeomagnetic reversal from 29R to 29N, but the sampling density is not high enough to determine it exactly.

The flow morphology changes slightly from here (669 m) to the top of the pass at 700 m asl. The thickness of the units decreases markedly and they become small lobes and toes, some only centimetres thick (Figure 2.50). The first two sheet flow lobes are welded together and are 5 m and 10 m thick respectively, both contain 1% of 5 mm long, plagioclase needles. The remaining units of this 50 m thick flow-field are aphyric. The reddened flow top at 690 m shows some pāhoehoe ropes, so the weathering was either not destructive or short-lived.

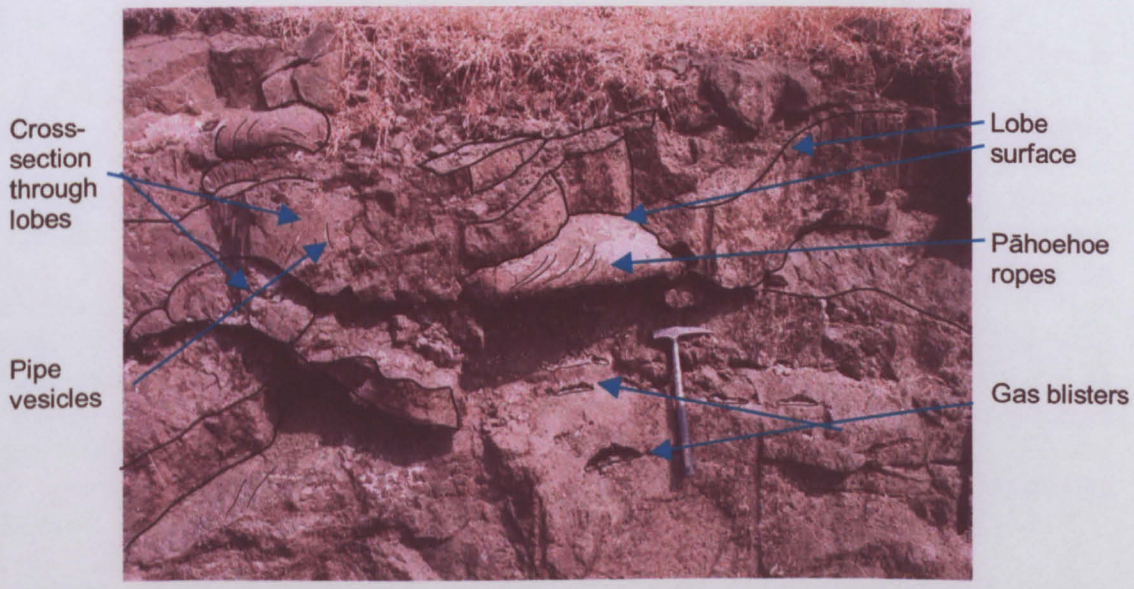

Figure 2.50. A series of small pāhoehoe lobes and toes, some showing rope structures, pipe vesicles and HVZ. Khumbarli Ghat ~685 m asl in the Mahabaleshwar Formation. Lat. long. 17°23'53.3"N 73°40'09.9"E. (Photo by S. Self)

The final road-level unit is a single sheet lobe 10 m thick. The petrography has changed considerably as it contains 10% of 2-3 mm blocky plagioclase crystals. It is capped by a red saprolite up to 10 cm thick at 700 m, and this single sheet lobe constitutes a flow-field. There are approximately three thick sheet flow lobes visible in the cliff above the road. A sample taken from a road-side boulder, assumed to come from the cliff, above

the road contained 10% of 1-1.5 cm plagioclase crystals, and is assumed to either be a continuation of the Mahabaleshwar Formation chemotype lavas or be of mixed Ambenali/Mahabaleshwar chemotype, as observed on the Mahabaleshwar Plateau traverses.

2.6.7 *Matheran-Neral road*

- *Appendix A7,*
- *Geochemical data Appendix C8,*
- *Palaeomagnetic data appendix B8,*
- *Static GPS data Appendix D2,*

The Matheran-Neral section was logged up the road to the Matheran tableland. This mesa is situated ~ 125 km north west of Mahabaleshwar and about 50 km east of Mumbai (Figure 2.1). This traverse is lower in the DVP sequence than the previous sections, as it contains basalt from the Neral, Thakurvadi, Bhimashankar and Khandala Formations. The base of the section is at 50 m and the top of the section is at approximately 680 m.

Neral Formation succession

Elev. 50-166 m asl

The lowest exposure is in a river bed, where moderately small, aphyric pāhoehoe sheet flow lobes occur. These show infill from the flow above into the depressions between the flow lobes. Thin aphyric sheet flow lobes continue up to approximately 160 m with sporadic sections of poor or no exposure. At 120 m one lobe is welded to the lobes below. In this series of decimetre scale lobes, ropey flow tops and some moderately unaltered volcanic glass were identified (Figure 2.51). At 160 m the petrography is beginning to change, below 160 m the flow tops appear to contain some small glomerocrysts of olivine and clinopyroxene, above this elevation aphyric units dominate. The flow boundary itself is slightly rubbly but there is no reddening. A similar horizon is observed at 166 m. It is impossible to say if these represent time breaks.

Figure 2.51. Ropey texture on a small pāhoehoe lobe. The average sheet lobe thickness in this outcrop is 1 m. This basalt is the lowest outcrop of the Neral Formation in the area and is located next to the Neral, Matheran road, 50 m asl, close to electricity pylons. Lat. long. 19°01'04.2"N 73°18'54.0"E (Photo by S. Self)

Elev. 166-175 m asl

A single sheet flow lobe 9 m thick (166-175 m) is a GPB containing ~20% plagioclase crystals up to 2 cm long. These mark the final units of the Neral Formation. The majority of the flow lobes from 175-555 m are aphyric.

Thakurvadi Formation succession

Elev. 175-243 m asl

The first sheet lobe of the Thakurvadi Formation at 175-184 m asl contains 2-3% of 3-4 mm plagioclase laths, and another at 193-202 m contains 5% plagioclase crystals 1-4 mm. Similar sequences of lobes continue to 230 m; 10 m of no exposure occurs before Jammu Patti Railway Station is encountered at 243 m asl.

Elev. 243-260

Light coloured lobes occur in the cutting of Jammu Patti Railway Station and above. Crude columnar joints are observed in some of the lobes. These lobes are on average 1-2 m thick.

Elev. 260-515 m asl

The final unit below the main bench (~260 m asl) is either a very weathered flow or a colluvial deposit. The bench provides a zone of no exposure from 263-320 m. There are a series of centimetre-scale lobes from 337-362 m, in which occasional dark spots are seen that may be weathered mafic minerals. The next series of sheet flow lobes, from 362-476 m forms a dry waterfall and therefore the majority of the units are not accessible for close inspection (Figure 2.52). The top flow of this sequence, at 476-485 m, contains small (1-2 mm) thin acicular plagioclase crystals which can be observed despite the highly weathered nature of this unit. Due to this unit's position immediately below a topographic bench (485-515 m), it is difficult to know if this is modern or original alteration.

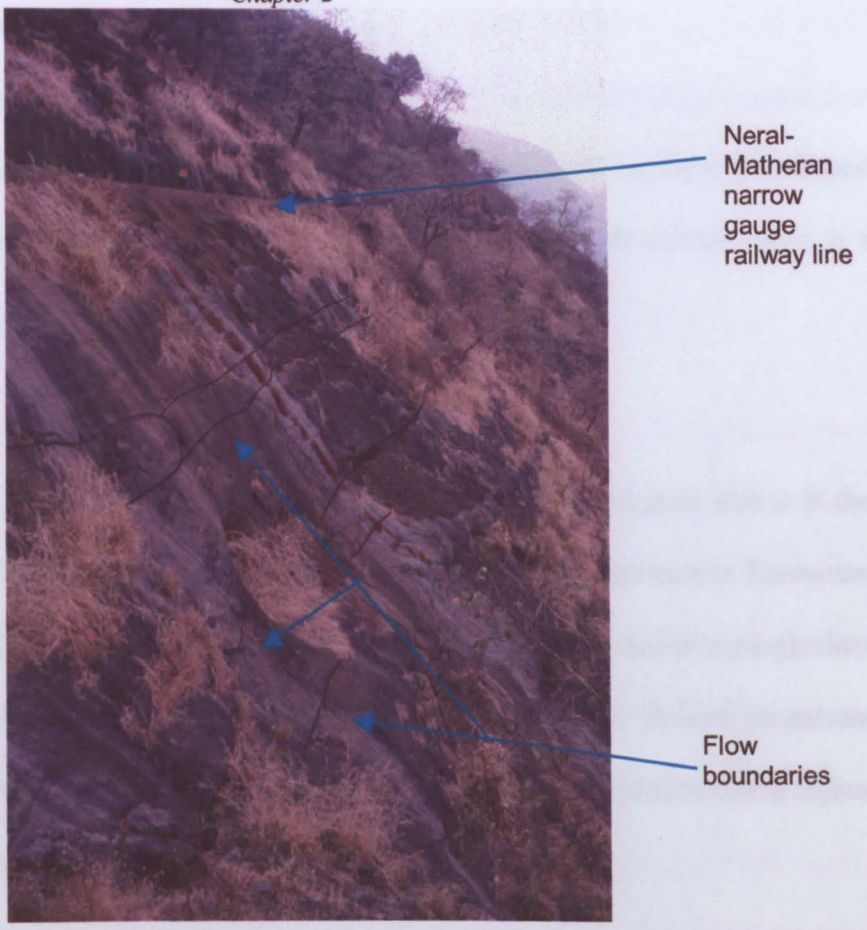

Figure 2.52. A series of stacked sheet lobes exposed on a very steep slope between 362 and 476 m asl on the Matheran Ghat traverse, in the Thakurvadi Formation. This exposure forms a waterfall in the wet monsoon and hence has limited vegetation cover, but erosion has masked many of the features, flow boundaries however, can be observed. Lat. Long. unavailiable.

Elev. 515-562 m asl

On top of the topographic bench is an exposure of black aphyric rock at 515 m. This is the first exposed unit in a 45-m-thick pile of 1-2-m-thick pāhoehoe lobes which are welded together. The boundaries between them are best distinguished using vesicle distributions. At the top of this section is an 8 m thick sheet flow lobe which contains 15% plagioclase needles but no glomerocrysts. Above this unit is the first red bole of the section; it is discontinuous so is only seen in small pockets. Subbarao et al. (2000) state that this is the Thakurvadi-Bhimashankar Formation boundary.

Bhimashankar Formation succession

Elev. 562-581 m asl

The flow lobe above the pockety bole at 562 m asl contains 20% star-shaped glomerocrysts. There is a possible contact at 570 m and the sheet flow lobe above is a spotty rock which is, again, possibly weathered mafic minerals.

Elev. 581-596 m asl

The coarse-grained nature of the next well-exposed flow suggests that it is the 'Giravali flow' (~581-595 m) and is the top-most unit of the Bhimashankar Formation (Subbarao et al., 2000). It is a GPB and contains 2 to 3 cm-long weathered plagioclase crystals. Thus the Bhimashankar Formation is different to all the other defined formations studied in that it consist of only three lava units at this location, both with different crystal content but with no weathering between them, i.e., it is one flow field.

Khandala Formation succession

Elev. 596-641 m asl

From 596-603 there is no exposure. From 603-616 m is a basalt with a coarse groundmass with small red crystals which may be weathered pyroxene, this has been named the 'Khandala KGC unit' (Subbarao et al., 2000). Above this is the 25 m thick 'Khandala aphyric flow', this is a dark fine-grained lava, which again contains a few red crystals. At the top of this sheet flow lobe is a rubbly slightly reddish flow top, marking the top of an 80 m thick flow-field, one of the thickest found in this study.

Elev. 641-680 m asl

The next two flow-fields are similar to some of those seen around the Mahabaleshwar Plateau, i.e., one sheet flow lobe forming one flow-field. The lower, 641-660 m is the 'Upper Khandala Aphyric flow' (Subbarao et al., 2000) and again contains a few red crystals. The bole at the top of this unit is 5 cm thick. The penultimate unit is only

7 m thick, it has the same petrography as the flow lobe below. The red horizon on this flow top is very thin, probably altered glass. The final flow observed at road level is possibly the 'Khandala phyric unit' (Subbarao et al., 2000). It is a hard, dark rock with a fine-grained glassy groundmass containing sparse plagioclase and pyroxene glomerocrysts. Another flow is visible above the road but it was not visited on this occasion.

2.7 Summary of the observed volcanic features

The volcanological features observed during field work in the DVP are typical of those commonly observed in many stacks of inflated pāhoehoe lava flows dominated by sheet flow lobes. The lobes themselves occur in a variety of sizes from small Hawaiian-sized, P-type lobes, (i.e., a few tens of centimetres thick, to a few metres thick) to massive sheet lobes up to 60 m thick, and presumably many hundreds to perhaps kilometres long. However, in general, these basaltic sheet lobe units tend to be ~20-25 m thick.

Many of the units observed during field work display the three divisions typical of an inflated sheet flow lobe, that is, the basal crust, lava core and upper crustal zone. However, in some units, poor or no exposure obscured various parts of these divisions. Nevertheless, this three-fold division aided the identification of different sheet lobes even if the actual contact was not visible; for instance, the upper core is often identifiable by the slight increase in vesicularity from the normally non-vesicular centre, into a zone with large sparse vesicles or mega-vesicles. If a section of no exposure occurs above the zone identified as the upper core, and the next visible outcrop has a very low vesicularity, then it is probable that this exposure is the core of the next sheet lobe in the sequence, and that the intervening upper crustal zone, flow contact and basal crust have been obscured because they are more easily weathered and erodible. On the occasions that the basal crust is visible, it is common for small pāhoehoe lobes and toes to occur below the highly vesicular

basal zone (Figure 2.53). Bigger sheet lobes often show little evidence of basal crusts and hence have low vesicularity except in the top of the upper crustal zone.

2.7.1 Flow-fields, lava flows and sheet flow lobes

The flow-fields have been identified on the logs, and each one is shown by brackets. The number of flow fields observed in each section is shown in Table 2.4 and discussed in Section 2.7.2.

Ghat section	Minimum number of flow fields	Section thickness m	Ave. exposed sheet lobe thickness m
Ambenali Ghat	29	1235	17
Tapola Road	8	563	21
Kelgar Road	16	455	16
Wai-Panchgani Road	15	450	19
Varandah Ghat	8	572	
Khumbarli Ghat	12	580	19
Matheran Ghat	5	632	

Table 2.4. The number of flow-fields, as defined in Section 2.2.1, in each traverse, and the average thickness of exposed sheet lobes, Matheran and Varandah Ghats are not shown as the average thickness of thin lobes is not known.

The identification of the number of lava flows (in the context that this term is defined in Section 2.2.1) has, however, proved difficult to count. It is probable that if a flow-field could be followed across a large area, i.e., the Mahabaleshwar Plateau, then the units seen would most probably be composed of different lava flows.

All of the traverses have varying proportions of no and poor exposure so it is not always possible to calculate the exact number of thick sheet lobes in each traverse, but this has been estimated in Section 2.7.2. The percentage of exposure of logged section which contains lobes less than or greater than 15 m thick can be calculated (Table 2.5). It is clear that the thicker lobes (>15 m) dominate except in the Matheran Ghat section, which is the only section in a different part of the DVP sequence to the Mahabaleshwar regional formations.

Ghat section	% of good exposure in traverse section dominated by lobes over 15 m	% of good exposure in traverse section dominated by lobes under 15 m
Ambenali Ghat	92	8
Tapola Road	97	3
Kelgar Road	100	0
Wai-Panchgani-Road	98	2
Varandah Ghat	70	30
Khumbarli Ghat	87	13
Matheran Ghat	23	77

Table 2.5. The percentage or good exposure containing lobes more than and less than ~ 15 m thick in each traverse studied

2.7.2 Summary of the traverses

This section provides a brief summary of the volcanostratigraphical characteristic of the seven traverses logged and an estimate of the number of flow-fields and sheet lobes in each chemostratigraphical formation along each traverse. As this is an estimation of the volcanological units within each formation chemotype, the elevations and thicknesses given correspond to the actual known thicknesses of formations and generally leaves out the zones of exposure with unknown chemotype.

Ambenali Ghat

Overall Ambenali Ghat is dominated by thick sheet lobes, but the lowest exposed section, in the Bushe Formation, is formed of thin pāhoehoe lobes and toes, usually less than 2 m thick, with a maximum thickness of 4 m. The Poladpur Formation is generally very poorly exposed. However, the sections of sheet lobes which are exposed have the characteristics of thick sheet lobes rather than small lobes and toes. There are very few red boles in the Poladpur Formation possibly due either to the poor exposure or to a real absence of extended periods between eruptions. The number of boles increases towards the top of the Formation and into the Ambenali Formation. This latter Formation is dominated by thick sheet lobes. In the lower part of the Ambenali Formation it is relatively common for a single sheet lobe to form a flow-field. However, the characteristics of the units changes between 573-610 m where the lava returns to small lobes and toes, the thickest being ~ 7 m, but the flow-fields become thicker and contain more but smaller sheet lobes. This reverts back again to thinner flow-fields towards the

top of the Ambenali Formation and into the Mahabaleshwar Formation and the mixed Mahabaleshwar/Ambenali Formation chemotype. The quality of the exposure decreases markedly above 1107 m to the top of the Plateau.

There is only 17 m of the Bushe Formation exposed on Ambenali Ghat. No red boles or erosion horizons are observed in this part of the succession, so it can be assumed that the outcrop of small pāhoehoe lobes form one flow-field. The Poladpur Formation is identified in the Ambenali Ghat section from 58 m to 333 m asl although it may be as high as 367 m asl (Pg. 62) (283 or 256 m thick). It is impossible to determine the number of eruptive units, although the upper 60 m contains at least four flow-fields, which represent four separate eruptions. Thus, if these are representative of the typical thickness of a flow-field (~15 m) in the Poladpur Formation, it is probable that this formation is formed from seven or eight flow-field-forming eruptions.

On Ambenali Ghat the total thickness of the exposed Ambenali Formation from (333 m or) 367-934 m (567 or 601 m thick) contains about sixteen or seventeen flow-fields and approximately twenty four sheet lobes. Not including: precursor lobes, break-out lobes and the small lobes and toes between 570 and 610 m asl, i.e., all those lobes under 5 m thick, (lobes under 5 m thick are not included in all the descriptions in this Section).

The Mahabaleshwar Formation is exposed from 934-1059 m (125 m thick) and contains ~ four flow-fields and ~ seven sheet lobes. The mixed Mahabaleshwar/ Ambenali Formation chemotype occurs from 1059-1205 m (~146 m thick) although much of this is no exposure. Portions of three flow-fields are visible and it is formed of at least four sheet lobes. Due to no exposure covering the boundary between the mixed chemotype and the upper Ambenali Formation chemotype above it is only possible to say that the upper Ambenali Formation chemotype is exposed from 1252-1255 m and that this is part of a single flow-field and two sheet lobes.

Tapola Road

The Tapola traverse is dominated by poor and no exposure. It is difficult to work out the characteristics of the units, as so much detail is obscured. Both the Ambenali and Mahabaleshwar Formations are dominated by thick sheet lobes, with one or two sheet lobes forming each flow-field. Towards the top of the traverse the sections of no exposure become smaller but are still frequent, but the characteristics of the outcrops suggest that thick sheet lobes still dominate.

The section of Ambenali Formation which is observed on this traverse occurs from 690-857 m and contains at least four flow-fields and at least six sheet flow lobes. The Mahabaleshwar Formation on this traverse (857-1005 m, 149 m thick) contains at least two flow-fields a minimum of three sheet flow lobes but the large amount of no exposure probably masks many more sheet lobes and boles which would indicate more flow-fields. Mixed Ambenali/ Mahabaleshwar Chemotype is from 1005-1140 m (135 m thick) and consists of at least three flow-fields and three sheet lobes. The upper part of the traverse, with a return to Ambenali Formation chemotype from 1175-1222 m (46 m thick), contains at least one flow-field and two sheet lobes, but again exposure limits the full understanding of the nature and number of units in this section.

Kelgar Road

The Kelgar traverse has the highest percentage of good exposure of all the sections studied. The Ambenali Formation in this section is dominated by flow-fields formed of more than one sheet lobe. This continues into the Mahabaleshwar Formation but after the first flow-field the majority of the flow-fields are formed from only one sheet lobe. Between 1032-1043 m the section is dominated by thin lobes a few metres thick, but not as small as those that typify the Bushe Formation. The characteristics of the remaining units are similar to those immediately below the thin lobes.

On the Kelgar traverse the exposed section of the Ambenali Formation (770-858 m, 89 m thick) is formed from only two flow-fields and ~six inflated pāhoehoe sheet flow lobes. The Mahabaleshwar Formation chemotype on the Kelgar traverse (858-1032 m, 174 m thick) contains ~ six flow-fields and ~ nine sheet lobes. The mixed Ambenali/ Mahabaleshwar Formation chemotype on the Kelgar Road (1043-1150 m) contains three flow fields which together comprise of at least three sheet flow lobes. The upper section of the traverse which has Ambenali Formation chemotype (1150-1225 m, 75 m thick) contains at least three flow-fields and ~seven sheet lobes.

Wai-Panchgani

The Ambenali Formation exposed on the Wai-Panchgani Road is dominated by thin flow-fields which have only one sheet lobe forming them. With the exception of the first flow-field in the Mahabaleshwar Fm, which is thick and contains a few small lobes, and the second flow-field which consists solely of lobes up to a few metres thick, the remaining traverse has the same characteristics with flow-fields dominated by single sheet lobes, however the sheet lobes are thicker than lower down in the section.

The exposed part of Ambenali Formation in this section is approximately 145 m (770-915 m) thick and contains six flow-fields, composed of at least eight sheet flow lobes. The Mahabaleshwar Formation is formed of five flow-fields consisting of at least seven sheet lobes. The zone, of mixed Ambenali and Mahabaleshwar Formation chemotype (1089-1165 m) contains at least two flow-fields and two sheet lobes. In this traverse the occurrence of the upper Ambenali chemotype Formation (1165-2020 m) is formed from at least two flow-fields and two or three sheet lobes.

Varandah Ghat

Varandah Ghat has large tracts of poor exposure (Appendix A5) but the outcrops in the lower parts are dominated by thin toes and lobes with no occurrence of a bole

horizon until 267 m asl. Poor or no exposure makes up 54% of the first ~ 400 m of the Varandah Ghat section and it is therefore not possible to determine if this is only two flow-fields. The upper third of this traverse (in the upper section of the Poladpur Formation and the lower Ambenali Fm.) is dominated by much thicker units, similar to those seen on the Mahabaleshwar Plateau, and red boles are common between each thick sheet flow lobe. In contrast, a considerable number of small, either precursor or break-out lobes, are much more common or well-preserved than in the main study area.

On Varandah Ghat the Bushe Formation (from 10-216 or 231 m, pg. 101) contains at least one flow field and at least five sheet flow lobes. The lack of exposure in this section may mask the occurrence of other sheet lobes and boles, which would indicate separate flow-fields. The Poladpur Formation on this traverse contains two flow-fields consisting of at least six sheet lobes, but again poor and no exposure dominates this section of the traverse. The section of the Ambenali Formation (from 470 to 560+ m) which is exposed on this ghat section consists of four flow-fields and three sheet lobes (one of the flow fields consists entirely of lobes less than 5 m thick). Although sampling stopped at 560 m, the Ambenali Formation is assumed to continue well above this point.

Khumbarli Ghat

The lower sections of Khumbarli Ghat, in the Ambenali Fm., (Appendix A6) are poorly exposed and so it becomes problematical to determine the thickness of the sheet lobes and flow-fields. As exposure increases up the section, 20-35 m thick sheet flow-lobes are often separated by red boles and weathering horizons dominate, as seen in the Mahabaleshwar Plateau region. However, this changes above the palaeomagnetic reversal horizon (towards the base of the Mahabaleshwar Formation) and a 30 m section of small pāhoehoe lobes dominates. The units above this were inaccessible but are exposed above road level and appear to be dominated again by thicker sheet flow-lobes.

The section of Ambenali Formation (120-605 or 640 m) exposed on Khumbarli Ghat contains at least nine flow fields consisting of at least seventeen sheet flow lobes. Although poor exposure may have masked some sheet lobes, flow boundaries and boles. The exposed section of the Mahabaleshwar Formation on this traverse (605 or 640 -700+ m) contains at least four flow-fields formed of six big sheet lobes, but many small lobes and toes are also observed in this formation.

Matheran Ghat

It is important to note that the Matheran traverse differs greatly from the previously described sections. The whole section, barring the upper few units (in the Khandala Formation) is formed from relatively small pāhoehoe lobes and toes. The first red bole horizon appears after approximately 500 m of section. Although the exposure is not perfect it seems probable that enough is visible to suggest that this may be all one flow-field or that eruptions followed each other very quickly. The exposure towards the top of the section becomes poorer, and the occurrence of boles increases.

The Neral Formation on Matheran Ghat (50-175 m) contains no boles, so it is not possible to determine if different flow-fields exist. There are four sheet lobes thicker than approximately 5 m. The Thakurvadi Formation (175-562 m) contains no observed weathering horizons, except for the one that marks the termination of this formation. It contains only five sheet lobes which are definitely thicker than 5 m, the remainder being smaller pāhoehoe lobes and toes. One or possibly two sheet lobes form the Bhimashankar Formation on Matheran Ghat (from 562-577 m). No red bole is found capping this formation, so under the classification used in this thesis it is not a flow field, although the geochemical signature (Beane, 1988; Subbarao et al., 2000) indicates that it must be. The Khandala Formation in the Matheran Traverse (577-680+ m) contains at least four flow

fields and at least seven sheet flows, although again sections of poor and no exposure must mask more units.

Traverse	Number of exposed flow-fields	% good and poor exposure	Approx. total number of flow-fields
Ambenali Ghat	30	70	43
Tapola Road	9	68	13
Kelgar Road	14	92	15
Wai-Panchgani Road	15	100	15
Varandah Ghat	10	69	14
Khumbarli Ghat	13	94	14
Matheran Ghat	-	-	-

Table 2.6. Approximate total number of flow-fields in each traverse calculated by taking the number of flow-fields identified and dividing by the percentage good and poor exposure. Matheran has not been calculated due to the difficulty in defining flow fields in the sections where there are no boles.

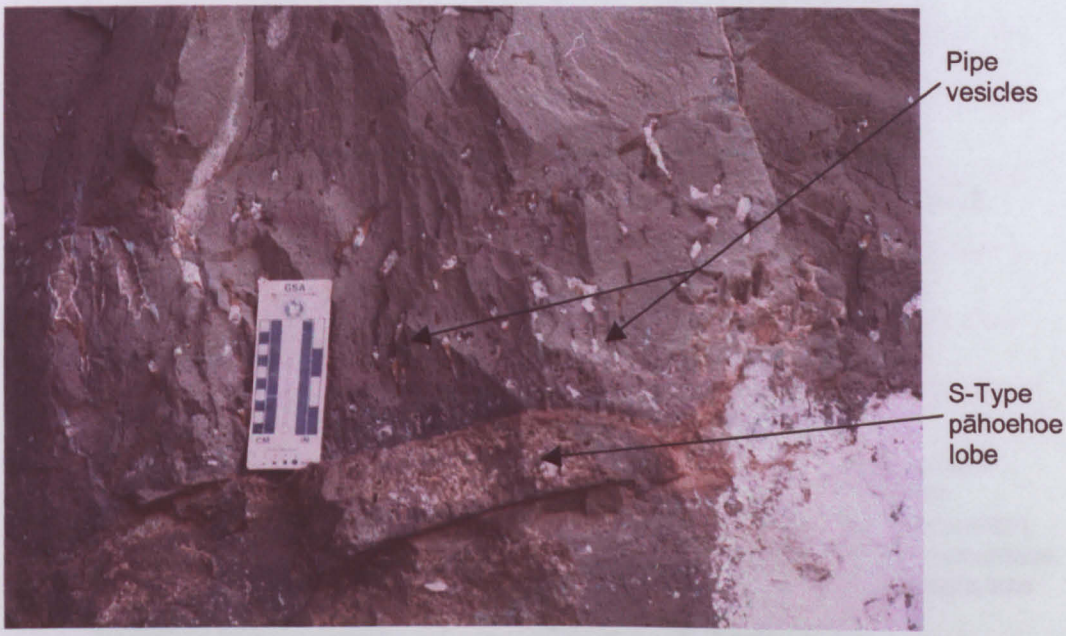

Figure 2.53. Basal zone of a ~ 2 m thick sheet lobe in the Ambenali Formation, showing moderate vesicularity and pipe vesicles. Note the S-type (spongy pāhoehoe) toe beneath (this is a close up of the lava flow above the bole in Figure 2.43). Varandah Ghat 470-474 m asl. Lat. long. not available (Photo by S. Self)

2.7.3 Vesicles

The type and degree of vesiculation seen in this area of the DVP varies considerably. The basal crust of the thick sheet lobes often contains vesicles up to 1 cm (Figure 2.53) but rarely contain pipe vesicles, which are only common in the smaller lobes and toes (e.g., Varandah Ghat 383-399 m). The vesicles in the core can generally be divided into three categories: mega-vesicles, gas blisters and bell-jar vesicles, although smaller vesicles do occur. Mega-vesicles are wider than they are deep, whereas, bell-jar vesicles, as their name suggests are deeper than they are wide. The lava cores in the study

area are, however, poorly vesicular. The lower upper crustal zone is marked by an upwards increase in vesicularity (Figure 2.54). Lower down the vesicles are big but few in number and, this pattern reverses towards the top of the sheet lobe. HVZ can often be observed at localities were the upper crust is visible (Figure 2.8 and Figure 2.54). Many of the vesicles are in-filled or partially in-filled with secondary minerals; the smaller vesicles are more prone to be fully amygdaloidal. Large vesicles observed in the upper crust are called gas blisters.

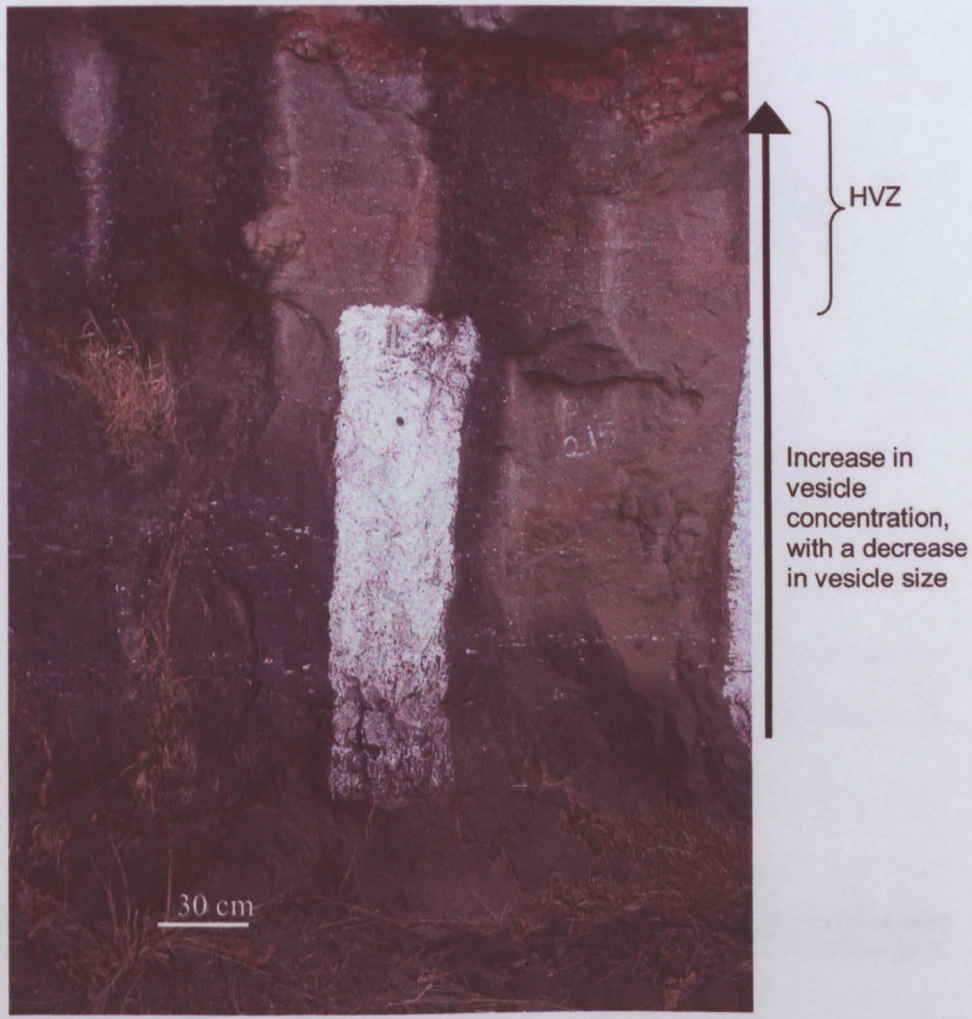

Figure 2.54. Upper crustal zone of an amygdaloidal sheet lobe (Ambenali Formation) showing the discrete size banding and the increase in vesicle concentration but decrease in vesicle size up through the upper crustal zone, grading into the red weathering horizon at the flow top. Varandah Ghat ~470 m asl, adjacent to the small lobes in Figure 2.43. Lat. long. unavailable

2.7.4 *Jointing*

The jointing in the sheet lobes studied varies in style and degree of development. The smaller lobes and toes rarely display columnar jointing, but this was, nevertheless, observed in some localities. The thicker inflated sheet lobes often show poorly-developed, wide columnar joints (Figure 2.55). Some units show well developed jointing, although they are dominated by hackly (Figure 2.11) and fanned (Figure 2.41), or vertical (Figure 2.55), joints with secondary smaller perpendicular joints (Figure 2.11).

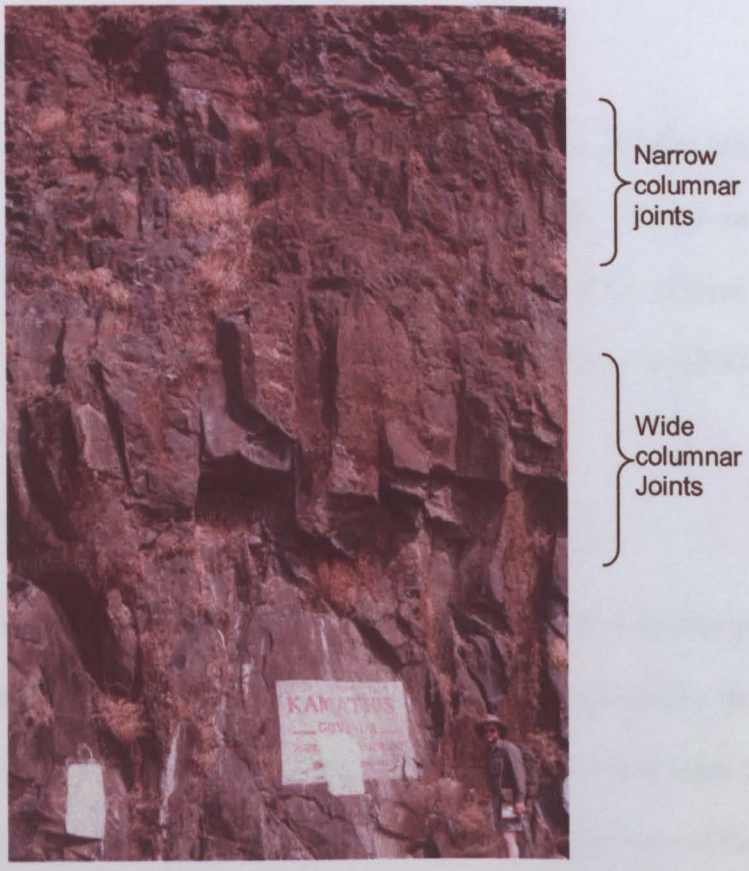

Figure 2.55. Wide, poorly developed columnar joints below narrow, poorly developed joints in a flow core above the green bole on Ambenali Ghat ~1100 m asl. Lat. long. 17°54'45.5"N 73°37'27.2"E (Photo by S. Self)

2.7.5 *Rare volcanic features observed*

Other, less-common features were observed in the field area and are described here.

Tumuli (Section 2.2.2)

A number of probable pāhoehoe tumuli (Walker, 1991) were identified on the Wai-Panchgani road (968-972 m) and Kelgar road (1148-1150 m). They were only seen in two dimensions and have a central solid core surrounded by highly vesicular dipping 'walls' (Figure 2.34).

Segregation features (Section 2.2.2)

A small percentage of the sheet lobes, both thick and thin, display segregation features (e.g., ~1000 m Kelgar Ghat and 525 m Varandah Ghat). Occasionally only vertical vesicle cylinders are seen but more commonly they feed HVS (Figure 2.4 and Figure 2.10). The frequency of these features is low compared with other CFBs such as the CRBG (S. Self, pers. comm., 2004).

Pāhoehoe surfaces

The upper surface of many of the small Hawaiian-sized lobes display pāhoehoe ropes (e.g., 50 m Matheran Ghat and ~685 Khumbarli Ghat) and, occasionally (relatively) unaltered volcanic glass (~135 m Matheran Ghat). The thicker sheet flow lobes are often topped by weathering horizons and/ or smaller breakout lobes so the features of their upper surface are usually destroyed, although stretched vesicles, typical of the upper surface of a pāhoehoe lobe are occasionally found (Figure 2.23).

Vesicular masses and war-bonnets

The only structures observed that remain unidentified and unexplained were seen on Ambenali Ghat and Khumbarli Ghat. Large, often 3-4 m deep and the same or wider, highly vesicular masses, often highly amygdaloidal were observed on two traverses. Two

were seen on Ambenali Ghat, (1040 m), the larger showing some possible signs of quenching in the host lava and trains of vesicles that appear to be rising around it but no obvious jointing relating to the vesicular mass. On Khumbarli Ghat, the masses are more typical of so-called 'war-bonnet structures' (Figure 2.49) (Viswanathan and Misra, 2002), although some did not have radiating columnar joints but show signs of chilling (Figure 2.56). These masses are also highly amygdaloidal but usually display cooling joints which radiate from the mass. War-bonnet structures in the CRBG are sometimes small but relatively thick inflated lobes with well-developed radial columnar joints and low vesicularity. They are not the same as these features (S. Self, pers. comm., 2004)

Figure 2.56. Dark, chilled margin around an unidentified vesicular, amygdaloidal object, similar to the war bonnet structure in Figure 2.49 within a sheet lobe. Khumbarli Ghat at ~480 m asl in the Ambenali Formation. Lat. long. not available (Photo by S. Self)

2.8 Discussion

2.8.1 The number of flow-fields/ eruptive events contributing to the DVP in the study area

The identification of flow-fields (Section 2.2) provides an indication of the number of eruptive events that formed the DVP in the areas of study, but the distance from the vent

and the degree of exposure will influence the number of flow-fields observed at any location.

Ambenali Ghat has the highest number of flow-fields identified, mostly because the section is almost twice as thick as the other ghat sections, although it does have a low percentage of good exposure (47 %; Table 2.3). The approximate number of flow-fields in the whole traverse is 43 (Table 2.6). Kelgar and Wai-Panchgani traverses have a similar number of observed and estimated flow-fields (Table 2.3 and Table 2.6) and this is probably a good representation of the number of units present in the section as the amount of exposure is good (Table 2.3). The similar number of flow-fields in both the Kelgar and Wai-Panchgani traverses is possibly due to the same flow-fields and possibly sheet lobes forming both sections. This could also be the reason for the percentage of good, poor and no exposure being similar in both traverses because lava units with the same characteristics and susceptibility to weathering occur on both traverses. Tapola, however, has only eight observed flow-fields, the lowest of all the Mahabaleshwar Plateau traverses, but it is estimated to have 13 (Table 2.6). This difference between observed and estimated is due to the low percentage of good exposure, only 45 %, which makes firm identification of flow-fields difficult by limiting the exposure of weathering horizons. Varandah Ghat also has a paucity of flow-fields. This could be due to two things: i) there is poor exposure of the first 400 m, in the lower Poladpur Formation (N.B this was also seen on Ambenali Ghat), which may have obscured weathering horizons. ii) Despite the poor exposure there may simply be fewer flow-fields in the Poladpur Formation. The estimated total number of flow-fields is 14 (Table 2.6). Khumbarli Ghat however, despite having a low percentage of good exposure only 54 %, has only a slightly lower number of observed flow-fields (12) than the Kelgar (16) and Wai-Panchgani (15) traverses, but the Khumbarli Ghat section is 130 m thicker. This indicates that even 60 km to the south of the Mahabaleshwar Plateau there are similar numbers of flow-fields and so units do not appear

to 'die out'. The estimated total number of flow-fields is 14, similar to the traverses of the Mahabaleshwar Plateau. By contrast, Matheran Ghat has a very low number of flow-fields, but a relatively high percentage of good exposure. However, the number of boles observed is low in much of this section and hence making the division into flow-fields (Section 2.2) using the definition used in this work, rather uncertain.

It is possible to deduce the lateral extent of some of the flow-fields from the number of flow-fields in the different traverses round the Mahabaleshwar Plateau. The number of flow-fields between recognised 'marker' horizons (the 29R/29N reversal horizon and the change between two chemotypes, for instance) in each logged section around the Mahabaleshwar Plateau varies. It is therefore clear that not all the flow-fields cover the entire Mahabaleshwar Plateau area. There is also insufficient information to say how wide the flow-fields are in extent, as it is not known how far each flow-field extended towards the west, as this area has been eroded off by the regression of the Western Ghats Escarpment. However, it is possible to say, however, that each flow-field may not cover the vast majority of the volcanic edifice i.e., the DVP, but some do cover an area at least equal to the size of Mahabaleshwar Plateau (~30-40 km across).

2.8.2 The location of the vents

The distribution of thin pāhoehoe lobes in the Matheran Ghat study area (Deshmukh, 1988) was believed to be related to the closer proximity to the vent areas (Walker, 1972), although no vent systems or deposits have been found. In fact, as no vents have been located, all it is possible to say is that the older formations which constitute Matheran Ghat are generally made of thinner and smaller pāhoehoe units, and the younger formations are composed of thicker and larger units. This, however, could also be an incorrect assumption, as due to erosion it is impossible to observe whether the younger units, e.g., those of the Wai Sub-group, were smaller and more Hawaiian-like further north than those

observed at Matheran Ghat and similar areas. The only older unit which is visible to the south is the Bushe Formation, and the outcrops of this formation in my field areas are dominated by small, Hawaiian-sized, lobes and toes, but sheet lobes up to 15 m thick do occur in Varandah Ghat.

It seems probable that at least some of the DVP vents were in areas which are now offshore, as no evidence for vents has been found on land. If this is the case then from Mahabaleshwar the minimum distance that lava would have had to have travelled to the Mahabaleshwar area is ~70 km. However, if it is assumed that the compound nature of the lavas near the vents is related to the proximity to the vents, then it is also possible that the source vents for the lavas of Mahabaleshwar could be near Nasik (Walker, 1972) or even off shore at a similar latitude to that of Nasik or Mumbai. If this is the case, then the lavas at Mahabaleshwar would have had to travel a minimum distance of 250 km. Unfortunately for volcanological interpretation, the off-shore area of the Deccan volcanics was rifted away as part of the Seychelles-Mascarene Plateau (Devey and Stephens, 1991) and is not preserved.

Defining the source area of the lavas would be easier if it were possible to determine the overall direction of flow. Unfortunately this is not possible as methods for determining flow direction, such as pipe vesicle inclination and magnetic fabric studies (e.g., Herrero-Bervera et al., 2002), are very unreliable and only provide information of the direction of lava flow at the point that the sample or observation was taken. Pāhoehoe flows are known to be emplaced by a kind of 'random walk' thus almost any direction can be indicated anywhere in a flow-field (Baloga and Glaze, 2003). Pipe vesicles are rare in much of the Wai Sub-group lavas. A large volume of pipe vesicle inclination directions would have to be collected from lobes and toes all over the DVP in order to get an indication of source area, and this was beyond the scope of this work. The only other

source of directional information gathered came from a thick inflated sheet flow lobe at the top of Varandah Ghat. 'Scrape' marks on the base of the unit (Figure 2.46), formed as the lava flowed over the flow below, indicated that at that point the lava was flowing in a south easterly direction, i.e., away from the Mumbai region. This is not enough information to conclude that the vents were in the Mumbai area, or even off-shore, but it is the only information that could be collected.

Some workers (e.g., Deshmukh and Sehgal, 1988; Subbarao et al., 1988; Devey and Stephens, 1991) have looked at the occurrence and distribution of dykes in the DVP, but have not found anything that resembles a feeder dyke, i.e., a dyke which becomes a sheet lobe or other type of lava flow (West, 1985) and there is no evidence of spatter or other vent deposits. The best way of locating vents is to attempt to match the geochemical signature of specific dykes with individual sheet lobes but this has not been successful in the DVP although it has been attempted (Devey, 1982). No dykes were encountered in the fieldwork carried out for this study, although Devey (1982) states the occurrence of a dyke close to Mahad (Figure 2.2) which has Poladpur Formation geochemical characteristics. This overall lack of dykes in the field area of this study indicates that the units probably were distal to their source and did not originate locally.

2.8.3 Evidence for inflation being the dominant emplacement mechanism

This study has investigated in detail the structure of over 100 thick sheet lobes and determined that the lava units seen are predominantly inflated pāhoehoe. The three-fold division of lower basal crust, central lava core and upper crustal zone, as observed in the inflated pāhoehoe flow lobes of Hawai'i (Section 2.3.2), although not always visible due to poor exposure, is always present. This is the typical internal structure which develops during the endogenous growth of pāhoehoe lavas and so proves that inflation is the mechanism for sheet lobe formation in the areas studied and probably the DVP as a whole.

A few flow lobes showing the classic features of inflation also have a rubbly flow top which may not be due to the development of a weathering profile. This is observed at 1207 m on the Kelgar Road (Figure 2.36), and ~ 1089 m on the Wai-Panchgani Road. I interpret this as rubbly pāhoehoe (Section 2.2), which is observed in the CRBG and the 1783 Laki flow-field (Keszthelyi, 2000).

A further indication of the inflation process occurring is the presence break-out lobes. These are thought to be caused by an influx of lava at slightly higher pressure which breaks through the upper crust and forms small surface lobes (Hon et al., 1994). Although smaller lobes are found on top of a thick and highly vesicular upper crust, such lobes and toes did not necessarily form when the unit had inflated to its final size. It is probable that the break-outs occurred when the sheet lobe was much smaller than its final size, and still inflating. This is a scenario where the age of the basalt and its stratigraphic position do not follow the law of superposition, as the basalt in the core of the thick main unit may have been injected after the break-out lobes formed.

Small precursor lobes are also often seen (Section 2.2) at the base of sheet lobes and if no bole is present it can be difficult to distinguish breakout lobes from precursor lobes either side of a contact. This produces an often repeated sequence of early precursor lobes followed by the thick main sheet lobes topped with small break-out lobes. Break-out lobes are more difficult to distinguish than precursor lobes as they have a similar vesicularity to upper crustal zones and hence weather in the same way.

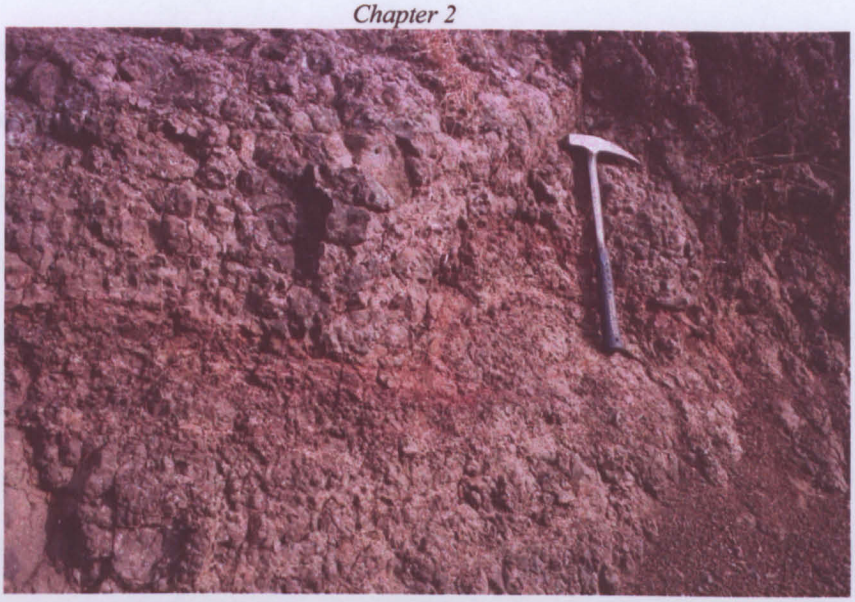

Figure 2.57. A break-out lobe with a red weathering rind on Khumbarli Ghat at ~680 m in the Mahabaleshwar Formation Lat. long. not available.

2.8.4 Evidence for ʹaʻā

During the field work the only evidence for ʹaʻā-like flows uncovered was raggedy vesicles at ~ 477 m and spinose clasts at 639 m, on Khumbarli Ghat, but both were part of a lava body with a sheet lobe type morphology not a channelised ʹaʻā-like form. The other features typically associated with ʹaʻā, a thick section of rubbly material on the upper surface and a thinner rubbly horizon on the lower surface (Section 2.2), were not observed. This is in contrast to much of the previously published volcanological investigation of the DVP (e.g., Sahasrabudhe et al., 1977; Deshmukh and Pal, 1984). More recently workers such as Bondre et al. (2004) have admitted that the sheet lobes are not ʹaʻā, yet did not recognise the inflation-related features in the thick sheet lobes. They also classify all the rubbly flow tops as primary flow related features rather than secondary weathering features, which are, in fact more common (Section 2.5.3).

2.8.5 The origin of intraflow cool, vesicular masses

It would be simple to assume that these highly vesicular bodies are sections of the upper crustal zone which had been entrained in to the lava core. However, if this were the case then it would seem probable that they would be found in the upper part of the core, but

often they are in the middle of the core. It would also seem probable that some, if not all, would show sections of the HVZs typical of the upper crust zone of a pāhoehoe lobe, yet none was observed. A further, and probably the most important, problem associated with this hypothesis is that pāhoehoe flows do not generally have disrupted crusts. A second suggestion put forward for the origin of these very vesicular masses is that they are small highly vesicular precursor lobes which where engulfed and then plucked off the surface they were resting on and became isolated vesicular masses within a much thicker sheet lobe (S. Self, 2004 pers. comm.). This would account for the radiating cooling joints in the host core. However, the internal structure of these objects is not similar to that of pāhoehoe lobes.

2.8.6 Vesicularity

The vesicularity of basalt can vary considerably between and within individual sheet lobes, formations and volcanic provinces. The lavas studied on the Mahabaleshwar Plateau have relatively low vesicularity. The upper crust vesicularity appeared to be normal compared to Hawaiian and CRBG lobes, but the lava cores are exceptionally vesicle-poor, suggesting efficient degassing during flow emplacement. There are few large vesicles, the largest being 30 cm long and about 15 cm thick, much smaller on average and fewer in number than in the CRBG where mega-vesicles are much more prevalent and large blister-shaped vesicles over 50 cm long are seen (S Self, 2004 pers. comm.). The reason for the lower vesicularity of the DVP basalts observed in the study area is debatable; perhaps it is due to the magma having a low initial volatile content (the magma degassing in the magma chamber or conduit), or the lava degassing as it moved to the flow front and hence becoming low in volatiles and degassed before it froze. This is important for the understanding of the environmental impact of the DVP, but is, unfortunately, beyond the scope of the current work.

2.8.7 *Relationship between the geochemical stratigraphy and the physical volcanology*

The volcanological logging has shown little correlation between the geochemical formations and the physical volcanology in the Wai Sub-group (Appendix A1-A7). There are, however, a few exceptions. The first is the marked change in style of physical volcanology at the Bushe-Poladpur Formation boundary which is observed on both Varandah and Ambenali Ghat (Appendix A1 and A5). The Bushe Formation is dominated by small Hawaiian-like lobes which give way to much thicker ~ 20 m thick sheet lobes, at the Poladpur Formation boundary, typical of the Wai Sub-Group. The second is observed on the Matheran Ghat section. It has already been noted that the lavas units here are generally thinner than further south but there are also changes within the traverse itself. The Neral and Thakurvadi Formation both have the same physical volcanology, that is small pāhoehoe lobes and toes (Appendix A7). Once into the Bhimashankar Formation, however, the sheet lobes become thicker (on average 5 m thick) and once into the Khandala Formation the units become thicker still (on average 15 m thick) and the number of red boles increases. The reason for this is uncertain, but it could be because eruptions are becoming fewer, although the occurrence of more boles and thicker sheet lobes does indicate a shift towards sheet lobes similar in appearance to the Mahabaleshwar Plateau, Wai-Sub group units. Perhaps this is because the Matheran area was becoming more distal to the vents as time progressed and, hence, only the bigger sheet lobes could reach that area?

2.8.8 *Boles*

The occurrence of boles or weathering horizons varies greatly throughout the DVP. These red or, rarely, green horizons develop as a result of the weathering of an exposed flow top, or pyroclastic material, as discussed in Section 2.5.3. The number of boles in the Mahabaleshwar Plateau traverses is high with a bole occurring between almost every sheet

lobe (Appendix A1-A4). This is interpreted as due to the waning in the number and frequency of eruptions. It is not thought that the volume of material being erupted was significantly less, but that the time between eruptions was much longer to allow for the development of the, often thick, weathering profiles (Widdowson et al, 1997). The lowest formation in the Wai Sub-group, the Poladpur Fm., is poorly exposed in both Ambenali Ghat and Varandah Ghat so it is difficult to determine the number of boles. However, as none are observed in Poladpur Formation on Ambenali Ghat and only one on Varandah Ghat, it is likely that they are fewer in number and that the repose between each eruption was relatively short.

Interestingly, the entire Matheran Ghat contains only three bole horizons and those which are present are near the top of the section, thus presenting just over 500 m of basalt without a single weathering horizon. This is an extremely large amount of basalt to be erupted without an apparent significant time break and could be due to the fact that the lavas observed on Matheran Ghat was close to vents which were erupting almost constantly and so boles could not develop. Perhaps, if it were possible to observe these same formations more distally, then only a few would have grown big enough to travel great distances (Figure 2.58). The same may be true of the thick units seen around the Mahabaleshwar Plateau and beyond. If it were possible to view them in a more proximal position, perhaps the thickness of the units would be less but the number of units greater, and the number of bole horizons fewer.

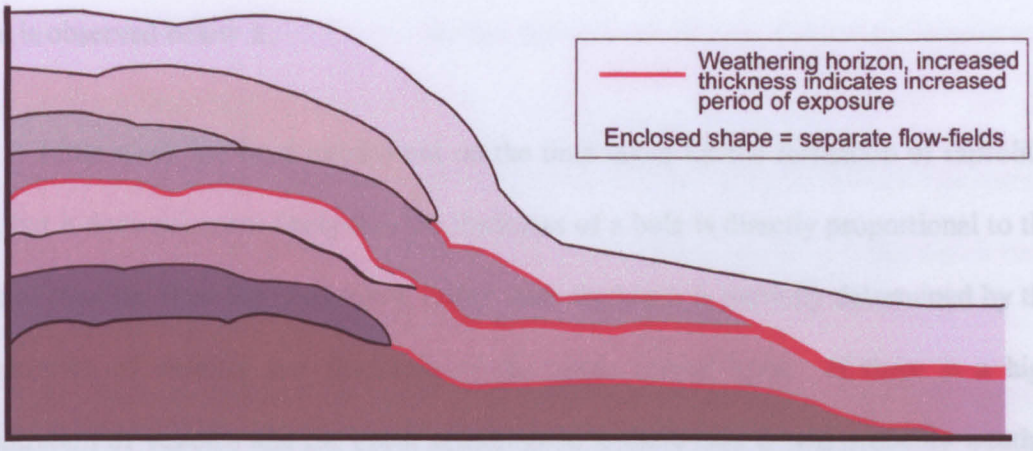

Figure 2.58. A diagram much exaggerated in the vertical, providing a possible explanation for the sparse number of weathering horizons at Matheran Ghat, assuming that it is proximal to the eruptive vent. This also demonstrates how boles are more likely to form distally to the vent as fewer sheet lobes travelled that far, allowing time for weathering horizons to develop.

The style of the boles also varies. The thinnest type is approximately 1 cm of reddened material with the upper crust below virtually intact, this probably represents only the altered glassy rind on top of the lobe. Many of the boles observed had more red material than just an altered glassy rind, these are referred to as saprolitic boles (Section 2.5.3). The majority of the boles encountered in this study are saprolitic boles. Some have a saprolite itself, with progressively less weathered material below it. Others do not have a saprolite and have a proportion of the bole containing relatively unaltered material at the top of the weathering profile (Section 2.5.3). The saprolitic boles regularly show small 'balls' of unaltered solid basalt surrounded by red weathered material, below this is altered, but solid basalt (Section 2.5.3 and Figure 2.15). If the weathering does not progress to the stage of thick saprolite balls of basalt, relic structures are observed such as amygdales and break-out lobes, which may also display red altered glassy rinds.

The second type of bole is the pyroclastic or cherty bole (Section 2.5.3). The bole observed at 757 m on the Tapola road appears to contain lithic fragments and may therefore have been a pyroclastic bole but unfortunately due to the friable nature of the material, the sample was destroyed during attempted thin sectioning. Another candidate for a pyroclastic bole is the 'big red bole' on Ambenali Ghat (693 m), as in places this

appears to lie directly on an unweathered flow top, but in other locations a weathering profile is observed below it.

Little work has been carried out on the time taken for the formation of saprolitic boles, but it does not seem likely that the thickness of a bole is directly proportional to the length of time the flow top is exposed; rather their thickness is partially determined by the concentration of vesicles and thickness of the upper crustal zone. If there is a high concentration of vesicles and the upper crustal zone is thick then it will probably weather more quickly and produce a thicker bole. However, sheet lobes with an upper crust having a lower vesicularity will weather more slowly, but if weathered for longer will also produce a thick bole. To investigate this suggestion, further work would involve detailed palynology of the bole horizons to study whether the species were pioneer colonising flora or else established forest ecosystems (Jolley, 1997). The latter would indicate a long period of bole exposure prior to the next sheet lobe emplacement. This is beyond the scope of this work, but was investigated in some detail by Cripps et al. (2002)

2.9 Conclusions

- The lavas in the study area are dominated by pāhoehoe lava flow-fields consisting of small toes and lobes down to 10 cm thick and up to 1 m thick and inflated pāhoehoe sheet flow lobes up to 60 m thick.
- The sheet flow lobes commonly observed contain the same three-fold division seen in Hawaiian lavas and the CRBG.
- The only evidence for ʻaʻā-like texture was raggedy vesicles in a single lobe, but rubbly flow tops were observed on a few occasions indicating the possible presence of rubbly pāhoehoe.

- The rubbly flow top material observed in many bole horizons which was thought to be evidence for ʻaʻā flows by earlier workers is, in fact, part of the weathering profile of the lavas.
- Smaller lobes are often associated with a single large sheet lobe; small precursor lobes precede the sheet lobe which is often overlain by break-out lobes which form during the inflation of the main unit.
- The sequences of lavas within the Wai Sub-group observed on the type section (Ambenali Ghat) and the other sections towards the south of the DVP, are dominated by thick, inflated pāhoehoe sheet lobes, but the older units (as seen in Matheran Ghat) appear to be dominated by small, thin Hawaiian-sized pāhoehoe lobes, although thicker sheet lobes do occasionally occur, especially towards the top of the section (Appendix A7).
- Boles are common in the Ambenali and Mahabaleshwar Formations, indicating that there were longer hiatuses between the emplacement of successive pāhoehoe flow-fields and thus eruptions.
- Boles are not common in the Poladpur, Bushe, Neral, Thakurvadi and Bhimashankar Formations. This probably indicates that the time between eruptions was short or that the sites were more proximal to the eruptive centres at the time of eruption of these formations.

Chapter 3
Interpretation of palaeomagnetic results

3.1 Introduction

The palaeomagnetic data gathered for this work were originally collected in an to attempt to constrain the eruption rate of the DVP, and as a tool to provide a means of correlating the volcanological units across the Mahabaleshwar Plateau. However, during the course of this work the data have also provided further volcanological insights which are discussed in Chapter 5.

The seven logged sections were selected with the aim of 'bracketing' the important, KTB bearing, chron 29R (Figure 3.1). It was expected, from $^{40}Ar/^{39}Ar$ data (Widdowson and Kelley, in prep.), that palaeomagnetic samples taken from the Matheran area (Figure 3.2), would locate the lowermost (30N/29R) palaeomagnetic reversal horizon of the Deccan Volcanic Province (DVP). The upper 29R/29N boundary was already known to occur on Ambenali Ghat (Figure 3.3). Together these palaeomagnetic reversals (i.e., 30N/29R and 29R/29N) would have provided timelines towards the top and the bottom of the volcanic pile, and so would have provided a means to calculate a more accurate average eruption rate of the DVP. However, as will be shown in this chapter, the lower reversal horizon (30N/29R) was not identified. Only the 29R/29N boundary was found, occurring towards the base of the Mahabaleshwar Formation in five traverses (Mahabaleshwar Plateau and Khumbarli Ghat). The new data do not greatly alter previous constraints on the timing of the DVP, but pinpoints the 29R/29N boundary accurately with respect to elevation, outcrop, geochemical stratigraphy and, most important to this study, the volcanological detail. Moreover, this study has used the new palaeomagnetic data in a novel way, to attempt to correlate sheet flows and flow fields across the Mahabaleshwar

Plateau and to investigate the topography that was created on the active surface of the DVP. These are discussed further in detail in Chapter 5.

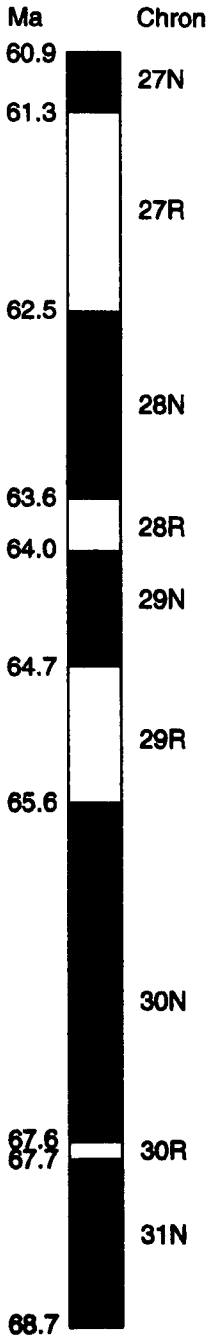

Figure 3.1. Palaeomagnetic timescale for Late Cretaceous to Palaeocene, showing normal chrons (black) and reverse chrons (white) and their ages. This work samples chron 29R and 29N; the KTB is within Chron 29R (after Cande and Kent, 1995).

The first part of this chapter provides an overview of the previous palaeomagnetic work that has been carried out on the DVP, and seeks to briefly document the first investigations into the palaeomagnetism of the DVP through to the realisation that the

Deccan eruptions spanned the KTB event, and to the current understanding that the majority of the succession was erupted in approximately 1 million years (e.g., Duncan and Pyle, 1988; Vandamme et al., 1991). The methodology (Section 3.3) explains the techniques that were carried out in the field and those that were carried out in the laboratory. Section 3.4 explains the methodology of displaying the palaeomagnetic data in a manner which clearly demonstrates both the magnitude and the direction of the palaeomagnetic vector. The results (Section 3.5) describe the occurrence of the palaeomagnetic reversal and its elevation in the five most southerly logged sections. The discussion section (3.6) is deliberately brief since the palaeomagnetic data were collected to be used as a tool to aid the understanding of the volcanological architecture, structure, and the lateral extent of the lava units. A more detailed discussion is undertaken in Chapter 5 where the palaeomagnetic data are combined with the geochemical and volcanological detail outlined in Chapter 2 and Chapter 4.

3.2 Previous work on the palaeomagnetic data in the Deccan Volcanic Province.

3.2.1 Early palaeomagnetic studies of the DVP

Palaeomagnetic studies on the DVP have been carried out since the 1950s. Early work was hampered by the lack of understanding of the occurrence of demagnetization and by the relative insensitivity of laboratory equipment (Vandamme and Courtillot, 1992). Despite these limitations, however, much useful work was carried out and provided information into the understanding of tectonic plate motion, the movement of the Indian landmass (McElhinny, 1968; Wensink and Klootwijk, 1971), and ideas as to the duration of the Deccan Traps eruptive period (McElhinny, 1968). However, the problem of remagnetization, and a lack of understanding of the structural warping of the DVP, initially led to a varying number of magnetic chrons being determined within the Deccan volcanic pile.

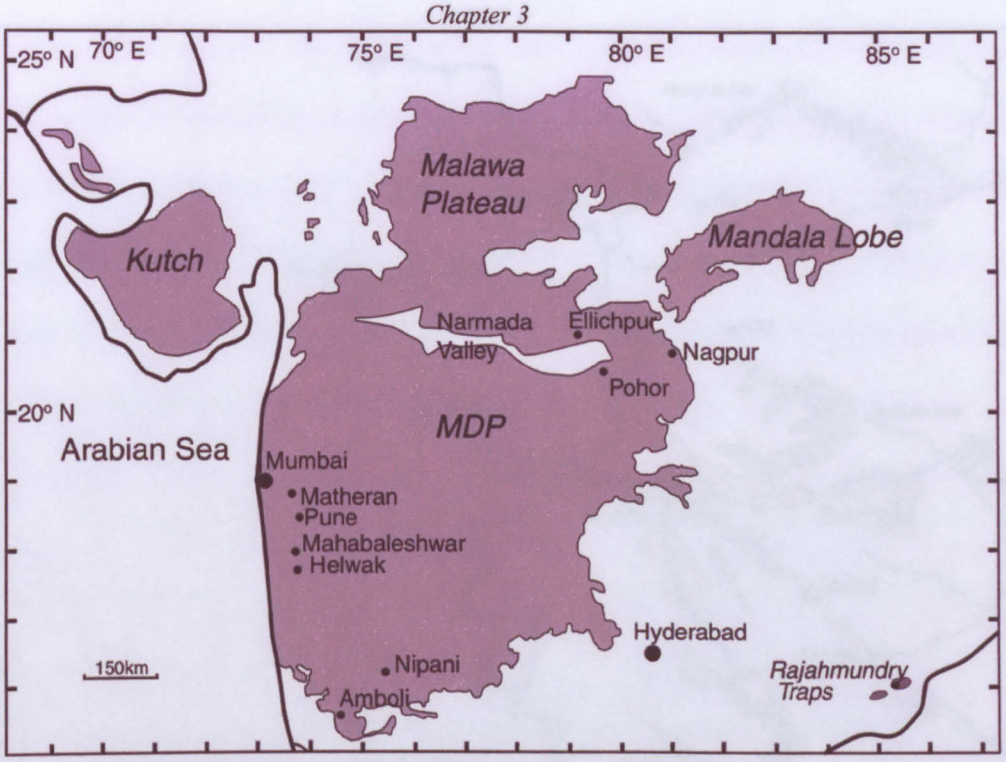

Figure 3.2. Location map of DVP and Rajahmundry Traps

Sahasrabudhe (1963) and McElhinny (1968) both concluded that there was a two-fold magnetic stratigraphy to the DVP that consisted of a lower section with reversed polarity (i.e., Chron 29R) and an upper with normal polarity (i.e., 29N). This reversal was observed to occur at approximately 2000 ft asl (~600 m) and it was assumed that this would be consistent over the entirety of the DVP, due to the horizontal appearance of the lavas. The identification of this single reversal led McElhinny (1968) to suggest that "it seems unlikely that the Deccan Traps cover a period of much longer than 5×10^6 yr".

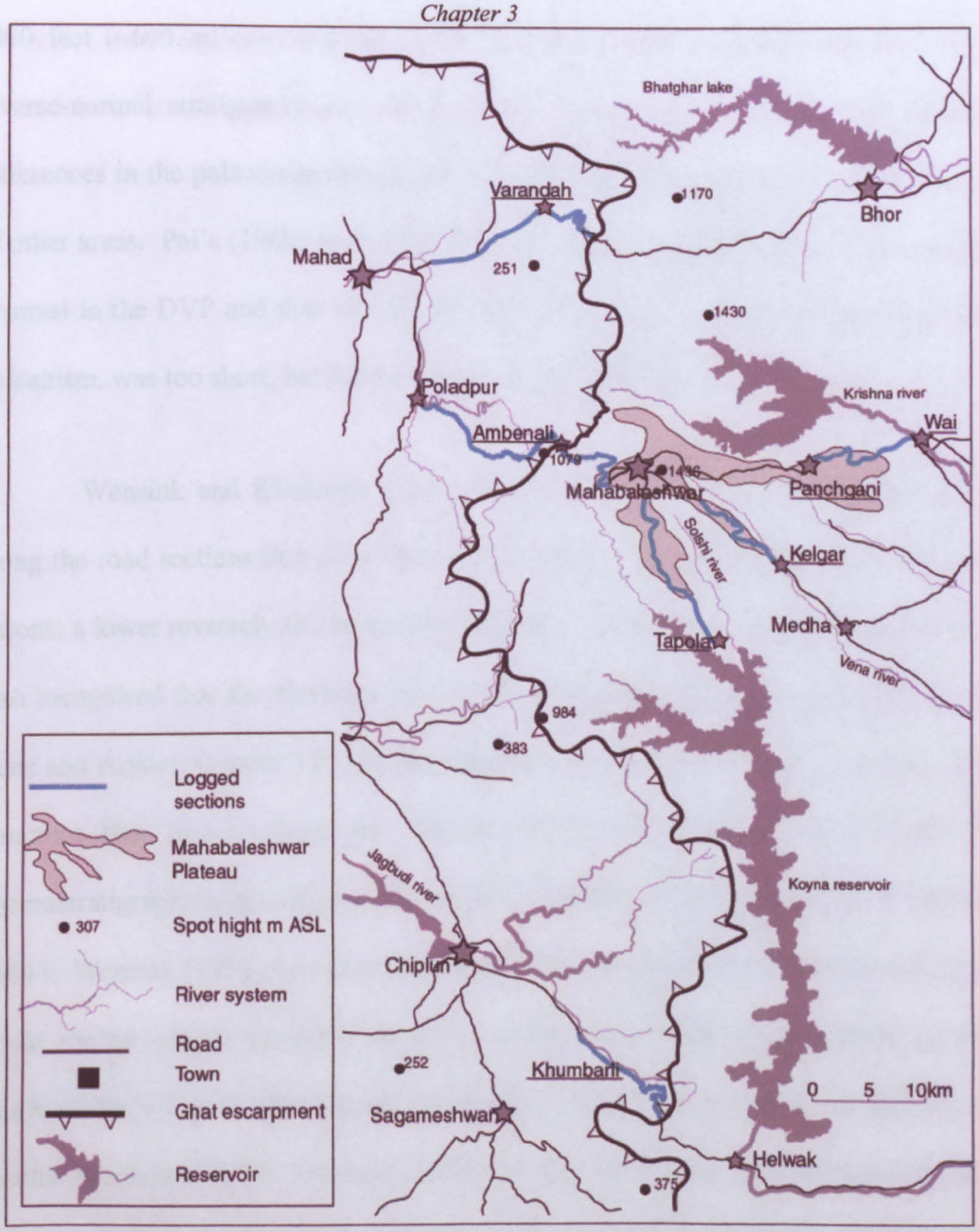

Figure 3.3. Detailed location map showing the main logged sections, indicated by a blue line. Section names are underlined. The Matheran Ghat section is not shown.

Pal (1969) reported on a number of investigations around the DVP which show more than one reverse and normal horizon, and some intermediate polarity flows. These data also indicated that reverse-to-normal polarity transitions occur at various elevations across the DVP. Pal (1969) identified reversely polarised basalt at 3000 ft (~900 m), while according to previous work (Sahasrabudhe, 1963; McElhinny, 1968) lava at this elevation should be normally polarised, to the normally polarised basalt at sea level in the Rajahmundry Traps. This demonstrated that the palaeomagnetic reversal did not occur at

2000 feet (~600 m) over the whole DVP, and Pal (1969) suggested that the two-fold reverse-normal stratigraphy was only valid in the Western Ghats and that significant differences in the palaeomagnetic reversal elevation and stratigraphy were seen in studies of other areas. Pal's (1969) work concluded that there was more than one palaeomagnetic reversal in the DVP and that McElninny's (1968) estimate, of a less than 5 Ma period of volcanism, was too short, but did not suggest a figure himself.

Wensink and Klootwijk (1971) undertook a series of palaeomagnetic traverses along the road sections that climb the Western Ghats. They identified only two magnetic chrons; a lower reversely (R) magnetised and upper normally (N) magnetised chron. They also recognised that the elevation of the palaeomagnetic reversal horizon varied between Pune and Amboli (Figure 3.2). In fact they had partially identified the plunging anticlinal structure that occurs along the Western DVP, which was discovered later using chemostratigraphical techniques, (Devey and Lightfoot, 1986; Mitchell and Widdowson, 1991). Wensink (1973), however, determined that this simple R-N palaeomagnetic pattern could not be reliably extended elsewhere in the Western Ghats and instead agreed with much of Pal's (1969, 1971) work. In order to attempt to correlate the palaeomagnetic results Wensink (1973) reviewed much of the DVP data available and proposed a palaeomagnetic stratigraphy. For instance, Pascoe (1964) and Deutsch (1959) had already identified a reversed series of basalts in the Eastern Deccan, which Wensink (1973) named "Nagpur Reversed Polarity Epoch" (Figure 3.4). Above this, at elevations between 300-400 m, Wensink proposed the "Pohor Normal Epoch" (Figure 3.4) for a higher elevation series of lavas cropping out in the east and north-east DVP. The next reversely magnetised lavas occurred further north still, at Ellichpur (Figure 3.1) where a 530-m thick section of reversely magnetised basalt was correlated with the lower reversed series of lavas, identified in the Western Ghats, which Wensink (1973) called the "Deccan Reversed Polarity Epoch" (Figure 3.4). The upper, normally magnetised flows recorded in the

Western Ghats (Deutsch, 1959; Wensink and Klootwijk, 1971) were named the "Nipani Normal Polarity Epoch" (Figure 3.4) by Wensink (1973).

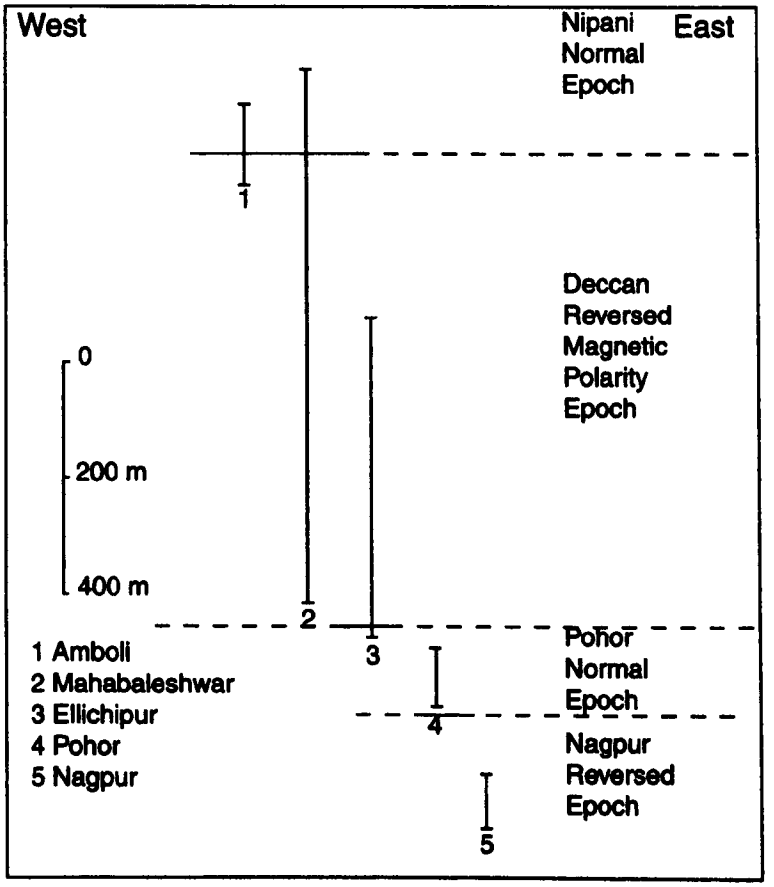

Figure 3.4. The preliminary palaeomagnetic polarity time scale proposed by Wensink (1973), showing a progressive younging from east to west (after Wensink 1973)

3.2.2 Using palaeomagnetism to constrain the date of the DVP and link it to the KTB

In the late 1970s and 1980s more sensitive laboratory equipment was developed and the occurrence of remagnetization was better understood. The date and duration of the DVP was also being narrowed through the use of improved $^{40}K/^{39}Ar$ and $^{40}Ar/^{39}Ar$ studies. This led Courtillot et al. (1986) to undertake a detailed study of the DVP using new palaeomagnetic, palaeontological and geochronological data collected from 22 sites from Nagpur in the far east of the DVP to Mumbai in the west (Figure 3.2). They noted that reversely magnetised basalt dominates, with only 15% of the sites normally polarised. This agreed with a compilation and re-evaluation of much of the previously published data (Rao et al., 1985; Courtillot et al., 1986). Courtillot et al.'s (1986) collection of data showed that

in all of the ghats sections studied, most only showed one palaeomagnetic reversal, and none showed more than two. In fact, much of the previous confusion concerning more complex reversal patterns had arisen from the occurrence of remagnetization and the failure to take into account the regional dip for the DVP which, although small (~0.3°), becomes significant with respect to the palaeomagnetic stratigraphy over long distances. From these discoveries Courtillot et al. (1986) proposed the following simple palaeomagnetic stratigraphy for the DVP: i) A thin, often absent, lower normally polarised sequence, (Chron 30N) occurring in the north DVP, overlain by, ii) a thick reversed sequence (Chron 29N), which dominates much of the DVP (Chron 29R), followed by, iii) an upper normal sequence (Chron 29 N), typically found in the south west DVP, (including this current study area). This demonstrated that the simple, reversed-normal, stratigraphy of the Western Ghats determined by Wensink and Klootwijk (1971) could be traced over the whole of the DVP, and that the eastern and northern areas may have slightly older basalts at their base, but are largely of a similar age (i.e., c.67-64 Ma).

Most importantly, the palaeomagnetic data indicate that the total duration of the DVP did not exceed parts of three successive magnetic chrons (Figure 3.1). In order to determine which three chrons coincide with the DVP eruptions Courtillot et al. (1986) studied a number of magnetic reversal time scales (Courtillot et al., 1986 and references therein), which link geochronology to the palaeomagnetic chrons. Courtillot et al. (1986) deduced that the reverse chron which contains the majority of the DVP lavas was chron 29R (833,000 yrs long ;Cande and Kent, 1995), as 30R is only 90,000 years long and 31R is too old to fit with the geochronology (Cande and Kent, 1995). Thus the sequence of chrons in the DVP becomes 30N–29R–29N (Figure 3.1), and the duration of the main pulse of basaltic volcanism. i.e., the Jawhar to lower Mahabaleshwar Formations (Table 2.1) probably did not exceed 1 Ma. The discovery that the majority of the DVP lavas were produced during 29R is very important since the KTB occurs during this chron (Courtillot

et al., 1986), and has thus produced much debate on the possibility that the DVP caused or promoted the KTB mass extinction event (e.g. McLean, 1985; Hallam, 1987; Glasby and Kunzendorf, 1996; Wignall, 2001; Phipps Morgan et al., 2004).

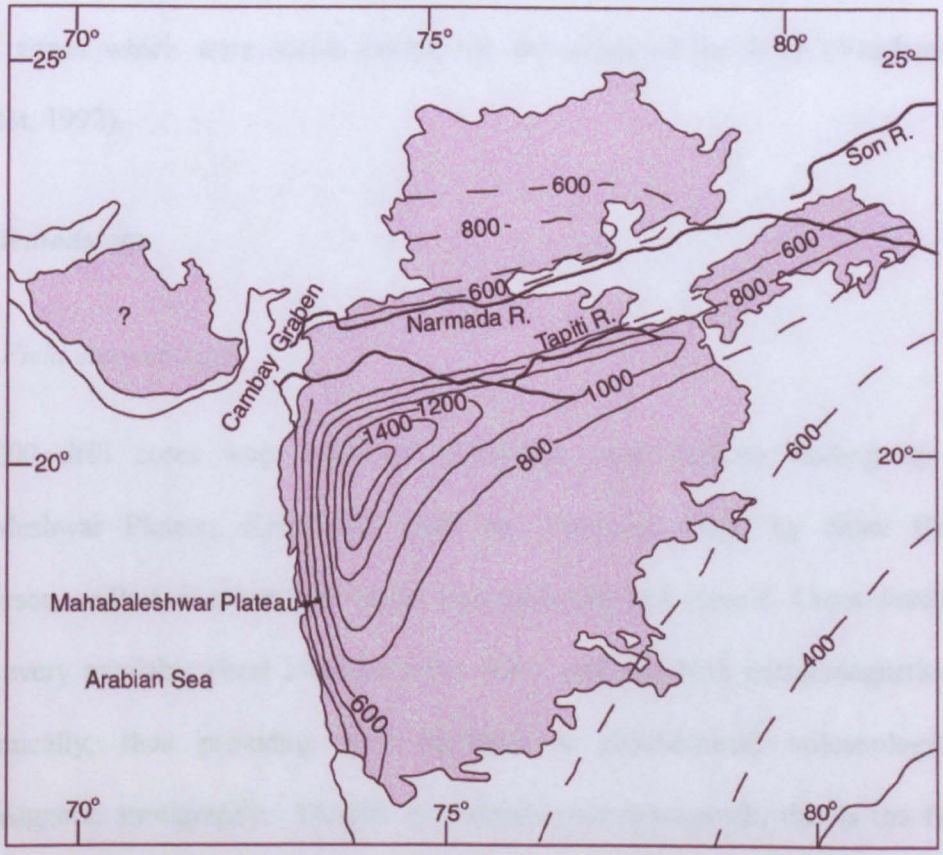

Figure 3.5. A Schematic (interpolated) map of elevation contours of the of the 29R/29N palaeomagnetic horizon across the DVP. Elevations are in metres above sea-level. After Vandamme and Courtillot (1992).

Further work by the French IPGP group (Vandamme and Courtillot, 1992) investigated the palaeomagnetism in the extremities of the DVP. Studies in the Mandala Lobe and the Rajahmundry Traps (Figure 3.2) further strengthened the N-R-N palaeomagnetic stratigraphy and the proposal that the eruptions occurred across the 30N, 29R and 29N chrons. Interpolation of the data collected shows the isochronous 29R-29N palaeomagnetic boundary (Figure 3.5) across much of the DVP. This can be assumed to reflect the epeirogenic warping which affects the DVP basalts (Widdowson, 1997). It shows a long narrow antiform to the south of the Narmada, and another, smoother antiform to the north, with a synform between. This folding has a wavelength of ~150 km and an amplitude of ~500 m and extends down the west coast of India, conferring a boomerang

shape to the contours as the east-west trending antiform to the south of the Narmada valley curves round to the south to trend parallel to the Western Ghats. The decrease in elevation of the 29R-29N boundary (Figure 3.5) along the Narmada river and the western coast of India is probably due to down faulting, or warping of the lavas along two of the 'arms' of the rift zones which were active during the formation of the DVP (Vandamme and Courtillot, 1992).

3.3 Methodology

3.3.1 Field methodology

Over 200 drill cores were collected along the road sections leading up to the Mahabaleshwar Plateau, Khumbarli Ghat and Matheran Ghat, by either Dr. Mike Widdowson, or Prof. Stephen Self, or Dr. Dougal Jerram and myself. Cores were taken at almost every available sheet lobe and these were analysed both palaeomagnetically and geochemically, thus providing a comprehensive geochemical, volcanological and palaeomagnetic stratigraphy. Despite considerable previous work, this is the first time such a comprehensive and detailed survey has been conducted along these classic ghat sections. The palaeomagnetic data were acquired in the Palaeomagnetic Laboratory of the Department of Earth Sciences, University of Oxford. The laboratory work, core preparation and stepwise demagnetisation experiments and subsequent data interpretation was undertaken by Dr. Conall Mac Niocaill, Will Turner and myself.

At each locality at least two palaeomagnetic drill cores, of varying length, were taken in the freshest rock available using a rock drill with a 2.2 cm diameter, diamond-tipped drill bit (Figure 3.6). Usually each sheet lobe encountered was sampled, although in the case of sheet lobes less than ~2 m thick some units were missed, since sampling each would have proved impractical. Each sample was oriented using both a magnetic and sun

compass (to ensure against the possibility of highly magnetised samples affecting the magnetic compass), and the exact time and position of the sample was recorded using a hand held GPS. The cores were marked with their Y-azimuth direction and the plunge of the sample was noted using an attached clinometer. This allowed precise recreation of the orientation of the sample during the laboratory palaeomagnetic analysis (Appendix B10).

During this study the elevations were acquired using handheld GPS and barometric altimeters (Section 2.6) providing much more accurate elevations for this study than any previous work. The sampling density during this work has also proved important. The location of the palaeomagnetic reversal horizon was identified on the Ambenali Ghat, Kelgar Road and Tapola road as accurately as possible in the first field season. Thus in the second field season it was possible to return and take more samples around the reversal horizon to increase the accuracy of the location in relation to the volcanostratigraphy and the exact elevation. With the precision GPS used during this study (Appendix D) it is now possible to identify the position of the 29R-29N palaeomagnetic reversal horizon on the Kelgar Road and Wai-Panchgani Road exactly, on the Tapola Road to within ± 40 m, and on Ambenali Ghat and Khumbarli Ghat to within ± 5 m (see logs Appendix A).

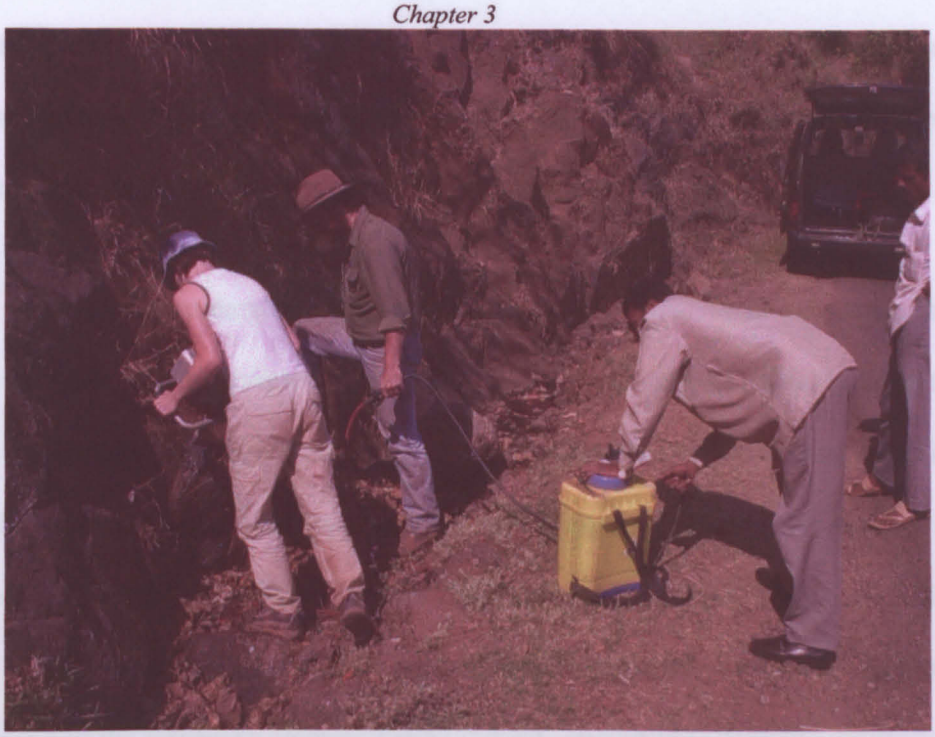

Figure 3.6. The author drilling a rock core for palaeomagnetic studies on the Kelgar section. Dr Mike Widdowson controlling the water flow, and Chotu Patel, our driver, maintaining water pressure. Lat and long. unknown (photo by Dr. Dougal Jerram).

3.3.2 Laboratory methodology

The cores were cut into 2.2 cm sections and measurements of the natural remanent magnetisation (NRM) were made using either a 3-axis 2G *cryogenic* magnetometer or a Geofysika Brno JR5A spinner magnetometer, in a field-free room, at the University of Oxford palaeomagnetic laboratory (Appendix B10). Further investigations were carried out on a limited number of sister samples using thermal demagnetisation in a magnetically shielded room to confirm the reliability of the remanence components identified using AI demagnetisation (Appendix B10).

3.4 Methods of displaying the data

3.4.1 Zijderveld Plots

The data were displayed using Orthogonal Vector Component plots or Zijderveld plots (Zijderveld, 1967). These display the magnitude and direction of the 3-D magnetic vector on a (2-D) plane using two sets of superimposed axes (Figure 3.7 and Figure 3.8). In the

horizontal plane the axes are N-S and E-W, and the data points are plotted as solid symbols. In the vertical plane the axes are E-W and up-down, and the data points are plotted as open symbols.

As the samples demagnetize, and the magnitude of the vector decreases, the graph shows two lines of data points tracking back towards the origin. Straight lines trending towards the origin (Figure 3.8 A) indicate that the vector has a constant direction; this shows that there is no secondary overprint. If the lines have two or more straight sections then there are multiple components to the sample's magnetisation (Figure 3.8 B & C). A curved line between two segments indicates an overlap in the coercivity spectra of the grains carrying the magnetic vectors (Figure 3.8 D). In a sample with two or more straight sections to the plotted line, the final straight section which tracks towards the origin is called the Characteristic Remanent Magnetisation (ChRM) and is regarded as the primary magnetisation.

3.4.2 Equal area stereographic projections

Stereographic projections also provide a method of displaying 3-D data, i.e., the magnetic vectors, on a flat plane (Figure 3.9). As the data plotted for palaeomagnetism is a true vector the data are projected into both the upper and lower hemispheres. A datum point will have a declination and an inclination. The declination of a point plots as if the stereo-net is a compass with north at the top, and the inclination increases from 0° at the edge to 90° in the centre. Magnetic vectors which intersect the lower hemisphere are downward inclinations and are therefore reversely polarized and are plotted as solid data points, those projected onto the upper hemisphere, normally polarized, are open data points. If a sample has more than one magnetic component, i.e., there are two sections to the line plotted on a Zijderveld plot, the datum point for each step of the demagnetization plots along a great circle. When only the stable, ChRM remains the points plot on top of one another.

The declination and inclination of each sample (Appendix B9) is calculated using principal component analysis (Kirschvink, 1980). Magnetic components are considered stable where they are defined by at least three points on orthogonal diagrams and have a maximum angular deviation not exceeding 15°.

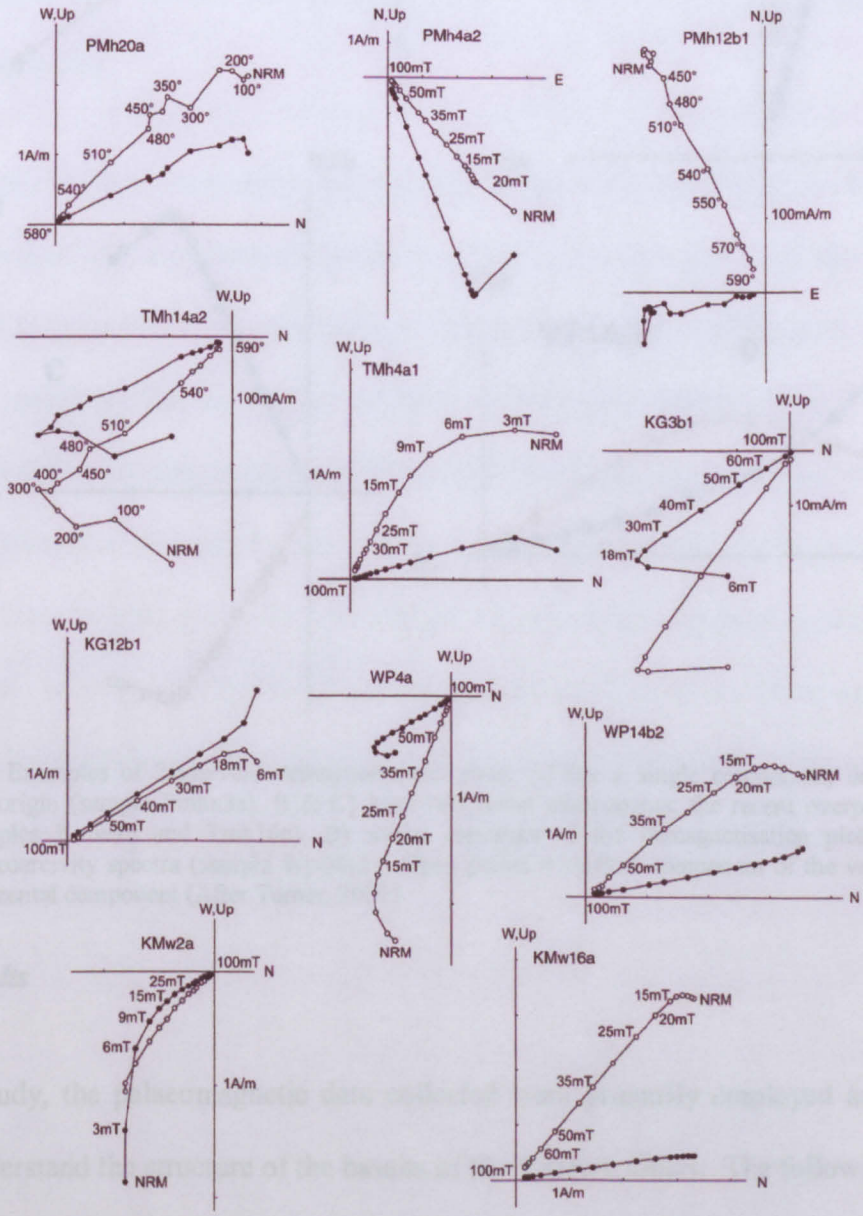

Figure 3.7. Examples of demagnetisation behaviour observed in each of the five sections. An example of a normal polarity sample and reverse polarity sample is given for Ambenali Ghat (PMh20a1 & PMh4a2), Tapola (TMh14a2 & TMh4a1) Khumbarli Ghat (KG3b1 & KG12b1), Wai Panchgani (WP4a & WP14b2) and Kelgar (KMw2a & KMw16a). Sample PMh12b1 exhibits a transitional direction at the 29R/29N reversal boundary in the Ambenali Ghat section. On orthogonal plots, solid (open) symbols are horizontal (vertical) projections. All plots are shown in geographic coordinates.

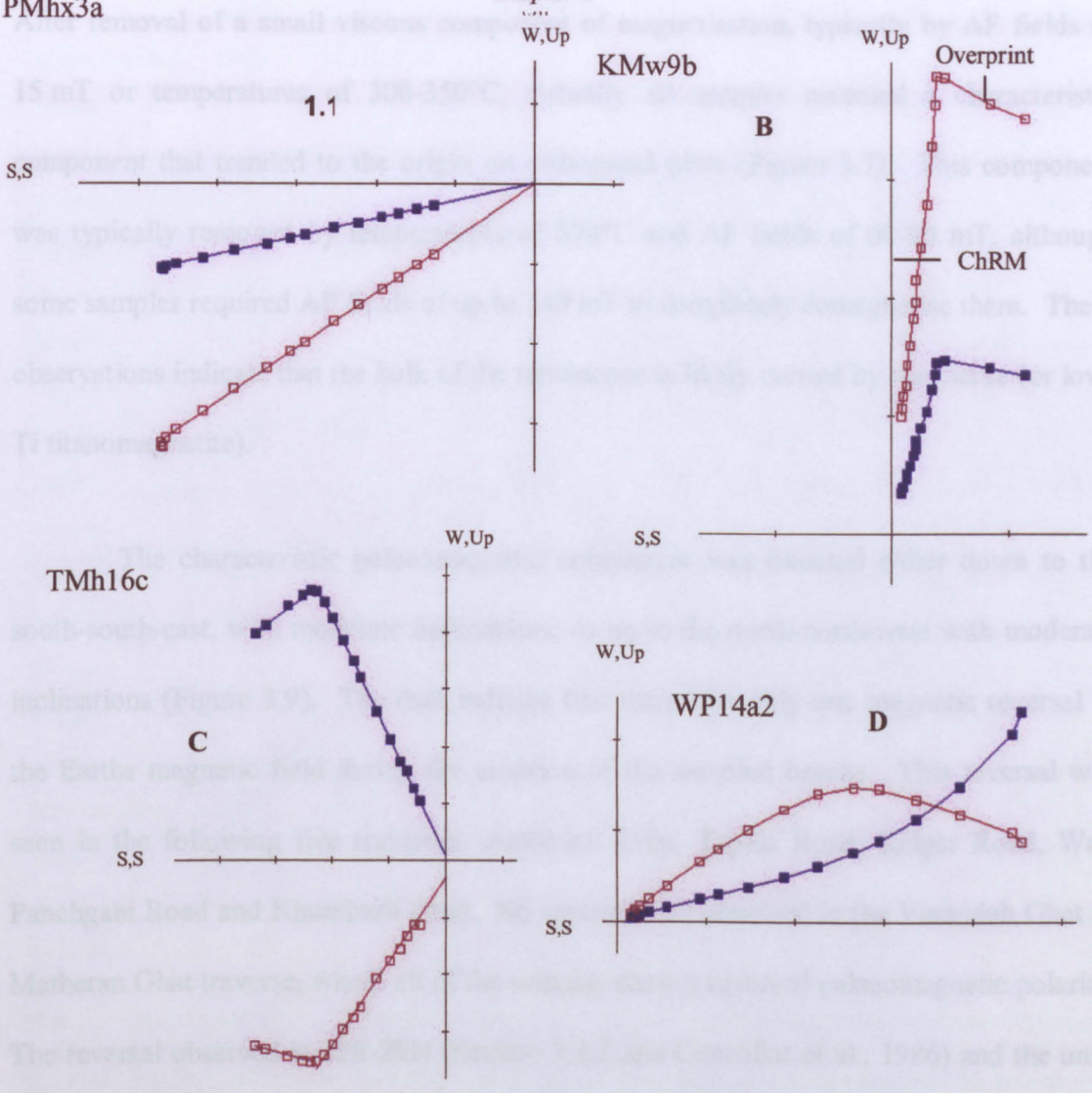

Figure 3.8. Examples of Zijderveld demagnetisation plots. A) has a single component, demagnetising towards the origin (sample Pmhx3a). B & C) have two linear components; the recent overprint, and the ChRM (samples Kmw9b and Tmh16c). D) shows curvature of the demagnetisation plot, suggesting overlapping coercivity spectra (sample Wp14a2). Open points = vertical component of the vector, Closed points = horizontal component (After Turner, 2003)

3.5 Results

For this study, the palaeomagnetic data collected were primarily employed as a tool to further understand the structure of the basalts of the Western Ghats. The following results, summarized in Table 3.1, concentrate on that aspect of the data accumulated. All the data collected for this palaeomagnetic work are shown in Appendix B1-8.

NRM intensities varied from 0.2 to ~10 A/m, with a mean intensity of 2.7 A/m. The response of the samples to progressive demagnetisation proved to be straightforward.

After removal of a small viscous component of magnetisation, typically by AF fields of 15 mT or temperatures of 300-350°C, virtually all samples revealed a characteristic component that trended to the origin on orthogonal plots (Figure 3.7). This component was typically removed by temperatures of 590°C and AF fields of 60-90 mT, although some samples required AF fields of up to 140 mT to completely demagnetise them. These observations indicate that the bulk of the remanence is likely carried by magnetite (or low-Ti titanomagnetite).

The characteristic palaeomagnetic component was directed either down to the south-south-east, with moderate inclinations, or up to the north-north-west with moderate inclinations (Figure 3.9). The data indicate that there was only one magnetic reversal in the Earths magnetic field during the eruption of the sampled basalts. This reversal was seen in the following five traverses: Ambenali Ghat, Tapola Road, Kelgar Road, Wai-Panchgani Road and Khumbarli Ghat. No reversal was observed in the Varandah Ghat or Matheran Ghat traverse, where all of the samples show a reversed palaeomagnetic polarity. The reversal observed is 29R-29N (Section 3.2.2 and Courtillot et al., 1986) and the units on Varandah and Matheran Ghats are proposed to also have been erupted during chron 29R (Courtillot et al., 1986). This is logical as they are made up of formations lower in the sequence.

	Lat (°N)	Lon (°E)	Dec.	Inc.	N	k	α_{95}	PLat.	PLong	Dp	dm
Ambenali Ghat	17°56'	73°37'									
Normal			339.0	-36.2	16	29.4	6.9	-46.7	103.0	4.7	8.0
Reverse			152.5	47.3	47	12.6	6.1	-36.5	104.0	5.1	7.9
Combined			154.5	44.4	63	14.1	4.9	-39.5	103.7	3.9	6.2
Tapola	17°48	73°42'									
Normal			344.5	-47.4	20	26.5	6.5	-41.3	091.9	5.5	8.4
Reverse			151.8	52.1	15	10.9	12.1	-32.7	101.9	11.4	16.6
Combined			159.5	49.5	35	16.1	6.2	-38.0	096.2	5.5	8.2
Kelgar	17°52'	73°50'									
Normal			342.5	-44.7	21	15.6	8.3	-42.6	095.2	6.6	10.5
Reverse			168.2	53.6	11	10.2	15	-36.6	085.9	14.6	20.9
Combined			164.2	47.7	32	13.1	7.3	-40.9	092.1	6.2	9.5
Wai Panchgani	17°25'	73°40,									
Normal			359.0	-45.0	13	21.2	9.2	-45.5	075..1	7.4	11.6
Reverse			159.3	56.7	19	23.7	7.0	-31.4	093.1	7.4	10.1
Combined			168.5	52.4	32	18.8	6.0	37.9	086.1	5.7	8.2
Khumbarli Ghat	17°25'	73°40'									
Normal			350.2	-18.3	5	12.0	23.0	-61.5	094.3	12.4	23.9
Reverse			149.9	4104	24	32.2	5.5	-39.6	110.3	4.1	6.7
Combined			154.0	37.6	29	17.8	6.5	-43.8	108.2	4.5	7.7

Table 3.1. Palaeomagnetic data from the Mahabaleshwar Plateau and Khumbarli Ghat sections. Notation is as follows: Lat. and Long. are the approximate latitude and longitude of the sampled sections determined by hand held GPS; Dec. and Inc. are the mean declination and inclination (based on samples) of the section; N is the number of samples used in the calculation of the mean direction; k is the Fisher (Fisher, 1953) precision parameter; α_{95} is the half-angle of cone of 95% confidence about the mean direction; PLat and PLong are the latitude and longitude of the resultant palaeopole for each section; dp and dm are the semi-axes of 95% confidence about the palaeopole; and Combined is the sum of the inverted normal polarity directions, combined with the reverse polarity directions to produce and overall mean.

The elevation of the palaeomagnetic reversal horizon is taken to occur between the final reversely magnetised sample and the first normally magnetised sample. Due to the sample spacing in this work there must be at least one flow boundary between these samples. I thought it probable that the palaeomagnetic reversal occurred during the hiatus between the emplacement of the sheet flows, rather than during an eruption. However, closer inspection of the data from three of the sections (Ambenali Ghat, Wai-Panchgani and Tapola), shows that there are samples that do not cluster with either the 29R or 29N samples, these have a transitional palaeomagnetic direction (grey points, Figure 3.9;

Tapola Road points may not be transitional, the signal may be due to over printing). This appears to indicate that lava was being emplaced over much of the Mahabaleshwar Plateau whilst the palaeomagnetic reversal was occurring. These transitional sheet lobes are the first sheet lobes after the final 29R sheet lobe in the traverses (i.e., the first sheet lobe above the thin red bole).

However, in all but Tapola (where the reversal cannot be pinpointed precisely due to poor exposure) and, possibly the Khumbarli sections, the exact reversal appears to coincide with the presence of a red bole horizon. This suggests that there may have been a hiatus of unknown duration in volcanic activity during the palaeomagnetic reversal. However, due to the occurrence of samples with transitional palaeomagnetic directions (in the first sheet lobe above the red bole) it is possible to state that the hiatus is likely to have been relatively brief. This is due to the fact that palaeomagnetic reversals are thought to take ~ 5000 years (Merrill et al., 1996), so for a transitionally magnetised flow to occur it must have been erupted within 5000 years, therefore the hiatus between must be less than 5000 years. It is not possible to use these data to help constrain the time taken to form a bole as it is thought that the thickness of a bole is not necessarily related to the length of exposure (M. Widdowson pers. com. 2005).

The elevation at which the palaeomagnetic reversal occurs varies in each traverse (Figure 3.10). On Ambenali Ghat, the only traverse which has been studied palaeomagnetically before, the reported elevation is 1000 m asl (Subbarao et al., 2000) or 955 m (Wensink and Klootwijk, 1971), the precise elevation for this R-N boundary determined in this study is 964 m asl. The discrepancy between the elevations is most likely due to the different methods of obtaining elevations during field work and the density of sampling. The Tapola section is difficult to interpret as there is a large area of no and poor exposure over the reversal horizon and consequently there is an error of ±

40 m. However, the reversal horizon must occur between 898 m and 945 m asl. On the Kelgar Road the reversal is observed at 952 m, on the Wai Panchgani Road reversal it occurs at 981 m, and on Khumbarli Ghat it is between 659 and 672 m asl (Figure 3.10).

As the two other sections (Matheran and Varandah Ghats) do not show a palaeomagnetic reversal their results are not discussed, but the data are presented in Appendix B7 and B8.

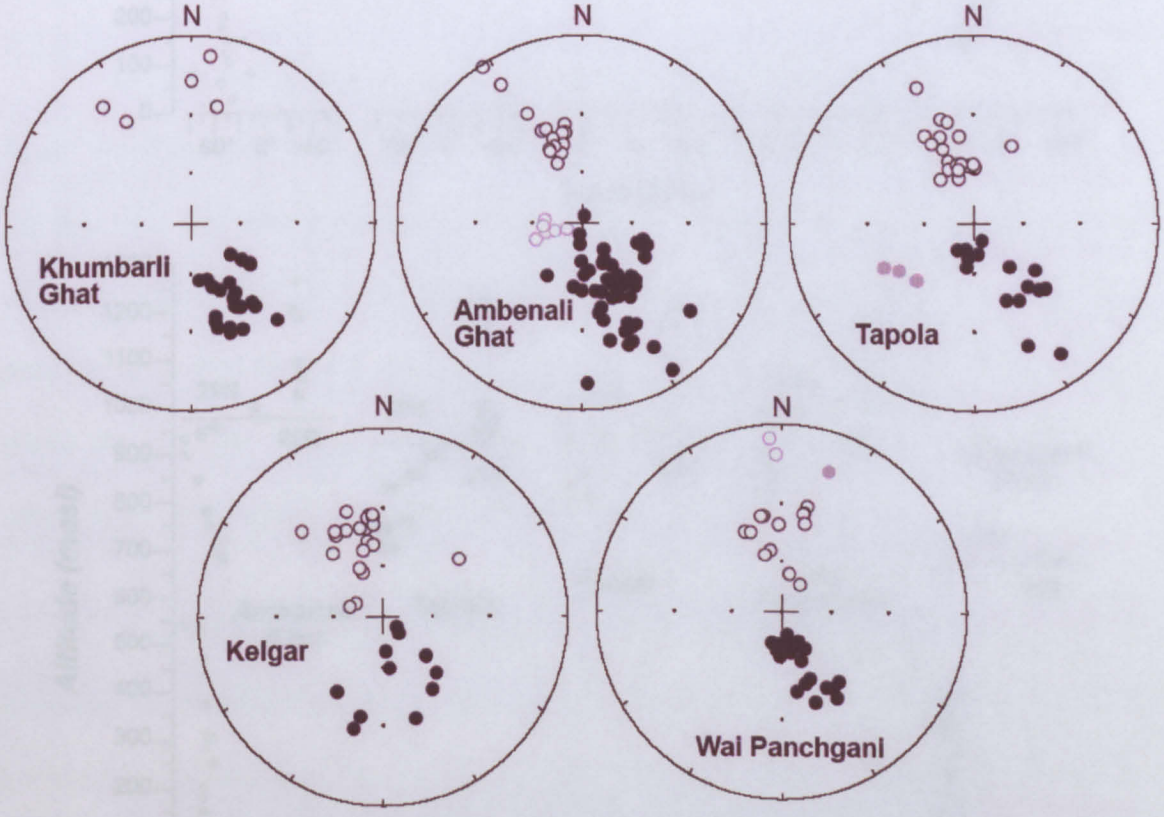

Figure 3.9. Equal area projections of site mean directions from each of the studies sections. Solid (open) symbols represent lower (upper) hemisphere projections. Samples outlined in grey are samples that yielded transitional direction at the 29R/29N reversal boundary, but have not been included in the calculation of the overall statistics.

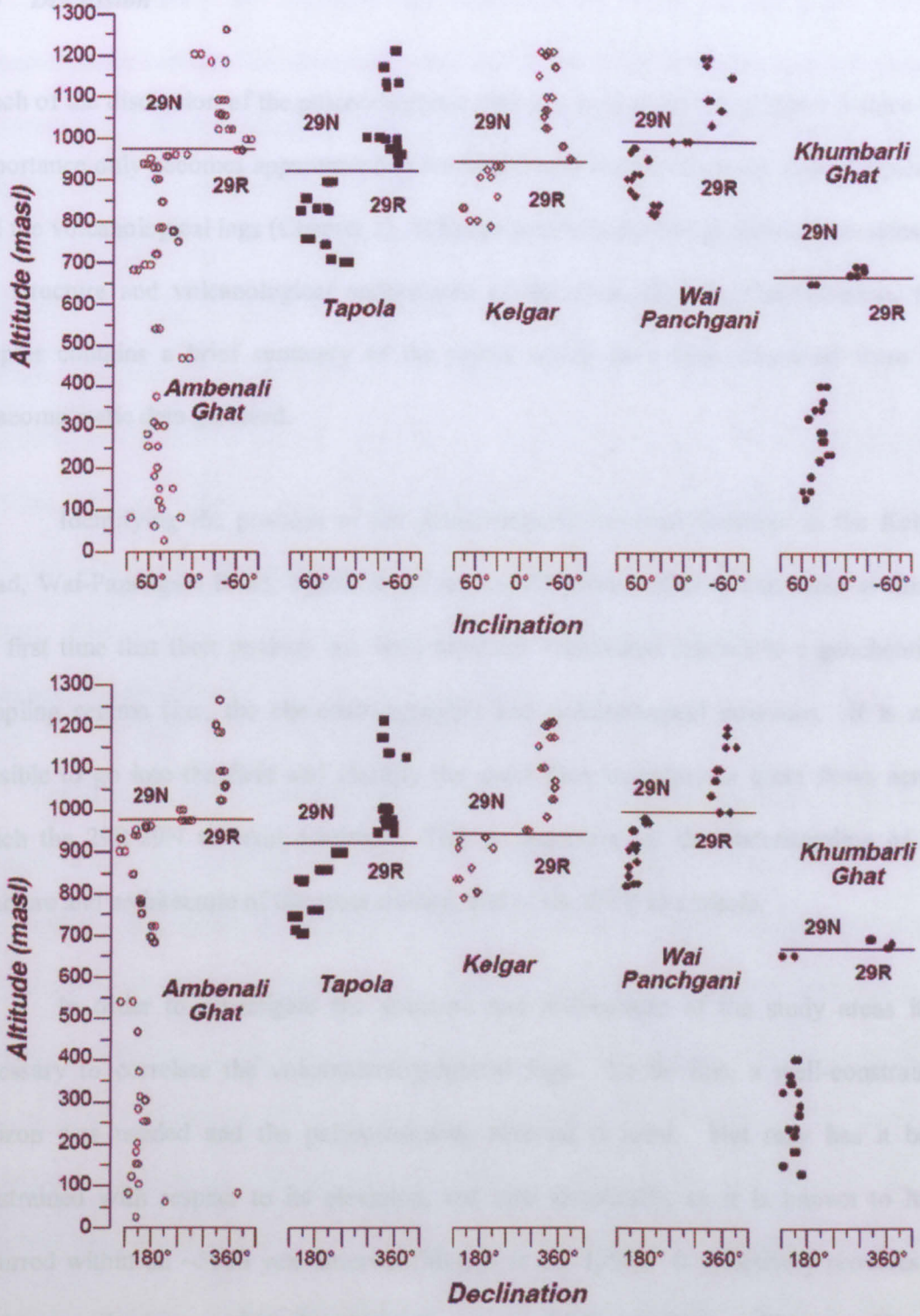

Figure 3.10. Altitude versus magnetic inclination and declination, which shows magnetostratigraphic correlation of each of the traverses sampled in the Western Ghats. It can clearly be noted that the 29N/29R reversal boundary occurs at a different altitude within each section, indicating that there has been differential vertical movement between the various sections post-dating their emplacement. Some of this altitude variation may also be due to the topography present on the active surface of the DVP. masl = metres above sea level. Sections are aligned around the Mahabaleshwar Plateau as they are encountered from east to west, in an anti-clockwise direction, Khumbarli Ghat is 60 km south of the Mahabaleshwar Plateau.

3.6 Discussion

Much of the discussion of the palaeomagnetic data is provided later in Chapter 5 since the importance only becomes apparent when combined with the geochemical data (Chapter 4) and the volcanological logs (Chapter 2). It has primarily been used to draw conclusions on the structure and volcanological architecture of the areas studied. Nevertheless, this chapter contains a brief summary of the topics which have been discussed from the palaeomagnetic data gathered.

Identifying the position of the palaeomagnetic reversal horizons in the Kelgar Road, Wai-Panchgani Road, Tapola Road and on Khumbarli Ghat is important as this is the first time that their position has been precisely established relative to a geochemical sampling regime (i.e., the chemostratigraphy) and volcanological structure. It is now possible to go into the field and identify the exact flow boundary or sheet flows across which the 29R/29N reversal occurred. This is important for the understanding of the structure and architecture of the areas studied, and of the DVP as a whole.

In order to investigate the structure and architecture of the study areas it is necessary to correlate the volcanostratigraphical logs. To do this, a well-constrained horizon was needed and the palaeomagnetic reversal is ideal. Not only has it been constrained with respect to its elevation, but also temporally, as it is known to have occurred within an ~5000 year interval (Merrill et al., 1996). It effectively provides an isochronous horizon within the timescale of the DVP eruptions. This provides an opportunity to compare the sheet lobes and flow-fields in the different traverses in which the reversal occurs, but as will be shown later, the sheet lobes, flow fields and bole horizons are not so easily correlated across the Mahabaleshwar Plateau as might first be expected (See Chapter 5).

Nevertheless, by aligning the volcanological logs with respect to the palaeomagnetic horizon (29R/29N), the post-eruptive warping can effectively be removed (Figure 5.11). For convenience sake the plateau-wide palaeomagnetic reversal horizon has been taken as horizontal, although in reality there would have been some topography on it. Once the logs are aligned it is possible to estimate the amount of palaeotopography that existed on the active surface of the DVP by comparing the different thicknesses of lava between the base of the Mahabaleshwar Formation and the 29R/29N boundary, and 29R/29N and the laterite surface. This showed that there was up to 95 m of topography (Section 5.4.3 and Figure 5.10). This topography indicates that not all the sheet lobes extended across the entirety of the Mahabaleshwar Plateau and/or that inflation was uneven. This observation and attempts at correlation of sheet lobes and flow-fields across the Mahabaleshwar Plateau are further discussed in Chapter 5.

Chron 29R is one of the most important palaeomagnetic times periods as the KTB occurred within its ~ 833,000 year span (Cande and Kent, 1995). It was hoped that by undertaking a palaeomagnetic study of sections of the Western Ghats Escarpment the base of Chron 29R, the 30N-29R boundary, would also be discovered which would then have provided a thickness of material to which a volume, and then an eruption rate could be applied. Unfortunately the 30N-29R reversal was not located. This is surprising, however, as dating carried out by Widdowson and Kelley (in prep) suggests that the base of 29R should be in the Matheran Ghat section (e.g., in the Bhimashankar or Neral Fms). Detailed drilling of the whole section, even down into the top of the Neral Fm failed to find this. Subsequent work by the IPGP team from Paris indicates that the 30N/29R reversal horizon probably occurs stratigraphically lower in the sequence (M. Widdowson, Pers. comm. 2005). Locating this important horizon in relation to the sections from this study will provide an important insight into the emplacement of the DVP.

3.7 Conclusions

- The palaeomagnetic reversal 29R-29N is found in five traverses, four around the Mahabaleshwar Plateau, and along Khumbarli Ghat, 60 km to the south.

- The elevation at which the palaeomagnetic reversal occurs varies in each section in which it is found and is approximately 100 m lower in Khumbarli Ghat, than the Mahabaleshwar Plateau. The majority of this difference is a product of the gentle, southward regional dip of the DVP lavas in this area, but some is thought to be due to sheet lobes not extending over the whole Mahabaleshwar Plateau, or inflating unevenly.

- The basalts observed in Varandah Ghat and Matheran Ghat all fall solely within chron 29R.

- The 29R-29N horizon appears to be concordant with a thin red bole horizon in all but the Tapola road section where it cannot be pinpointed due to a lack of exposure.

- The first exposure sampled above the final 29R sample on the Ambenali Ghat, Tapola and Wai-Panchgani traverses appears to have a transitional palaeomagnetic direction, indicating that the sheet lobe was emplaced during the palaeomagnetic reversal and that the bole nearest to the reversal developed in a geologically short period of time, i.e., less than 5000 years.

Chapter 4
Chemostratigraphy of the Western Ghats

4.1 Introduction

Much of the stratigraphic work carried out on the DVP has evolved using extensive geochemical studies in order to form a robust geochemical stratigraphy (Cox and Hawkesworth, 1985; Beane et al., 1986; Devey and Lightfoot, 1986; Subbarao and Hooper, 1988). During this current work, detailed sampling was undertaken along seven sections (See Chapter 2 and Appendix A1-A7), ascending the Western Ghats Escarpment (between 17°20'E and 19°N) and, as such, consolidates previous studies. More importantly however, the current work offers, for the first time, an integration of detailed volcanostratigraphical logging, palaeomagnetic sampling and flow-by-flow chemostratigraphy. Moreover, one logged section of this work, the Tapola road (Section 2.6.2; Figure 2.2), has never been studied before. This chapter aims to identify the formation boundaries within the seven sections studied. Chapter 5 uses these results and the palaeomagnetic data (Chapter 3) in an attempt to correlate individual sheet lobes and flow fields across a small area of the DVP, namely the Mahabaleshwar Plateau, and slightly further a field (Khumbarli Ghat and Varandah).

The DVP geochemical stratigraphy of the Deccan Group, (i.e., the entire volcanic succession) is divided into three sub-groups (Table 2.1), and these sub-groups into subsequent formations. Formations are defined as the 'smallest mappable or traceable unit' (Holland et al., 1978; Whittaker et al., 1991), and the formation must have internal lithological consistency and mappability. Generally, in sedimentary successions a change in lithological characteristics would define a formation boundary. However, in the DVP, this definition is not appropriate as it is predominantly tholeiitic lava units, and therefore

basalt petrography, mineralogy and, most importantly, the geochemical characteristics are used to define formations.

The DVP volcanic pile has been divided into formations based upon geochemical criteria, most reliably $^{87}Sr/^{86}Sr$, and these packages have been shown to be traceable, not just around the Mahabaleshwar Plateau area where they were originally defined, but to the far south and east of the Western Ghats (Devey and Lightfoot, 1986; Mitchell and Widdowson, 1991; Bilgrami, 1999; Jay and Widdowson, in prep.) and even to the Rajahmundry Traps (Figure 3.2), an outlier of the DVP on the east coast of India (Knight et al., 2003; Self et al., in prep).

The first part of this chapter (Section 4.2) provides an overview of the previous chemostratigraphic work undertaken on the DVP over the past two to three decades. Firstly, there is a summary of the petrogenesis of the basaltic lavas encountered in the main field area around the Mahabaleshwar Plateau. This is followed by a description of the development of the Deccan chemostratigraphy, from the first geochemical study carried out in the Western Ghats in the late 1970s, to the development and refinement of the geochemically defined formations as they are known to day. The early work has led to the establishment of criteria now used for defining the Bushe, Poladpur, Ambenali, Mahabaleshwar and Panhala Formations (Devey and Lightfoot, 1986) and an understanding of the broad stratigraphy and structure of the DVP (Devey and Lightfoot, 1986; Mitchell and Widdowson, 1991). More recent work has investigated the petrogenesis of basalts in the NW and NE provinces of the DVP and seeks to investigate their relationship with the basaltic sequences of the Western Ghats. Section 4.3, describes the geochemical characteristics of the formations of the Wai Sub-group and the Bushe Fm, as these are the Formations encountered around the Mahabaleshwar Plateau, along Varandah and Khumbarli Ghat. Section 4.4 briefly explains the data collection and

summarizes the data analysis. A more comprehensive treatment of the latter is covered more fully in Appendix C1. The results (Section 4.5) provides all the results of XRF analysis from all the samples collected, places them in their appropriate formations, defines them and their exact elevations within the context of this study. The discussion (Section 4.6) is divided into two parts: the first covers the more southerly traverses of the Mahabaleshwar Plateau, Varandah and Khumbarli Ghat, whilst the second describes the more northerly Matheran Ghat. This discussion is deliberately brief as the geochemical analysis has been used primarily as a tool during this study to enable the volcanostratigraphical logging to be incorporated into the current chemostratigraphy. However, combining the palaeomagnetic, geochemical and volcanological data collected, this work offers insights into the structure of the lava units. The implications of which are further discussed in Chapter 5.

4.2 Previous work on the geochemistry of the Western Ghats

4.2.1 Petrogenesis of the basaltic lavas

The variations in the chemical composition of the DVP tholeiitic basalts can be ascribed to three different processes. These occurred prior to the eruption of the basalt and are either fractional crystallisation of the magma, variations in the composition of the deep-seated source the amount of crustal contamination suffered by the magma during its ascent to the surface (e.g. Cox and Hawkesworth, 1984; Cox and Hawkesworth, 1985). Fractional crystallisation can explain the variation in concentration of incompatible elements e.g., 50-100 ppm Ba in the Ambenali Formation can be ascribed to 50% fractionation of gabbroic assemblages (e.g. Cox and Devey, 1987). The effects of this fractional crystallisation on basalt geochemistry can be seen through by using incompatible element ratios and isotopic ratios (Mitchell and Widdowson, 1991). However, any variation in the ratios themselves is related to differences in the incompatible element ratios within the parental magmas i.e.,

source variations (Cox and Hawkesworth, 1985; Mitchell and Widdowson, 1991). Minor within-suite variation of Sr is consistent with fractional crystallisation because Sr concentrations are buffered during the fractionation of a gabbroic assemblage containing 50% plagioclase (Cox and Hawkesworth, 1985). Larger changes in the geochemistry of the basalts can therefore be ascribed to either crustal contamination or heterogeneity of the source.

Archaean granitic basement is thought to be one of the main sources of contamination of the DVP basaltic magmas. This is most clearly demonstrated by the basalts of the Bushe Formation, which have a markedly different chemistry to the other DVP successions. Bushe lavas are characterised by high initial $^{87}Sr/^{86}Sr$ and $^{206}Pb/^{204}Pb$ ratios, as well as a significant elevation in K, Rb and Ba, but without a comparable enrichment in Sr, Ti, Nb and P (Mahoney et al., 1982; Cox and Hawkesworth, 1985). The Mahabaleshwar and especially the Ambenali Formations show only limited evidence of crustal contamination. Moreover, Cox and Hawkesworth (1985) state that the geochemistry of the Poladpur and Mahabaleshwar Formation basalts can be extrapolated back to that of the Ambenali Formation at lower ε_{Sr} and higher ε_{Nd}, demonstrating a degree of magma mixing and further indicating the uncontaminated state of the Ambenali Formation lavas. Despite this indication of a similar magma source, the Mahabaleshwar Formation has a geochemical signature which is different to the other formations, and Cox and Hawkesworth (1984) suggest the reason is that either a trace element enriched mantle source, or contamination by continental crust of a different composition to that affecting the other formations.

Petrogenesis of the lower six formations (Jawhar to Khandala) has been discussed by Peng et al. (1994). They described the formation of magma for these formations as being characterised by a) the abundant presence of magmas with a limited spread of

isotopic and incompatible element ratios (they termed this the common signature) and by b) the variable contamination of this common signature by at least three different continental end members. The common signature's range of Nd-Sr and Pb ratios lies outside that of oceanic lavas and Peng et al. (1994) suggest that this is due to either crustal contamination which could be achieved with hypothetical mixtures of Ambenali or Reunion-like parental magmas and high-degree melts of Archaean basic amphibolites (seen out-cropping to the north and south of the DVP), or a mantle source(s) in old Indian lithosphere. If either of these are the source of the common signature, then the contaminants must be abundant and the magma must be formed in an open system. This common signature is not identified in any of the later DVP formations (i.e., Bushe to Desur Formations).

4.2.2 The development of the Western Ghat stratigraphy

The original theories on the stratigraphy of the DVP developed in the 19th century, when it was understood that the DVP younged from the east to west (see Krishnan, 1956 and references therein). The modern geochemical stratigraphy developed over time from the late 1970s as the understanding of the development of the DVP grew with progressive geochemical and stratigraphical studies.

This first detailed study of the Western Ghats geochemistry was carried out by Najafi et al. (1981). The section studied was from Mahad (18°03'59"N 73°25'07"E), (near to the turn off to Varandah Ghat section) to Mahabaleshwar (Figure 2.2), which is essentially the same as the section in this work called Ambenali Ghat. Najafi et al. (1981) undertook a study of the petrography, and trace and major element geochemistry of each flow he encountered (though the definition of 'flow' is not given although it is probable that his term 'flow' corresponds to the term 'sheet lobe' in this work). They discovered that the section was composed of 47 exposed 'flows' and provided the first stratigraphic

division of the DVP. Najafi et al. (1981) divided the Mahad to Mahabaleshwar section into three chemically distinct groups: the Lower, Middle and Upper groups. The Lower Group, flows 1-16, were characterised by high K, Rb, and Ba combined with high Zr/Nb (15.6-21.8) and high Y/Nb (3.1-5.8) ratios; overall these flows are Fe-poor. The Middle Group, flows 17-31, were described as having low K, Rb and Ba contents and Zr/Nb ratios (12.4-14.4) and Y/Nb ratios (3.1-3.9) which are lower than those of the Lower Group. These rocks however, are mainly Fe-rich. The Upper Group flows, 32-47, were classified as having high K, Rb and Ba, similar to the Lower Group, but much lower Zr/Nb (7.5-12.2) and Y/Nb (1.6-2.80) ratios. These rocks were also found to be mainly Fe-rich. The petrogenic origins of these divisions was also touched upon, with contamination of the basaltic melt by varying amounts of more acidic, granitic continental crust suggested as the possible cause of the differences (Najafi et al., 1981).

A study carried out by Mahoney et al. (1982), also included the Ambenali Ghat section. Their work concentrated more on the chemical origin of the DVP lavas as opposed to using the geochemistry to form a stratigraphy. Mahoney et al.'s (1982) work used major and trace element data, but also included REE and isotopic ratios. This work divided the Ambenali Ghat basaltic pile into only two groups, the Lower and Upper Groups, based on Nd and Sr ratios, with the boundary at ~ 954 m asl. This division is at a similar elevation to the later-defined Ambenali-Mahabaleshwar Formation boundary of Cox and Hawkesworth (1984).

Najafi et al. (1981) produced the basis for much of the chemostratigraphic work that was to be later extended across much of the MDP. However, in order to accomplish this, the Western Ghats was divided up between a combined study group comprising workers from the USA, UK and India. Their preliminary work was presented at IAVCEI 1983 (Beane et al., 1983), and was mainly reconnaissance mapping of 7000 km^2 of the

western DVP, north of the Mahabaleshwar area between 18° 20' and 19°15', accompanied by trace and major element analysis which defined twelve major stratigraphic units (Table 4.1).

Unit	Discriminatory Features	TiO_2	Thickness (m)
Sinhaghad (S)	Well defined flows with oxidised tops, high CaO	2.0-3.0	500
Fort (F)	Well defined flows with some amygdaloidal features	1.75-2.15	450
Ambavne (A)	Well defined phyric to aphyric flows. Fine-grained matrix with glomeroporphyritic ol + plag.	2.20-2.50	50
Bushe (B)	A massive medium-grained amygdaloidal units, aphyric to plag. And cpx microphyric	1.00-1.45	150-300
Khandala (K)	A conspicuous, variable group of well defined flows fine-grained matrix glomeroporphyritic plag + ol.	2.20-2.90	150-200
Monkey Hill Flow	Giant plag. phenocrysts flow with fine-grained matrix	3.1-3.2	40
Bhimashankar (BIM)	Massive coarse-grained, plag., phyric amygdaloidal with microphenocrysts of ol and cpx.	1.85-2.50	50-125
Mancher Flow	Giant plag. phenocrysts flows	2.8	10
Thakurvadi (TH)	Massive coarse-grained, aphyric amygdaloidal with locally abundant ol and cpx	1.0-2.00	200
Tunnel 5 Flow	Giant plag. phenocryst flow	3.15-3.40	20
Neral	Small glomeroporphyritic groups of cpx and ol in a fine-grained matrix	1.40-1.70	100
Kashale	Giant plag. Phenocryst flow	2.70-3.00	25

Table 4.1. Twelve stratigraphic divisions of the Western Ghats, as defined by Beane et al. (1983). (From Beane et al., 1983)

Beane et al. (1983) studied the more northerly area of the Western Ghats between 18°20'N and 19°15'N, while Cox and Hawkesworth (1985) produced a detailed stratigraphy of the basalt pile of the Ambenali Ghat section. Five formations were defined; these were, from bottom to top: the Bushe, Upper and Lower Poladpur, Ambenali and Mahabaleshwar formations (Table 4.2). This work determined that Poladpur basalts were contaminated with crustal material, as were Ambenali Formation basalts but to a much lesser degree. The Mahabaleshwar Formation basalts are either derived from a relatively trace element enriched mantle source or were contaminated with a different crustal component to the lower two Formations. Correlations by Cox and Hawkesworth (1985) between their work and that of Beane et al. (1983) concluded that the lower units (Table 4.1) described by Beane et al. (1983) were absent further south at the Mahabaleshwar Plateau, Varandah Ghat and Khamshedi Ghat (~5 km south of Poladpur on the main, Mumbai-Chiplun road), due to the southerly regional dip of the Main Deccan Province

(MDP). The upper units of the Pune sequence and those of the Mahabaleshwar area however, show a strong correspondence, Cox and Hawkesworth (1985) therefore renamed the lowest portion of their Poladpur Fm, as defined in Cox and Hawkesworth (1984), the Bushe Formation to coincide with Beane et al.'s (1983) classification. The thin Ambavne Formation (Beane et al., 1983) appears to be absent in the Ambenali Ghat section (Mahad-Poladpur-Ambenali-Mahabaleshwar, (Figure 2.2)) and consequently the Poladpur Formation was divided into two (Cox and Hawkesworth, 1985).

Formation Name	Approximate thickness
	(top not seen)
Mahabaleshwar	256 m
Ambenali	550 m
Upper Poladpur	160 m
Lower Poladpur	140 m
Bushe Formation	124 m
	(base not seen)

Table 4.2. The stratigraphy of the Mahabaleshwar area as defined by Cox and Hawkesworth (1985)

The geochemical stratigraphy of the more northerly area of the MDP, encompassing Matheran Ghat, was mostly carried out by the workers from the Indian Institute of Technology (IIT) and Beane (1988). Bodas et al. (1984) geologically and geochemically mapped an area between Nasik and Junnar (19°-20° N), which is stratigraphically below (i.e. older) than the units further south. Four formations were identified, (from oldest to youngest) the Jawhar, Igatpuri, Thakurvadi and Bhimashankar Formations, (Table 4.3). Note that the Neral Formation is absent as it was not found in the study area of Bodas et al. (1984).

These three teams of Cox and Hawkesworth, Beane et al., and the group from IIT and subsequent workers, produced the majority of the stratigraphy of the DVP that is

known and used today. Beane et al. (1986) is a much more detailed study of the earlier 1983 data published by Beane et al. (1983) and, as a result, the stratigraphy defined in Table 4.1 from Beane et al. (1983) was abandoned and the modern stratigraphy, based around 3 sub-groups and 10 (later 12) formations was developed (Table 2.1). The criteria that Beane et al. (1986) used for determining these formations were based upon various major and trace element abundances, and field and thin section observations, this was confirmed by isotope and trace element ratios (Table 4.3). This stratigraphy was further refined and expanded (including the discovery of the Panhala and Desur Formations) by Devey and Lightfoot (1986) and Lightfoot (1985).

The three sub-groups defined are: the Kalsubai Sub-group, the Lonavala Sub-group and the Wai Sub-group (Table 4.3). The Kalsubai Sub-group (~ 2000 m thick) is the lowest in the stratigraphy and consists of the Jawhar, Igatpuri, Neral, Thakurvadi and Bhimashankar Formations. Of these, the Neral, Thakurvadi and Bhimashankar Formations were encountered during this study (i.e., Matheran Ghat). The middle, Lonavala Sub-group (max. thickness 525 m thick) consists of only the Khandala and Bushe Formations. The upper, Wai Sub-group (~1100 m thick) is arguably the most voluminous of the three and is composed of the Poladpur (during this current study the Poladpur Formation was not divided into its Upper and Lower Members, nor was the Ambavne Member identified), Ambenali, Mahabaleshwar, Panhala and Desur Formations. The Desur Formation however was not identified in any of the study areas during this work, and is only known to outcrop in the Belgaum region (c.16°N).

Group	Subgroup	Formation	Members and Chemical Types (CT)		(3) Flow Type	Texture (4) Phenocrysts ol	cpx	opx	pl	Grain Size	(5) % MgO	(6) % TiO_2	(7) $^{87}Sr/^{86}Sr$
DECCAN BASALT	WAI	Mahabaleshwar (1)	(Incomplete)			X (8)	X		X	C&F			
		Ambenali	Ambenali CT			X	X		X	F			
		Poladpur	Main Poladpur			X	X		X	F			
			Ambavne			X			X	F			
	LONAVALA	Bushe	Bushe CT			X			X	C			
			Pingalvadi			X				F			
			Bushe CT			X			X	C			
			Shingi Hill			X			X	C			
			Bushe CT			X			X	C			
			Picrite basalt			X	X		X	C			
			Bushe CT			X			X	C			
		Khandala	See Fig. 2b			Alternating phyric and aphyric flows						See Fig. 2b	
	KALSUBAI	Bhimashankar	Bhimashankar CT			X			X	C			
			Manchar GPB (9)			X			X	C			
		Thakurvadi	Thakurvadi CT			X	X			C			
			Water Pipe Member			X	X			C			
			Thakurvadi CT			X	X			C&F			
			Picrite basalt			X	X			F			
			Jammu Patti Member	3		X				F			
				2		X			X	C			
				1		X				F			
		Neral	Tunnel 5 GPB (9)			X			X	F			
			Picrite basalt			X				C			
			Neral CT			X	X			F			
			Tembre basalt			X				F			
			Ambivili picrite basalt			X	X	X	X	F			
		Igatpuri	Kashele GPB (9)			X			X	F			
			Igatpur CT			X				F			
			Thal Ghat GPB (9)			X			X	F			
		Jawhar (2) (Incomplete)	Jawhar CT			X				C			
			Kasara phyric basalt			X			X	F			

Table 4.3. Stratigraphic nomenclature and selected diagnostic features for the MDP, Western Ghats, from Beane et al. (1986). 1) Mahabaleshwar Formation described by Cox and Hawkesworth (1985). 2) Jawhar Formation described by Bodas et al. (1984). 3) Predominantly amygdaloidal compound flows (cross-hatch); predominantly simple flows (stipple). 4) F=fine grained matrix; c=coarse grained matrix; x=present. 5) Cross-hatch > 9.8% MgO; oblique hatch=9.8%-8.1% MgO; stipple < 8.1 MgO. 6) Cross-hatch=2.75-3.60% TiO_2; oblique hatch=2.75-1.65% TiO_2; stipple=1.65-0.90% TiO_2. 7) Cross-hatch > 0.7100; vertical hatch=0.7100-0.7060 (all lie between 0.785 and 0.760 except coarse and fine grained aphyric Khandala flows, the Water Pipe member and the Thakurvadi, and two specific flows in the Poladpur); oblique hatch=0.7060-0.7055; stipple=0.7050-0.7040. 8) Virtually all Deccan Flows contain phenocrysts or microphenocrysts of olivine, but most are completely replaced. 9) GPB, giant plagioclase basalts.

The culmination of this previous work was a geological map of the Western Ghats, that combined all the geochemical data collected (Subbarao and Hooper, 1988). This provided, for the first time, a compilation of all the previous work showing the progressive younging of the lavas from north to south. This work still provides an

excellent tool for explaining and investigating the large scale stratigraphy (e.g. Devey and Lightfoot, 1986; Mitchell and Widdowson, 1991; Khadri et al., 1999), and for further discussing the origin and development of the magmas (e.g. Lightfoot et al., 1990; Peng et al., 1994; Sano, 2001.

The more recent work on the DVP has concentrated on the geochemistry and petrogenesis of the lavas from the Mandala Lobe (North East), Kutch (North West), and Malwa Plateau (North) regions (Figure 1.2). Drill holes from the Kutch show picrites and basaltic lavas with two distinct trends: 1) a mixing between a mantle end-member (similar to the modern Reunion Island) and continental lithosphere; very different to the lavas seen in the Western Ghats, and 2) mixing between the same or similar continental lithospheric material and a mantle end member resembling the Ambenali Formation. These trend 1 and trend 2 lavas are interbedded, which Peng and Mahoney (1995) suggest indicates a compositionally zoned plumed head. They also suggest that the variation in lavas from north to south DVP is due to the average degree of partial melting increasing gradually southward, possibly because of increased lithospheric thinning.

Basalts from the north east DVP (Mandala Lobe) show strong isotopic and elemental affinities to lavas in the Western Ghats but with some differences, especially in $^{87}Sr/^{86}Sr$ and $^{206}Pb/^{204}Pb$. The isotopic array overlaps the Ambenali Formation field towards the common signature (Peng et al. 1994), which is important for the basis of the lower six Western Ghats formations. In the north east DVP some of the uppermost lavas are chemically and isotopically indistinguishable from the Ambenali Formation and beneath these are flows that chemically resemble the Poladpur and Khandala Formations. Peng et al. (1998) suggested that these north east flows may be petrogenetically related to the Western Ghats formations but are probably erupted from different feeder systems. Peng

et al. (1998) do not rule out some Ambenali Formation flows having travelled the 900 km from the proposed vents, near Nasik in the Western Ghats.

The Tapi Rift, to the north of the MDP contains lavas which are similar isotopically and geochemically to the Wai Sub-group lavas. Chandrasekharam et al. (1999) suggested that this demonstrates that the Wai Sub-group lavas extended further north than had previously been demonstrated, although no Ambenali formation lavas are found here (unlike in the Mandala Lobe; Peng et al., 1994) suggesting that the Ambenali units flowed in a more north easterly direction.

These, more recent, papers demonstrate that the lavas of the Western Ghats probably extended further than the MDP alone. Further isotopic investigation of lavas and dikes is necessary to clear some of the confusion over their origin, be it local or from the same vents as form the lavas of the Western Ghats. If they did not originate from the Western Ghats, then further work is needed to demonstrate more precisely the actual extent of the formations and their path between the Western Ghats and their outcrops in the periphery of the DVP.

4.3 Definitions of geochemical formations used in this thesis

This study used chemostratigraphy to aid the correlation of units across the Mahabaleshwar Plateau, and to Varandah and Khumbarli Ghat. The geochemical stratigraphy and criteria important to the correlation are discussed below. For an over-view of the chemistry of the lower formations, see Table 4.3, Beane et al.(1986) and Khadri et al. (1999).

The criteria by which the geochemical formations were distinguished during this study were determined by Devey and Lightfoot (1986) (see Table 4.4 and Figure 4.1). They identified $^{87}Sr/^{86}Sr$ ratios as the most reliable criteria for defining the geochemical formations and combining this with the Ba/Y, Zr/Nb and Sr vs. height plots improved the

criteria for bracketing the geochemical formations and therefore defining the formation boundaries Table 4.4). This method is sufficient to identify to which formation the majority of samples belong, but the reliability of these trace element criteria decreases close to formation boundaries since the flows here often display hybrid geochemical signatures, probably due to switches in the magma source. Ideally, to determine the formation boundaries precisely $^{87}Sr/^{86}Sr$ ratios would have been obtained, but this would have proved time consuming and was beyond the remit of the current study. Instead I have relied upon the trace element concentrations and ratios from Devey and Lightfoot (1986) (Table 4.4).

Formation	Criteria					Thickness (m)
	Sr (ppm)	Ba (ppm)	Ba/Y	$^{87}Sr/^{86}Sr$	Zr/Nb	
Panhala	< 200	< 90	-	-	> 13	25 to > 175
Mahabaleshwar	> 250	> 100	> 4	>0.705	< 10.5	280
Ambenali	200-250	< 100	< 3.5	<0.705	10.5-15	500
Poladpur	-	> 100	> 3.5	0.705-0.712	15-20	370
Bushe	-	> 100	-	> 0.713	> 20	> 160

Table 4.4. Criteria used to determine the geochemical formations during this current study, from Devey and Lightfoot (1986).

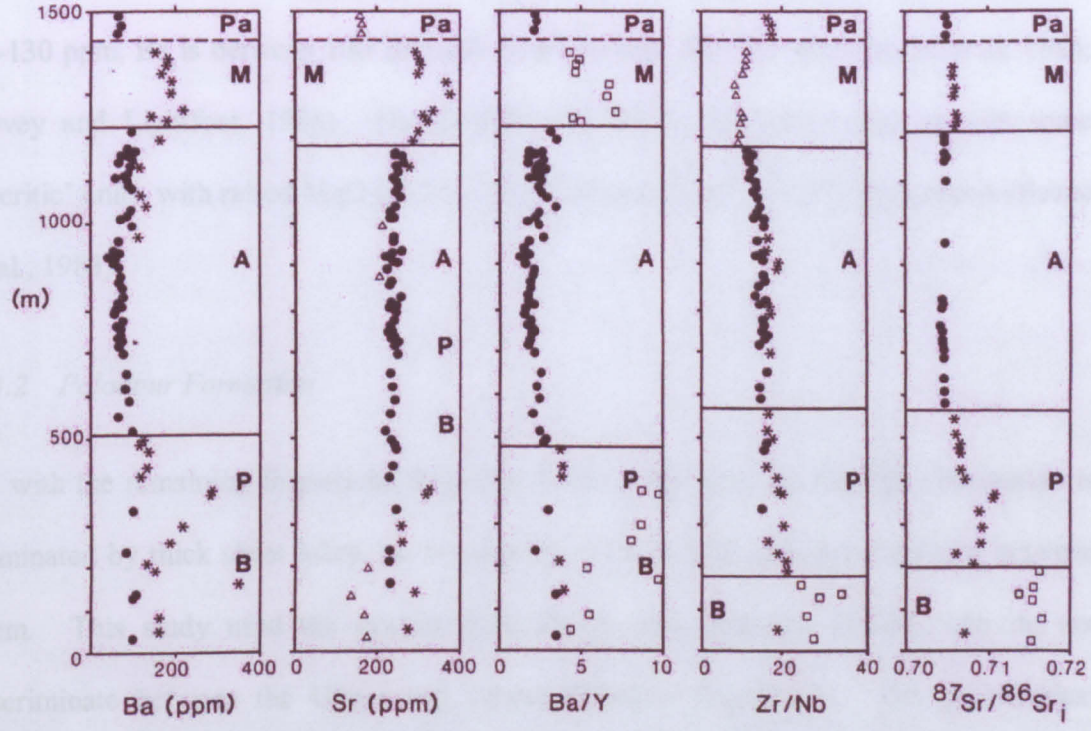

Figure 4.1. The Ba, Sr, Ba/Y, Zr/Nb and $^{87}Sr/^{86}Sr$ vs. height above sea level for the combined Torna and Raigad sections (Figure 2.1). The individual datum points are classified in accordance with Table 4.4 as follows: Ba: solid circle < 100 ppm, star > 100 ppm; Sr: triangle < 200 ppm, circle 200-250 ppm, star>250 ppm; Ba/Y: circle < 3.5, star 3.5-4, square > 4; Zr/Nb: triangle < 10.5, circle 10.5-15, star 15-20, square >20; $^{87}Sr/^{86}Sr_i$: circle < 0.705, star 0.705-0.713, square > 0.713. B=Bushe Fm, P=Poladpur Fm, A=Ambenali Fm, M=Mahabaleshwar Fm, Pa=Panhala Formation Note how the $^{87}Sr/^{86}Sr$ data jump sharply at the boundary of each formation and the similarity of the Panhala Formation geochemical signature to the Ambenali Formation geochemical signature. (from Devey and Lightfoot, 1986)

4.3.1 Bushe Formation

In outcrop this formation can often be relatively easily identified as in the area of this study it is mainly formed of small Hawaiian sized lobes and toes with some sheet lobes as thick as 15 m (Beane et al., 1986). Further north, out of the current study area, this is not necessarily the case as the majority of the sheet lobes are thicker (Devey and Lightfoot, 1986). It is often aphyric or sparsely plagioclase-phyric, but the groundmass is coarse grained, altered, and overall the basalt is amygdaloidal. Generally, it is also the easiest MDP formation to identify geochemically. The Bushe Formation lavas have very high $^{87}Sr/^{86}Sr$ values, > 0.713 (Devey and Lightfoot, 1986), very small concentrations of high field strength (HFS) incompatible elements (Ti, P, Zr and Y), Sr and Fe, with large concentrations of large ion lithophiles (LIL), specifically K and Ba (Beane et al., 1986).

The Bushe Formation is characterised though by its Zr concentrations which are between 80-130 ppm, Ba is between 100-200 and Sr is between 100-300 ppm (Beane et al, 1986; Devey and Lightfoot, 1986). Nevertheless, the Bushe Formation does contain some 'picritic' units, with raised MgO (~12%), Ni (>280 ppm) and Cr (>400 ppm) levels (Beane et al., 1983).

4.3.2 Poladpur Formation

As with the remaining formations described in the study area, the Poladpur Formation is dominated by thick sheet lobes, on average 20 m thick, with bole horizons rare between them. This study used the criteria from Devey and Lightfoot (1986), who do not discriminate between the Upper and Lower Poladpur Formations. The geochemical boundary between the Bushe and Poladpur Formation is marked by an abrupt decrease in the $^{87}Sr/^{86}Sr$ values, allowing the Poladpur to be defined as having $^{87}Sr/^{86}Sr$ ratio < 0.713. Generally TiO_2, Sr and Zr occur in higher concentrations than in the Bushe Formation (Figure 4.2; Cox and Hawkesworth, 1985).

4.3.3 Ambenali Formation

Cox and Hawkesworth (1985) arbitrarily define Ambenali Formation lavas on the basis of their Ba content being <100 ppm, as they concluded that there was no sharp change in any element concentration between the Upper Poladpur Formation and the Ambenali Formation. Beane et al. (1986), however, demonstrated that the $^{87}Sr/^{86}Sr$ ratio is much lower in the Ambenali Formation than in any other formation. The Ambenali Formation is also characterised by low LIL element concentrations, Ba, Rb and K_2O, and moderate to large HFS element abundances (Beane et al., 1986). The basalts of the Ambenali Formation are often moderately to highly porphyritic, but this characteristic decreases in the upper 100 m of the formation.

4.3.4 *Mahabaleshwar Formation*

The base of the Mahabaleshwar Formation is again best defined by an abrupt, but small increase in the $^{87}Sr/^{86}Sr$ ratio to ≥ 0.705, and an increase in the Ba/Y ratio (Cox and Hawkesworth, 1985). On the Kelgar Road (Figure 2.2), the base of the Mahabaleshwar Formation is marked by the Kelgar Mafic Unit (KMU, Cox and Hawkesworth, 1985), which is three sheet lobes characterised by high Mg-numbers and high Ni, Ba and Sr concentrations, it was not, however, identified on Ambenali Ghat or any of the other sections studied (Cox and Hawkesworth, 1985). Overall the Mahabaleshwar Formation is identified by its high Sr, Ba, Nb, and K_2O, although the concentrations of these elements decrease up through the formation (Figure 4.2), and the uppermost sections become difficult to discriminate geochemically and isotopically from Ambenali and Panhala Formation chemotype lavas (Mahoney et al., 1982; Cox and Hawkesworth, 1985).

4.3.5 *Panhala Formation*

This was first identified near Panhala (~16°42'42"N 74°20'08"E) in the south of the DVP (Devey and Lightfoot, 1986). The Panhala Formation has similar geochemical characteristics to the Ambenali Formation. The basalts of the Panhala Formation have high Zr/Nb ratios but low Sr, Rb, TiO_2 and Ba (Table 4.4), and also has generally higher $^{87}Sr/^{86}Sr$ ratios than the Ambenali Formation (Devey and Lightfoot, 1986). Panhala Formation lavas are not obviously exposed in the road sections of the Mahabaleshwar Plateau since if they were present, they would occur only at the highest elevations, consequently they were not identified there by Devey and Lightfoot (1986). Geochemical analysis showed that the Zr/Nb ratios of the overlying laterite cap together with basaltic samples retrieved from isolated exposures in the summit region, are higher than those typical of the Mahabaleshwar Formation and therefore more like the Ambenali or Panhala Formations (Table 4.4). Widdowson and Cox (1996) take this as evidence that the laterite

protolith was Panhala Formation. However, the identification that the upper units of the Mahabaleshwar Formation resemble the Ambenali Formation (and hence the Panhala Formation (Table 4.4)) has been noted in this work (Table 4.3 and Table 4.4) and that of Mahoney et al. (1982), who demonstrated that the upper Mahabaleshwar and Ambenali Formations are geochemically and isotopically indistinguishable from each other. Lightfoot (1985), who first discovered the Panhala Formation in the south MDP, did not find the Panhala Formation as far north as the Mahabaleshwar Plateau, but he did not sample at as high an elevation as Widdowson and Cox (1996) or this thesis. Lightfoot (1985) may provide a method by which the upper Mahabaleshwar, Ambenali and Panhala Formation lavas may be distinguished, by plotting Ce vs Ce/Y each formation plots in their own discreet field.

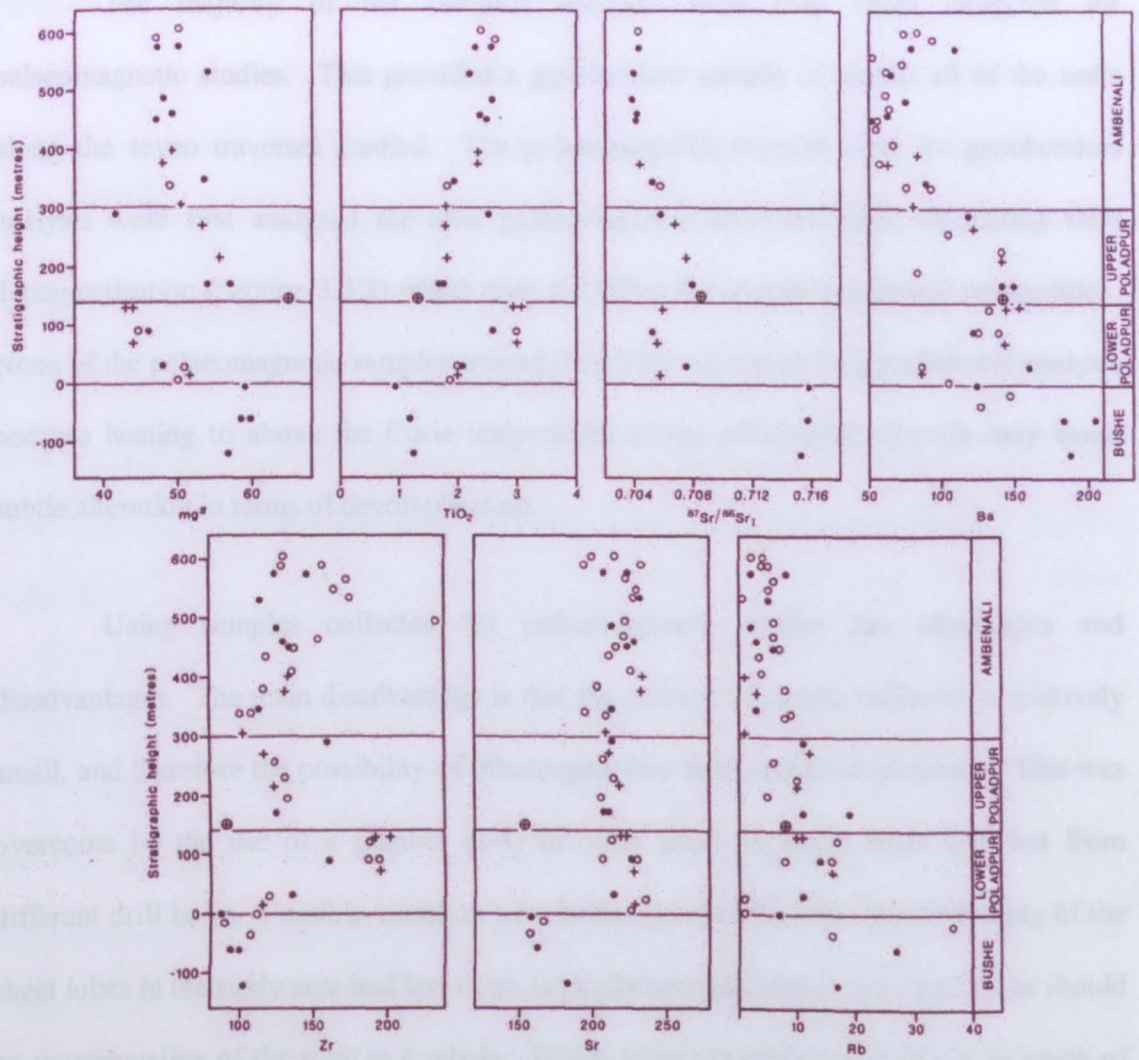

Figure 4.2. Graphs from Cox and Hawkesworth (1985) showing the analytical parameters plotted against calculated stratigraphic height for the lower part of the Mahabaleshwar Plateau sequence (height datum arbitrarily placed at top of Bushe Formation). Solid circles Varandah section; open circles Poladpur-Mahabaleshwar section; crosses Khamshedi section; cross in circle-Khamshedi picrite (Khamshedi section). This does not contain data for the Mahabaleshwar and Panhala Formations.

4.4 Data collection

The geochemically analysed samples were collected in conjunction with the volcanostratigraphic logging. Many of the basalt units in the field area are amygdaloidal with a range of zeolites and, locally, whole exposures can be highly decomposed (Cox and Hawkesworth, 1985) resulting in sections where no worthwhile samples could be taken. However, in some locations the centres of spheroidally weathered sheet lobes contain basalt fresh enough for geochemical analysis.

The majority of the samples analysed were drill cores collected for palaeomagnetic studies. This provided a geochemical sample of almost all of the units along the seven traverses studied. The palaeomagnetic samples used for geochemical analysis were first analysed for their palaeomagnetic direction using alternating field demagnetisation (Section 3.3.2) which does not affect the sample's chemical composition. None of the palaeomagnetic samples treated thermally were used for geochemical analysis because heating to above the Curie temperature of the constituent minerals may cause subtle alteration in terms of devolatilisation.

Using samples collected for palaeomagnetic studies has advantages and disadvantages. The main disadvantage is that the amount of sample collected is relatively small, and therefore the possibility of inhomogeneities being sampled increases. This was overcome by the use of a number (2-4) of cores from the same sheet lobe but from different drill holes. Possible variation was further decreased by the fact that many of the sheet lobes in the study area had few or no large phenocrysts; thus, even small cores should be representative of the rock as a whole. Where large phenocrysts did occur, as much of the available sample as possible was crushed. The main advantage of this method of sampling is that in order to drill, the rock must be as fresh as possible. Such fresh material is essential for good geochemical analyses, and it also allows for any outside weathering rind to be easily discarded before the samples were prepared for analysis. This approach meant that samples could be taken from areas that may previously have been ignored. Some samples were collected as hand specimens using a hammer, but only from locations which were not drilled for palaeomagnetic studies.

All the geochemical data collected during this study was done using XRF analysis. Each sample was crushed to a fine powder in an agate Tema mill, having first

removed as much of any zeolites or amygdales as possible. Further details of preparation and analytical parameters are given in Appendix C1.

4.5 Results

As with the palaeomagnetic data collected and described in Chapter 3, the geochemical data presented here are employed primarily as a tool to place the studied lavas within a stratigraphical context and to further understand the structure of the basalts of the Western Ghats, specifically the Mahabaleshwar Plateau. All the geochemical data are presented in Appendix C2-C8.

The geochemical data collected during this work have enabled the logged sections to be divided into their respective geochemical formations. The geochemical formations of the Wai Sub-group, which form the bulk of the Mahabaleshwar Plateau lava units, Khumbarli Ghat and Varandah Ghat lava units, may be categorized using the easy-to-use criteria developed by Devey and Lightfoot (1986) (Table 4.4), and as such it has proved easier to determine the formations there than on Matheran Ghat (Khadri et al., 1999), which, although it has been extensively studied, does not have an easy to apply discriminatory criteria like that provided by Devey and Lightfoot (1986)

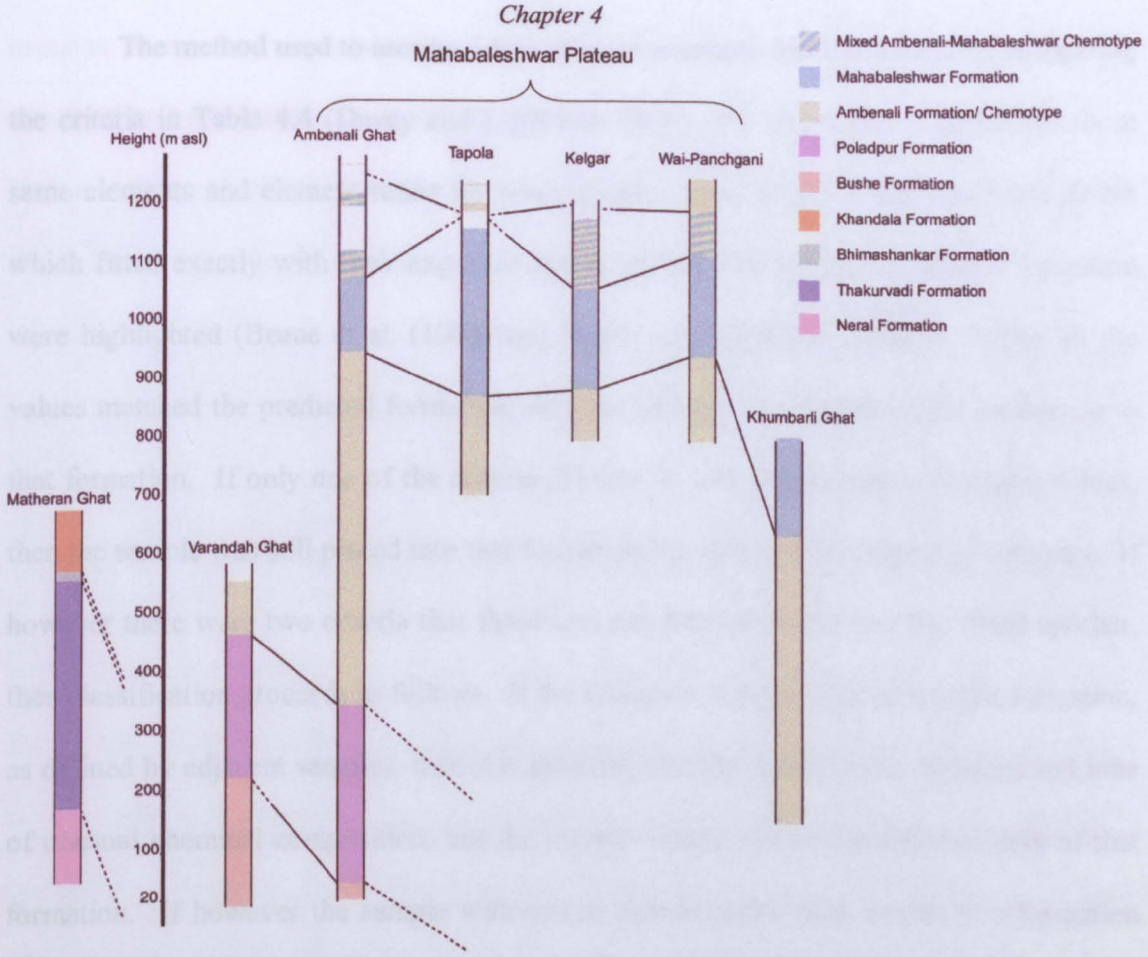

Figure 4.3. Stratigraphic logs for all sections showing the elevation above sea-level of the formation boundaries (change in lava chemotype). The Matheran Ghat section (125 km to the north west) is aligned to its elevation above sea-level, but is separate from the other sections as it is farther north and so the lower formations are exposed. Note how the mixed Ambenali Formation chemotype and the upper Ambenali occur above the Mahabaleshwar Formation. The dotted lines indicate where the exact elevation of the change in chemotype is not known. Note that Khumbarli Ghat is 60 km south of the Mahabaleshwar Plateau and Varandah Ghat is 25 km north of the Mahabaleshwar Plateau.

The elevations of the geochemical boundaries identified in this study are in Figure 4.3 and Figure 4.4 (and in more detail in Appendix A1-A7). Occasionally, close to formation boundaries it proved difficult to ascribe samples to a specific formation, and so in the absence of unequivocal criteria, a designation was made by reference to the element ranges for each formation identified by Widdowson et al. (2000). Widdowson et al. (2000) provides a comprehensive compilation of much of the available geochemical data collected by previous workers and provides the maximum, minimum and average of element concentrations and discriminatory element ratios for the Wai Sub-group, which can considerably aid the determination of formations.

The method used to ascribe a formation to a sample was carried out by comparing the criteria in Table 4.4 (Devey and Lightfoot, 1986) with the values acquired for those same elements and element ratios for each sample. Values for Sr, Ba, Ba/Y and Zr/Nb which fitted exactly with their expected ranges (Table 4.4) for their predicted formation were highlighted (Beane et al. (1986) and Devey and Lightfoot (1986)). Where all the values matched the predicted formation, then the sample was ascribed with confidence to that formation. If only one of the criteria did not fit with the expected formation values, then the sample was still placed into that formation but with a lower degree of certainty. If however there were two criteria that fitted into one formation and two that fitted another, then classification proceeds as follows. If the sample is in the middle of a given formation, as defined by adjacent samples, then it is probable that the sample came from a sheet lobe of unusual chemical composition, but the sample would still be classified as part of that formation. If however the sample with mixed criteria came from nearer to a formation boundary, then in the absence of $^{87}Sr/^{86}Sr$ data (as in this work), two strategies were undertaken. Firstly, some of the criteria from Table 4.4 are more reliable for some formations than others. To distinguish the Ambenali Formation from the Mahabaleshwar Formation it is best to use Ba/Y and Zr/Nb ratios, whereas determining the Mahabaleshwar Formation from the Panhala Formation it is best to use Ba/Y, Sr or Zr/Nb (Devey and Lightfoot, 1986). Key criteria for determining the location of the boundary between the Bushe and Poladpur Formation are an increase in % TiO_2 and P_2O_5, and a decrease in K_2O from the Bushe to the Poladpur Formation. Secondly, reference was made to Widdowson et al. (2000) who determined maximum, minimum and average values of all the elements in the Poladpur, Ambenali, Mahabaleshwar and Panhala Formations. By using these data it was usually possible to assign a sample to a formation. Occasionally samples did not fit in with any of the Devey and Lightfoot (1986) criteria and these have been named 'unique'. The process of placing a sample in a formation is not a precise art especially if the samples are near a formation boundary. This has been most common in the upper

sections of the Mahabaleshwar Plateau where the samples do not always exhibit their expected Mahabaleshwar Formation criteria, and have either, mixed Mahabaleshwar/Ambenali Formation characteristics or purely Ambenali characteristics; this is further discussed Section 4.3.5.

The formation boundaries can be best displayed on graphs, showing elemental concentrations, ratios or percentages, plotted against elevation. Graphs in Figure 4.4 show the four geochemical criteria used to define the formations, which often show a 'jump' at each formation boundary. Some elements or element ratios display the formation boundaries more clearly than others, but using a combination of the four criteria from Devey and Lightfoot (Devey and Lightfoot, 1986), together with Table 4 from Widdowson et al. (2000), it has not proved difficult to identify the formations and formation boundaries. However, the Matheran section falls outside the criteria laid down by Devey and Lightfoot (1986), and hence the criteria used to define the formations are derived from the Penrose Field Guide (Subbarao et al., 2000, taken from Beane et al., 1986 and Khadri et al., 1999).

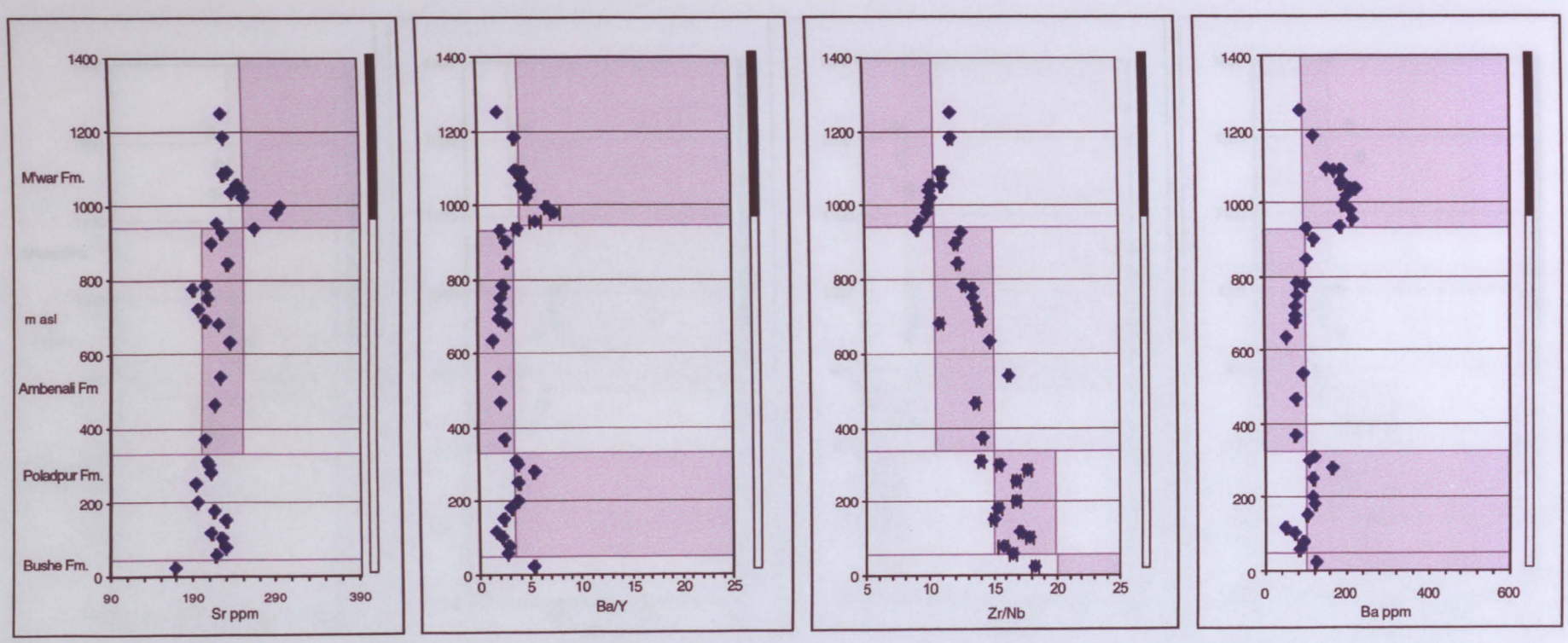

Figure 4.4a Ambenali Ghat

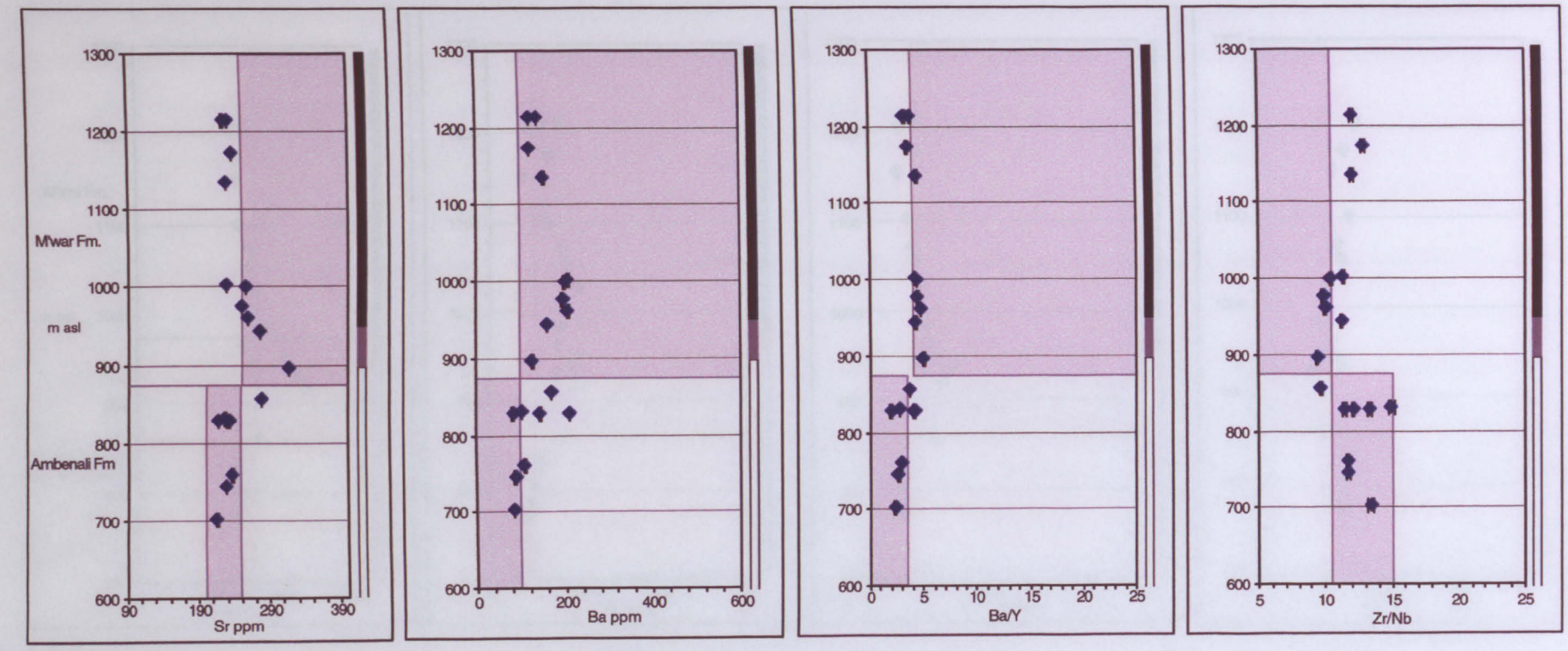

4.4b. Tapola road

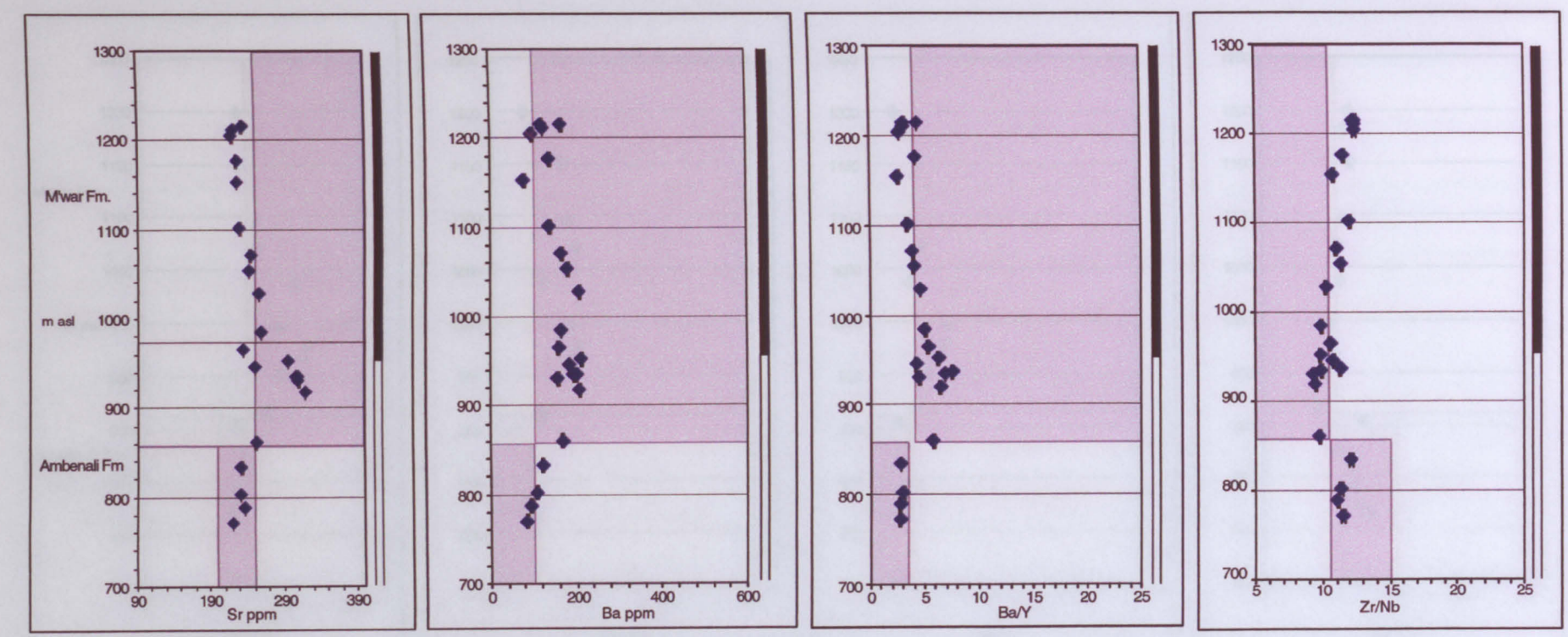

4.4c. Kelgar road

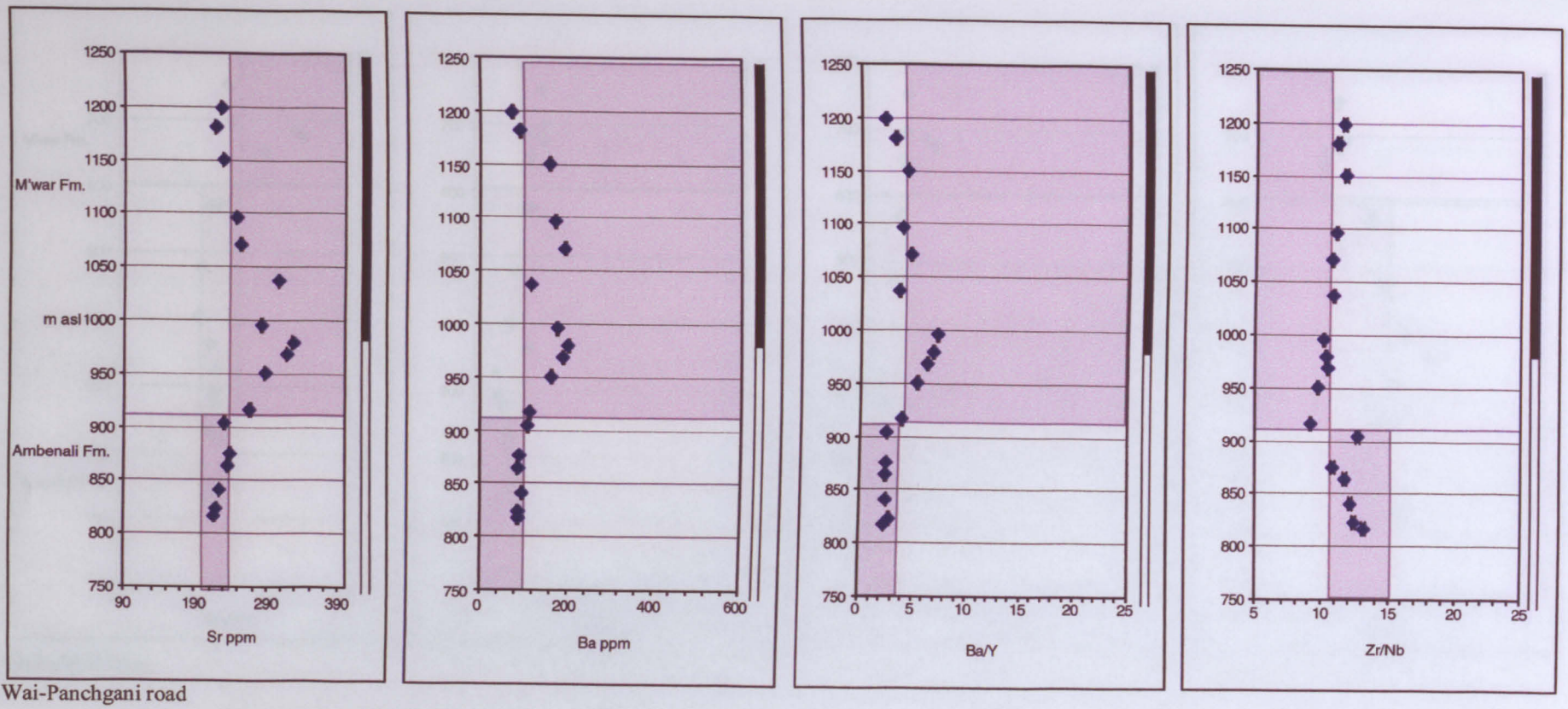

4.4d. Wai-Panchgani road

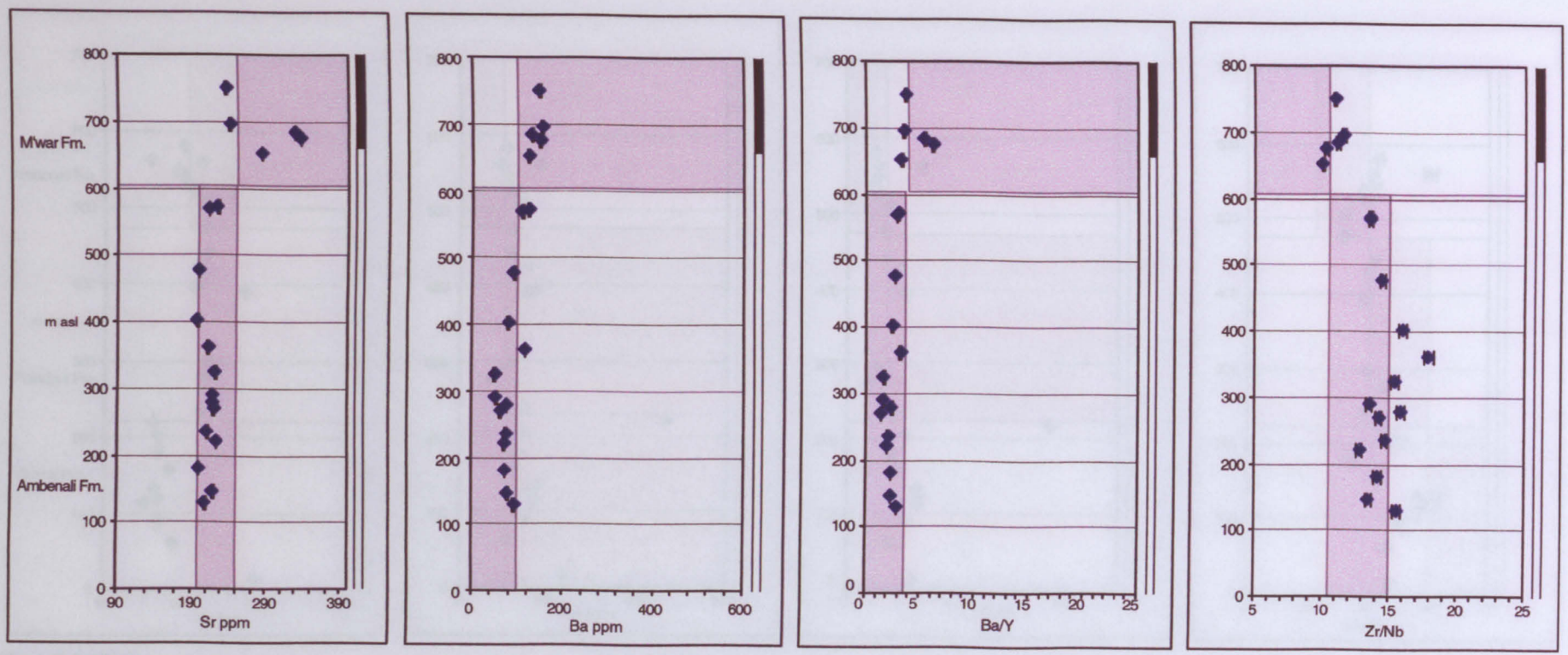

4.4e. Khumbarli Ghat

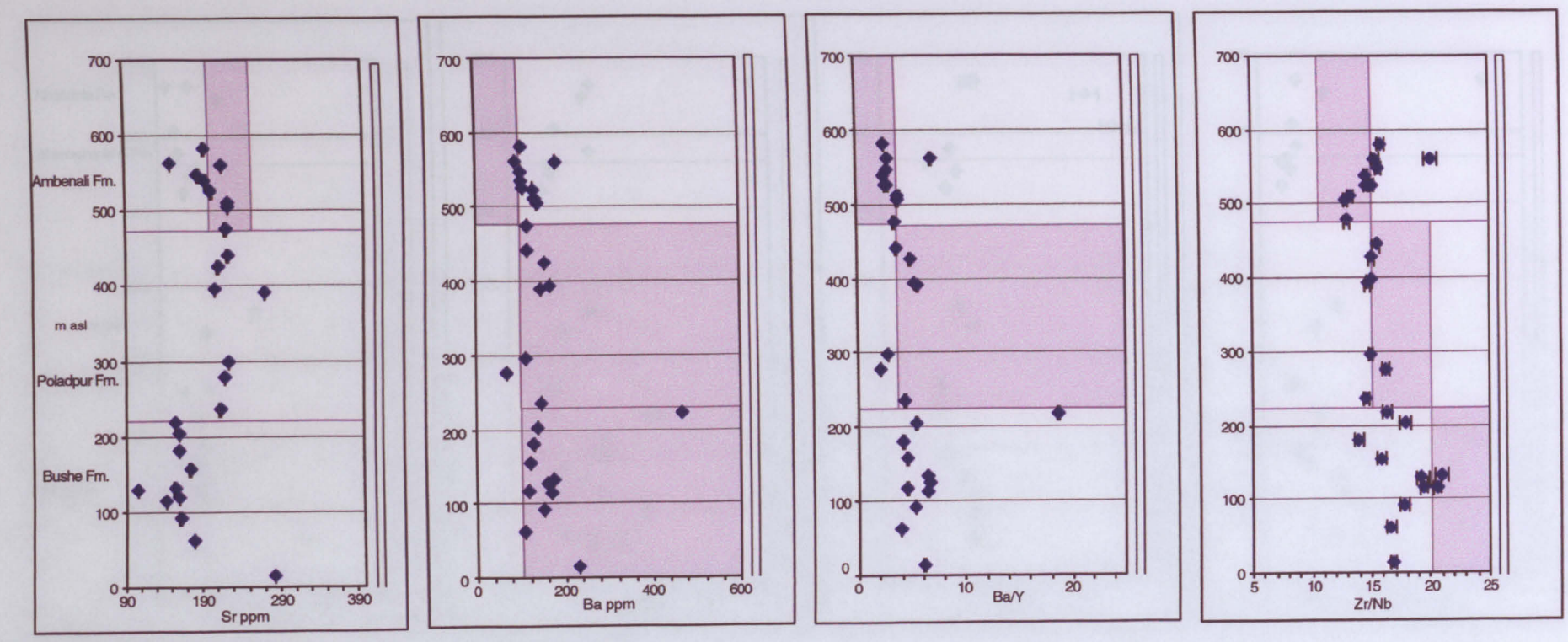

4.4f. Varandah Ghat

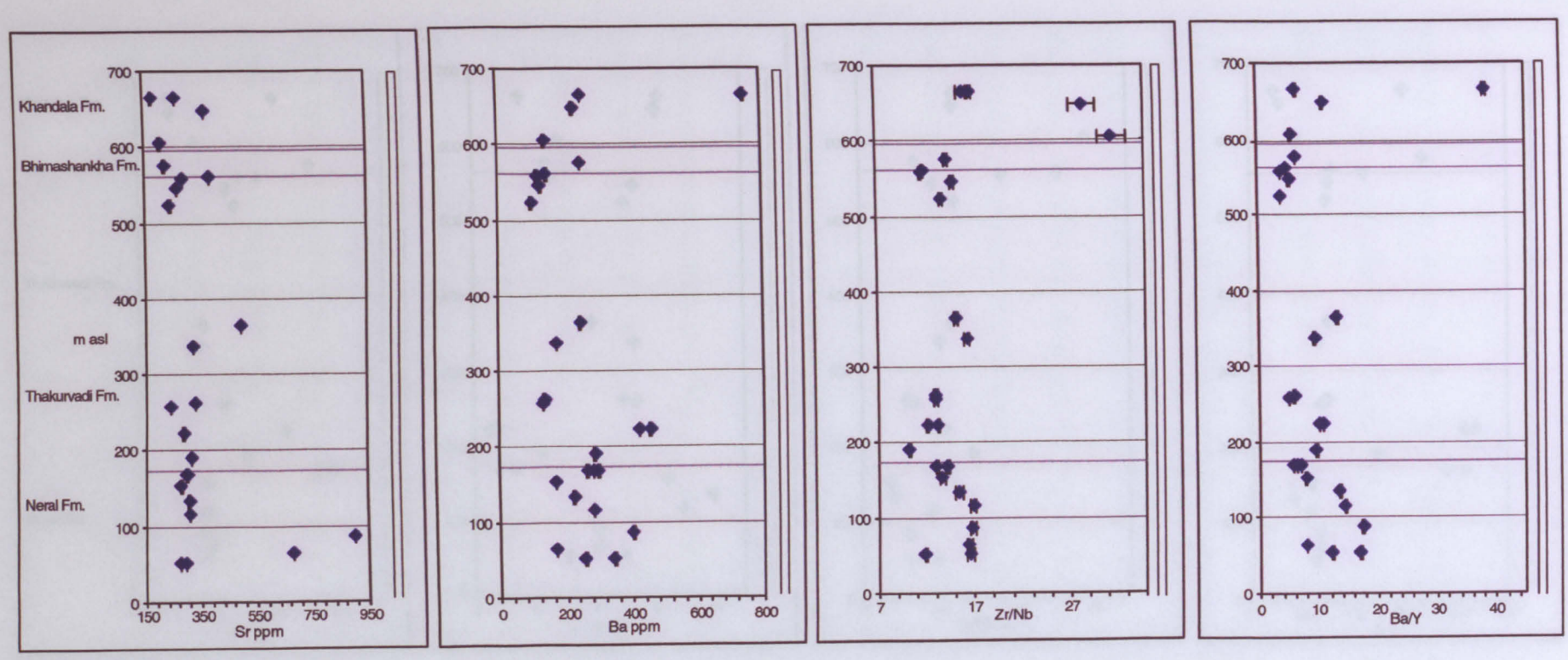

4.4g(i)Matheran Ghat

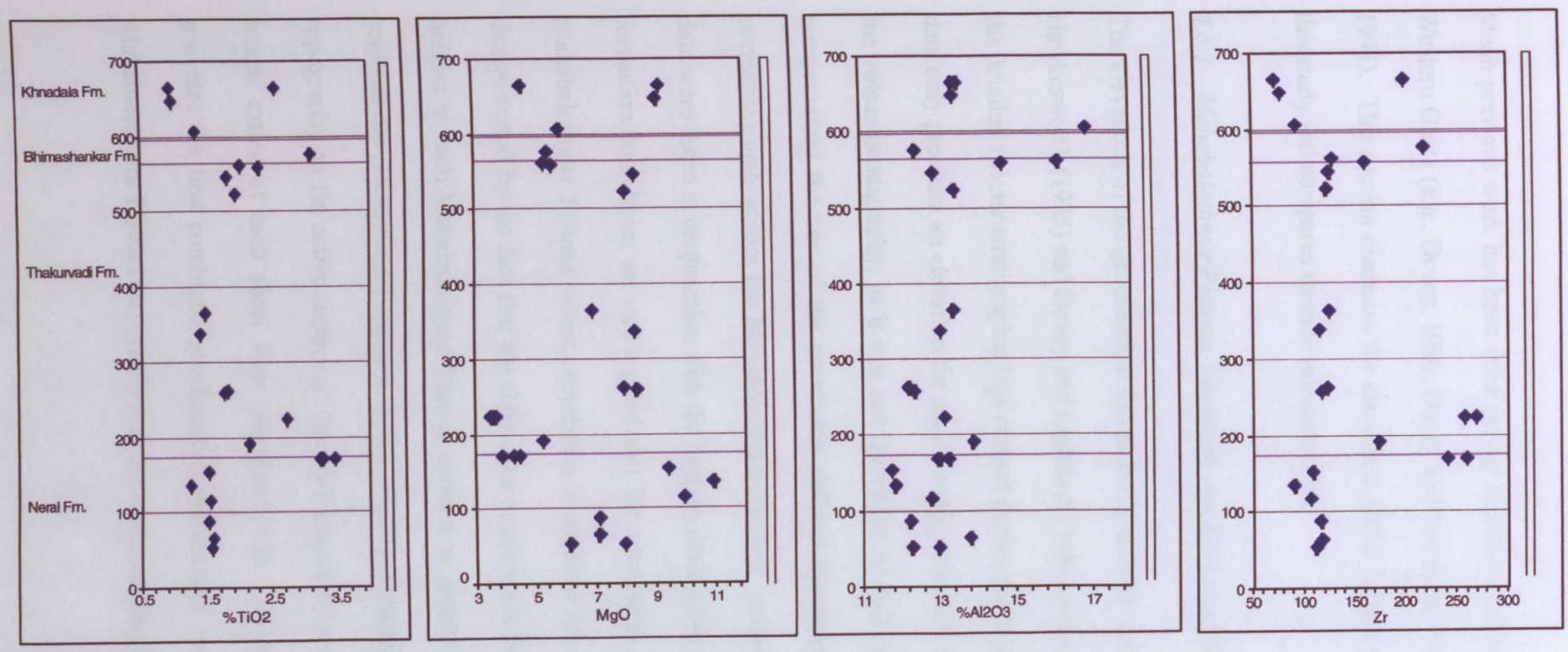

4.4g(ii) Matheran Ghat

Figure 4.4. Graphs a-g display the geochemical data used to define formations, plotted against elevation above sea level. Note however that the criteria used (from Devey and Lightfoot, 1986) only apply to the Wai Sub-group and the Bushe Formation. Formation boundaries on the Matheran section have been applied using criteria in the Deccan 2000 Penrose field guide (Subbarao et al., 2000, from Beane et al., 1986 and Khadri et al., 1999), but for interest the Devey and Lightfoot (1986) Wai Sub-group criteria have also been used. Grey shading indicates the fields of the criteria for each formation, although this is only applicable for Devey and Lightfoot (1986) criteria. Devey and Lightfoot (1986) did not specify a concentration of Sr for the Bushe and Poladpur Formations and the Ba/Y ratio for the Bushe Formation therefore the elevation of these formation boundaries has been added to the relevant plots. Column to the right of each graph is palaeomagnetic polarity; black is chron 29N, white chron 29R. Note also that the Mahabaleshwar Formation criteria fields have been extended to the top of the plots as it is not certain that the Panhala Formation is present.

4.6 Discussion

Much previous work has been done on the elevations of the formation boundaries in the Western Ghats (e.g., Devey, 1986; Devey and Lightfoot, 1986; Mitchell and Widdowson, 1991). This section discusses the elevations of the formation boundaries acquired during this study and compares them to previous work.

4.6.1 Mahabaleshwar Plateau, Varandah and Khumbarli Ghat sections

The elevations of the geochemical formation boundaries previously identified by Cox and Hawkesworth (1985) and Devey and Lightfoot (1986) proved insufficient to correlate with the detailed volcanostratigraphic logs created during this work (Section 2.6). The previous data only provides an elevation for each sample collected, and little account was taken of the volcanostratigraphy, as it was not the object of their work. This therefore seriously compromised the use of the previously defined geochemical formation boundaries for correlating units across the Mahabaleshwar Plateau. In fact, even when the geochemical data were taken in conjunction with the logging during this study, the chemostratigraphical formation boundaries are not a good tool for correlation over such a small area as the Mahabaleshwar Plateau where correlation is required on a flow-by-flow basis. This is demonstrated by the fact that the difference in elevation between the formation boundary heights in each Mahabaleshwar Plateau traverse is greater than that predicted by the 0.3° regional dip (Devey and Lightfoot, 1986). This discrepancy is probably because there was topography on the active surface of the DVP caused by non-uniform inflation and limited lateral extent of each sheet flow (Section 5.4.3). Despite this, the data set collected provides the first combined geochemical and detailed volcanostratigraphic study of the Mahabaleshwar Plateau and greatly aids the understanding of the DVP (Chapter 5).

Overall, the previous published elevations of the formation boundaries (Devey and Lightfoot, 1986; Mitchell and Widdowson, 1991) coincide well with the elevations established during this study using high precision Static GPS. A major problem occurred when trying to assign chemostratigraphic formations to the sheet lobes at the top of the Mahabaleshwar Plateau. Using the accepted criteria (Devey and Lightfoot, 1986), the upper ~ 150 m of all four traverses appeared to have a mixed Ambenali–Mahabaleshwar chemotype and some of the topmost samples show a distinctly Ambenali-like chemotype. This illustrates well one of the key problems with a stratigraphy based solely on trace element geochemistry. If a sample lacking relevant elevation and stratigraphic data were to be analysed it could then become possible to confuse an upper Mahabaleshwar Formation basalt with an Ambenali Formation sample. This is not so important in the Western Ghats where the stratigraphy and structure are well established, but in other parts of the DVP where less detailed have been carried out, this could cause recognition problems. The change back towards Ambenali chemotype basalt towards the top of the Mahabaleshwar Plateau has been noticed previously (Mahoney et al., 1982; Cox and Hawkesworth, 1985), but no explanation was given A probable explanation is the similarity in the geochemistry of the upper Mahabaleshwar, Ambenali and Panhala Formation lavas (Section 4.3.5).

4.6.2 Matheran Ghat section

The formation boundaries (Figure 4.3) assigned to the Matheran section were defined by Beane et al. (1986), Subbarao and Hooper (1988) and Khadri et al. (1999). Much of their work was done in conjunction with local geological mapping and field observations, and as such there are good physical descriptions of the units at the formation boundaries. However, a set of geochemical criteria, like the one developed by Devey and Lightfoot (1986) for the Bushe Formation and Wai Sub-group, has not been developed. Consequently, it proved difficult to assign the samples I took to formations on the basis of

their geochemical composition alone. However, the most comprehensive, yet simple, description of the location of the formation boundaries is found the Penrose fieldtrip guide (Subbarao et al., 2000) as this describes the outcrops and geochemistry of each formation boundary. Using the field data and geochemistry described in this field guide (originally from data in Beane et al. 1986 and Khadri et al. 1999a) the formation boundaries have been assigned to the log created during this study (Appendix A7).

The nature of the formation boundaries seen on the Mahabaleshwar Plateau sections and those of the Matheran sections are very different (see Appendix A1-A4 and A7). Those visible in the sections further south all coincide with weathering horizons, which might be expected as it seems likely that there would be some sort of a pause in the emplacement of lava whilst the magma source was changing. On the Matheran section however, the Neral-Thakurvadi Formation boundary occurs at a flow boundary, but there is no bole or indication of a hiatus between the emplacement of the units. This could be because the new magma system started erupting as soon as the previous one stopped. Or else a small time break may have occurred, but the new lava inundated the area much quicker than it could do further away from the vent, thus implying that the Matheran area was more proximal to the vent systems. Therefore if it were possible to view this formation boundary more distally, a bole may occur. A final possibility is that the majority of the lava units in Matheran Ghat section were erupted from a single magma system and perhaps the Neral and Thakurvadi Formations should be merged, and a new formation not assigned until the first bole is encountered, towards the top of the section at 561 m asl. This is contentious, however, because the current chemostratigraphy of the Matheran Ghat section relies much more heavily on field based observations and petrography than the chemostratigraphy developed for the Wai Sub-group, and no criteria exist for discrimination like those developed by Devey and Lightfoot (1986). Hence it is not possible to take a sample and identify its formation by its geochemistry alone; associated

field observations must be carried out. In order to investigate occurrence of the Neral-Thakurvadi Formation boundary further, geochemical studies including $^{87}Sr/^{86}Sr$ ratios and rare earth element data need to be undertaken and investigations of the outcrops of these formations in areas that may be more distal to the source need to be made.

Undertaking a fully integrated study including volcanostratigraphical logging (Chapter 2), geochemical analysis and high precision Static GPS (Appendix D2) has provided the exact elevation of most flow boundaries and, more importantly, formation boundaries around the Mahabaleshwar Plateau. A few more samples and better exposure would improve this still, but the data collected here provide the most comprehensive integrated study completed in the DVP. This, combined with the palaeomagnetic studies also carried out, has provided the first opportunity to attempt to understand the volcanostratigraphical complexities of the DVP. These are further discussed in Chapter 5.

4.7 Conclusions

- The majority of the formation chemotype boundaries have been identified precisely using Static GPS and detailed logging, therefore, in most instances, the formation boundary can be assigned to coincide with individual flow boundaries.

- The geochemical stratigraphy works well on a regional scale, but over the small area of the Mahabaleshwar Plateau, on an individual flow-by-flow basis, the geochemical stratigraphy is insufficiently accurate for correlation. This is partly due to the hybrid nature of the lavas at the formation boundaries, especially towards the top of the Mahabaleshwar Formation, and partly due to the realisation that the elevations of the formation boundaries on each traverse around the Mahabaleshwar Plateau vary. This variation is too great to be due to post-eruptive warping alone,

and indicates the possibility of topography of up to 95 m having been present on the surface of the active DVP (see Chapter 5).

- The Panhala Formation may have been identified in the top lava units of the Mahabaleshwar Plateau traverses whereas previously they have only been identified as the protolith of the laterite cap (Widdowson and Cox, 1996), but rare earth element data are needed to determine this.

- The validity of the lower formations on Matheran Ghat may need to be reassessed as there is no obvious hiatus at the Neral-Thakurvadi chemotype Formation boundary. This may be due to the Matheran area being proximal to the vents, and therefore the time between eruptions was too small for a weathering horizon to form. Alternatively, the Neral and Thakurvadi Formations could be combined as there is no bole between them. This needs further investigation to improve the chemostratigraphy of the Matheran section to try to identify different magma batches and hence formations.

Chapter 5
Volcanic architecture and stratigraphical correlations

5.1 Introduction

Although much work has been carried out on the DVP in recent times, it has mainly concentrated on the geochemistry and palaeomagnetism; the nature of the volcanic architecture (i.e., structure of individual eruptive units and flow packages) is only now beginning to be investigated (Keszthelyi et al., 1999; Bondre et al., 2000; Duraiswami et al., 2001; 2002; Bondre et al., 2004). The most recently published work (Bondre et al., 2004) investigates the wider issues of DVP lava emplacement, whereas much of the earlier authors' work concentrates on individual features and structures such as tumuli (Duraiswami et al., 2001; 2002), entablature structures (De, 1996) and proposed lava tubes and channels (Section 2.5, Sharma and Vaddadi, 1996; Thorat, 1996). This chapter brings together my results from Chapters two, three, and four on geochemistry, palaeomagnetism, individual volcanological structures and volcanostratigraphy, respectively, in order to understand the three-dimensional structure and lava unit characteristics (the volcanic architecture) of a 50 km by 200 km section of the Western Ghats.

Investigating the lava flow architecture of the DVP is very important as it provides information on the lateral extent of sheet lobes and flow-fields; this will help in the understanding of the mechanism of lava emplacement, give insights into the topography of the DVP edifice, and provide useful information for the future estimation of the environmental impact of the DVP by helping to constrain the amount of material produced by eruptions.

The first part of this chapter (Section 5.2) provides a brief overview of the previous lithostratigraphy, palaeomagnetic and geochemical stratigraphy that has been

used for broad correlations in the DVP. Sections 5.3-5.5 look at correlations on various spatial scales using the data collected during this study. Section 5.3 investigates short distance correlations of sections from approximately 100 m apart and up to 9 km apart, and observations made of the cliffs around the Mahabaleshwar Plateau, demonstrating the lateral discontinuity of sheet lobes. Section 5.4 looks at correlations around the Mahabaleshwar Plateau, and investigates the use of lithology, boles and geochemistry for correlating the lavas, particularly those between the 29R/29N palaeomagnetic reversal horizon and the base of the Mahabaleshwar Formation. From this, it is possible to demonstrate that there was considerable topography on the active surface of the DVP. Section 5.5 attempts correlation between the Mahabaleshwar Plateau and distant logged sections of Khumbarli, Varandah and Matheran Ghats and compares their volcanic architecture. Section 5.6 discusses how this work affects the current theories of eruption rates in the DVP. Section 5.7 demonstrates how the volcanic architecture observed in various parts of the Western DVP is similar on a variety of scales.

5.2 Previous work on correlations in the Deccan Volcanic Province

Much work has been carried out in the past on broad correlations within the DVP. This has mostly concentrated on the development of a chemostratigraphy which has proved to be MDP wide (e.g., Devey, 1986; Mitchell and Widdowson, 1991; Bilgrami, 1999). Palaeomagnetic and lithostratigraphies have also been attempted and developed, but they have not proved as robust or successful as the geochemical stratigraphy.

5.2.1 Lithostratigraphy

A number of previous attempts have been made to correlate flows and flow packages using lithostratigraphy rather than chemostratigraphy (Choubey, 1973; De, 1978; Godbole et al., 1996). This uses criteria such as the occurrence of giant plagioclase basalts (GPBs),

general hand specimen petrography, degree and appearance of weathering, 'flow' (sheet lobe in the naming system used in this work) thickness, presence and extent of boles, jointing and the occurrence of fossiliferous beds. For example, Godbole et al. (1996) proposed a stratigraphy for the MDP (Table 2.2), based upon the occurrence of GPBs and compound and simple flows, which was discussed in Section 2.1.1 and 2.5.1.

One of the first correlations of individual 'flows' was undertaken by Choubey (1973) in an area of the Malwa Plateau in the northernmost Deccan, and surrounding outliers, of the MDP (Figure 1.2). Choubey's (1973) work claims to have correlated five 'lava flows' (probably sheet lobes in the naming system used in this work) and interbedded sedimentary rocks between five traverses across distances of up to 160 km using primary structures, weathering, thickness, hand specimen petrography and plagioclase-pyroxene ratios. In a discussion of Choubey's (1973) work, Gupte et al. (1974) claim that Choubey's (1973) 'lava flow' correlations between sections are flawed because there is a 40 m elevation difference between the outcrop elevation of a 'lava flow' in two different sections. Gupte et al. (1974) state that in order for 'lava flows' to correlate they must be at the same elevation in each section in which they outcrop, and therefore Choubey's (1973) correlations are false. This, however, may be an erroneous argument since it is probable that there is some regional dip which will cause a variation in elevation of a specific 'lava flow' between two different traverses. However, my work also suggests that it is unrealistic to expect that a single body of lava exhibiting the same characteristics will persist over a distance of 160 km. This caveat also applies to all previous work attempting to correlate CFB lavas on field or other characteristics (Section 5.4.1).

5.2.2 Palaeomagnetic stratigraphy

The coarsest stratigraphic division of the DVP is palaeomagnetic (as discussed in Chapter 3). This divides the whole of the DVP into three divisions (N/R/N). The uppermost

reversal horizon 29R/29N provides a stratigraphic marker which is present across much of the southern MDP (Figure 3.5). The palaeomagnetic reversal has not been used specifically for correlations across the DVP before, but it is a useful correlation tool as the reversal occurs across a single flow boundary (with a laterally discontinuous, transitionally magnetised flow above) and it can be taken as an isochronous horizon. It has been used extensively as a marker horizon in this study as it can be pinpointed in five of the traverses studied.

5.2.3 Geochemical stratigraphy

Wider correlation across the DVP using a geochemical stratigraphy began with the advent of detailed geochemical mapping projects (Subbarao and Hooper, 1988; Mitchell and Widdowson, 1991; Bilgrami, 1999; Khadri et al., 1999) (Section 4.2.2). These studies show that the older formations of the Kalsubai Sub-group and the overlying lower Lonavala Sub-group are typically found in the central to northern Western Ghats, whereas the younger units of the upper Lonavala and overlying Wai Sub-groups are absent further north (Figure 5.1). This absence is either due to these units never having occurred there, or else considerable erosion has removed these lavas, and this erosion was exacerbated by the more elevated nature of this part of the Western Ghats (the Nasik-Kalsubai region, Figure 5.1). Very few laterite caps, which formed on the final eruptive emplacement surface of the DVP after the emplacement of the LIP was over (Widdowson, 1997), are found north of Mahabaleshwar, indicating that some erosion must have taken place to help expose these older units (Widdowson, 1990). Despite the evidence of some erosion to the north of Mahabaleshwar Plateau it is still probable that the younger units, especially those of the Wai Sub-group, probably did not extend far north (Figure 5.1) (Mitchell and Widdowson, 1991; Widdowson and Cox, 1996) since many formations of the Wai Sub-group appear to thin northwards (Devey and Lightfoot, 1986). The younger formations, the Bushe and those of the Wai Sub-group (Poladpur to Desur), are typically found farther south along the

Western Ghats. This is thought to be due to the northward migration of India over the Reunion Plume and caused a southerly migration of the volcanic edifice so that each Sub-group is further south than the last (Figure 5.1). The base of the Ambenali Ghat traverse marks the farthest south outcrop of the Bushe Formation (Devey and Lightfoot, 1986), and the Wai Sub-group dominates much of the remaining areas of the southern MDP and extends (Figure 5.1 and Figure 5.2) to the south, west and east periphery (Devey and Lightfoot, 1986; Bilgrami, 1999).

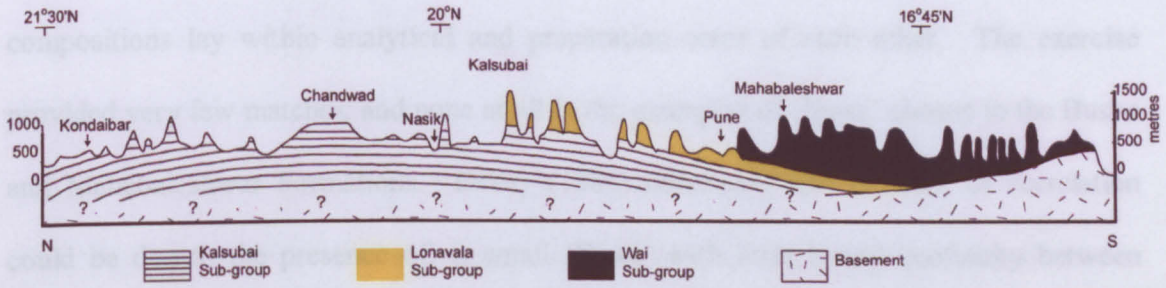

Figure 5.1. A north-south sketch section along the Western Ghats crest from approximately 21°30'N to 16°15'N. This shows the regional extent of the sub-groups and demonstrates the progressive younging and overstepping of the younger formations to the south. The section is about 650 km long (after Widdowson and Cox, (1996), who modified it from Subbarao and Hooper (1988)).

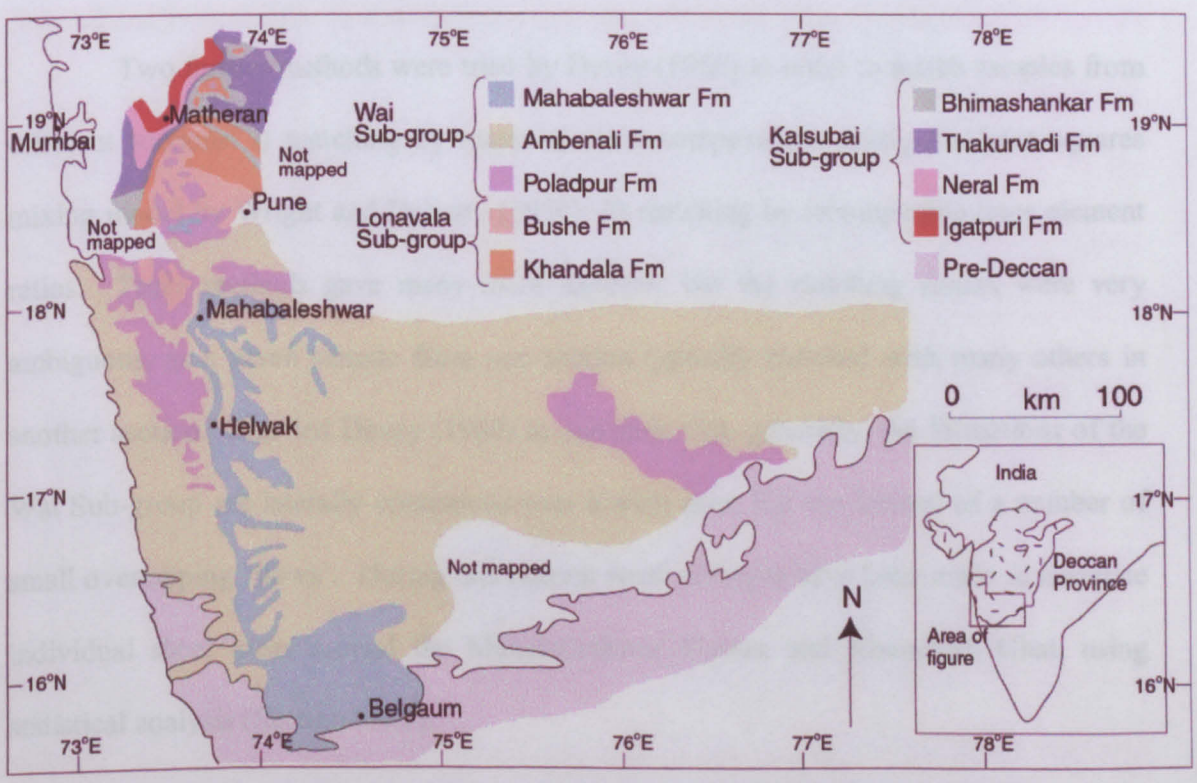

Figure 5.2. Simplified geological map of the southern DVP, from Mitchell and Widdowson (1991).

Geochemical correlation between individual 'flows' (most probably sheet lobes in the terminology used in this work) was attempted by Devey (1986) who investigated the possibility of compositional similarities between 'flows' on a number of pairs of different sections (Raigad and Goregaon, Torna and Purandha/Sasawad, Torna and Khumbarli, and Khumbarli and Purandha/Sasawad, (Figure 2.1)). Initially, this was attempted by the direct comparison of the 'flows' using trace and major elements, except K, Rb, Ba (not used because of concern over their post-solidification mobility) and Cu (not used because the XRF analyses of this element were in doubt). The units were deemed to match if their compositions lay within analytical and preparation error of each other. The exercise provided very few matches, and none at all in the examples of 'flows' chosen in the Bushe and Mahabaleshwar Formations. Devey (1986) concluded that the lack of correlation could be due to the presence of: i) small 'flows' with little lateral continuity between sections or, ii) larger flows which are inhomogeneous with respect to their degree of fractionation and/or contamination.

Two further methods were tried by Devey (1986) in order to match samples from different sections: i) matching by major element compositions, using the least squares mixing model by Wright and Doherty (1970); ii) matching by incompatible trace element ratios. These methods gave many more matches, but the matching results were very ambiguous, as a given sample from one section typically matched with many others in another section. This led Devey (1986) to conclude that, generally, the formations of the Wai Sub-group are laterally continuous over a wide area, but are formed of a number of small overlapping 'flows'. During this current work attempts have been made to correlate individual sheet lobes around the Mahabaleshwar Plateau and Khumbarli Ghat, using statistical analysis (Section 5.4.5).

Broader scale correlations using formation boundaries (Devey and Lightfoot, 1986; Mitchell and Widdowson, 1991) demonstrated that despite the seemingly horizontally extensive appearance of the units around the Mahabaleshwar Plateau and the DVP as a whole, post-eruptive regional warping has formed a gently dipping, southerly-plunging anticline that plunges at ~0.3° (Figure 5.3), and runs parallel to the Western Ghats Escarpment. A component of this dip must also be due to the dip of the volcanic edifice itself. The eastern limb of the anticline dips at ~ 0.5° to the southeast (Devey and Lightfoot, 1986), this is equivalent to an 8.7 m drop per 1 km. However, the western limb dips at a maximum of 0.15° to the southwest in the southern Western Ghats (Mitchell and Widdowson, 1991), and which is equivalent to a drop of 2.6 m per 1 km. Moreover, the regional dip and plunge in the southern Western Ghats was calculated using the elevation of the base of the Mahabaleshwar Formation, which, as this work will show, may have provided erroneous dip measurements over shorter distances (this will be further discussed in Section 5.4.3). Due to the occurrence of regional dip, correlating logged sections by lining the logs up relative to the elevations above sea level was not possible.

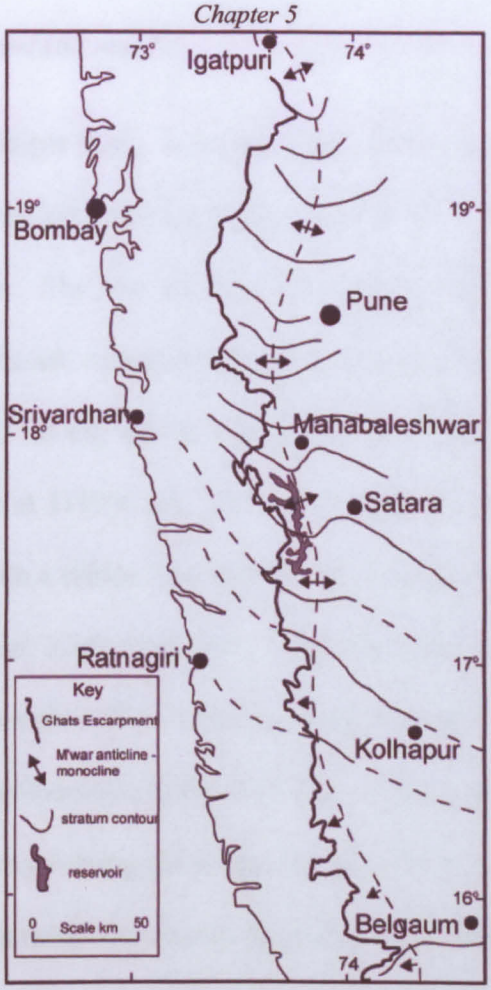

Figure 5.3. Stratum contours drawn to the base of the Mahabaleshwar Formation from the southern DVP to Mahabaleshwar, to the base of the Bushe Formation from Mahabaleshwar to Pune, and to the base of the Thakurvadi Formation from Pune to Igatpuri. These together define the large, southerly-dipping, anticline feature which becomes essentially monoclinal south of 17°15'N. It is important to note that the axis of the feature is not coincident with the Western Ghats scarp line, but between 19° 30'-15°30' commonly lies 10-30 km inland (east) of the Western Ghats escarpment. Dashed lines indicate where the precise position of the contours is in doubt (from Widdowson, 1997).

5.3 Short-range lava architecture and stratigraphic correlation: comparing adjacent sections

Along the Kelgar Road and Ambenali Ghat it has been possible to investigate short-range correlations using two traverses that cover duplicate sections of the stratigraphy but are separated by 50-100 m (Kelgar Road) and around 9 km (Ambenali and Arthur's Seat). Insights on short-range correlations can also be gathered from tracing sheet lobes along cliff sections (Section 5.3.3).

5.3.1 Kelgar Road: 1225-1160 m asl

After logging the main Kelgar Road, a second much shorter log was undertaken along a small road (which branched off the main Kelgar road at 17° 53' 40.5"N 73° 43' 00.8"E) leading down to a village. The two sections are no more than 50-100 m apart yet they appear to have quite different volcanostratigraphy (Figure 5.4). The main road section shows a red bole at 1167 m asl, above which there is a 40 m thick sheet lobe which terminates at the flow top at 1199 m asl. The overlying 20 m of stratigraphy is formed of an 8 m thick sheet lobe with a rubbly flow-top at 1207 m asl, overlain by a very distinctive, highly amygdaloidal (Figure 2.36) sheet lobe. This lobe is terminated by a low angle fault or fracture above which is a sheet lobe containing large vesicles. By contrast, the side road section is dominated by no exposure from 1167 m to 1198 m, and shows a vesicular flow top at 1202 m asl which may correspond to that seen at 1199 m in the main section. Above the flow top at 1202 m is a thick columnar-jointed sheet lobe, which terminates at the same elevation as the main section, at 1225 m. This is very different to the highly vesicular nature of the thinner sheet lobe in the main section and the low angle fracture is not seen. This variation between two such close sections suggests that the rubbly-topped and vesicular lobes in the main section do not persist more than 100 m laterally, where they are replaced at the same horizon by a thicker sheet lobe. It is not known whether they are both part of the same flow-field or not.

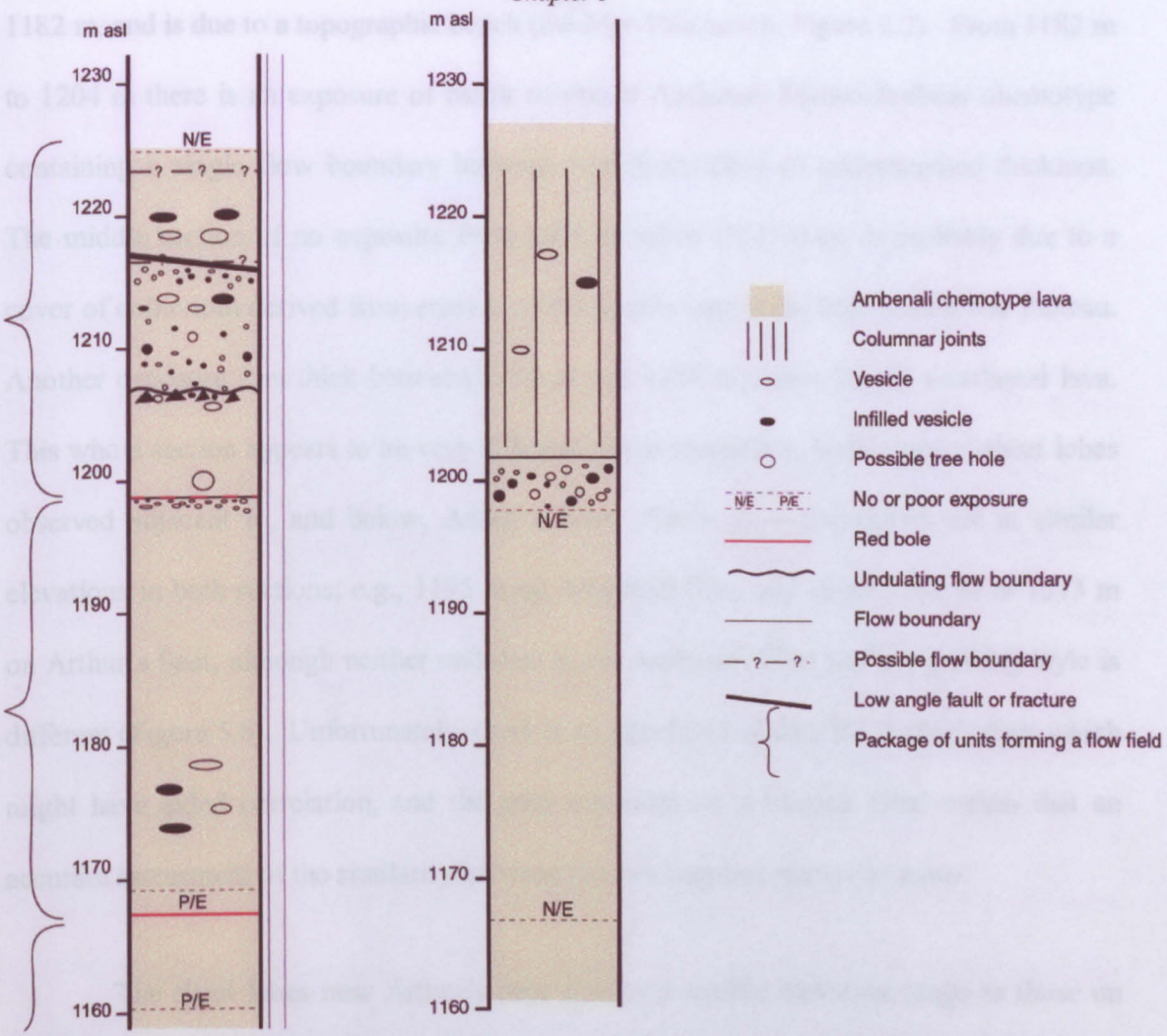

Figure 5.4. To the left is the top of the Kelgar Road main section, and to the right is the section logged 50-100 m away along a small track, off the main road.

5.3.2 *Ambenali Ghat and Arthur's Seat*

Part of the main Ambenali Ghat section can be compared with the cliff-forming section below and adjacent to the lookout point of Arthur's Seat (approximately 1250 m asl; Figure 2.2 and Figure 5.5) on the north west side of the Mahabaleshwar Plateau. The two sections are 9 km apart. The vertical Arthur's Seat cliff section contains approximately five sheet lobes, each between 25 m and 60 m thick, although this is an approximation as thicknesses were estimated by eye and hand-held GPS. This makes correlating more complex but the information permits an estimate of the similarity between the two sections. The Ambenali Ghat section is dominated by no exposure from 1106 m to the top of the Ghat at ~1290 m (Figure 5.6). The lowest section of no exposure is between 1106 m to

1182 m, and is due to a topographic bench (the Met-Tala bench, Figure 2.2). From 1182 m to 1204 m there is an exposure of basalt of mixed Ambenali-Mahabaleshwar chemotype containing a single flow boundary between two sheet lobes of undetermined thickness. The middle section of no exposure from 1204 m asl to 1252 m asl is probably due to a cover of colluvium derived from erosion of the laterite cap of the Mahabaleshwar Plateau. Another exposure 2 m thick between 1252 m and 1254 m shows highly weathered lava. This whole section appears to be very different to the competent, well-exposed sheet lobes observed adjacent to, and below, Arthur's Seat. Some flow boundaries are at similar elevations in both sections; e.g., 1195 m on Ambenali Ghat and either 1180 m or 1213 m on Arthur's Seat, although neither undulate as on Ambenali Ghat and the jointing style is different (Figure 5.6). Unfortunately, there is no geochemical data for Arthur's Seat which might have aided correlation, and the poor exposure on Ambenali Ghat means that an accurate assessment of the similarity between the two sections cannot be made.

The sheet lobes near Arthur's Seat occupy a similar elevation range as those on Ambenali Ghat, and so should be their lateral equivalent, despite an ~ 47 m drop between Arthur's Seat and Ambenali Ghat due to the regional dip. However, the exposure on both sections is very different. There are two possible reasons for the differences in the characteristics of the two sections: 1) the erosion rate on the cliff by Arthur's Seat is higher, as it is on the main ghat scarp and at the headwater of the Savitri river, whereas the top of Ambenali Ghat is slightly protected, as it is slightly east of the main ghat scarp (Figure 2.2). The higher erosion rate of the Arthur's Seat cliff may be sufficient to prevent benches, such as Met-Tala on Ambenali Ghat, from forming. 2) Alternatively, some of the lava units present in the two sections could be different, with those near Arthur's Seat being thick inflated sheet lobes, some of which appear welded together whereas the lobes on the main Ambenali Ghat section are much thinner and vesicular making them more prone to weathering, and hence to forming benches and extensive areas of no exposure. If

the latter is correct then this change in 'degree of weathering' between the two sections suggests that the big sheet lobes of Arthur's Seat do not extend to the main Ambenali Ghat road (a distance of ~9 km) and, if the same eruptive units/flow-field are present at both sections, there is a change to thinner and/or more weathered lobes towards the south.

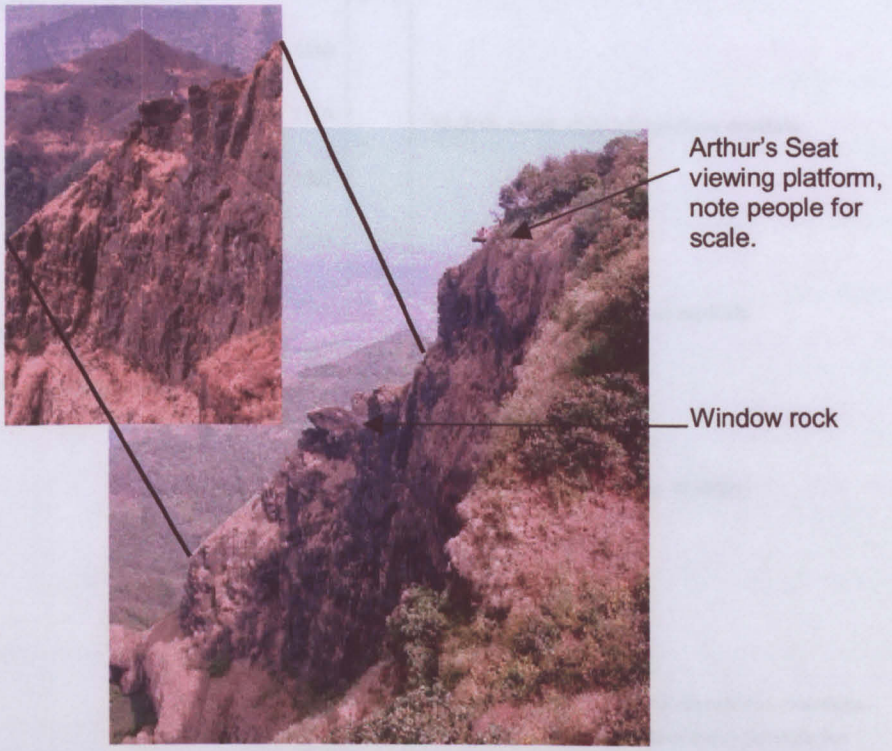

Figure 5.5. Thick inflated, sheet lobes at Arthur's Seat. Insert shows a section of the cliff from a better angle.

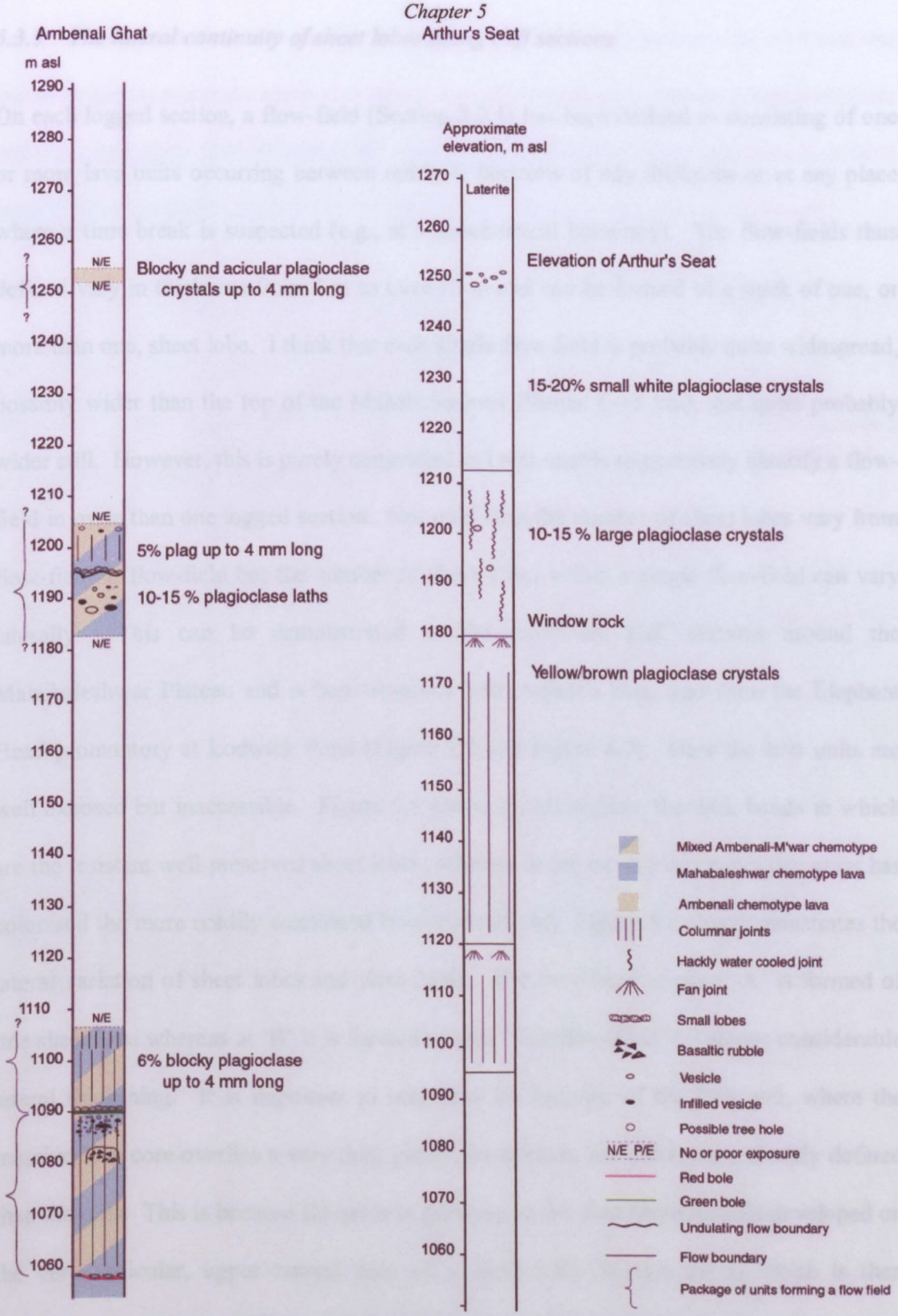

Figure 5.6. Comparison between the exposure on the Ambenali Ghat traverse and the sheet lobes observed adjacent to, and below Arthur's Seat at a similar elevation. The thicknesses and elevations for the Arthur's Seat log are approximate as they were judged by eye. Note, there is no geochemical data for Arthur's Seat.

5.3.3 The lateral continuity of sheet lobes along cliff sections

On each logged section, a flow-field (Section 2.2.1) has been defined as consisting of one or more lava units occurring between red bole horizons of any thickness or at any place where a time break is suspected (e.g., at a geochemical boundary). The flow-fields thus defined vary in thickness from 2 m to over 70 m and can be formed of a stack of one, or more than one, sheet lobe. I think that each single flow-field is probably quite widespread, possibly wider than the top of the Mahabaleshwar Plateau (~15 km), and quite probably wider still. However, this is purely conjecture as I was unable to positively identify a flow-field in more than one logged section. Not only does the number of sheet lobes vary from flow-field to flow-field but the number of sheet lobes within a single flow-field can vary laterally. This can be demonstrated in the prominent cliff sections around the Mahabaleshwar Plateau and is best observed near Arthur's Seat, and from the Elephant Head promontory at Lodwick Point (Figure 2.2 and Figure 5.7). Here the lava units are well exposed but inaccessible. Figure 5.8 shows a cliff section; the dark bands in which are the resistant well-preserved sheet lobes, whereas in the intervening zones dry grass has colonised the more readily weathered flow-top material. Figure 5.8 also demonstrates the lateral variation of sheet lobes and flow-fields. The flow-field at point 'A' is formed of one sheet lobe whereas at 'B' it is formed of two. The flow-field 'C' shows considerable lateral thickening. It is important to note how the bottoms of the lava unit, where the massive lava core overlies a very thin, glassy, basal crust, are much more sharply defined than the tops. This is because the grass is growing on the weathering profile developed on the very vesicular, upper crustal zone of a sheet lobe (Section 2.3.2) which is then terminated by the very thin, lower vesicularity of the basal crust of the sheet lobe above. The thickness of these bands of grass varies; perhaps the thicker bands of grass are due to the sheet lobe having a thicker upper crust, or perhaps the sheet flow or flow-field was exposed and weathered for a greater length of time. It is possible therefore, that the thicker

grass bands may represent the top of a long-exposed flow-field and the thinner bands the top of single sheet lobes or breakout lobes above the upper crust, which, because they are within a flow-field, and therefore not the final surface, may have been exposed for a shorter period of time.

It can be seen (Figure 5.7) in many of the flow-fields that the number of units, most probably sheet lobe, varies along section, usually from between one and three over a distance of a few hundred metres. These observations are only in two dimensions and it must be remembered that this complexity occurs in three-dimensions.

Figure 5.7. View north from Elephant Head, Lodwick Point, showing a typical Deccan section. The sheet lobes look very flat and continuous here, but in fact the lateral continuity of the individual sheet lobes is variable. At point X there are, apparently two sheet lobes in this flow-field and at point Y there is only one.

Figure 5.8. View towards the north west from the path towards Arthur's Seat. The complex and discontinuous nature of the sheet lobes within a package or flow-field is shown here clearly. A single thick sheet lobe is visible at point 'A' but ~70 m along the section two sheet lobes are observed, 'B'. The sheet lobe labelled 'C' shows lateral thickening from right to left.

The only observed example of a large sheet lobe terminating was observed on Ambenali Ghat. Above the 'Green Bole' is an approximately 20 m thick sheet lobe which forms the prominent cliff below the Met-Tala bench at 1106 m asl (Figure 2.2). If this cliff is traced northwards (i.e., walking down Ambenali Ghat towards Ambenali village,) the cliff disappears and is covered by forest and does not reappear (Figure 5.9). It is probable that the sheet lobe has thinned out and disappeared, and the trees are growing on highly weathered smaller infill, or break-out lobes.

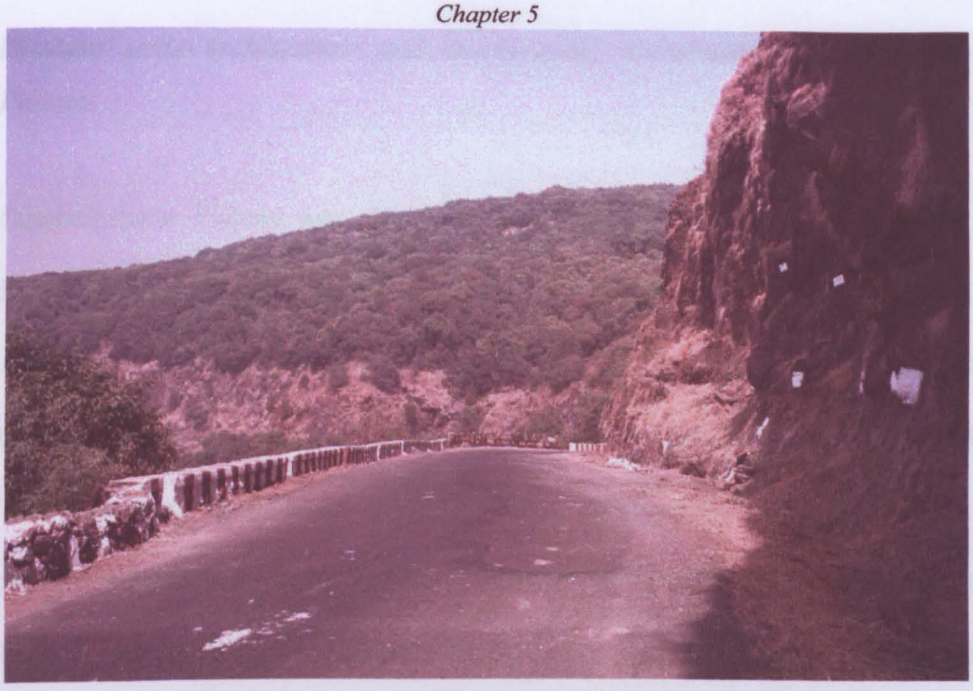

Figure 5.9. Photo demonstrating the lateral discontinuity of thick sheet lobes. To the right of the image, in shadow, is the 'green bole' on Ambenali Ghat (see sitting person for scale at light/shadow boundary). Above the bole is a thick, resistant sheet lobe. This sheet lobe is not visible in the distance, where sloping forest occurs at the elevation that the vertical basalt cliff should occur. It is probable that the sheet lobe above the green bole has pinched-out and terminated. Lat. Long. 17°55'00.0''N 73°37'32.9''E

The majority of the sheet lobes in the study area are ~20 m thick, but scattered throughout all of the sections are much smaller sheet flow lobes. These are either precursor or break-out lobes, as discussed earlier, (Section 2.2.2), or else isolated packages of lobes and toes usually no thicker than 2 m which do not appear to be directly associated with a large sheet lobe above or below. These latter probably represent the small lobes that form on the periphery of a sheet lobe or flow-field. This may explain, for instance, why there are thin lobes and toes above the palaeomagnetic reversal horizon on Khumbarli Ghat (Appendix A6), yet on the sections on the Mahabaleshwar Plateau above the palaeomagnetic reversal horizon there are none. It is possible that the small lobes viewed on Khumbarli Ghat are the periphery of a much larger sheet lobe or flow-field which may be present at the Mahabaleshwar Plateau, and has either been eroded or is not yet exposed there.

5.4 *Medium scale architecture and stratigraphic correlation: the Mahabaleshwar Plateau*

The Mahabaleshwar Plateau was chosen for this work because it has four roads which ascend it on three of its four sides, and from this it was hoped to be able to form a three-dimensional picture of how the sheet lobes and flow-fields were related to each other in order to investigate the volcanic architecture. This section looks at the problems of field-based correlations involving sheet lobes and boles and then describes the sections of the Mahabaleshwar Plateau traverses, between the base of the Mahabaleshwar Formation and the 29R/29N palaeomagnetic reversal horizon, which have been used in this study to investigate the correlation of individual sheet lobes (using statistical analysis) and the topography which was developed on the DVP.

5.4.1 Lava unit correlations using lithology

Although the lateral discontinuity and pinching out of sheet lobes is easily observed in the exposed cliff faces, especially from the Arthur's Seat and Elephant Head viewpoints (Figure 2.2, Figure 5.5, Section 5.2.1) the slopes of the Mahabaleshwar Plateau are steep, near-vertical in places, and often vegetated, preventing individual sheet lobes being 'walked out' around the Plateau, traced with binoculars or followed on digitized photographs. Thus, tracing and correlating individual sheet lobes, lava flows or flow-fields between the four Mahabaleshwar Plateau sections was not possible in the field. However, it is probable that sheet lobes are between 100s of metres and perhaps a few kilometres wide.

The petrography of the basaltic sheet lobes observed around the Mahabaleshwar Plateau, and specifically between the palaeomagnetic reversal and the base of the Mahabaleshwar Formation where the majority of correlation attempts were made, also hampered field-based correlations. The majority of the sheet lobes were indistinguishable

since many have a medium-grained groundmass with 2-3% of 2-5 mm plagioclase crystals and glomerocrysts. It was noted that plagioclase abundance varies even within one sheet lobe so its percentage cannot be diagnostic. Along with the petrographic similarities between the observed basalts which limit the identification and correlation of individual sheet lobes, it was noticed that the physical appearance of a sheet lobe can vary significantly within a few metres from almost pristine basalt to spheroidally weathered or not exposed at all. Both factors reduce the chance of being able to make correlations on the basis of lithologic characteristics.

The main exception to the monotony of the petrography is a GPB below the palaeomagnetic reversal horizon which was observed only on Ambenali Ghat and the Kelgar Road (Section 2.6.1 pg. 67 and Section 2.6.3 pg. 81), and four GPB sheet lobes (between 612 and 682 m asl) in the Ambenali Formation on the Ambenali Ghat traverse (Figure 2.2, Section 2.6.1, pg 63). These lavas contain up to 30% 1-2 cm-long plagioclase crystals and should be easily recognisable, and hence aid correlations. Unfortunately, they lie below the lowest exposures on the other three ghat sections. Although the mid-Ambenali Formation outcrops on Khumbarli Ghat, no GPBs were observed in the Ambenali Formation on Khumbarli Ghat. Only the lower Ambenali Formation is observed on Varandah Ghat so this would not contain these GPBs (Appendix A1-A7).

5.4.2 Boles as a tool for correlation

Although lithologically distinct, the mode of occurrence and formation of boles limit their use as correlation tools. For example, the lateral extent of boles can be highly variable. Cherty boles, thought to be formed from volcanic ash fall ((Widdowson et al., 1997); Section 2.5.3), could be expected to be more widespread and laterally continuous than saprolitic boles if they originate from an eruption with a large zone of ash fall-out. However, if the ash fall-out zone is small and/or the volume of ash deposited is small, the

cherty bole's extent would be concentrated to areas close to the vent. It is also probable that some reworking of volcanic ash may occur, so cherty boles may only be laterally continuous if covered by lava soon after deposition. Exposure for any prolonged period of time may allow remobilisation which could cause cherty boles to be thicker in palaeodepressions than on highs, where it may be absent altogether, this would further complicate the correlation of boles. The lateral continuity and depth of saprolitic boles depends on the period of time between the emplacement of one sheet lobe and its inundation by another sheet lobe. Sheet lobes which are exposed at any one time can be of very different ages and hence have been exposed, and weathered, for varying periods of time. This will produce a bole which, i) undulates, due to the topography which develops on the surface of the lava, and, ii) is of varying age and therefore probably thickness. This varying degree of weathering may be exacerbated by the inundation of the next sheet lobes, which may not cover the entire bole area. This will effectively fossilize the bole beneath the newly emplaced lava, and leave kipukas which will continue to be weathered. Due to these problems of lateral discontinuity, varying elevations of a continuous saprolitic bole, and varying thickness due to differing duration of exposure, the use of boles as tools for correlation within the Mahabaleshwar Plateau and Deccan-wide is limited. The exception however, is the thin bole at the palaeomagnetic reversal horizon, which was correlatable only because of its association with the palaeomagnetic reversal. It may be possible to correlate cherty boles on the basis of their chemical compositions, but this is beyond the scope of this study.

It had been hoped that some of the thicker bole horizons, e.g., the 'Big Red Bole' (17°57'03.07"N 73°35'00.19"E, in the Ambenali Formation at 693 m) and the 'Green Bole' (17°55'00.0"N 73°37'32.9"E, in the mixed Ambenali/ Mahabaleshwar Formation at 1090 m) observed on Ambenali Ghat, would be recognisable on other Mahabaleshwar Plateau traverses. However, the 'Big Red Bole' outcrops too low in the sequence to be

exposed on the other three traverses up the Mahabaleshwar Plateau, and nothing similar was found at the corresponding stratigraphic position on the Khumbarli Ghat section (65 km to the south, Figure 2.1)). This does not mean that an equivalent to the 'Big Red Bole' weathering horizon does not occur on Khumbarli Ghat. It may well do, but boles can vary in thickness and appearance over a relatively short distance making it impossible to distinguish one individual bole from other boles that occur on Khumbarli Ghat, even when the regional dip is taken into account.

The 'Green Bole' should also be an ideal marker horizon as it is easily recognisable on Ambenali Ghat at 1090 m asl (Section 2.6.1, pg. 70). However, it has not been positively identified in any of the three other Mahabaleshwar Plateau sections. The 'Green Bole' is not dark grey/green for its entire outcrop length; further along its length, above the road, it can be seen as a much thinner, red bole (Section 2.6.1 pg. 70). On the Wai-Panchgani Road at 1089 m there is a pale grey/green undulating rubbly bole which also displays a change to red in small patches on the flow top (Appendix A4, Figure 2.27). This may be an equivalent horizon to that of the 'Green Bole' on Ambenali Ghat. The two boles are along strike from each other and essentially at the same elevation. The bole on the Wai-Panchgani Road is slightly more rubbly than the 'Green Bole' and a paler colour. An explanation for the darker, greener colour of the 'Green Bole' on Ambenali Ghat could be due to the water content of the bole on the Ambenali Ghat outcrop. The 'Green Bole' is saturated with water, as it is the location of a number of small springs. The much lower rainfall, and hence less groundwater and fewer springs, on the Panchgani side of the Plateau (Section 1.3.3) may be the reason for this lighter appearance of the bole on the Wai-Panchgani traverse.

5.4.3 *Volcanic topography on the surface of the DVP*

Within the study area of the Mahabaleshwar Plateau, three surface datums of different types and quality have been established, all of which relate to the way in which the lava pile was constructed. These are the palaeomagnetic 29R/29N horizon, the chemostratigraphic Ambenali-Mahabaleshwar Formation boundary and the post-eruptive laterite surface that marks the final eruptive surface of the DVP. For the purpose of this work it is assumed that these three datums are time horizons, although the reliability of this assumption varies for each horizon, as will be discussed below.

The palaeomagnetic reversal is unequivocally a time horizon as it was created in a geological instant (Section 3.6). The geochemical boundary horizon (the base of the Mahabaleshwar Formation) is also a type of time horizon, provided that it is assumed that lava emplacement was terminated at the end of the Ambenali Formation times, over the area of the Mahabaleshwar Plateau before the onset of the Mahabaleshwar Formation chemotype. Even if the changeover was not perfectly synchronous over the Mahabaleshwar Plateau it must nevertheless represent a relatively short period of time in relation to the DVP as a whole. The third and uppermost of the three horizons is the laterite horizon. This is the highly altered upper surface of the final lava field (or fields) that was left exposed after the eruption ceased. Although it has been highly altered this surface can be taken as representing the final surface of the DVP as the current surface of the (Mahabaleshwar Plateau) laterite is conformable with the wider surface morphology of the Western Ghats laterite (Widdowson, 1997), the stratigraphic structure (taken from the base of the Mahabaleshwar Fm; (Devey, 1986)), and the palaeomagnetic reversal horizon (Figure 3.5; Vandamme and Courtillot (1992)).

In order to investigate the shapes of these surfaces and any variations in the thickness of the intervening lava, the elevations of the top of the Ambenali Formation, the

palaeomagnetic reversal and the laterite were noted on each of the four traverses around the Mahabaleshwar Plateau. These were either taken from the high precision GPS work carried out in the field or by calculating the elevation of the laterite surface at the latitude and longitude of the palaeomagnetic horizons from detailed laterite contour maps (Widdowson, 1990). The elevations for these (Table 5.1) were plotted to form a graph which clearly demonstrates the variations in thickness (Figure 5.10). In comparing the thicknesses from the graph, any post-eruptive deformation is irrelevant.

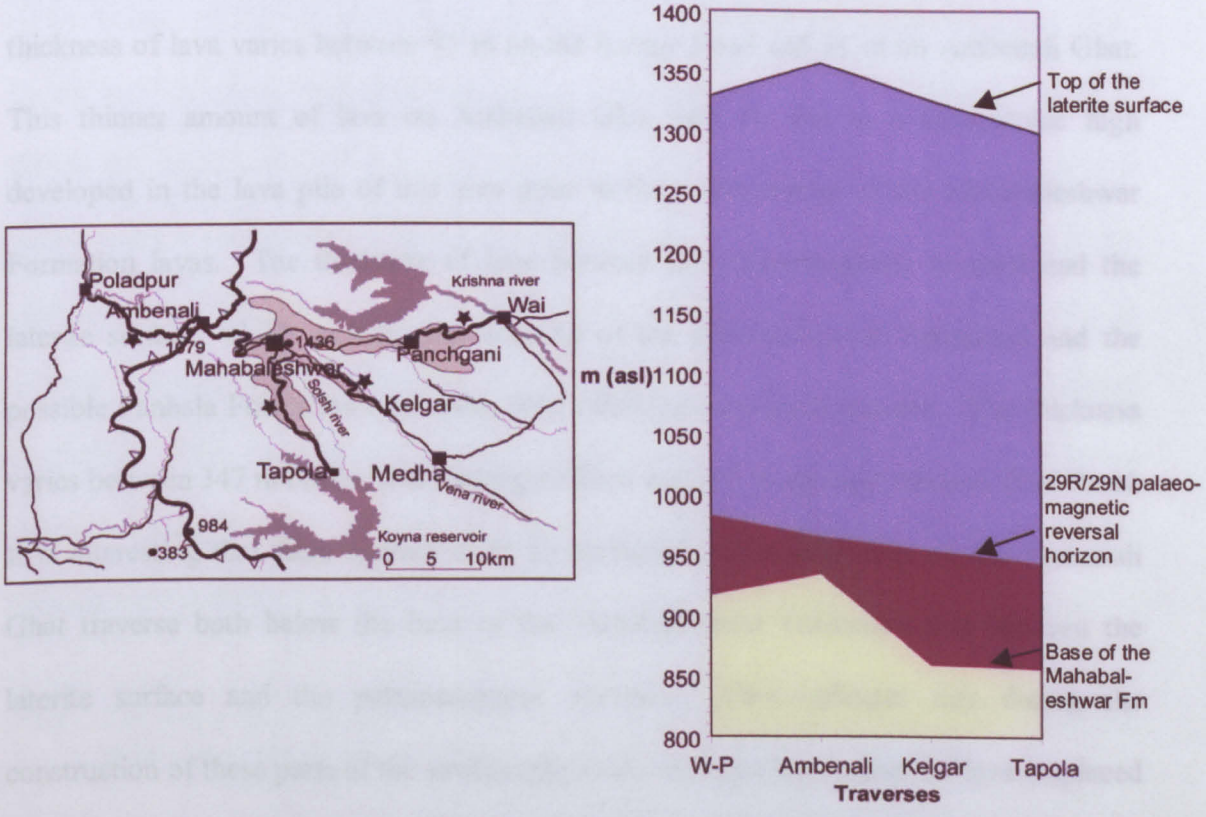

Figure 5.10. A graph showing the elevation of, and differing thicknesses of material between, the base of the Mahabaleshwar Formation, the palaeomagnetic reversal and the laterite horizon at the latitude and longitude of the palaeomagnetic reversal on the four traverses around the Mahabaleshwar Plateau, from north to south. Map shows the position of the traverses, light brown area is the upper surface of the Mahabaleshwar Plateau; starred, thicker lines are the logged sections.

	Wai-Panchgani (W-P) Road (m)	Ambenali Ghat (m)	Kelgar Road (m)	Tapola Road (m)
Laterite	1329	1356	1332	1302
Palaeomagnetic reversal	982	965	954	944
Base of the Mahabaleshwar Fm.	916	934	859	856

Table 5.1. The elevations of the three horizons used to determine palaeotopography on surfaces of the DVP in the Mahabaleshwar Plateau area, which were measured at the position of the palaeomagnetic horizon[1].

In comparing the thickness of the lava on each traverse between the palaeomagnetic horizon and the base of the Mahabaleshwar Formation it is seen that the thickness of lava varies between 95 m on the Kelgar Road and 31 m on Ambenali Ghat. This thinner amount of lava on Ambenali Ghat may be due to a topographic high developed in the lava pile of this area prior to the emplacement of the Mahabaleshwar Formation lavas. The thickness of lava between the palaeomagnetic reversal and the laterite surface, which includes the majority of the Mahabaleshwar Formation and the possible Panhala Formation type units, also varies between each traverse. The thickness varies between 347 m on the Wai-Panchgani Road and 391 m on the Ambenali Ghat Road. It is interesting that there appears to be an increased thickness of lava on the Ambenali Ghat traverse both below the base of the Mahabaleshwar Formation and between the laterite surface and the palaeomagnetic reversal. This indicates that during the construction of these parts of the stratigraphy there was a greater amount of lava emplaced over the Ambenali Ghat area than there was in the other three traverses around the Mahabaleshwar Plateau. However, between the base of the Mahabaleshwar Formation and the palaeomagnetic reversal only a small amount of lava was emplaced. This shows that topographic highs were present on the active surface of the DVP. Over time these highs appear to be evened out, which may account for the appearance of a layer-cake

[1] The elevation of the laterite surface was extrapolated using the laterite contour map, Widdowson, M., 1990. The Uplift History of the Western Ghats, India. D. Phil. Thesis, University of Oxford, Oxford..

stratigraphy of sheet lobes within the DVP. This pattern is evident in other CFB sequences (Jerram and Widdowson, 2005).

From these data, the apparent dip of the three surfaces can be calculated along the same north-south line. If the volcanic topography demonstrated above did not exist, then the dip of all three surfaces would be the same. However, the dip on the laterite surface is 0.5° S, the dip on the palaeomagnetic surface is 0.095° S, and the dip on the Mahabaleshwar Formation surface is 0.029° S. Most workers, however, have taken the dip on the surface of the Mahabaleshwar Formation to be due to post-eruptive warping (e.g., Devey and Lightfoot, 1986) but this work reveals that the plunge and dip calculated by Devey and Lightfoot (1986), cannot solely be due to post-eruptive warping. There is bound to be a component of the surface topography in the 0.3° plunge and the 0.5° dip measurement. Obviously, this is not a significant problem on a Deccan-wide scale, but on a small area such as the Mahabaleshwar Plateau the calculated regional dip may become unreliable. This observation may help explain why, even when taking into account regional dip, the elevation of the base of the Mahabaleshwar Formation or palaeomagnetic horizon were at anomalous elevations when relying on them separately for correlations.

5.4.4 The units between the Ambenali – Mahabaleshwar Formation boundary and the palaeomagnetic reversal horizon

The units between the accurately defined palaeomagnetic reversal horizon and the Ambenali-Mahabaleshwar Formation boundary (Figure 5.11) are important in this study because they have been used to investigate the volcanological structure and the correlation of sheet lobes and/or flow-fields across the Mahabaleshwar Plateau. As both horizons occur on all four traverses they provide upper and lower stratigraphic boundaries between which any sheet lobes or flow-fields should outcrop, in two or more traverses, if they are laterally continuous. This can be deduced because sheet lobes cannot cross either of these horizons, and the same sheet lobe cannot be reversely polarised in one traverse and

normally polarised in another traverse. This means that the units between the palaeomagnetic reversal and the Ambenali-Mahabaleshwar Formation boundary are indispensable for the problem of studying the correlation of units and in the investigation of the development of topography on the active surface of the DVP. Due to the precise and accurate elevation data acquired for these two horizons (from static GPS work, Appendix D2), accurate information on the lava thickness and volcanostratigraphy can be revealed. The exposure quality and the sheet lobes and flow-fields between these two important horizons are summarised as follows.

On Ambenali Ghat (Figure 2.2) there is a bole at the palaeomagnetic reversal which is only visible in an extremely weathered outcrop (Figure 2.24). Below this there is almost no exposure, with samples being taken from small isolated roadside outcrops (sample numbers in Appendix A1). Between the palaeomagnetic reversal and the base of the Mahabaleshwar Formation there is only c. 30 m of vertical section. This is the smallest thickness of lava occurring between these two horizons on any of the examined Mahabaleshwar Plateau traverses (Figure 5.11). Unfortunately, the number of individual lava units within this 30 m section cannot be precisely determined due to a lack of suitable exposure at this elevation on the traverse (Section 2.6.1, pg. 67).

On the Kelgar Road (Figure 2.2) traverse, an apparently equivalent red bole can be identified at the palaeomagnetic reversal horizon (953 m). Here, the exposure is better, and the bole is visible in partially weathered rock. By contrast, the thickness of Mahabaleshwar Formation material between the reversal and the base of the Mahabaleshwar Formation is 95 m (Figure 5.11). Moreover, within this succession, three sheet lobes can be readily identified with a possible further two within a 20-m-thick section of poorer exposure. These five sheet lobes form two flow-fields (Section 2.6.3, pg. 81).

The Wai-Panchgani Road (Figure 2.2) offers much better exposure than the other three traverses up the Mahabaleshwar Plateau. Again, a thin red bole is identified at the reversal horizon (982 m asl; Figure 5.11) and the units above and below it are well-preserved inflated pāhoehoe sheet lobes that form prominent vertical cliffs (c.10-20 m). Here, there is 55 m of Mahabaleshwar Formation lava between the reversal and the base of the Mahabaleshwar Formation. This consists of two sheet flows and two flow-fields (Section 2.6.4, pg. 91).

On the Tapola Road (Figure 2.2), the reversal horizon occurs within an area of poor to no exposure on a topographic bench (Section 2.6.2, pg. 75); a zone of unknown magnetic polarity is between 897-945 m asl. The number of units between the palaeomagnetic reversal and the base of the Mahabaleshwar Formation is uncertain because of the poor exposure. Similarly, the thickness of lava within this interval is uncertain but must be between 50 and 90 m (Figure 5.11).

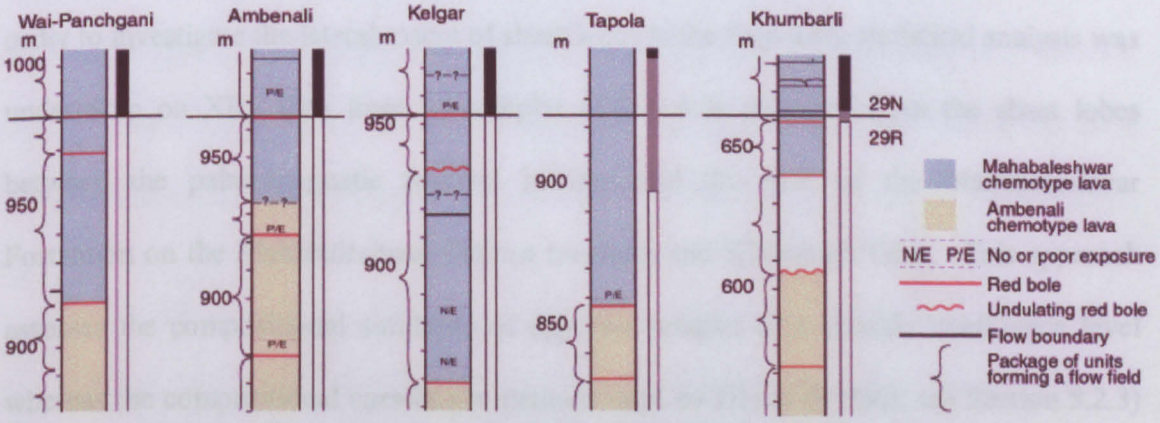

Figure 5.11. Simplified log sections from north to south around the Mahabaleshwar Plateau and Khumbarli Ghat. This shows the similarity of the style of sheet lobe in all sections below the palaeomagnetic reversal, but above, in Khumbarli Ghat, the style changes to thin lobes and toes. The thin columns to the right of each log, indicates the palaeomagnetic polarity: white, reverse; black, normal and grey, not determined. The section of white on Khumbarli Ghat is due to a lack of geochemical data. Detailed versions of these logs are found in Appendix A

Having acquired the location and elevation of the formation boundaries (Chapter 4) in all the seven logged sections, together with their detailed volcanostratigraphy (Chapter 2) it becomes possible to attempt the correlation of sheet lobes across sections of

the Western Ghats. While the main location for attempted correlations is the Mahabaleshwar Plateau, Khumbarli Ghat was also investigated (see pg. 241 for a Khumbarli Ghat description). The four logs were aligned using the base of the Mahabaleshwar Formation as the datum. This provided a horizon across the Mahabaleshwar Plateau but the variation in elevation of this horizon, between 934 m (Ambenali Ghat) and 856 m asl (Tapola Road) on the four Mahabaleshwar Plateau traverse and was irregular and not at a constant dip as would have been expected with the previously established 0.3° S and 0.5° SE tectonic dip ((Devey and Lightfoot, 1986); Section 5.2.3). This led to the conclusion that the formation boundaries alone were not precise enough for correlating sheet lobes across the Mahabaleshwar Plateau at the scale required for this work

5.4.5 Geochemical data as a means of correlating the volcanostratigraphic logged sections

Geochemical data can be used to attempt to correlate sheet lobes between traverses. In order to investigate the lateral extent of sheet lobes in the field area, statistical analysis was undertaken on XRF data from 15 samples (Table 5.2) collected from the sheet lobes between the palaeomagnetic reversal horizon and the base of the Mahabaleshwar Formation on the Mahabaleshwar Plateau traverses and Khumbarli Ghat. This approach assesses the compositional similarity of any two samples at a specific confidence level whereas the compositional correlation methods used by Devey ((1986); see Section 5.2.3) did not involve a statistical measure of similarity.

The statistical analysis undertaken is based upon the methodologies of Perkins et al. (1995) and tests the potential correlation between all the samples chosen (Table 5.2) based on the degree of similarity in their composition. The assessment of similarity is undertaken by using the statistical distance function D; where D is the Euclidean distance (in standard deviation units) between two chemical analyses. The lower the value of D the

more similar the chemical compositions of the samples are to each other. The equation for the square of D is:

$$D^2 = \sum_{k=1}^{n} \left[\frac{(x_{k1} - x_{k2})^2}{2\sigma_k^2} \right]$$

where x_{k1} = concentration of element k in sample 1, x_{k2} = concentration of element k in sample 2, σ_k = standard deviation for analytical precision of element k, and n = the number of elements used in the comparison.

D^2 will have a χ^2 distribution with n degrees of freedom, provided the samples being compared have identical composition and provided analytical errors are estimated precisely and distributed normally (Perkins et al., 1995). A D value which is less than a critical value of χ (at the 95% confidence level this value varies from 6.6 for 30 elements to 4.58 for 12 elements) is taken to show that the two samples are statistically identical i.e., from the same sheet lobe. This does not mean, however, that samples with values just outside the 95% confidence level are not from the same sheet lobe for one or more reasons. For example, there may be lateral or vertical compositional variations within the sheet lobes or uncertainties in measurement error may have been under-estimated (Perkins et al., 1995).

In order to estimate values of σ_k data from sixteen samples taken at heights of between 10 cm and 27 m from the base of a single sheet lobe (the sheet lobe below 'the Green Bole' on Ambenali Ghat, a mixed Ambenali-Mahabaleshwar Formation chemotype), were used (Table 5.3). The compositional variation between the samples is small with little sense of systematic correlation between the elevation of the sample (indicated by the sample name, e.g., APMh0.17 is 17 cm above the base of the sheet lobe) and the composition. For example, MgO and CaO have a range of only 0.8 wt.% but they

appear to correlate in the manner expected for plagioclase plus augite fractionation. The lowest MgO sample also has the lowest concentration of incompatible elements, such as TiO_2, P_2O_5 and Zr. This particular sample (APMh17) has higher K_2O than the other samples, which have scattered K_2O (Figure 5.12 C). The immobile elements (Zr, P_2O_5, TiO_2) are well correlated (e.g., Figure 5.12 D; Zr/TiO_2) but do not vary regularly with CaO, MgO or K_2O (Figure 5.12 A,B,C), suggesting small variable amounts of alteration have affected the latter elements.

The range in each incompatible element requires at most 10% fractional crystallisation and is similar to that reported by Hooper (1988) for multiple samples from CRB lavas. The range of compositions is therefore interpreted to reflect the combined effect of minor internal differentiation, post-eruptive alteration, sampling error and analytical error. As such, the standard deviations (σ_k values) of the samples given in Table 5.3 are taken to characterize the random uncertainty in the composition of a sheet lobe that is based on a single sample.

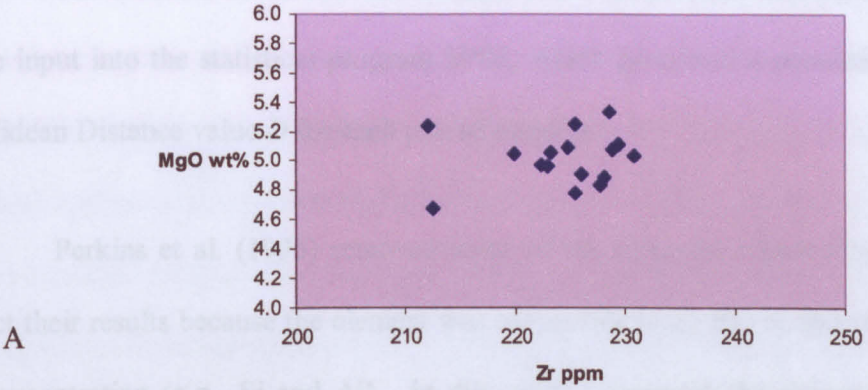

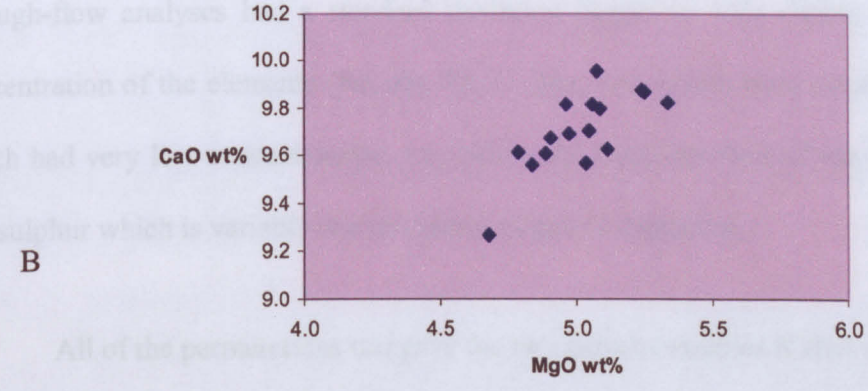

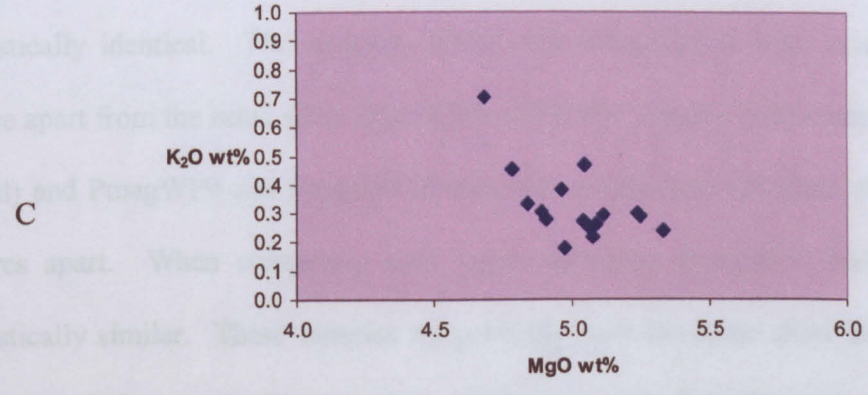

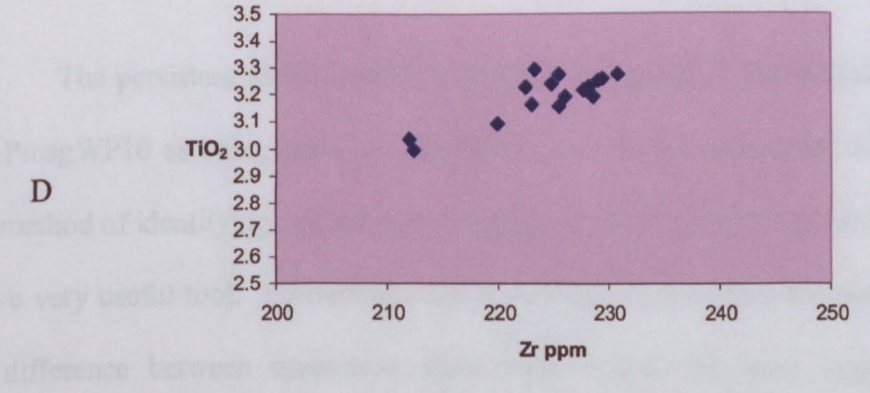

Figure 5.12 A, B, C, D. Plots demonstrating the range of compositions of the samples taken from within a single sheet lobe. (see text for details)

The standard deviations of the major and trace element data from the 15 samples were input into the statistical program SPSS, which generated a proximity matrix of the Euclidean Distance value *D* for each pair of samples.

Perkins et al. (1995) removed some of the elements which they thought would affect their results because the element was too mobile (e.g., Ba) or showed little variation in concentration (e.g., Si and Al). In this work I removed the elements for which the through-flow analyses had a standard deviation bigger or only slightly lower than the concentration of the elements (Rb, Pb, Th, U, Mo, As), which were mostly also elements which had very low concentrations, i.e., below the detection limit of the XRF equipment, and sulphur which is variable due to various stages of degassing.

All of the permutations run gave the two pairs of samples KMh2 and PMagKMw8 and PmagWP9 and PmagWP10 low *D* values, i.e., above the 95% confidence level and so statistically identical. The samples, KMh2 and PmagKMw8 were taken one (vertical) metre apart from the same sheet lobe (KMh and KMw samples both come from the Kelgar Road) and PmagWP9 and PmagWP10 were also taken from the same sheet lobe but ten metres apart. When comparing only major elements, PmagWP7 and 8 also become statistically similar. These samples are probably from the same sheet lobe, but are 34 m apart; PmagWP8 may be from a tumulus above or on top of the sheet lobe.

The persistent identification of samples PmagKMw8 and KMh2, and PmagWP9 and PmagWP10 as being identical and therefore from the same sheet lobe indicates that this method of identifying statistically similar geochemical samples is very sensitive, and is thus a very useful tool. Furthermore the Euclidean distance function statistics recognises the difference between successive sheet lobes within the same logged traverse and formation. However, considering that PmagWP9 and 10 are thought to be from the same sheet lobe, but are only identified when including major elements in the analysis, it is

important to ensure very careful sample location and investigate further the possibility of internal variation within a sheet lobe. These positive identifications indicate that this method is ideal to show whether any of the sheet lobes between the palaeomagnetic reversal horizon and the base of the Mahabaleshwar Formation are identifiable in more than one traverse.My results (Table 5.4, Table 5.6 and Table5.6) indicate that none of the sheet lobes from different traverses are statistically similar, and hence that the lateral extent of any individual sheet lobes is less than the distance between the traverses, approximately 20 km. This means that there were at least thirteen sheet lobes emplaced in this area between the beginning of the Mahabaleshwar formation and the 29R/29N palaeomagnetic reversal (assuming none of the variation is due to variable composition within eruptions).

Elev. M asl	861	919	930	935	936	945	957	938	652	903	925	945	954	856	896
	Kelgar Road	Kelgar Road	Kelgar Road	Kelgar Road	Kelgar Road	Kelgar Road	Ambenali Ghat	Ambenali Ghat	Khumbarli Ghat	Wai- Pnchgani	Wai- Panchgani	Wai- Panchgani	Wai- Panchgani	Tapola road	Tapola road
wt. %	PMaqKmw5	KMh1	03kMh1	PMaqKmw8	KMh2	03kMh2	PMhv3	PMaqPMh10	PMaqKG15	PMaqWP7	PMaqWP8	PMaqWP9	PMaqWP10	PMaqTMh15	PMaqTMh16
SiO2		48.50	48.24	49.53	48.46	49.01	47.43	47.68	48.17	49.39	50.13	49.28	48.14	47.89	49.27
TiO2		2.443	2.724	2.062	2.079	3.127	3.180	4.255	3.319	2.471	2.451	2.538	2.514	3.901	2.184
Al2O3		15.12	14.58	13.39	13.02	14.52	15.97	12.33	13.78	14.73	14.31	13.66	13.35	12.99	14.33
Fe2O3		12.73	14.09	12.85	12.79	14.97	15.19	17.63	16.02	13.28	13.06	13.20	13.68	15.89	12.12
MnO		0.167	0.179	0.268	0.265	0.219	0.166	0.218	0.301	0.196	0.198	0.202	0.165	0.218	0.168
MgO		5.19	5.68	7.84	7.31	5.22	4.70	5.26	5.69	6.25	6.12	6.49	6.20	5.09	6.60
CaO		9.41	9.96	10.76	10.57	9.73	6.91	9.25	10.02	10.81	10.53	9.89	10.05	9.69	11.04
Na2O		2.43	2.36	2.26	2.24	2.48	1.49	2.45	2.48	2.39	2.55	2.54	2.49	2.61	2.26
K2O		0.31	0.20	0.48	0.42	0.36	0.28	0.52	0.26	0.34	0.37	0.59	0.68	0.38	0.22
P2O5		0.251	0.280	0.225	0.221	0.323	0.303	0.418	0.324	0.223	0.254	0.298	0.295	0.379	0.225
LOI		2.12	1.73	0.48	1.44	0.31	4.56	0.13	0.06	0.38	0.69	0.68	2.5	-0.26	1.41
Total		98.67	100.02	100.14	98.81	100.26	100.17	100.13	100.43	100.45	100.66	99.37	100.06	98.77	99.82
ppm	PMaqKmw5	KMh1	03kMh1	PMaqKmw8	KMh2	03kMh2	PMhv3	PMaqPMh10	PMaqKG15	PMaqWP7	PMaqWP8	PMaqWP9	PMaqWP10	PMaqTMh15	PMaqTMh16
Rb	10	3	2	5	7	11	16	7	4	6	8	12	11	14	5
Sr	252	320	310	309	306	250	218	264	284	286	288	318	327	278	318
Y	28.6	32.3	34.6	28.3	26.6	44.0	37.5	49.2	37.7	28.6	30.8	30.5	30.4	46.5	25.3
Zr	140	161	177	152	150	218	198	255	189	138	156	180	176	245	147
Nb	14.3	17.0	19.0	15.3	13.2	19.7	21.2	27.9	18.8	15.1	16.0	17.3	16.9	25.2	15.5
Ba	157	207	166	194	200	183	215	186	124	113	164	190	205	170	126
Pb	3	2	2	3	2	4	4	3	3	1	4	4	2	5	1
Th	0	2	3	0	4	4	5	3	2	3	5	2	2	4	1
U	0	1	0	0	2	1	2	2	1	1	2	2	0	1	0
Sc	31	28	31	34	32	34	34	40	40	35	36	31	35	36	33
V	326	306	375	333	327	413	338	463	421	366	326	337	316	429	330
Cr	498	306	384	390	439	144	152	46	104	159	246	284	387	106	499
Co	50	38	35	46	50	35	33	42	40	44	40	47	40	36	38
Ni	184	96	98	136	137	75	85	70	79	101	107	128	117	60	113
Cu	150	163	181	134	123	263	211	337	250	157	175	172	145	314	154
Zn	110	106	121	100	110	116	126	166	149	99	101	109	108	144	97
Ga	19	25	25	20	21	24	27	26	23	23	23	22	23	25	23
Mo	0	0	0	0	0	0	0	0	0	0	0	0	0	0	0
As	0	2	4	0	0	1	0	4	0	3	0	0	1	0	2
S	57	61	87	52	41	33	111	173	31	63	68	63	233	30	130
	M'wer Fm.	M'wer Fm.	M'wer Fm.	M'wer Fm.	M'wer Fm.	M'wer Fm.	M'wer Fm.	M'wer Fm.	M'wer Fm.	M'wer Fm.	M'wer Fm.	M'wer Fm.	M'wer Fm.	M'wer Fm.	M'wer Fm.

Table 5.2. The sample numbers, elevations and geochemistry of the samples used in the Euclidean distance function analysis

wt. %	APMh0.17	APMh0.28	APMh0.41	APMh0.65	APMh0.97	APMh1.27	APMh1.58	APMh5	APMh11	APMh14	APMh17	APMh18	APMh23	APMh24	APMh25	APMh27	st dev
SiO2	47.71	47.86	48.71	48.81	48.19	48.31	48.96	48.70	49.52	48.68	49.46	48.94	47.64	48.24	46.59	47.01	0.81432
TiO2	3.262	3.230	3.196	3.218	3.276	3.231	3.169	3.163	3.098	3.281	2.999	3.039	3.293	3.243	3.198	3.253	0.08591
Al2O3	13.51	13.81	13.60	13.42	13.44	13.56	13.62	13.79	13.65	13.89	14.02	14.10	13.53	13.55	14.02	14.04	0.23010
Fe2O3	15.81	16.04	15.64	15.60	15.86	15.71	15.12	15.32	15.11	15.27	14.49	14.99	15.99	15.68	15.51	15.94	0.42646
MnO	0.254	0.219	0.229	0.257	0.240	0.218	0.215	0.189	0.211	0.279	0.169	0.203	0.207	0.200	0.183	0.202	0.02899
MgO	5.11	4.97	4.91	4.84	5.04	4.89	4.96	4.79	5.05	5.25	4.68	5.24	5.06	5.09	5.33	5.08	0.17491
CaO	9.63	9.70	9.67	9.56	9.57	9.61	9.82	9.61	9.71	9.87	9.27	9.88	9.82	9.80	9.83	9.96	0.16745
Na2O	2.40	2.44	2.56	2.59	2.51	2.61	2.62	2.57	2.64	2.52	2.54	2.41	2.36	2.49	2.14	2.33	0.13109
K2O	0.30	0.18	0.28	0.34	0.27	0.31	0.38	0.46	0.47	0.29	0.70	0.30	0.25	0.26	0.24	0.22	0.12697
P2O5	0.356	0.336	0.347	0.341	0.345	0.335	0.331	0.331	0.337	0.341	0.323	0.328	0.336	0.334	0.327	0.345	0.00843
LOI	1.23	0.90	0.92	0.82	1.35	0.83	0.50	0.91	0.22	0.53	0.80	0.81	0.92	0.66	1.47	1.06	
Total	99.58	99.67	100.06	99.78	100.10	99.60	99.70	99.83	100.01	100.21	99.45	100.23	99.41	99.54	98.84	99.44	0.35984
	APMh0.17	APMh0.28	APMh0.41	APMh0.65	APMh0.97	APMh1.27	APMh1.58	APMh5	APMh11	APMh14	APMh17	APMh18	APMh23	APMh24	APMh25	APMh27	St dev
Rb	3	2	9	12	4	3	9	6	16	4	20	3	3	3	4	5	5.37586
Sr	245	255	252	248	249	252	249	249	245	253	250	252	243	249	244	252	3.44093
Y	46.5	45.2	44.8	45.5	44.7	46.8	43.3	46.9	43.1	44.2	42.8	41.9	44.5	43.6	43.2	45.1	1.47579
Zr	229	222	226	228	231	228	223	226	220	226	212	212	223	225	229	229	5.53193
Nb	20.5	20.1	20.5	21.2	20.3	20.4	19.8	20.1	19.0	20.1	19.1	19.1	19.7	19.0	20.6	20.8	0.68139
Ba	123	131	160	173	173	185	192	200	193	200	195	153	149	183	115	146	28.16333
Pb	4	4	3	1	3	0	4	4	5	4	5	3	4	4	4	5	1.38911
Th	4	3	4	4	3	4	3	4	3	4	3	4	1	3	4	4	0.73663
U	0	2	2	2	1	2	1	2	1	2	0	0	3	2	0	1	0.92376
Sc	40	36	37	35	38	38	37	39	35	39	35	36	42	36	40	37	1.99165
V	418	411	418	413	416	402	426	424	407	424	383	356	390	398	436	443	21.30415
Cr	123	128	125	120	123	122	131	131	140	131	135	155	178	125	285	183	41.69495
Co	39	35	35	36	39	38	38	40	37	40	35	35	35	37	36	38	1.87368
Ni	67	65	68	63	66	62	66	67	67	67	75	77	67	71	71	71	3.91629
Cu	314	330	342	326	358	301	283	254	264	254	219	221	284	238	293	209	46.14603
Zn	131	126	126	123	129	123	125	117	121	117	119	110	122	117	128	131	5.80481
Ga	23	24	25	23	26	25	25	25	24	25	26	25	25	24	24	25	0.89645
Mo	0	0	0	0	0	0	0	0	0	0	0	0	0	0	0	0	0.02500
As	5	0	0	0	0	0	3	1	0	1	0	0	3	0	5	0	1.89416
S	59	62	44	37	42	54	47	43	33	43	39	68	65	64	80	71	13.99185

Table 5.3 The geochemical analyses of the samples through a single sheet lobe and the standard deviation.

All major elements	χ=4.2													
	Kelgar Road					Ambenali Ghat		Khumbarli	Wai-Panchgani Road				Tapola Road	
	2:KMh1	3:03KMh1	4:PMagKMw8	5:KMh2	6:03KMh2	7:PMagPMh10	8:PMhn3	9:PMagKG15	10:PMagWP7	11:PMagWP8	12:PMagWP9	13:PMagWP10	14:PMagTMh15	15:PMagTMh16
2:KMh1	0.00	6.44	14.10	12.71	11.08	26.88	16.18	15.18	8.02	6.85	8.42	8.98	20.02	10.01
3:03KMh1	6.44	0.00	13.24	12.17	6.19	21.80	15.88	9.40	7.32	5.86	6.05	5.73	15.10	10.69
4:PMagKMw8	14.10	13.24	0.00	2.77	18.26	31.13	26.40	19.04	8.70	8.94	9.91	10.87	25.22	7.09
5:KMh2	12.71	12.17	2.77	0.00	17.35	30.38	25.32	18.29	8.00	8.02	9.05	9.72	24.32	6.48
6:03KMh2	11.08	6.19	18.26	17.35	0.00	16.37	14.23	5.30	12.87	11.19	9.76	9.10	9.72	16.46
7:PMagPMh10	26.88	21.80	31.13	30.38	16.37	0.00	22.05	13.65	27.91	26.29	23.37	22.30	7.56	31.16
8:PMhn3	16.18	15.88	26.40	25.32	14.23	22.05	0.00	16.92	21.59	20.69	19.13	19.11	18.54	24.65
9:PMagKG15	15.18	9.40	19.04	18.29	5.30	13.65	16.92	0.00	14.98	13.72	12.01	11.14	7.95	13.69
10:PMagWP7	8.02	7.32	8.70	8.00	12.87	27.91	21.59	14.98	0.00	3.43	8.02	8.47	21.22	4.96
11:PMagWP8	6.85	5.86	8.94	8.02	11.19	26.29	20.69	13.72	3.43	0.00	5.20	5.93	19.46	5.67
12:PMagWP9	8.42	6.05	9.91	9.05	9.76	23.37	19.13	12.01	8.02	5.20	0.00	2.68	16.92	9.37
13:PMagWP10	8.98	5.73	10.87	9.72	9.10	22.30	19.11	11.14	8.47	5.93	2.68	0.00	15.96	10.14
14:PMagTMh15	20.02	15.10	25.22	24.32	9.72	7.56	18.54	7.95	21.22	19.46	16.92	15.96	0.00	24.40
15:PMagTMh16	10.01	10.69	7.09	6.48	16.46	31.16	24.65	13.69	4.96	5.67	9.37	10.14	24.40	0.00

Table 5.4. Euclidean distance matrix of the fifteen samples (from between the base of the Mahabaleshwar Formation and the 29R/29N palaeomagnetic reversal horizon) from four sections around the Mahabaleshwar Plateau and Khumbarli Ghat. The element compared are all the major elements. Statistically similar samples are highlighted ($D < 4.2$). Sample 1 is missing because there is no major element data for it.

All trace elements-Rb,Pb,Th,U,Mo,As,S				χ=4.73												
	Kelgar Road						Ambenali Ghat		Khumbarli	Wai-Panchgani Road				Tapola Road		
	1:PMagKMw5	2:KMh1	3:03KMh1	4:PMagKMw8	5:KMh2	6:03KMh2	7:PMagPMh10	8:PMhx3	9:PMagKG5	10:PMagAP7	11:PMagAP8	12:PMagAP9	13:PMagAP10	14:PMagTMh15	15:PMagTMh16	
1:PMagKMw5	0.00	22.85	22.37	15.01	14.26	25.64	33.57	24.81	24.45	17.04	17.42	18.53	21.07	32.32	19.69	
2:KMh1	22.85	0.00	5.34	9.91	11.26	18.32	24.92	22.71	12.97	13.11	7.96	7.75	5.69	20.38	6.99	
3:03KMh1	22.37	5.34	0.00	11.18	12.74	15.28	21.07	20.03	9.97	13.11	8.16	8.52	7.00	16.75	8.80	
4:PMagKMw8	15.01	9.91	11.18	0.00	3.40	21.59	28.78	24.67	16.65	12.20	8.16	5.68	7.13	25.54	6.68	
5:KMh2	14.26	11.26	12.74	3.40	0.00	22.68	30.10	25.35	17.72	12.56	9.39	7.40	8.93	27.01	7.84	
6:03KMh2	25.64	18.32	15.28	21.59	22.68	0.00	18.21	8.80	9.82	15.06	14.95	19.79	20.43	10.27	21.65	
7:PMagPMh10	33.57	24.92	21.07	28.78	30.10	18.21	0.00	17.17	15.09	25.06	23.85	25.26	26.05	6.34	29.05	
8:PMhx3	24.81	22.71	20.03	24.67	25.35	8.80	17.17	0.00	15.36	16.40	17.95	23.88	24.78	16.34	25.02	
9:PMagKG5	24.45	12.97	9.97	16.65	17.72	9.82	15.09	15.36	0.00	12.37	10.85	14.34	14.63	11.65	16.29	
10:PMagAP7	17.04	13.11	13.11	12.20	12.56	15.06	25.06	16.40	12.37	0.00	6.07	13.73	14.83	22.03	12.81	
11:PMagAP8	17.42	7.96	8.16	8.16	9.39	14.95	23.85	17.95	10.85	6.07	0.00	8.74	9.10	20.19	8.31	
12:PMagAP9	18.53	7.75	8.52	5.68	7.40	19.79	25.26	23.88	14.34	13.73	8.74	0.00	4.61	21.93	8.10	
13:PMagAP10	21.07	5.69	7.00	7.13	8.93	20.43	26.05	24.78	14.63	14.83	9.10	4.61	0.00	22.07	6.03	
14:PMagTMh15	32.32	20.38	16.75	25.54	27.01	10.27	6.34	16.34	11.65	22.03	20.19	21.93	22.07	0.00	24.90	
15:PMagTMh16	19.69	6.99	8.80	6.68	7.84	21.65	29.05	25.02	16.29	12.81	8.31	8.10	6.03	24.90	0.00	

Table 5.5. Euclidean distance matrix of the fifteen samples (from between the base of the Mahabaleshwar Formation and the 29R/29N palaeomagnetic reversal horizon) from four sections around the Mahabaleshwar Plateau and Khumbarli Ghat. The elements compared are all the trace elements except Rb, Pb, Th, U, Mo, As and S. Statistically similar samples are highlighted ($D < 4.73$).

All major and trace elements -Rb,Pb,Th,U,Mo,As,S						χ=5.93								
	Kelgar Road					Ambenali Ghat		Khumbarli	Wai-Panchagani Road				Tapola Road	
	2:KMh1	3:03KMh1	4:PMagKMw8	5:KMh2	6:03KMh2	7:PMagPMh10	8:PMhk3	9:PMagKG15	10:PMagWP7	11:PMagWP8	12:PMagWP9	13:PMagWP10	14:PMagTMh15	15:PMagTMh16
2:KMh1	0.00	8.37	17.24	16.98	21.41	36.65	27.89	19.96	15.37	10.50	11.45	10.63	28.57	12.21
3:03KMh1	8.37	0.00	17.33	17.62	16.49	30.32	25.56	13.70	15.01	10.05	10.45	9.05	22.55	13.84
4:PMagKMw8	17.24	17.33	0.00	4.39	28.27	42.40	36.13	25.30	14.98	12.10	11.43	13.00	35.89	9.74
5:KMh2	16.98	17.62	4.39	0.00	28.55	42.76	35.83	25.46	14.90	12.35	11.68	13.20	36.34	10.17
6:03KMh2	21.41	16.49	28.27	28.55	0.00	21.04	16.73	11.15	19.81	18.68	22.06	22.36	14.14	27.20
7:PMagPMh10	36.65	30.32	42.40	42.76	21.04	0.00	27.94	20.35	37.51	35.49	34.41	34.29	9.87	42.61
8:PMhk3	27.89	25.56	36.13	35.83	16.73	27.94	0.00	22.85	27.11	27.39	30.60	31.29	24.71	35.12
9:PMagKG15	19.96	13.70	25.30	25.46	11.15	20.35	22.85	0.00	19.42	17.49	18.71	18.39	14.11	24.79
10:PMagWP7	15.37	15.01	14.98	14.90	19.81	37.51	27.11	19.42	0.00	6.97	15.90	17.08	30.59	13.73
11:PMagWP8	10.50	10.05	12.10	12.35	18.68	35.49	27.39	17.49	6.97	0.00	10.16	10.87	28.04	10.06
12:PMagWP9	11.45	10.45	11.43	11.68	22.06	34.41	30.60	18.71	15.90	10.16	0.00	5.33	27.70	12.38
13:PMagWP10	10.63	9.05	13.00	13.20	22.36	34.29	31.29	18.39	17.08	10.87	5.33	0.00	27.24	11.80
14:PMagTMh15	28.57	22.55	35.89	36.34	14.14	9.87	24.71	14.11	30.59	28.04	27.70	27.24	0.00	34.86
15:PMagTMh16	12.21	13.84	9.74	10.17	27.20	42.61	35.12	24.79	13.73	10.06	12.38	11.80	34.86	0.00

Table 5.6. Euclidean distance matrix of the fifteen samples (from between the base of the Mahabaleshwar Formation and the 29R/29N palaeomagnetic reversal horizon) from four sections around the Mahabaleshwar Plateau and Khumbarli Ghat. The elements compared are all the major and trace elements except Rb, Pb, Th, U, Mo, As and S. Statistically similar samples are highlighted ($D < 5.93$)

5.5 *Large scale architecture and stratigraphic correlation: geographically distinct sections*

Having investigated the correlations and volcanic architecture of sections which are relatively geographically close (Section 5.3 and 5.4) it is important to look at these relationships on a slightly larger scale, still within the central Western Ghats, but on sections north and south of the main study area (the Mahabaleshwar Plateau). The possibility of correlation obviously decreases with distance, but it is important in the understanding of the volcanic architecture of the DVP that areas other than the Mahabaleshwar Plateau are investigated and compared to the main study area.

5.5.1 Correlating between the Mahabaleshwar Plateau sections and Khumbarli Ghat.

Khumbarli Ghat is 60 km south of the main study area of the Mahabaleshwar Plateau (Figure 2.1). The road section is between Chiplun (17°31'40"N 73°50'50"E) and Helwak (17°23'05"N 73°40'10"E), at the southern end of the Koyna reservoir. The logged road section is 10 km long (Figure 2.1), and ascends the ghat scarp itself. A detailed description of the observations is given in Section 2.6.6 and the associated log in Appendix 6. The Khumbarli Ghat traverse contains the Ambenali and Mahabaleshwar Formations and hence the 29R/29N palaeomagnetic reversal. Here the palaeomagnetic reversal is at either 659 m or 663 m (due to time constraints it was not possible to drill palaeomagnetic cores in every sheet lobe and so the 29R/29N reversal can be placed at one of two flow boundaries), and provides an opportunity for Khumbarli Ghat to be broadly correlated with the four sections of the Mahabaleshwar Plateau. The elevations on this section were gathered using hand-held GPS and barometric altimeters only, as the static GPS was not available at the time of the logging. Consequently, this remains an unquantifiable error which adds to the problem of correlating between the Mahabaleshwar Plateau and Khumbarli logs.

Statistics undertaken on the compositions of the sheet lobes between the base of the Mahabaleshwar Formation and the palaeomagnetic reversal (Section 5.4.5) revealed that no sheet lobes sampled around the Mahabaleshwar Plateau or Khumbarli Ghat have statistically similar compositions and therefore cannot be taken as correlating. However, it is important to investigate the possibility of units being traceable between these two sections as it provides insights into the correlation of units and volcano architecture across an area wider than just the Mahabaleshwar Plateau.

The lowest formation identified on Khumbarli Ghat in this study is the poorly exposed Ambenali Formation (Figure 4.4e), although Devey and Lightfoot (1986) document 150 m of Poladpur Formation at the base of Khumbarli Ghat, not seen at similar elevations in my study. The Ambenali-Mahabaleshwar Formation boundary is at either 606 m or 640 m asl; this uncertainty is due to the lower sampling density (the same problem as encountered in identifying the 29R/29N reversal horizon). The uppermost samples collected at road level (700 m asl) are still in the Mahabaleshwar Fm, and it is probable that the top three thick sheet lobes, in an approximately 40-60 m high inaccessible cliff (~ 700 m asl), are typical of those seen towards the top of Ambenali Ghat and should have the mixed Mahabaleshwar-Ambenali Formation geochemistry.

Much of the lower Khumbarli Ghat is relatively poorly exposed (Table 2.3), however the upper section from 450 m (in the Ambenali Fm) to 730 m (in the Mahabaleshwar Formation), is well exposed (Figure 5.11). The section between the thin red bole (thought to mark the 29R/29N reversal horizon) and the base of the Mahabaleshwar Formation, is one (or two, depending on the exact location of the formation boundary) thick sheet lobe(s) (each) bounded top and bottom by a red bole. This is similar to the sequences seen on the Mahabaleshwar Plateau traverses. However, above the reversal the characteristics of the sheet lobes change to a sequence of small pāhoehoe

lobes each with a maximum thickness of 2 m, whereas thick sheet lobes are observed further north in the Mahabaleshwar Plateau area (Figure 5.11).

5.5.2 Correlating between the Mahabaleshwar Plateau sections and Varandah Ghat

The Varandah Ghat section is approximately 25 km directly west-north-west of the town of Mahabaleshwar (Figure 2.1). Due to the southerly regional dip (Figure 5.1), this places the lower lava units observed in Varandah Ghat lower down in the stratigraphy than the sections logged around Mahabaleshwar Plateau and Khumbarli Ghat. The formations encountered are the Bushe, Poladpur and lower Ambenali Fm, thus providing overlap with the lower part of the Ambenali Ghat traverse, and possibly the lower Khumbarli Ghat. Due to the absence of the palaeomagnetic reversal horizon in this traverse it is not possible to use the 29R/29N horizon for correlating individual sheet lobes between Varandah Ghat and the logged traverses to the south (i.e., Mahabaleshwar Plateau and Khumbarli Ghat). The only possibility is to use the geochemical characteristics of the formations, but it has been demonstrated that these are not reliable for correlations over short distances because of the topography which developed on the active surface of the DVP (Section 5.4.3). Again, correlation is hampered by the lack of high precision GPS on Varandah Ghat and so the elevations are reliant upon hand-held GPS and barometric altimeters, further increasing the difficulty in correlations. No successful correlations between Varandah Ghat and the Mahabaleshwar Plateau traverses were achieved. However, future work using digital elevation models could provide an opportunity to correlate this section, the Mahabaleshwar Plateau sections and Khumbarli Ghat using the topographic benches which occur in the DVP and including Varandah Ghat samples in future statistical comparisons of geochemical data using the Euclidean distance function analysis (Section 5.4.5).

5.5.3 Correlating between the Mahabaleshwar Plateau sections and Matheran Ghat

Matheran Ghat is ~125 km north west of Mahabaleshwar (Figure 2.1) and hence much lower in the DVP stratigraphy than the Varandah, Mahabaleshwar Plateau and Khumbarli sections. The formations encountered here are the Neral, Thakurvadi, Bhimashanka and Khandala. Although the lavas in this section do not overlap in time with any of the traverses further south, it does provide a useful comparison of the style of the eruptive units in the region around the main study area. As described in Section 0, (and summarised here), the Matheran Ghat, traverse is dominated by small pāhoehoe toes and lobes, from 10s of cm to approximately 10 m thick.

Apart from the different size of the sheet lobes, the most marked difference is the lack of boles or major weathering horizons. This is in considerable contrast to the situation on the Mahabaleshwar Plateau where there is a bole horizon between the majority of the sheet lobes of flow-fields. On Matheran Ghat, the section starts at ~50 m asl and the first bole is observed at ~562 m. It is possible that a bole could be obscured in the 25% of lavas not exposed (Table 2.3 and Appendix A7) but it seems probable that if there were many boles in this section some would be observed in the good exposure lower down in the sequence. Therefore, using the definition of a flow-field used in this work (Section 2.2.1), this forms a "flow-field" that is ~512 m thick. This is a huge amount of lava to be erupted without an apparent time break.

The reasons for this however, can only be speculated upon and may or may not relate to the reasons for the differing flow morphology between the lavas seen at Matheran and those observed further south. Walker (1972) suggested that lavas which were emplaced proximal to the vent formed compound flows, i.e., a series of small lobes or toes erupted on top of one another, in the style that is seen at Matheran Ghat. If this area, and hence these units, are proximal to the vent, each eruption would probably send some lava

over this area and thus there was never a hiatus long enough for a bole to form. Perhaps if it were possible to observe these formations more distally, the sheet lobes would be much thicker and similar to those seen around the Mahabaleshwar Plateau, as only the largest units would have reached the more distal zones. The reason for the boles occurring towards the top of the pile could be due to the active vent zones moving further away from the Matheran area (due to the northward drift of India (Mitchell and Widdowson, 1991), so that new sheet lobes covered the area less often, and boles developed. A second option is that the eruptive style changed from these earlier compound-type lavas to thicker lava inflation units later on in the DVP history and that the length of time between eruptions increased, thus providing time for the boles to form in the younger more southerly areas. A third option is that effusion rates in the early DVP's history were slower, and so the lavas could only form thin, relatively short, hummocky pāhoehoe flow-fields dominated by lobes and toes, and so the older, lower formations (typical of those around the Matheran area) did not reach far south and/or could not form thick sheet flows like those observed around the Mahabaleshwar area.

5.6 Eruption rates

It was hoped that the palaeomagnetic data collected on all of the sections would identify the lower, 30N/29R reversal as well as the 29R/29N. This would have provided two dated time horizons at 65.578 and 64.745 Ma respectively (Cande and Kent, 1995) which, when combined with the known and extrapolated thickness and the total extent of the relevant formations would have provided a time averaged eruption rate for this part of the stratigraphy. However, this may well be a relatively poor indicator of the environmental impact of the DVP as the environmental effect is dependent upon the magnitude, duration and style of individual eruptions and the length of the time between them. It has been suggested by Widdowson et al. (1997) that the high number of boles observed in the

southerly sections indicates that there were prolonged periods where no lava was emplaced over sizeable areas. These areas were probably as extensive, or more so, than the Mahabaleshwar Plateau. However, an ability to match boles across the Plateau would greatly increase the reliability of this statement.

The occurrence of boles becomes more frequent up through the DVP pile (Widdowson et al., 1997) and some of the top-most sheet lobes of the Mahabaleshwar Plateau, where they are visible, are some of the thickest seen. This suggests that towards the end of the DVP the eruptions became less frequent but were possibly larger than those which formed the lower Wai Sub-group sheet lobes. A further suggestion, that cannot be tested with current knowledge, is that the DVP could have been erupting almost continuously. Much of the work on CFBs speculates that the eruptions where huge and each lasted for at least a decade or more (Thordarson and Self, 1998), and were then followed by long periods of quiescence, of between 10 - 10^4 years (Jerram and Widdowson, 2005), when no eruptions took place. The areas of the DVP covered by lava from the Wai Sub-group Fms is so huge (Mitchell and Widdowson, 1991; Bilgrami, 1999) that it seems possible that the period of time taken to resurface the whole volcanic edifice, even if it was erupting almost continually, provides enough time for the thick boles to develop on inactive areas of the lava surface. Clearly this is only speculation and deserves further work in the future.

Figure 5.13 A cartoon (not to scale) demonstrating the complexities of the emplacement of flow-fields and hence the thickness and occurrence of boles. Each layer represents a new flow-field, 1 being the oldest and 8 the youngest. Flow-fields may be active for long periods of time forming first one 'arm' of the flow-field and then another on a completely different part of the edifice, thus allowing boles to form in some areas while lava is emplaced else where. This provides a mechanism for the formation of thick boles whilst allowing for the possibility of almost continuous eruption. Note also how the age of the lava in kipukas and exposed areas is of various ages, thicker boles will form on older lava therefore boles of different thicknesses can occur adjacent to each other yet be covered by the same flow-field or even sheet lobe.

5.7 *The scales of volcanic architecture*

The volcanic architecture of the DVP was investigated on a number of scales (in Sections 5.3-5.5). The results are now summarized and linked, and show that the same style of volcanic architecture occurs from a decimetre to tens of kilometres scale.

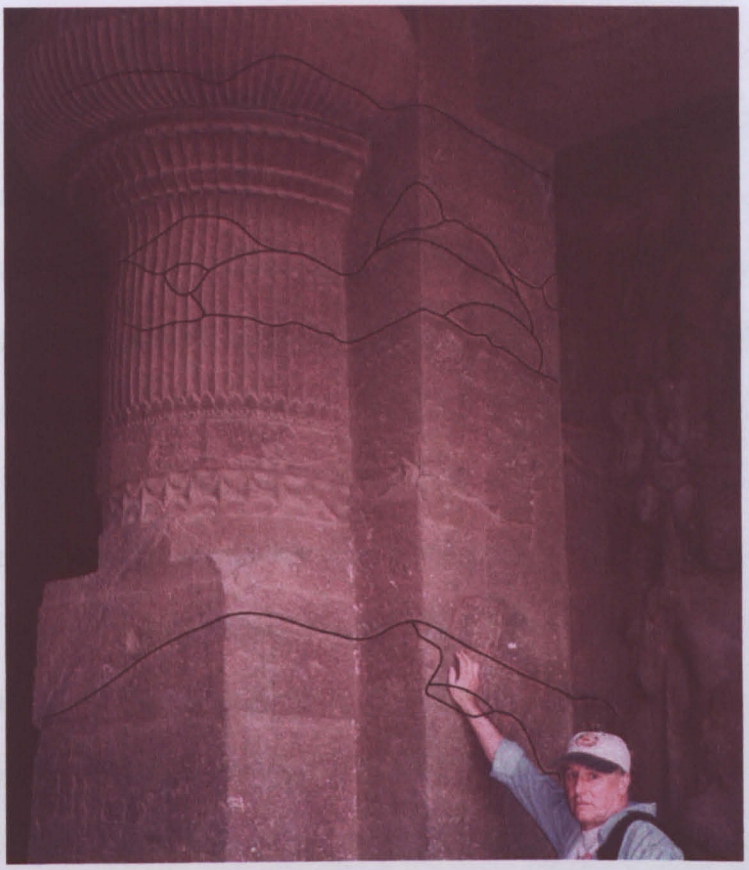

Figure 5.14. A series of small lobes from the Elephanta Caves, near Mumbai, which were carved into lavas in situ. This demonstrates the architecture of small (2 to 3-m-thick) inflated pāhoehoe lobes (such as the ones above the persons head) and small inter-stratified lobes and toes (outlined in black).

Starting at the smallest scale of observation, Figure 5.13 shows small toes and lobes and inflated sheet lobes, the majority of which are only tens of centimetres thick. Figure 5.7 and Figure 5.8 show inflated sheet lobes on a much larger scale in the cliff faces of the Mahabaleshwar Plateau. The lateral continuity of the sheet lobes on both scales is limited, and on following a sheet lobe laterally, the number of lobes increases and decreases as lobes vary in thickness and terminate against one another. The statistical analysis of geochemical data from the sheet lobes between the palaeomagnetic reversal and

the top of the Mahabaleshwar Formation (Section 5.4.5) has also supports the theory that the sheet lobes have limited lateral extent of in that none of the sheet lobes has been successfully identified on more than one traverse around the Mahabaleshwar Plateau (this however maybe due to chemical inhomogeneities within individual sheet lobes which are not yet fully understood), thus suggesting that individual sheet lobes are less than 20 km wide.

There are a number of reasons as to why it is not possible to correlate sheet lobes across the Mahabaleshwar Plateau. First, the quality of the exposure varies considerably in each logged section (Figure 5.11 and Appendix A), thus making it possible to miss sheet lobes preserved in one section in other sections. Second, the sheet lobes are areally restricted (i.e., they are not Plateau-wide). Section 5.4.3 has demonstrated that there was topography on the active surface of the DVP, and that this was probably caused by a different number of sheet lobes and flow-fields being emplaced onto different areas over a region the size of the Mahabaleshwar Plateau. This can be seen in Figure 5.11, where there are at least three and more probably five sheet lobes between the palaeomagnetic horizon and the base of the Mahabaleshwar Formation on the Kelgar Road, and two on the Wai-Panchgani Road. Third, a further factor which decreases the likelihood of correlating units across the Plateau is the non-vertical nature of the logged sections. The logs follow the road which ascend the Plateau and they are therefore, naturally, further apart at the base of the Plateau than at the top as the roads converge towards the top of the Plateau (Figure 2.2). This will obviously reduce the likelihood of correlating units between sections at lower elevations, as the sheet lobes would have to be wider to appear in more than one traverse. It is probable, however, that a number of the flow-fields encountered between the palaeomagnetic reversal and the base of the Mahabaleshwar Formation do occur in more than one traverse. Nevertheless, they will be formed of different sheet lobes so it is not possible to identify them in the different traverses.

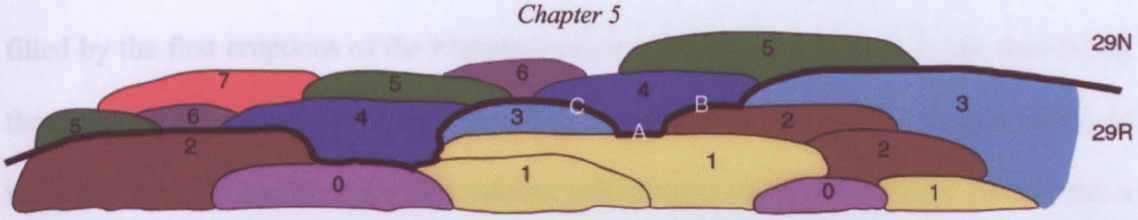

Figure 5.15. A cartoon (not to scale) demonstrating the complexities of a section of sheet lobes in a flood basalt province. Each number indicates a different flow-field: 0 is oldest, 7 is youngest. This shows that the elevation of the younger sheet lobes can be stratigraphically lower than the adjacent older units. Heavy line is the palaeomagnetic reversal horizon (which occurred in the interval between flow-fields 3 and 4) described in text.

Figure 5.15 (not to scale with no lateral dimension implied) illustrates the lateral discontinuity and complications of pāhoehoe sheet lobes. It demonstrates how an isochronous boundary, in this case 29R/29N (but it could be the top surface of a single flow-field), can appear at different levels within a number of pāhoehoe lava flow-fields. Each group of sheet lobes (the enclosed shapes, here much vertically exaggerated compared to their lateral extent) formed by one eruption are colour and number coded (0 is oldest 7 is youngest). Pāhoehoe flow-fields grow in a complicated way, often not covering whole areas and leaving kipukas (areas that are not covered by active flows). Therefore when the next sheet lobe arrives it can be emplaced upon different flow-fields of different ages. If a number of flow-fields are absent at a location and the kipuka is then covered by a subsequent flow, the difference in elevations of the base of that flow, at different locations, could be up to 100 m (Figure 5.10). For example, in Figure 5.14, at point 'A' a unit from flow-field 4 is resting directly on flow-field 1, at 'B' the same unit is resting on a unit from flow-field 2, and at 'C' it is resting on a unit from flow-field 3. The palaeomagnetic reversal horizon occurs at each of these places but at different elevations. Importantly, later sheet lobes will fill any low-lying topography as the lava will flow into the depression and then inflate to partially or totally fill it. This may explain what happened in the section of stratigraphy between the base of the Mahabaleshwar Formation and the palaeomagnetic reversal horizon around the Mahabaleshwar Plateau (Section 5.4.3). For instance if the area on Ambenali Ghat was a topographic high, as information suggests, the depression around it (seen on the other three traverses Figure 5.10) would be

filled by the first eruptions of the Mahabaleshwar Formation chemotype lavas, thus filling the available depression by the time the palaeomagnetic reversal occurred. If inflation of the sheet lobe(s) continued and the number and extent of lateral breakouts are limited, a topographic high may have developed in the areas where there was once a low. If this flow-field is then viewed in section across the plateau, it could appear to be a different flow-field in different localities, because the base will be at different positions in the stratigraphy and it can appear that a younger unit is below an older unit in the stratigraphy (Figure 5.15).

Further complications in stratigraphy can develop if a sheet lobe does not extend far laterally and during inflation the unit grows vertically with only a few small break-out lobes on what can be almost vertical flanks (Figure 5.16). This will provide a considerable amount of topography and subsequent younger flows will have to flow around it, again producing a stratigraphy which can be temporally misinterpreted.

Figure 5.16. Inflated sheet lobe with vertical sides and some break out lobes and toes, Mauna Loa, Hawai'i.

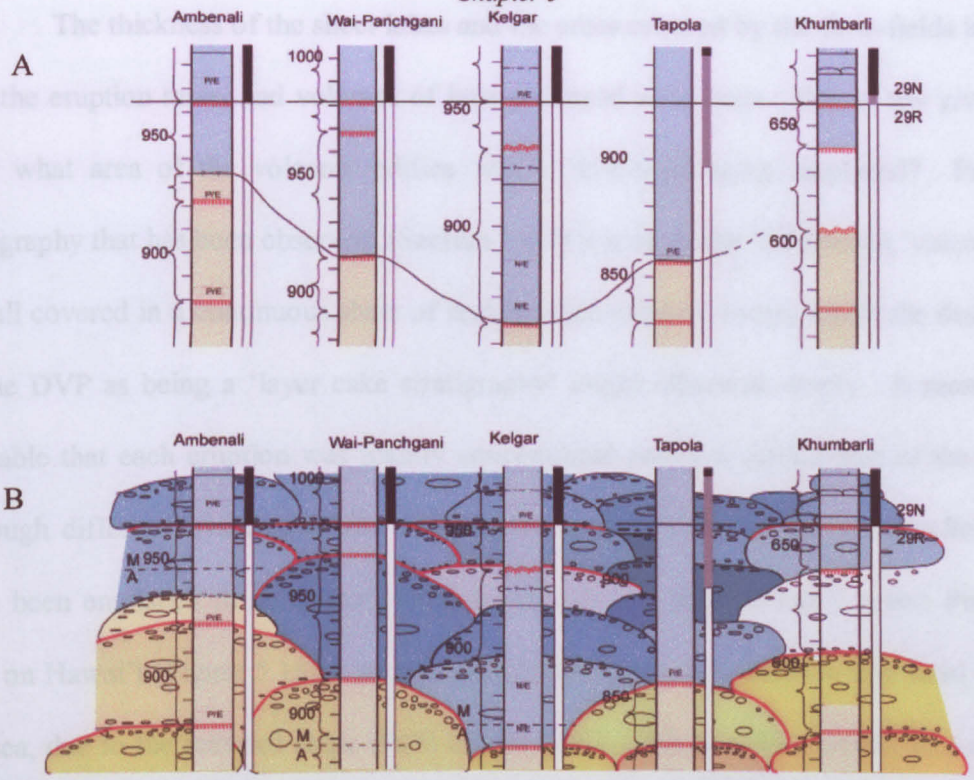

Figure 5.17 A) simplified version of the five sections which display the 29R/29N palaeomagnetic reversal horizon and the Mahabaleshwar – Ambenali Formation boundary. The logs have been aligned along the palaeomagnetic reversal horizon. B) A cartoon considerably magnified in the vertical, showing an idealised section of sheet lobes and how the topography may have been formed on top of the Ambenali Formation. Ambenali Formation is yellow, Mahabaleshwar Formation is blue.

Moving to the flow-field scale, Figure 5.16 shows the five logged sections which have been used to demonstrate the architecture of this area of the Western Ghats as they contain the two isochronous horizons which have aided attempted correlations and understanding of the topography (Figure 5.10) which built up on the active surface of the DVP. Figure 5.17 shows that there are varying numbers of flow-fields in between the two isochronous horizons and this demonstrates that the lateral continuity of flow-fields is limited in the same way that the lateral continuity of individual sheet lobes is limited. Neither lava flows nor (especially) sheet lobes are thought to cover very wide areas so their length to width ratio is very large. This demonstrates that on a sheet lobe, lava flow and flow-field scale the volcanic architecture of the Western Ghats is similar, units pinch out, and their lateral continuity is limited and disrupted, which leads to the development of topography on the active surface and problems in correlating units.

The thickness of the sheet lobes and the areas covered by the flow-fields indicates that the eruption rates, and volumes of lava produced were huge. But at any given time over what area of the volcanic edifice was a flow-field being emplaced? From the topography that has been observed, (Section 5.4.3) it is clear that the Deccan 'volcano' was not all covered in a continuous sheet of lava by each eruptive event, which the description of the DVP as being a 'layer cake stratigraphy' might otherwise imply. It seems more probable that each eruption was mainly concentrated across a certain part of the edifice, although different lava flows from the eruptive episode (which forms a flow-field) may have been emplaced in completely different directions. The currently active Pu'u' O'o vent on Hawai'i (Figure 5.18) is predominantly producing lava flows which head towards the sea, due to the seaward slope (Pali) but the 1983-1986 lava flow travels in a different direction and flows parallel to the coast. The DVP is unlikely to have been dominated by a seaward slope like Pu'u' O'o but as the individual sheet lobes inflated to thicknesses of ~20 m and as topography of up to 95 m is known to have developed, the shape of individual flow-fields may have been dominated by the topography of the surface it was erupted onto, just like Pu'u O'o (only the topography was formed in a different way). Thus producing lava flows which may have flowed in a variety of different directions.

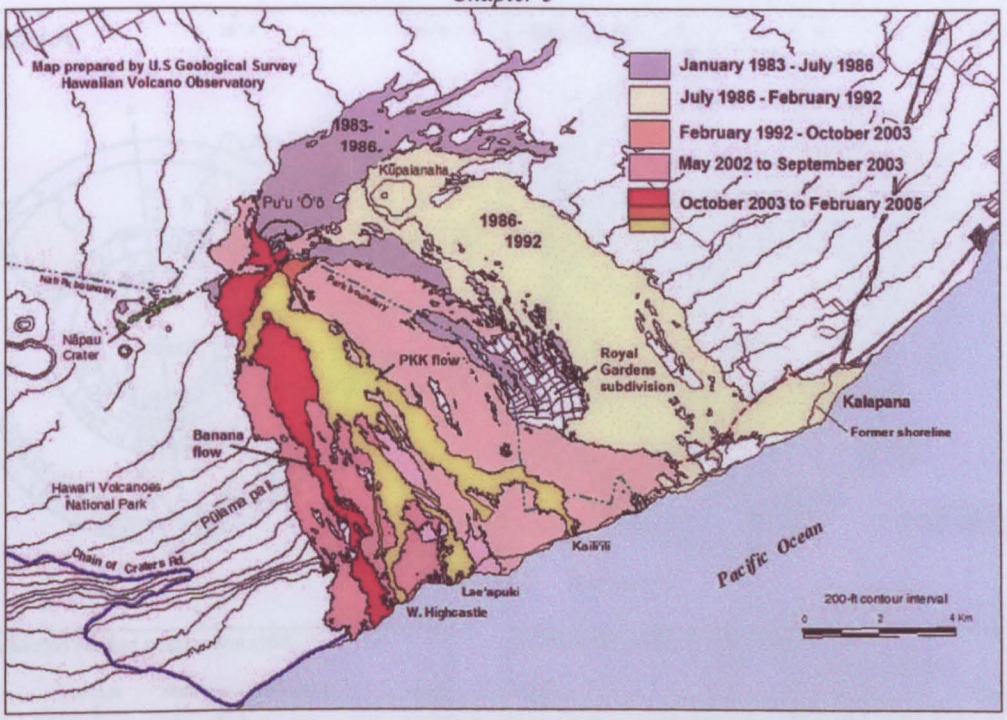

Figure 5.18. Map of the active Pu'u'O'o-Kūpaianaha flow-field, Kilauea, Hawai'i, showing the varying directions in which lava flows from the same flow-field can travel, note that white areas within the flow-field are still uncovered by lava since the eruption began n 1983. Image from HVO website.

At the next scale up, the geochemical formation scale, the volcanic architecture is not important. Here the correlations are almost plateau-wide (Figure 5.19) The geochemical formations terminate towards the edge of the DVP, with some formations being larger than others, and the southerly migration of the proposed sources has led to some overstepping of the formations (Figure 5.19, Figure 5.20 and Figure 5.1). The thicknesses of the formations appears to vary only slightly over distances of hundreds of kilometres (Devey and Lightfoot, 1986; Mitchell and Widdowson, 1991). This is the same for the sub-groups, they do not vary much in their thickness and each new sub-group occurs further south than the previous one (Figure 5.1). The final and largest sub-division of the DVP is defined by the 29R/29N palaeomagnetic reversal horizon. This occurs towards the base of the Mahabaleshwar Formation and an interpolated map of its proposed position over the DVP is seen in Figure 3.5. It is only observed in the south DVP and regionally it is not affected by the volcanic architecture.

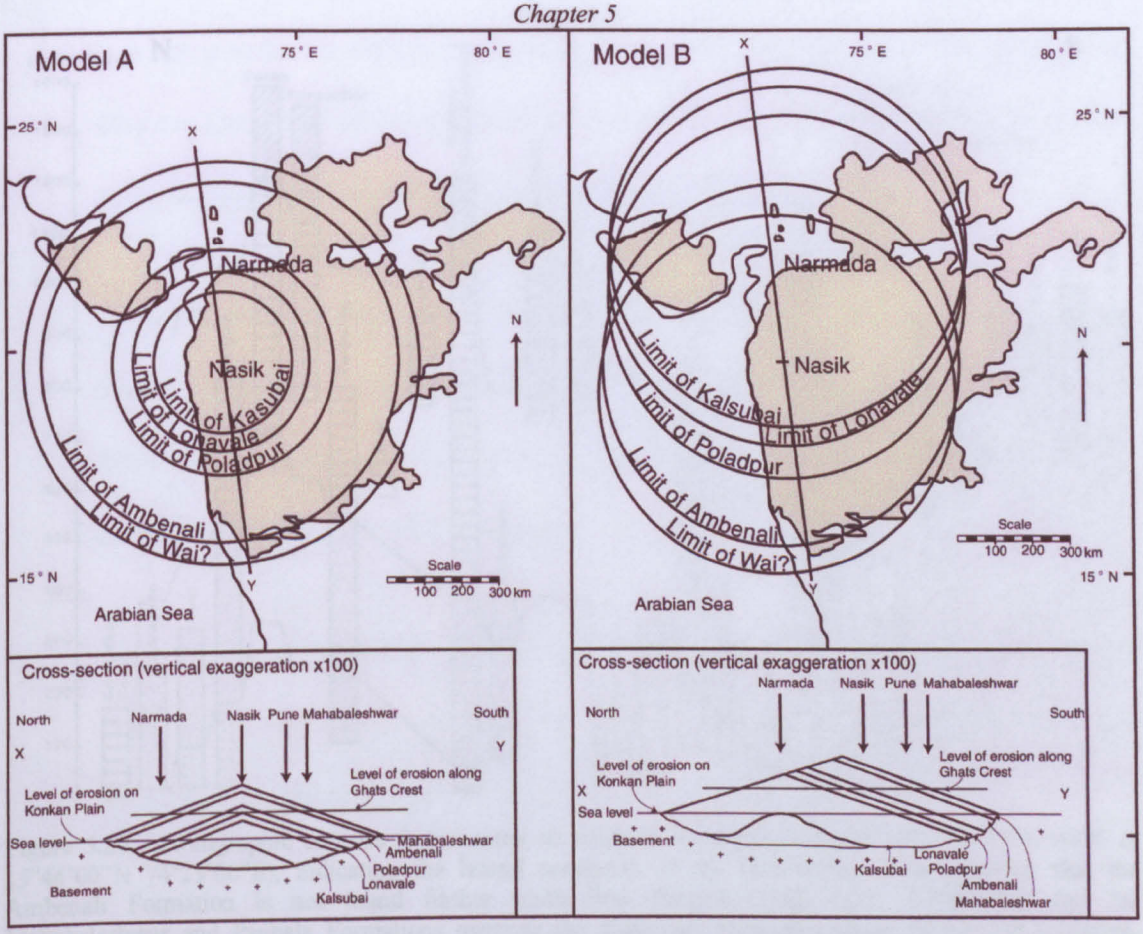

Figure 5.19 Diagrams demonstrating the two possible end-members for the distribution of formations with the development of the DVP. To the left the distribution if the mantle source and eruptive vents remain stationary relative to one another, to the right, the distribution if the eruptive vents move south relative to the movement of the mantle source. This is probably the more likely as India was moving rapidly northwards at the time of the DVP emplacement and its is observed that there is a progressive younging of units towards the south of the province. (From Mitchell and Widdowson, 1991)

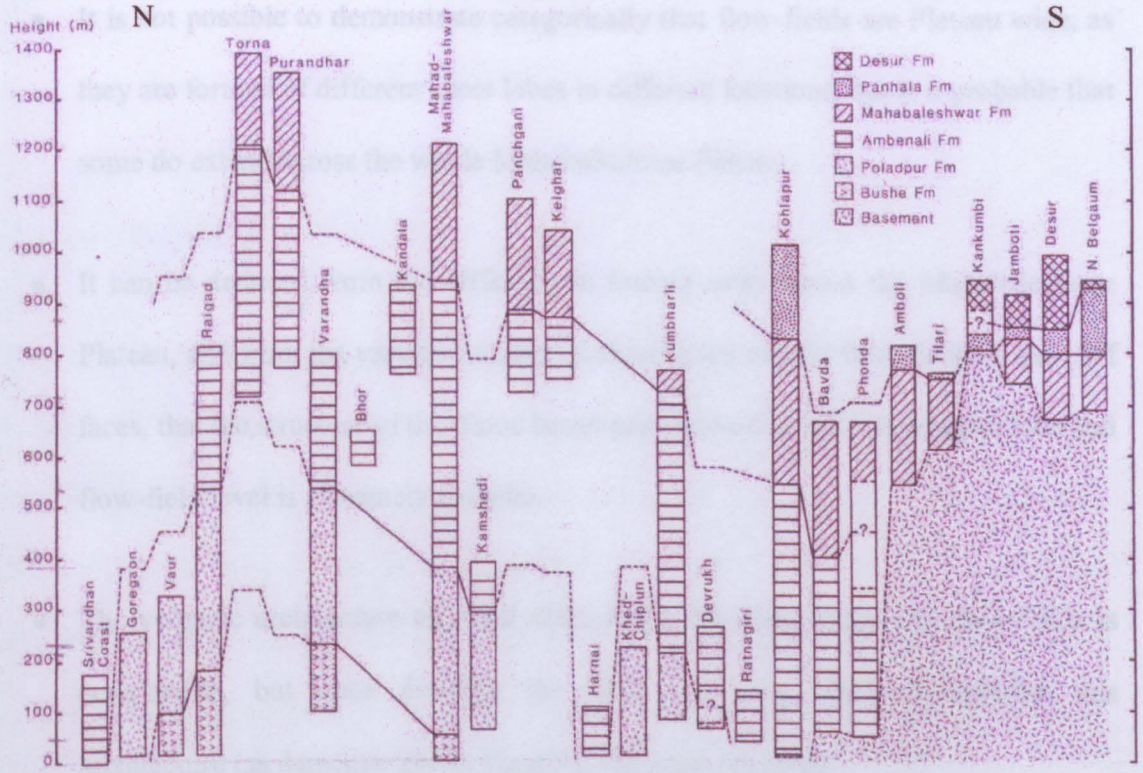

Figure 5.20. Stratigraphic sections from central to southern Western Ghats (18°13'13"N 73°12'46"E to 15°44'00"N 74°23'00"E), indicating the lateral continuity of the formations. Note however that the Ambenali Formation is not found further south than Phonda (16°23'00"N 73°49'00"E) and the Mahabaleshwar and Panhala Formations overstep the Ambenali Formation (from Devey and Lightfoot, 1986).

5.8 Conclusions

- The thickness, number of sheet flows and number of flow-fields in each formation are variable between each section studied.

- Comparing the thickness of the lava between the base of the Mahabaleshwar Fm, the palaeomagnetic reversal horizon and the laterite cap, indicates that there was as much as 95 m of topography over a distance of approximately 20 km on the active surface of the DVP.

- Euclidean distance function analysis of the composition of lava units indicates that no sheet lobe correlation can be proved between the logged sections around the Mahabaleshwar Plateau. This is probably because they are of limited lateral extent.

- It is not possible to demonstrate categorically that flow-fields are Plateau wide, as they are formed of different sheet lobes in different locations, but it is probable that some do extend across the whole Mahabaleshwar Plateau.

- It can be deduced from the difficulty in tracing units across the Mahabaleshwar Plateau, and from the varying number of sheet lobes seen in flow-fields in the cliff faces, that the structure of this flood basalt province on an individual sheet lobe and flow-field level is extremely complex.

- The volcanic architecture of small sheet lobes, big sheet lobes and flow-fields is comparable, but once dividing the DVP up using chemostratigraphy this architecture (as demonstrated in Figure 5.14) is not observed.

Chapter 6
Ancient compared with modern

6.1 Introduction

The aim of this thesis has been to investigate the volcanic architecture of the DVP (Chapter 5), but I feel that it is important to compare what I have observed in the DVP with a modern basaltic volcano. In this chapter I compare and contrast the DVP with Hawai'i (Table 6.1). Firstly, I use chemostratigraphy to suggest that Hawai'i's individual volcanoes could be seen as analogies for individual DVP formations. I then use this argument to investigate the length of time it takes individual DVP formations to form and how they interact with each other. Finally, I demonstrate that the volcanic architecture of the DVP and Hawai'i is the same but on a different scale.

	DVP	Hawai'i
Plume	Plume 'head'	Plume 'tail'
Basement	Continental lithosphere	Oceanic lithosphere
Plate speed	14 cm/yr *	10 cm/yr †
Time averaged lava emplacement rate	~1-2 km^3/yr	~0.1 km^3/yr §
Volcano slope	~0.1°	~4° ‡

Table 6.1. comparison of the 'vital statistics' of the DVP and Hawai'i. *Klootwijk and Peirce (1979), †DePaolo and Stolper (1996), ‡ Walker (1987), § Swanson (1972).

The chemostratigraphic formations of the DVP are defined by geochemical criteria (e.g., Devey and Lightfoot, 1986) (Chapter 4). Each of these formations is thought to represent the magma from a new magma chamber (Cox and Hawkesworth, 1985) where the magma may have tapped different melt from the plume, and have spent more time residing in the crust and hence had time to become more contaminated or been differentiated due to fractional crystallisation (Cox and Hawkesworth, 1985). This sourcing of a new magma chamber may have been due to the rapid movement north (approximately 14 cm a year ; Klootwijk and Peirce, 1979) of 'Greater India'. This would continually have caused the magma chamber system to be moved away from the centre of

the plume (Mitchell and Widdowson, 1991), which is the hottest part and is thought to be responsible for the surface magmatism. If the eruptive focus moved south in a series of jumps, interspersed by periods when the vent was fixed, and if each of these jumps represented the start of a new geochemical formation, then perhaps each formation could be thought of as a separate volcano. It might therefore be worthwhile to compare the lavas of the DVP with the lavas of another plume-fed volcano such as the island of Hawai'i, even if they are from different stages in a plume's development.

6.2 Chemostratigraphical comparison of DVP and Hawai'i

The island of Hawai'i is formed of five volcanoes, Kohala, Hualalai, Mauna Kea, Mauna Loa and Kilauea (Figure 6.1). Lavas from adjacent Hawaiian volcanoes have distinctive compositions (Rhodes, 1996). The best discriminants between adjacent shield volcanoes are TiO_2 and Nb correlated with Sr and Pb isotope ratios (e.g., Frey and Rhodes, 1993). Rhodes (1996) discusses the geochemical stratigraphy of the core recovered by the Hawai'i Scientific Drilling Project (~ 5 km east of Hilo, Figure 6.1), and has used the data to investigate the depth and nature of the boundary between Mauna Loa and Mauna Kea. It can be seen in Figure 6.2 that there is a distinct jump in Zr/Nb ratio (and Sr/Nb) with elevation. This represents the elevation of the Mauna Loa Mauna Kea boundary and it is similar to, and in some cases more distinct, than the Zr/Nb ratio change observed at formation boundaries in the DVP (Figure 4.4). Figure 6.3-Figure 6.7 also show graphs of isotope systems ($^{206}Pb/^{204}Pb$, $^{207}Pb/^{204}Pb$, $^{208}Pb/^{204}Pb$, $^{143}Nd/^{144}Nd$ and $^{87}Sr/^{86}Sr$) from the DVP and Hawai'i. It can be seen that the DVP systems have a much larger spread of data than the Hawaiian data and hence the spread for each DVP formation is much larger than that of the individual volcanoes of Hawai'i. The much larger spread of data for the DVP lavas is probably due to the DVP magmas having resided in the granitic continental basement and having therefore been contaminated with geochemical signatures of

continental crust, such as raised $^{87}Sr/^{86}Sr$. For example, the highest $^{87}Sr/^{86}Sr$ value for the Mauna Loa, Mauna Kea and Kilauea field in Figure 6.2 is approximately 0.70375 which is the lowest $^{87}Sr/^{86}Sr$ for the DVP lavas. Nevertheless, with the isotope systems (Figure 6.3-Figure 6.7), each volcano on the island of Hawai'i and the other Hawaiian islands can be distinguished from each other, as can be the formations of the DVP.

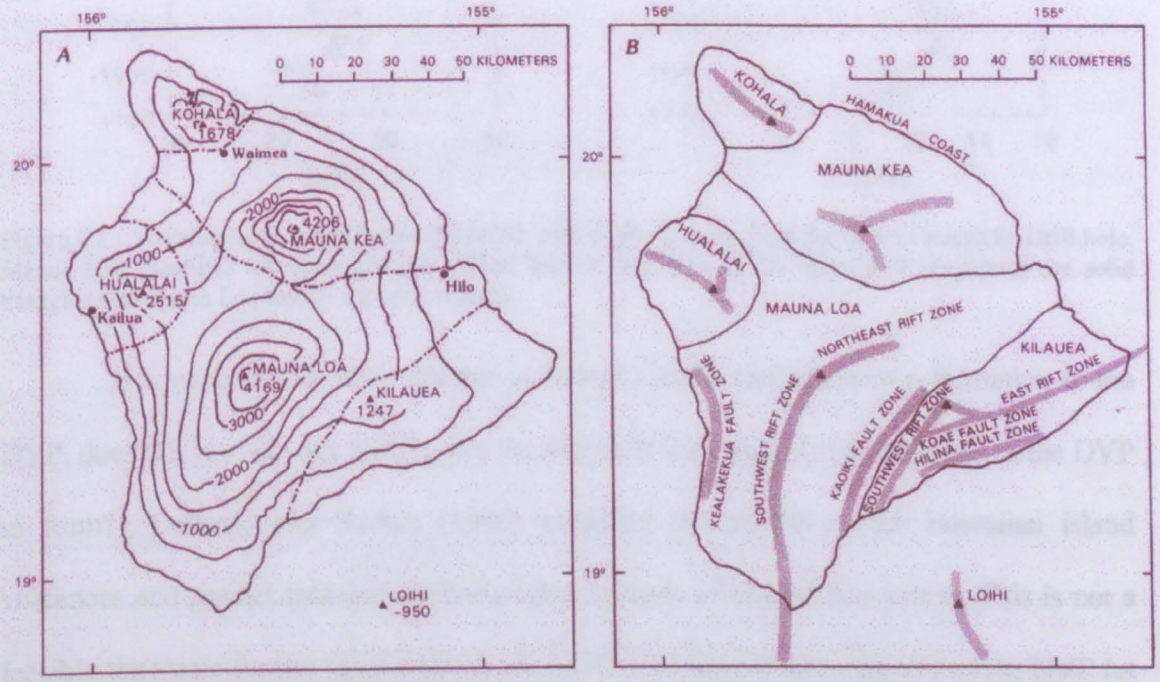

Figure 6.1. Topographic map of the Island of Hawai'i showing the boundaries between the five volcanoes which make up the island, and the position of the Loihi seamount. B, The major rift and fault zones of Hawai'i (from Peterson and Moore, 1987).

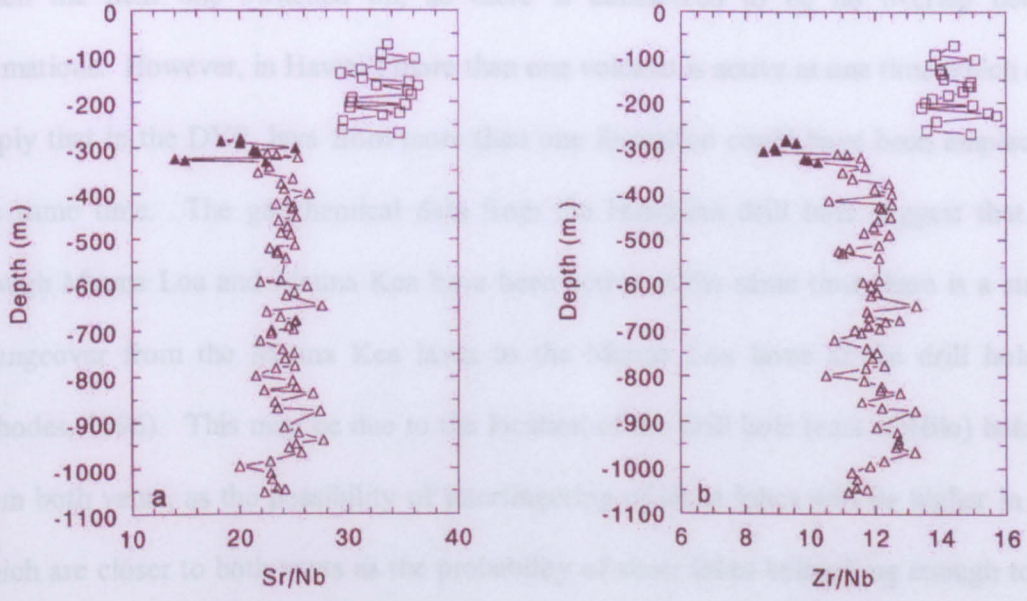

Figure 6.2. Variations of (a) Sr/Nb and (b) Zr/Nb with depth in lavas from the Hawaii scientific Drill hole. Mauna Kea tholeiites are open triangles, alkali basalts (not seen in the main DVP sequence) are solid triangles and Mauna Loa basalts are open squares.

If we accept that each volcano in Hawai'i is the equivalent of a formation in the DVP, does this provide any insight into the length of time taken for a formation in the DVP to form? DePaolo and Stolper (1996) modelled the growth of the Hawaiian island volcanoes and predict that each volcano has a lifetime of one million years. This is not a feasible timescale for the emplacement of a DVP formation as the majority of the DVP (at least eight formations) was erupted in chron 29R which is only 833,000 years long (Cande and Kent, 1995). Nine of the twelve formations in the MDP were erupted during chron 29R providing an average of one formation every 92,500 years. It is not surprising, however, that the lifetime of a Hawaiian volcano is much longer than that of a DVP formation as the DVP was formed from a plume 'head' which is capable of producing a much larger volume of magma more quickly than the plume 'tail' which feeds Hawai'i.

Studies of Hawaiian lavas and volcanoes may provide an insight into the boundary between formations. For instance do sheet lobes interdigitate or is there a single surface where one formation starts and the next one stops? In the DVP it has often been assumed that the magma system feeding one formation switched off at or before the time

when the next one switched on, so there is considered to be no overlap between formations. However, in Hawai'i more than one volcano is active at one time which could imply that in the DVP, lava from more than one formation could have been emplaced at the same time. The geochemical data from the Hawaiian drill hole suggest that even though Mauna Loa and Mauna Kea have been active at the same time there is a straight changeover from the Mauna Kea lavas to the Mauna Loa lavas at the drill hole site (Rhodes, 1996). This may be due to the location of the drill hole (east of Hilo) being far from both vents, as the possibility of interfingering of sheet lobes will be higher in areas which are closer to both vents as the probability of sheet lobes being long enough to abut the adjacent volcano increases. DePaolo and Stolper (1996) model the amount of interfingering between Mauna Loa and Mauna Kea and predict only a 200 m wide zone of interfingering between the two volcanoes. This figure of 200 m is for a Hawaiian-sized volcano with an average slope in the order of 4°. In the DVP the slope of the volcanic edifice is thought to be 0.1° so the zone of interdigitation has the possibility of being much larger although the width of this zone is probably also dependent on the length of time that both formations are being emplaced. If 'Greater India' was moving northwards at 14 cm/year (Klootwijk and Peirce, 1979) and Hawai'i is currently moving northwest wards at 10 cm/year (DePaolo and Stolper, 1996), the 4 cm/yr difference between the two may be enough to cause much less overlap in the emplacement of lava from two different DVP formations, as the magma systems may be cut off from their source more quickly.

Further investigations into the possibility that the formations of the DVP are equivalent to the volcanoes that make up the island of Hawai'i would make an interesting study and may provide further insight into the development of LIPs, but unfortunately it is beyond the scope of this study.

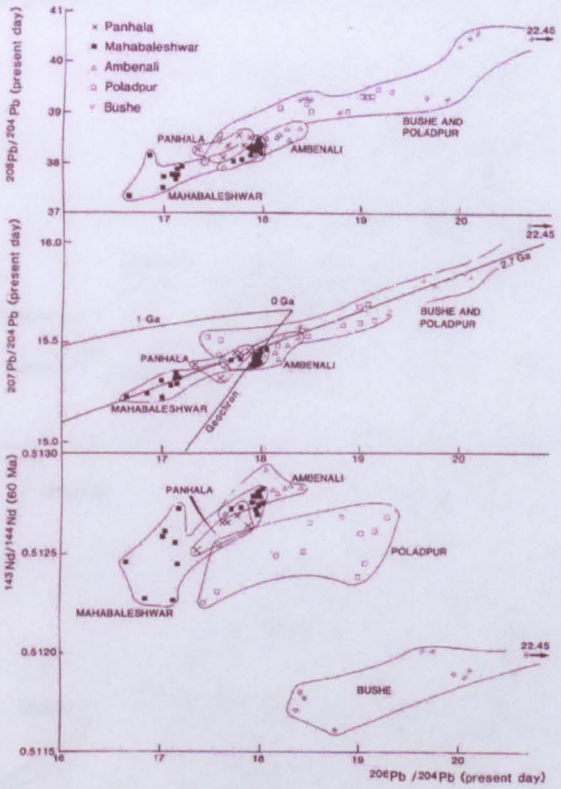

Figure 6.3. Pb- and Nd-isotope variations in the DVP basalts of the Bushe Formation and the Wai Sub-group (from Lightfoot and Hawkesworth, 1988).

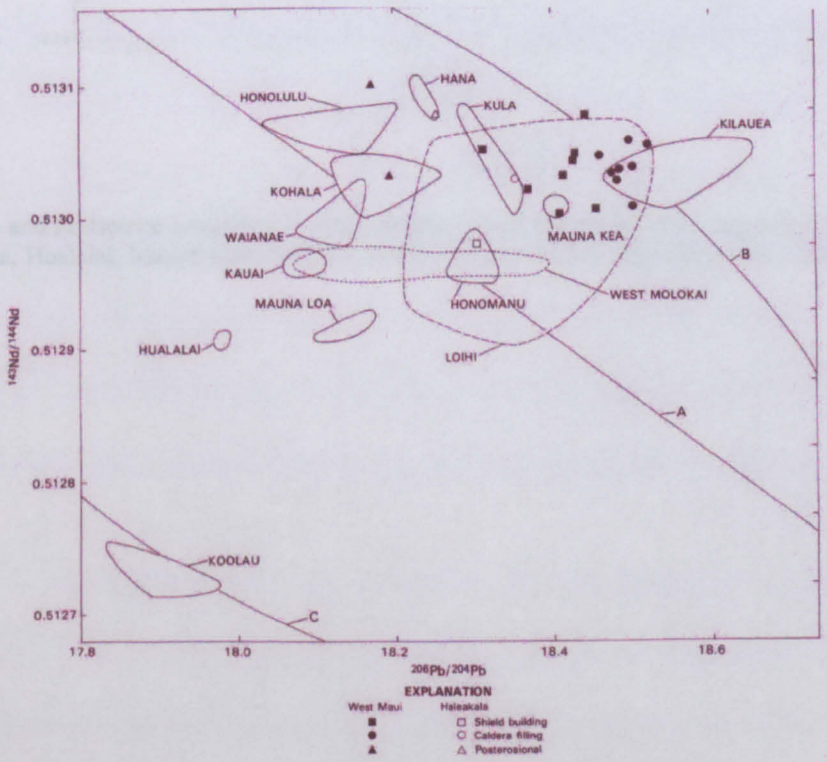

Figure 6.4. Pb- Nd- isotope variations for the Hawaiian island volcanoes. The volcanoes of the island of Hawai'i, Kohala, Hualalai, Mauna Kea, Mauna Loa and Kilauea all plot separately (from Tatsumoto et al., 1987)

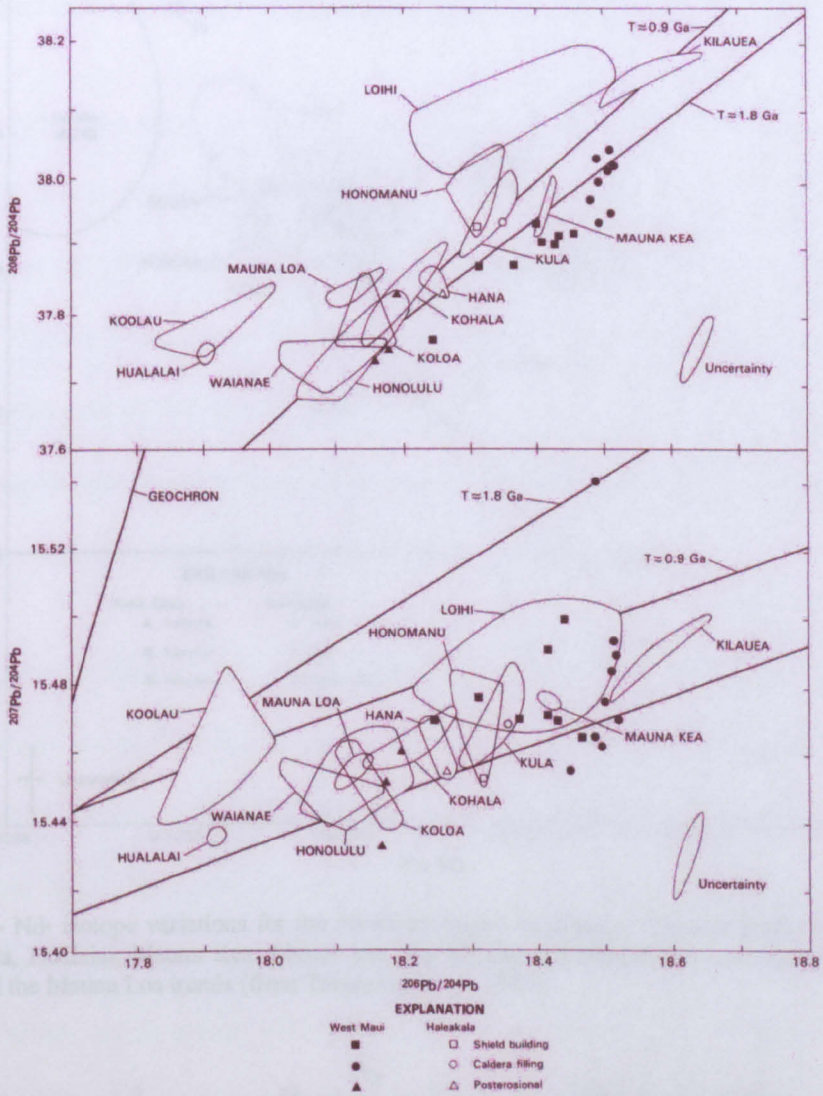

Figure 6.5. Pb- and Pb-isotope variations for the Hawaiian island volcanoes. The volcanoes of the island of Hawai'i, Kohala, Hualalai, Mauna Kea, Mauna Loa and Kilauea all plot separately (from Tatsumoto et al., 1987)

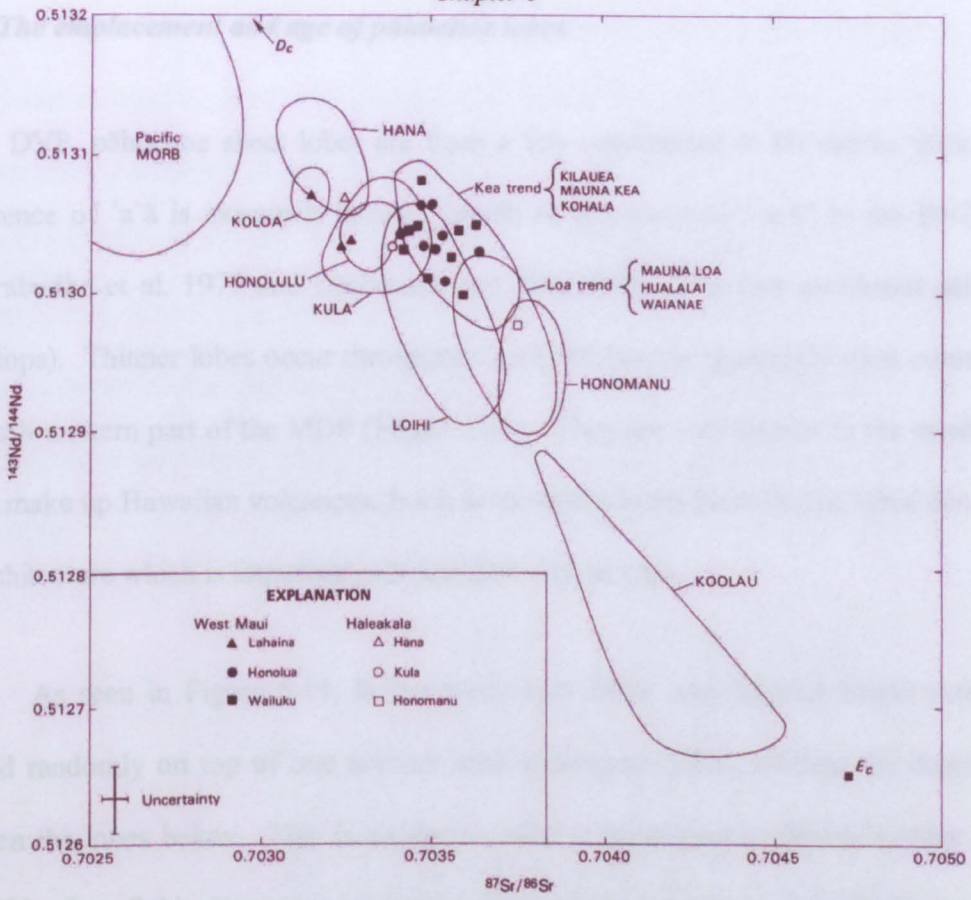

Figure 6.6. Sr- Nd- isotope variations for the Hawaiian island volcanoes. The volcanoes of the island of Hawai'i, Kohala, Hualalai, Mauna Kea, Mauna Loa and Kilauea are plotted into two separate groups, the Mauna Kea and the Mauna Loa trends (from Tatsumoto et al., 1987)

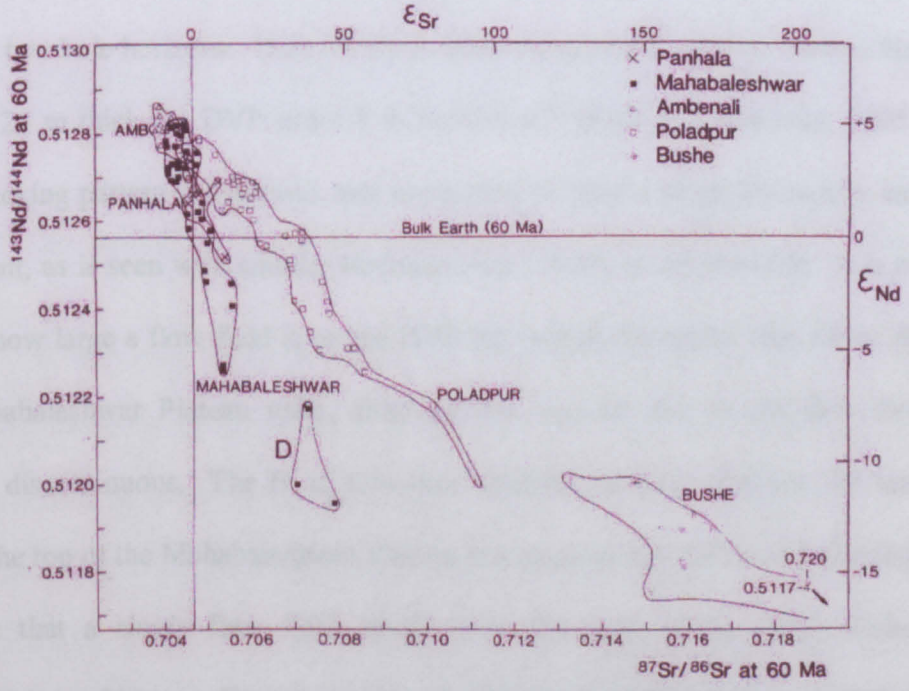

Figure 6.7. Sr- and Nd- isotope variations in DVP basalts from the Bushe Formation, the Desur Formations (D) and the Wai Sub-group (from Lightfoot and Hawkesworth, 1988).

6.3 *The emplacement and age of pāhoehoe lobes*

In the DVP, pāhoehoe sheet lobes are from a few centimetres to 60 metres thick. The occurrence of ʻaʻā is extremely limited (much of the reported "ʻaʻā" in the DVP, e.g., Sahasrabudhe et al. 1977 and Deshmukh and Pal (1984), is in fact weathered pāhoehoe sheet tops). Thinner lobes occur throughout the DVP but are apparently most common in the north western part of the MDP (Figure 2.12). They are very similar to the small lobes which make up Hawaiian volcanoes, but it is the relationship between the lobes that forms the architecture which is important, not just their size or type.

As seen in Figure 5.14, in the study area lobes with limited lateral extent are stacked randomly on top of one another with subsequent lobes infilling the depressions between the lobes below. This is similar to what is happening on Hawai'i today on the Pu'u' O'o flow field. However, identifying flow fields in regions of the DVP dominated by small lobes has proved difficult and had not been attempted before this study. It has been easier further south where it is proposed that a flow field is the package of lavas between two bole horizons. Here the sheet lobes are generally thicker than on Hawai'i, on average 20 m thick for DVP and 1.1 m for Hawai'i (Katz and Cashman, 2003), but the same stacking pattern is observed, and attempting to trace a single sheet lobe laterally for any extent, as is seen with smaller Hawaiian sized lobes, is not possible. It is not known exactly how large a flow field is on the DVP but it does not appear that all the flow fields are Mahabaleshwar Plateau wide, although this may be due to the flow fields being laterally discontinuous. The Pu'u' O'o flow field has an area of about 140 km^2 and the area of the top of the Mahabaleshwar Plateau is a maximum of 150 km^2 indicating that it is probable that a single flow field could cover the area of the upper surface of the Mahabaleshwar Plateau. By comparison, Bondre at al. (2004) provide a map which may give some insight into the lateral extent of individual flow fields. The map (Figure 6.8)

shows the extent of the Bhimashankar Formation which, from its extent and shape, S. Self (pers. comm.) suggests it may be a single flow field. On the Matheran Ghat traverse the Bhimashankar Formation is only 20 m thick, formed of either one or two sheet lobes, and bounded at the base by a bole, but the upper surface is obscured by poor exposure (Appendix A7). The Formation is approximately 100 km wide and may be an indication of the lateral extent of flow fields in the DVP, i.e., an order of magnitude wider than those occurring today on Hawai'i (the Pu'u' O'o flow field is currently only eight km wide Figure 5.18).

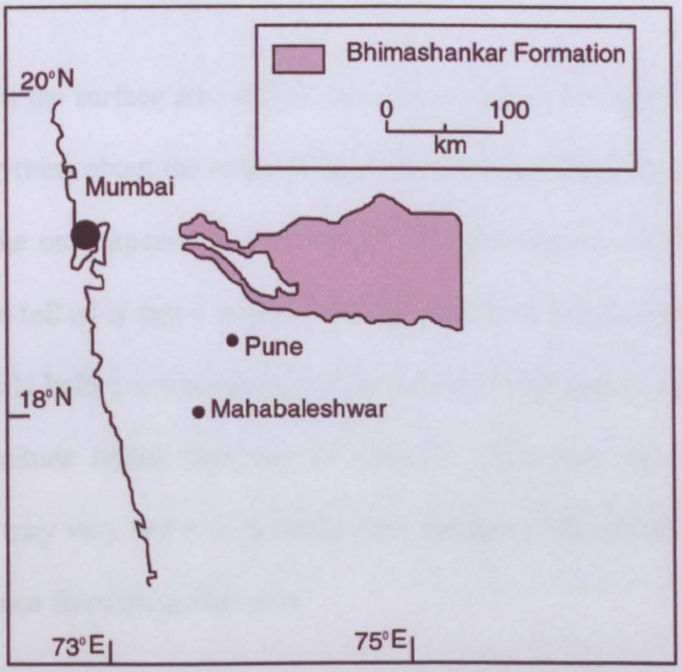

Figure 6.8. Map showing the mapped extent of the Bhimashankar Formation in the DVP (after Bondre et al., 2004).

If it were possible to strip away the layers of the DVP to look at a surface onto which lavas were being emplaced it is probable that the overall pattern of flow fields would look similar to the current surface of Kilauea, Hawai'i (Figure 6.9). It would be possible to map out individual flow fields which would form the topography observed on the surface of the DVP. New eruptions would successively resurface the DVP edifice, as is gradually occurring on Kilauea today. In fact, possibly the biggest difference in the volcanic architecture of the DVP compared to Kilauea (besides the time scale) is the

steeper gradient of the Kilauean edifice. However, if it were possible to see a section through Kilauea and remove the dip of the edifice the volcanic architecture would probably resemble Figure 5.15 with sheet lobes and flow fields being emplaced on top of units that have a variety of different ages. This results in younger units at an apparent stratigraphically lower position than older units above or adjacent to them, and therefore limits the ability to trace units laterally. The biggest limitation to tracing sheet lobes is the patchiness of the natural exposure, which while there is averagely good exposure in the study area, is insufficient to trace individual flow fields even with the detailed information available in this study.

The majority of the surface area of Kilauea (Figure 6.9) is less than 10,000 years old. Can this tell us anything about the range of ages of units exposed on an active surface of the DVP, such as the one exposed at the 29R/29N palaeomagnetic reversal horizon? Unfortunately, all it can tell us is that it is probable that the oldest units exposed would be less than 10,000 years old before it was covered in lava as the DVP had an eruption rate at least an order of magnitude higher than that of Hawai'i. However, the rate at which surfaces were covered may vary and it is probable that the age of the oldest lava exposed will increase with distance from the active vent.

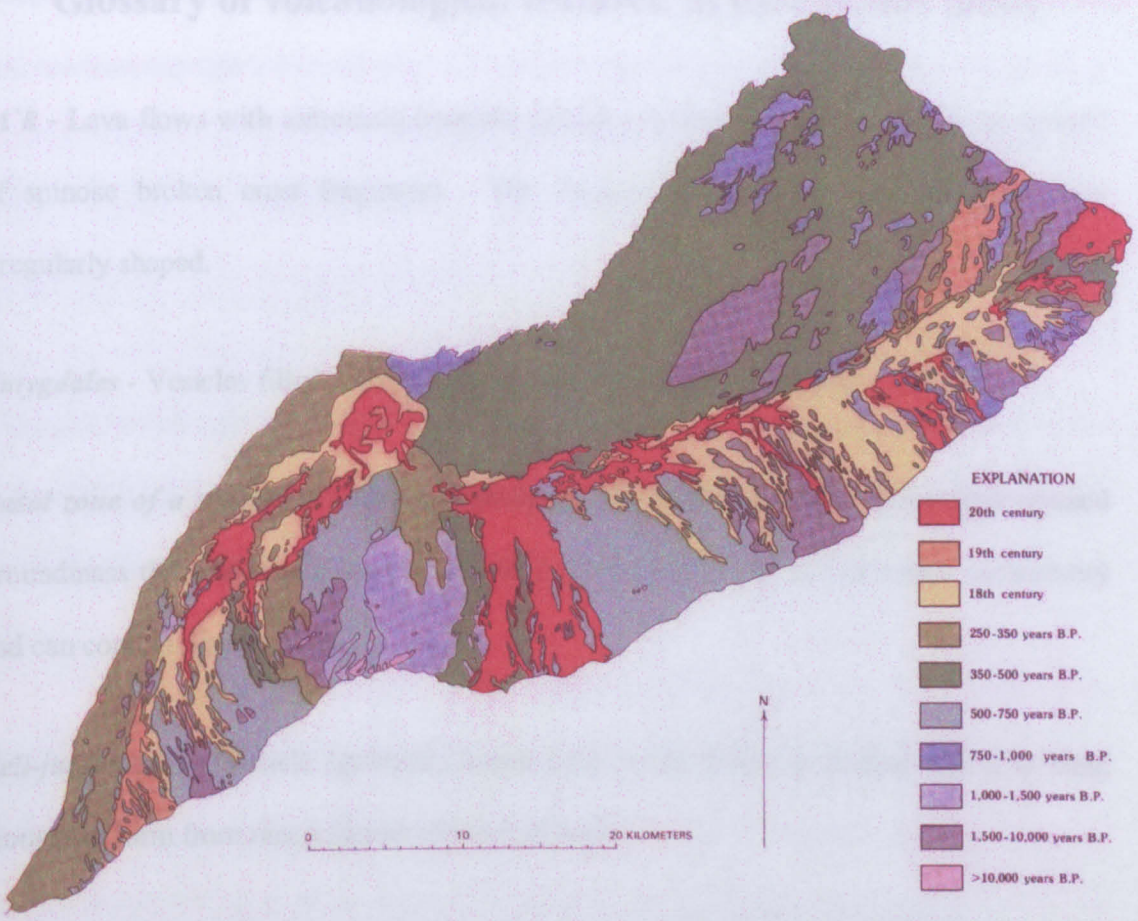

Figure 6.9. Stratigraphic map of Kilauea; some individual flow fields from the 20th, 19th and 18th centuries can be distinguished. It is probable that if it were possible to map the DVP in this way that it would resemble this type of flow-field distribution, but on a larger scale (from Holcomb, 1987).

The complexities demonstrated in this chapter and in this thesis should always be borne in mind in future investigations of LIPS. The volcanic architecture is extremely complicated, the lateral extent of sheet lobes, lava flows, flow-fields and the amount of exposure, is limited, and the lava unit stratigraphy on a small scale, i.e., on a scale smaller than geochemical formations, is highly complex.

Glossary of volcanological features, as used in this thesis

'A`ā - Lava flows with extremely irregular clinkery surface, covered in a crust composed of spinose broken crust fragments. The vesicles in the core are characteristically irregularly shaped.

Amygdales - Vesicles filled with secondary minerals e.g., calcite, quartz, zeolites.

Basal zone of a sheet lobe - Has a quenched glassy rind and usually has a finer grained groundmass than the lobe core, forms ≤ 10% of the sheet lobe; has moderate vesicularity and can contain pipe vesicles.

Bell-jar vesicles - Vesicle (generally larger than 5 cm) which is deeper than it is long, thought to form from rising diapirs of residual melt.

Bole - The upper section of a weathering profile, or altered pyroclastic material, usually red in colour sometimes green. Probably originally a soil.

CFB – Continental flood basalt

Columnar joints - Parallel prismatic joints, polygonal in cross section, formed as a result of contraction during the cooling of, commonly, a lava flow. Can be centimetres to a few metres in diameter, but normally more than 50 cm, and form perpendicular to a cooling surface.

Colonnade - A very well-formed set of columnar joints.

Compound flows - Multiple lobes visible in an exposure. The original description from Walker (1972) is; 'lavas which are divisible into flow units, commonly having a shield like form'.

Core of a sheet lobe - Form 40-60% of a sheet lobe, characteristically is poorly vesicular and contains segregation features.

CRG – Columbia River group.

DVP – Deccan volcanic province.

Flow field - The aggregate product of a single eruption or vent built up of one or more lava flows. However in locations may appear to be formed from a single sheet lobe. In this work, field recognition of flow fields is taken to be the lava unit or units between two boles.

Flow lobe - An individual unit of lava which is bounded top and bottom by a glassy rind or selvage.

Gas blisters - A void which is considerably longer than it is deep, usually found within the upper crustal zone of a sheet lobe.

GPB - Giant plagioclase basalt, a basalt with plagioclase phenocryst over 1 cm in length.

Hackly joints - Semi-vertical columnar joints with an irregular habit, caused by water-induced cooling.

Horizontal vesicular sheet (HVS) - The horizontal portion of segregation features formed when the rising residuum (in the vesicle cylinders) in a cooling and crystallising lava encounters the base of the upper crustal zone. They are often 1-5 cm thick and have 10-cm scale irregularities reflecting the uneven base of the upper crustal zone, also called segregation veins.

Horizontal vesicular zone (HVZ) - Formed within the upper crustal zone from bubbles which rise out of the lava. The bubbles are often in layers of similar sizes and their concentration tends to decrease, but size increase towards the base of the upper crustal zone.

Inflation - The process by which pāhoehoe units increase in size. The upper surface of a lava toe cools almost immediately on formation to form a brittle crust. Below this is a visco-elastic crust which retains the incoming lava and causes the toe to inflate like a balloon.

Kipuka - A island of land surrounded by younger lava.

Lava flow - The product of a single outpouring of lava.

Lava tube - A hollow space beneath a surface of solidified lava, formed by the draining of the interior liquid lava after the solidification of the crust.

Levees - Margins of a lava flow raised above the level of the channel; built up of solidified lava along the edges of a lava channel.

MDP – Main Deccan province

Mega vesicle - Vesicle in the core of a sheet lobe, which is over 15 cm long and is longer than it is deep.

Pāhoehoe - Lava or sheet lobe with a smooth continuous surface, sometimes folded into ropes. The lobes usually contain round or oval vesicles and are usually formed by inflation.

P-type pāhoehoe - Containing pipe vesicles, these have denser interiors than S-type pāhoehoe and more vesicular exteriors. Most lobes formed by inflation are typical P-type pāhoehoe even if they do not contain pipe vesicles.

Perpendicular joints - Secondary joints which form at right angles to the main joint set. Probably due to water flowing down the main joints.

Pipe vesicles - Small near-vertical vesicles commonly less than 10 cm long and 1 cm wide which form in the basal crust of a lava lobe.

Precursor lobes - Small pāhoehoe lobes which are emplaced before the main sheet lobe.

S-type pāhoehoe - Or 'spongy' pāhoehoe, describes pāhoehoe lobes which have spherical vesicles distributed throughout but have a higher concentration in the core. They form with minimal inflation.

Segregation features - General term for features formed by the residuum created during the crystallisation of a lava body, commonly highly silicic and rich in volatiles and incompatible elements.

Sheet flow lobe, (shortened to sheet lobe) - a large flow lobe, bigger than an outcrop.

Simple flow - A single lava unit (sheet lobe) which in outcrop cannot be divided into smaller units.

Tumuli (singular tumulus) - Positive topographic features found on hummocky pāhoehoe lava flow-fields. They form whale-back shaped mounds 1-10 m high and are deeply gashed by axial to radial gaping clefts. They are formed when basaltic lava flowing through lava tubes is blocked and as the pressure increases the upper crustal zone of the pāhoehoe sheet lobe is pushed up.

Upper crustal zone - The upper part of a sheet lobe with a quenched glassy rind. It comprises 40-50% of the total flow-lobe thickness and has high vesicularity, which decreases down into the flow with a corresponding increase in vesicle size.

Vesicle cylinder (VC) - Vertical columns of residual vesicular material (more evolved than the host) formed during the crystallisation of a lava unit. Forms part of segregation features.

War bonnet structure - Columnar joints radiating from a central mass.

Weathering profile - The section of a unit which has been altered by weathering before being covered with lava. The upper portion of the profile is usually red or green and is often capped by a bole, but this may be absent. The degree of weathering decreases down into the lava unit to solid but altered rock.

Bibliography

Acocella, V. and Neri, M., 2003. What makes flank eruptions? The 2001 Etna eruption and its possible triggering mechanisms. Bulletin of Volcanology.

Agashe, L.E. and Gupte, R.B., 1972. Mode of eruption of the Deccan Trap Basalts. Bulletin of Volcanologique, 55(30): 591-601.

Ali, J., R., Thompson Gary, M., Xieyan, S. and Yunliang, W., 2002. Emeishan basalts (SW China) and the 'end-Guadalupian' crisis: magnetobiostratigraphic constraints. Journal of the Geological Society, 159: 21-29.

Allegre, C.J., Birck, J.L., Capmas, F. and Courtillot, V., 1999. Age of the Deccan traps using ^{187}Re-^{187}Os systematics. Earth and Planetary Science Letters, 170: 197-204.

Allegre, C.J., Dupre, B., Richard, P., Rousseau, D. and Brooks, C., 1982. Subcontinental verses suboceanic mantle; II, Nd-Sr-Pb isotopic comparison of continental tholeiites with mid-ocean ridge tholeiites, and the structure of the continental lithosphere. Earth and Planetary Science Letters, 57(25-34).

Anderson, S.W., Stofan, E.R., Smrekar, S.E., Guest, J.E. and Wood, B., 1999. Pulsed inflation of pahoehoe lava flows; implications for flood basalt emplacement. Earth and Planetary Science Letters, 168(1-2): 7-18.

Arndt, N.T. and Christensen, U., 1992. Role of lithospheric mantle in continental volcanism: thermal and geochemical constraints. Journal of Geophysical Research, 97: 10967-10981.

Aubele, J.C., Crumpler, L.S. and Elston, W.E., 1988. Vesicle zonation and vertical structure of basalt flows. Journal of Volcanology and Geothermal Research, 35(4): 349-374.

Baksi, A., K., Byerly, G., R., Chan, L.-H. and Farrar, E., 1994. Intracanyon flows in the Deccan province, India? Case history of the Rajahmundry Traps. Geology, 22: 605-608.

Baloga, S.M. and Glaze, L.S., 2003. Pahoehoe transport as a correlated random walk. Journal of Geophysical Research, B, Solid Earth and Planets, 108(1): 10.1029/2001JB001739.

Bates, R.L. and Jackson, J.A., 1984. Dictionary of geological terms. American Geological Institute, 571 pp.

Bates, R.L. and Jackson, J.A., 1987. Glossary of geology. American Geological Institute, Alexandria, VA.

Beane, J.E., 1988. Flow stratigraphy, chemical variation and petrogenesis of Deccan flood basalts from the Western Ghats, India, Washington State University, Pullman, 576 pp.

Beane, J.E., Turner, C.A., Hooper, P.R., Subbarao, K.V. and Walsh, J.N., 1986. Stratigraphy, composition and form of the Deccan Basalts, Western Ghats, India. Bulletin of Volcanology, 48(1): 61-83.

Beane, J.E., Turner, C.A., Hooper, P.R., Subbarao, K.V., Walsh, J.N. and Beckinsale, R.D., 1983. A Preliminary Stratigraphy of Basalt Flows of Part of the Western Ghat, Deccan, India, IAVCEI, Hamburg, pp. 92.

Berner, R.A., 2001. GEOCARB III: a revised model of atmospheric CO_2 over Phanerozoic time. American Journal of science, 301(2): 182-204.

Besse, J. and Courtillot, V., 2002. Apparent and true polar wander and the geometry of the geomagnetic field over the last 200 Myr. Journal of Geophysical Research (Solid Earth), 107.

Bijwaard, H. and Spakman, W., 1998. Tomographic evidence for a narrow whole mantle plume below Iceland. Earth and Planetary Science Letters, 166(166): 121-126.

Bilgrami, S.Z., 1999. A reconnaissance geological map of the Eastern part of the Deccan Traps (Bidar-Nagpur). Memoir Geological Society of India, 43: 219-232.

Biswas, S.K., 1987. Regional tectonic framework, structure and evolution of the western marginal basins of India. Tectonophysics, 135: 307-327.

Bodas, M.S., Khadri, S.F.R. and Subbarao, K.V., 1988. Stratigraphy of the Jawhar and Igatpuri Formations, Western Ghats Lava Pile, India. Deccan Flood Basalts Memoir, Geological Society of India., 10: 235-252.

Bodas, M.S., Khadri, S.F.R., Subbarao, K.V., Hooper, P.R. and Walsh, J.N., 1984. Flow stratigraphy of a part of the western Deccan Basalt Province - a preliminary study. In: B. Bhaskar Rao (Editor), Indian Geological Congress. Proceedings of the fifth session I G C. Indian Geological Congress, Bombay, pp. 399.

Bondre, N.R., Dole, G., Phadnis, V.M., Duraiswami, R.A. and Kale, V.S., 2000. Inflation pahoehoe lavas from the Sangmner area of the western Deccan Volcanic Province. Research Communications, 78(8): 1004-1007.

Bondre, N.R., Duraiswami, R.A. and Dole, G., 2004a. A brief comparison of lava flows from the Deccan Volcanic Province and the Columbia-Oregon Plateau Flood Basalts: Implications for models of flood basalt emplacement. Proceedings of the Indian Academy of Science (Earth and Planetary Science), 113(4): 809-817.

Bondre, N.R., Duraiswami, R.A. and Dole, G., 2004b. Morphology and emplacement of flows from the Deccan Volcanic Province. Bulletin of Volcanology, 66(1): 29-45.

Buecker, C.J., Cashman, K.V. and Planke, S., 1998. Physical and magnetic characterization of aa and pahoehoe flows; Hole 990A. In: H.-C. Larsen et al. (Editors), Proceedings of the Ocean Drilling Program; scientific results, Southeast Greenland margin; covering Leg 163 of the cruises of the drilling vessel JOIDES Resolution, Reykjavik, Iceland, to Halifax, Nova Scotia, sites 988-990, 3 September-7 October 1995 Proceedings of the Ocean Drilling Program, Scientific Results 163 (199908). Texas A & M University, Ocean Drilling Program, College Station, TX, pp. 41-49.

Burke, K. and Dewey, J.F., 1973. Plume-generated triple junctions: key indicators in applying plate tectonics to old rocks. Journal of Geology, 81(4): 406-433.

Burkhard, D.J.M., 2002. Thermal interaction between lava lobes. Bulletin of Volcanology.

Butler, R., 1992. Paleomagnetism: Magnetic Domains to Geologic Terranes. Blackwell Science, Boston, 319 pp.

Byrnes, J.M. and Crown, D.A., 1999b. Relationships between pahoehoe surface units, topography, and lava tubes at Mauna Ulu, Kilauea Volcano, Hawaii. Journal of Geophysical Research, B, Solid Earth and Planets, 106(2): 2139-2151.

Caldeira, K. and Rampino, M.R., 1990a. Carbon dioxide emissions from Deccan volcanism and a K/T Boundary greenhouse effect. Geophysical Research Letters, 19(9): 1299-1302.

Caldeira, K. and Rampino, M.R., 1990b. Deccan volcanism, greenhouse warming, and the Cretaceous/Tertiary boundary. Geological Society of America special paper, 247: 117-123.

Caldeira, K., Rampino, M.R., Volk, T. and Zachos, J.C., 1990. Biogeochemical modeling at mass extinction boundaries: atmospheric carbon dioxide and ocean alkalinity at the K/T boundary. In: E. Kauffman, G. and O. Walliser, H. (Editors), Lecture notes in Earth sciences. Springer-Verlag, pp. 333-345.

Caldeira, K.G. and Rampino, M.R., 1989. The Deccan Traps and atmospheric CO (sub 2). Continental magmatism; abstracts Bulletin - New Mexico Bureau of Mines & Mineral, Resources: 36.

Camp, V.E. and Ross, M.E., 2003. Genesis of flood basalt and Basin and Range volcanic rocks from Steens Mountain to the Malhewr River gorge region. Geological Society of America Bulletin, 115(1): 105-128.

Campbell, I.H., 1998. The mantle's chemical structure: insights from the melting products of mantle plumes. In: I.N.S. Jackson (Editor), The Earth's Mantle: Composition, Structure and Evolution. Cambridge University Press, New York, pp. 259-310.

Campbell, I.H. and Griffiths, R.W., 1990. Implications of mantel plume structure for the evolution of flood basalts. Earth and Planetary Science Letters, 99: 79-93.

Campbell, I.H., Griffiths, R.W. and Hill, R.I., 1989. Melting in an Archean mantle plume: heads it's basalt, tails it's Komatiites. Nature, 339: 697-699.

Cande, S.C. and Kent, D.V., 1995. Revised calibration of the geomagnetic polarity timescale for the Late Cretaceous and Cenozoic. Journal of Geophysical Research, 100: 6093-6095.

Cas, R., Self, S. and Beresford, S., 1999. The behaviour of the fronts of komatiite lavas in medial to distal settings. Earth and Planetary Science Letters, 172(1-2): 127-139.

Cashman, K.V. and Kauahikaua, J.P., 1997. Re-evaluation of vesicle distributions in basaltic lava flows. Geology, 25(5): 419-422.

Cashman, K.V., Thornber, C., R. and Kauahikaua, J.P., 1999. Cooling and crystallization of lava in open channels, and the transition of pahoehoe lava to 'a'a. Bulletin of Volcanology, 61(5): 306-323.

Chandrasekhar, D.V., Mishra, D.C., Poornachandra Rao, G.V.S. and Mallikharjuna, J., 2002. Gravity and magnetic signatures of volcanic plugs related to Deccan volcanism in Saurashtra, India and their physical and geochemical properties. Earth and Planetary Science Letters, 201 (2): 277-292.

Chandrasekharam, D., Mahoney, J.J., Sheth, H. and Duncan, R.A., 1999. Elemental and Nd-Sr-Pb isotope geochemistry of flows and dikes in the Tapi rift, Deccan flood basalt province, India. Journal of Geothermal Research, 93: 111-123.

Chandrasekharam, D., 2003. Deccan Flood Basalts. Memoir Geological Society of India, 53: 197-214.

Chatterjee, K.K., Gupta, A. and Deshmukh, S.S., 2001. A theoretical approach to emplacement mechanism of Deccan Flood Basalts, Geological Survey of India Special Publication, pp. 529-541.

Chitwood, L.A., 1993. Inflated basaltic lava; processes and landforms. The Speleograph, 29(5): 55-64.

Choubey, V.D., 1973. Long-distance correlation of Deccan Basalt flows, Central India. Geological Society of America Bulletin, 84: 2785-2790.

Choubey, V.D., 1974. Long-distance correlation of Deccan Basalt flows, Central India: Reply. Geological Society of America Bulletin, 85: 1008-1010.

Coffin, M.F. and Eldholm, O., 2001. Large igneous provinces: progenitors of some ophiolites? In: R.E. Ernst and K.L. Buchan (Editors), Mantle Plumes: Their identification through time. Geological Society of America, Special Paper 352: 59-70.

Cook, E.F., 1966. Palaeovolcanology. Earth Science Reviews, 1: 155-174.

Courtillot, V., 1994. Mass extinctions in the last 300 million years: One impact seven flood basalts? Israel Journal of Earth Sciences, 43: 255-266.

Courtillot, V., Besse, J., Vandamme, D., Montigny, R., Jaeger, J.J. and Cappetta, H., 1986. Deccan flood basalts at the Cretaceous/Tertiary boundary? Earth and Planetary Science Letters, 80: 361-374.

Courtillot, V., Davaille, A., Besse, J. and Stock, J.M., 2003. Three distinct types of hotspots in the Earth's mantle. Earth and Planetary Science Letters, 205(3-4): 295-308.

Courtillot, V., E. and Renne, P., R., 2003. On the ages of flood basalt events. Comptes rendus geosciences, 335: 113-140.

Courtillot, V., Feraud, G., Maluski, H., Vandamme, D., Moreau, M.G. and Besse, J., 1988. Deccan flood basalts at the Cretaceous/Tertiary boundary. Nature, 333: 843-845.

Courtillot, V., Jaupart, C., Manighetti, P., Tapponnier, J. and Besse, J., 1999. On causal links between flood basalts and continental break-up. Earth and Planetary Science Letters, 166: 177-195.

Cox, K.G., 1980. A model for flood basalt vulcanism. Journal of Petrology, 21(4): 629-650.

Cox, K.G., 1989. The role of mantle plumes in the development of continental drainage patterns. Nature, 387: 888-891.

Cox, K.G. and Devey, C.W., 1987. Fractional processes in the Deccan Traps Magmas: Comments on the paper by G. Sen-Mineralogy and Petrogenesis of the Deccan trap Lava Flows around Mahabaleshwar, India. Journal of Petrology, 28: 235-238.

Cox, K.G. and Hawkesworth, C.J., 1984. Relative contribution of crust and mantle to flood basalt magmatism, Mahabaleshwar area, Deccan Traps. Philosophical Transactions of the Royal Society of London, A310: 627-641.

Cox, K.G. and Hawkesworth, C.J., 1985. Geochemical stratigraphy of the Deccan Traps at Mahabaleshwar, Western Ghats, India, with implications for open system magmatic processes. Journal of Petrology, 26(2): 355-377.

Cox, K.G. and Mitchell, C., 1988. Importance of crystal settling in the differentiation of Deccan Trap basaltic magmas. Nature, 333: 447-449.

Cripps, J.A., Widdowson, M., Spicer, R.A. and Jolley, D.W., 2002. Coastal ecosystem responses to late stage Deccan Trap volcanism; the post K-T boundary (Danian) palynofacies of Mumbai (Bombay), west India. Palaeogeography, Palaeoclimatology, Palaeoecology, 216(3-4): 303-332.

Crumpler, L.S., Aubele, J.C. and Elston, W.E., 1983. Basalt flow vertical structure and vesicle zonation. The Geological Society of America, Rocky Mountain Section, 36th annual meeting; Cordilleran Section, 79th annual meeting Abstracts with Programs - Geological Society of America, 15(5): 419.

Davies, G.F., 1988. Ocean bathymetry and mantle convection; 1, large scale flow and hotspots. Journal of Geophysical Research, 93: 10,467-10,480.

De, A., 1978. Short and long distance correlation of the Deccan trap lava flows by utilizing volcanic structures. Quarterly Journal of the Geological Mining and Metallurgical Society of India, 50: 151-162.

De, A., 1996. Entablature structure in the Deccan Trap Flows: its nature and probable mode of origin. Gondwana Geological Magazine, 2: 439-447.

DePaolo, D.J. and Stolper, E.M., 1996. Models of Hawaiian volcano growth and plume structure: Implications of results from Hawaii Scientific Drilling Project. Journal of Geophysical Research, 101(B5): 11,643-11654.

Deshmukh, S.S., 1988. Petrographic variations in compound flows of Deccan Traps and their significance. In: K.V. Subbarao (Editor), Deccan flood basalts Memoir - Geological Society of India. Geological Society of India, Bangalore.

Deshmukh, S.S. and Pal, R.N., 1984. Deccan basalt in Buldana Ghat Section, Maharashtra a geological and petrographic study. Records of the Geological Survey of India, 113(6): 52-69.

Deshmukh, S.S. and Sehgal, M.N., 1988. Mafic dyke swarms in the Deccan volcanic province of Madhya Pradesh and Maharashtra., A workshop on Deccan flood basalts, December 3-10, 1988. Geological Society of India, pp. 323-340.

Deutsch, E.R., 1959. Palaeomagnetic of the Deccan Traps. Annales de Geophysique, 15: 39-59.

Devey, C.W., 1986. Stratigraphy and Geochemistry of the Deccan Trap lava series, Western Ghats, India. D. Phil Thesis, University of Oxford, Oxford.

Devey, C.W. and Lightfoot, P.C., 1986. Volcanological and tectonic control of stratigraphy and structure in the western Deccan traps. Bulletin of Volcanology, 48(4): 195-207.

Devey, C.W. and Stephens, W.E., 1991. Tholeiitic dykes in the Seychelles and the original spatial extent of the Deccan. Journal of the Geological Society, London, 148: 979-983.

Dewey, J.F. and Burke, K., 1974. Hot spots and continental break-up: Implications for collisional Orogeny. Geology, 2(2): 57-60.

Dixon, J.E. and Stolper, E.M., 1995. An experimental study of water and carbon dioxide solubilities in mid ocean ridge basaltic liquids: part II: Applications to degassing. Journal of Petrology, 36: 1633-1646.

Duncan, R.A. and Pyle, D.G., 1988. Rapid eruption of the Deccan flood basalts at the Cretaceous/Tertiary boundary. Nature, 333: 841-843.

Duraiswami, R.A., Bondre, N., R., Dole, G. and Phadnis, V., M., 2002. Morphology and structure of flow-lobe tumuli from Pune and Dhule areas, Western Deccan Volcanic Province. Journal of the Geological Society of India, 60: 57-65.

Duraiswami, R.A., Bondre, N., R., , Dole, G., Phadnis, V., M., and Kale, V., S., 2001. Tumuli and associated features from western Deccan Volcanic Province, India. Bulletin of Volcanology, 63: 435-442.

Duraiswami, R.A., Bondre, N.R. and Dole, G., 2004. Possible lava tube system in a hummocky lava flow at Daund, western Deccan Volcanic Province, India. Proceedings of the Indian Academy of Science (Earth and Planetary Science), 113(4): 819-829.

Duraiswami, R.A., Dole, G. and Bondre, N.R., 2003. Slabby pahoehoe from the western Deccan Volcanic Province: evidence for incipient pahoehoe-aa transitions. Journal of Volcanology and Geothermal Research, 121: 195-217.

Eldholm, O. and Coffin, M.F., 2000. Large Igneous Provinces and Plate Tectonics. Geophysical Monograph 121, The History and Dynamics of Global Plate Motions: 309-326.

Elliot, D.H.F., Thomas H, 2000. Physical volcanology of the Jurassic Kirkpatrick Basalt, Antarctica, Geological Society of America, 2000 annual meeting Abstracts with Programs - Geological Society of America 32, pp. 395-396.

Ernst, R.E. and Buchan, K.L., 1997. Giant radiating dyke swarms: their use in identifying pre-Mesozoic large igneous provinces and mantle plumes. In: J.J. Mahoney and M.F. Coffin (Editors), Large Igneous Provinces: Continental, Oceanic, and Planetary Flood Volcanism. American Geophysical Union, Washington.

Ernst, R.E. and Buchan, K.L., 2001. The use of mafic dyke swarms in identifying and locating mantle plumes. In: R.E. Ernst and K.L. Buchan (Editors), Mantle Plumes: Their identification through time. Geological Society of America, Special Paper, pp. 246-265.

Ernst, R.E. and Buchan, K.L., 2002. Maximum size and distribution in time and space of mantle plumes; evidence from large igneous provinces. In: K.C. Condie, D.H. Abbott and D.J. Des Marais (Editors), Superplume events in Earth history; causes and effects. Pergamon Press, Oxford, pp. 309-342.

Ernst, R.E. and Buchan, K.L., 2003. Recognizing mantle plumes in the geological record. Annual Review of Earth and Planetary Sciences, 31: 469-523.

Ernst, R.E., Buchan, K.L. and Campbell, I.H., 2005. Frontiers in large igneous province research. Lithos, 79: 271-297.

Fagents, S., A. and Greeley, R., 2001. Factors influencing lava-substrate heat transfer and implications for thermomechanical erosion. Bulletin of Volcanology, 62: 519-532.

Fedorenko, V.A., Lightfoot, P.C., Naldrett, A.J., Czamanske, G.K., Hawkesworth, C.J., Wooden, J.L. and Ebel, D.S., 1996. Petrogenesis of the flood-basalt sequence at Noril'sk, north central Siberia. International Geology Review, 38(2): 99-135.

Finnemore, S.L., Self, S. and Walker, G.P.L., 1993. Inflation features in lava flows of the Columbia River basalts. AGU 1993 fall meeting Eos, Transactions, American Geophysical Union, 74(43): 555.

Fisher, R.A., 1953. Dispersion on a sphere. Proceedings of the Royal Society, London, 217: 295-305.

Foote, R.B., 1996. The Deccan Trap and associated formations. In: S.S. Ghosh and A. Chaudhuri (Editors), Annals of Deccan Traps study and bibliography on Deccan Traps Special Publication Series - Geological Survey of India 38 (1996). Geological Survey of India, Calcutta, India, pp. 43-65.

Francis, P., 1993. Volcanoes. A planetary perspective. Clarendon Press, 443 pp.

Frey, F.A. et al., 2000. Origin and evolution of a submarine large igneous province: the Kerguelen Plateau and Broken Ridge, southern Indian Ocean. Earth and Planetary Science Letters, 176(1): 73-89.

Frey, F.A. and Rhodes, J.M., 1993. Intershield geochemical differences among Hawaiian volcanoes: implications for source compositions, melting processes and magma ascent paths. Philosophical Transactions of the Royal Society of London, 342: 121-136.

Friedman, R.C., 1998. Petrologic clues to lava flow emplacement and post-emplacement processes. Doctoral Thesis, University of Hawaii, Honolulu, HI, 260 pp.

Gerard, M. and Fritsch, E., 2003. Pers. comm.

Gibson, S., 2002. Major element heterogeneity in Archean to Recent mantle plume starting -heads. Earth and Planetary Science Letters, 195: 59-74.

Glasby, G.P. and Kunzendorf, H., 1996. Multiple factors in the origin of the Cretaceous/Tertiary boundary: The role of environmental stress and Deccan Trap volcanism. Geologische Rundschau, 85(2): 191-210.

Godbole, S.M., Rana, S.R. and Natu, S.R., 1996. Lava stratigraphy of Deccan Basalts of Western Maharashtra. Gondwana Geological Magazine, 2: 125-134.

Goff, F., 1996. Vesicle cylinders in vapor-differentiated basalt flows. Journal of Volcanology and Geothermal Research, 71(2-4): 167-185.

Golonka, J. and Bocharova, N.Y., 2000. Hotspot activity and the break-up of Pangaea. Palaeogeography, Palaeoclimatology, Palaeoecology, 161(1): 49-69.

Grattan, J., 2005. Pollution and paradigms: lessons from Icelandic volcanism for continental flood basalt studies. Lithos, 79: 343-353.

Grattan, J. and Durand, M., 2003. Illness and elevated human mortality in Europe coincident with the Laki fissure eruption, Volcanic Degassing. Geological Society of London, pp. 401-414.

Greeley, R., Fagents, S. A., Harris, R. S. and Kadel, S. D., 1998. Erosion by flowing lava: Field evidence. Journal of Geophysical Research, 103(B11): 27,325-27,345.

Gregg, T., K. P. and Keszthelyi, L., 2004. The emplacement of pahoehoe toes: field observations and comparison to laboratory simulations. Bulletin of Volcanology, 66: 381-391.

Griffiths, R.W. and Campbell, I.H., 1991. Interaction of mantle plume heads with the Earth's surface and onset of small-scale convection. Journal of Geophysical Research, 96: 18295-19310.

Grossenbacher, K.A. and McDuffie, S.M., 1995. Conductive cooling of lava: Columnar joint diameter and stria width as functions of cooling rate and thermal gradient. Journal of Volcanology and Geothermal Research, 69(1-2): 95-103.

Guilbaud, M.-N., Blake, S. and Self, S., in press.

Gupta, H.K., Rastogi, B.K., Mohan, I., Rao, C.V.R.K., Sarma, S.V.S. and Rao, R.U.M., 1998. An investigation into the Latur earthquake of September 29, 1993 in southern India. Tectonophysics, 287(1-4): 299-318.

Gupte, R.B., Karmarkar, B.M., Kulkarni, S.R. and Marathe, S.S., 1974. Long-distance correlation of Deccan Basalt flows, Central India: Discussion. Geological Society of America Bulletin, 85: 1007-1008.

Hallam, A., 1987. End-Cretaceous mass extinction event: argument for terrestrial causation. Science, 238: 1237-1242.

Hansen, J.E., Lacis, A., Rind, D., Russell, G., Stone, P., Fung, I., Ruedy, R. and Lerner, J., 1984. Climate sensitivity: Analysis of feedback mechanisms. In: J.E. Hansen and T. Takahashi (Editors), Climate Processes and Climate Sensitivity. American Geophysical Union, Washington, D.C.. pp. 130-163.

Harland, W.B., Cox, A.V., Llewellyn, P.G., Pickton, C.A.G., Smith, A.G. and Walters, R., 1982. A geologic time scale. Cambridge Earth Sciences Series. Cambridge University Press, Cambridge.

Heirtzeler, J.R., Dickenson, G.O., Le Pichon, X. and Pittman W.C., 1967. Magnetic anomalies and ocean-floor spreading since Late Cretaceous. Transactions - American Geophysical Union, 48(1): 133.

Heliker, C. and Mattox, T., N., 2003. The first Two Decades of the Pu'u O'o-Kupaianaha Eruption: Chronology and selected Bibliography. In: C. Heliker, D. Swanson and T. Takahashi (Editors), The Pu'u O'o-Kupaianaha Eruption of Kilauea Volcano, Hawai'i: The first 20 Years. Unite States Geological Survey.

Herrero-Bervera, E., Canon-Tapia, E., Walker, G.P.L. and Tanaka, H., 2002. Magnetic fabrics study and inferred flow directions of lavas of the old Pali Road, O'ahu, Hawaii. Journal of Volcanology and Geothermal Research, 118: 161-171.

Ho, A., Cashman, K.V. and Reidel, S.P., 1997a. Emplacement and cooling rates in a flow of the Columbia River Basalt Group. AGU 1997 fall meeting Eos, Transactions, American Geophysical Union, 78(46): 748.

Ho, A.M., 1999. Emplacement of a large lava flow; the Ginkgo Flow of the Columbia River Basalt Group. Doctoral Thesis, University of Oregon, Eugene, OR, 188 pp.

Ho, A.M. and Cashman, K.V., 1997. Temperature constraints on the Ginkgo Flow of the Columbia River Basalt Group. Geology (Boulder), 25(5): 403-406.

Ho, A.M., Cashman, K.V. and Reidel, S.P., 1997b. Constraints on emplacement duration for Columbia River Basalt Group flows. Enriched: Geological Society of America, Cordilleran Section, 93rd annual meeting Abstracts with Programs - Geological Society of America, 29(5): 19.

Hofmann, C., Feraud, G. and Courtillot, V., 2000. $^{40}Ar/^{39}Ar$ dating of mineral separates and whole rocks from the Western Ghats lava pile: further constraints on the duration and age of the Deccan traps. Earth and Planetary Sciences letters, 180: 13-27.

Holcomb, R.T., 1987. Eruptive history and long-term behaviour of Kilauea volcano. In: R.W. Decker, T.L. Wright and P.H. Stauffer (Editors), Volcanism in Hawaii, (U.S. Geological survey Professional Paper 1350). U.S.G.S., Washington, pp. 261-350.

Holland, C.H., Audley-Charles, M.G. and Basset, M.G., 1978. A guide to stratigraphical procedure. Geological Society Special Report No. 10.

Hon, K., Kauahikaua, J., Denlinger, R. and Mackay, K., 1994. Emplacement and inflation of pahoehoe sheet flows; observations and measurements of active lava flows on Kilauea Volcano, Hawaii. Geological Society of America Bulletin, 106(3): 351-370.

Hon, K., Kauahikaua, J.P. and Mackay, K., 1993. Inflation and cooling data from pahoehoe sheet flows on Kilauea Volcano. Open-File Report - U. S. Geological Survey (1993). Reston, VA, U. S. Geological Survey.

Hon, K.A., Self, S., Thordarson, T. and Keszthelyi, L., 1995. The emplacement of flood basalts. International Union of Geodesy and Geophysics; XXI general assembly; abstracts International Union of Geodesy and Geophysics, General Assembly, 21: 436.

Hooper, P.R., 1985. A case of simple magma mixing in the Columbia River Basalt Group: The Wilbur Creek, Lapwai, and Asotin Flows, Saddle Mountains Formation. Contributions to Mineralogy and Petrology, 91: 66-73.

Hooper, P.R., 1988a. A case of simple magma mixing in the Columbia River Basalt Group; the Wilbur Creek, Lapwai, and Asotin flows, Saddle Mountains Formation. Contributions to Mineralogy and Petrology, 91(1): 66-73.

Hooper, P.R., 1988b. The Giant Plagioclase Basalts (GPBS) of the Western Ghats, Deccan Traps, India, Geological Society of India Memoir 10, pp. 135-144.

Hooper, P.R., 1997. The Columbia River Flood Basalt Province: Current status. In: J.J. Mahoney and C.M. F. (Editors), Large Igneous Provinces continental, oceanic, and planetary flood volcanism. American Geophysical Union, Washington, pp. 1-27.

Hoover, S.R., Cashman, K.V. and Manga, M., 2001. The yield strength of subliquidus basalts-experimental results. Journal of Volcanology and Geothermal Research, 107: 1-8.

http://asterweb.jpl.nasa.gov/.

http://boris.vulcanoetna.com/ETNA_maps.html, 1999.

http://www.ascscientific.com/JR5.html, 2004. ASC Scientific JR-5 / JR-5A Spinner Magnetometers. http://www.ascscientific.com/JR5.html.

HVO, http://hvo.wr.usgs.gov/kilauea/update/archive/2005/Feb/20050202_updatemap.jpg.

Ingle, S. and Coffin, M.F., 2004. Impact origin for the greater Ontong Java Plateau. Earth and Planetary Science Letters, 218: 123-134.

Jay, A.E. and Widdowson, M., in prep. A geological map of the south east Deccan Volcanic Province.

Jerram, D., Mountney, N., Holzfoerster, F. and Stollhofen, H., 1999a. Internal stratigraphic relationships in the Etendeka Group in the Huab Basin, NW Namibia; understanding the onset of flood volcanism. In: P.R. Renne, M. Ernesto and S.C. Milner (Editors), Tectonic and magmatic evolution of the Parana-Etendeka large igneous province and South Atlantic margins Journal of Geodynamics 28, no. 4-5 (199912). Pergamon Press, Oxford, United Kingdom, pp. 393-418.

Jerram, D., Mountney, N.P., Howell, J., Stollhofen, H. and Lorenz, V., 1998. Stratigraphical evolution of the Etendeka Group in the Huab Basin, Northwest Namibia. In: J. Almond et al. (Editors), Gondwana 10; event stratigraphy of Gondwana Journal of African Earth Sciences 27, no. 1A (199807). Pergamon, London-New York, International, pp. 119-120.

Jerram, D.A., Mountney, N. and Stollhofen, H., 1999b. Facies architecture of the Etjo Sandstone Formation and its interaction with the basal Etendeka Flood Basalts of Northwest Namibia; implications for offshore prospectivity. In: N.R. Cameron, R.H. Bate and V.S. Clure (Editors), The oil and gas habitats of the South Atlantic Geological Society Special Publications 153 (1999). Geological Society of London, London, United Kingdom, pp. 367-380.

Jerram, D.A. and Stollhofen, H., 2002. Lava-sediment interaction in desert settings; are all peperite-like textures the result of magma-water interaction? In: I.P. Skilling, J.D.L. White and J. McPhie (Editors), Peperite; processes and products of magma-sediment mingling Journal of Volcanology and Geothermal Research 114, no. 1-2 (20020515). Elsevier, Amsterdam, Netherlands, pp. 231-249.

Jerram, D.A., Stollhofen, H., Lorenz, V. and Milner, S.C., 1997. Pahoehoe lava flow structures and sediment/lava interaction in the basal Etendeka flood basalts of NW Namibia. AGU 1997 fall meeting Eos, Transactions, American Geophysical Union, 78(46): 748.

Jerram, D.A. and Widdowson, M., 2005. The Anatomy of Continental Flood Basalt Provinces: geological constraints on the processes and products of flood basalt volcanism. Lithos.

Jolley, D.W., 1997. Palaeosurface palynofloras of the Skye lava field and the age of the British Tertiary volcanic province. In: M. Widdowson (Editor), Palaeosurfaces: recognition, reconstruction and palaeoenvironmental interpretation. Geological Society Special Publication, London, pp. 67-94.

Jones, A.P., Price, G.D., Price, N.J., DeCarli, P.S. and Clegg, R.A., 2002. Impact induced melting and the development of large igneous provinces. Earth and Planetary Science Letters, 202: 551-561.

Kale, V.S., Kulkarni, S.R. and Peshwa, V.V., 1992. Discussion on a geological map of the southern Deccan Traps, India and its structural implications, *Journal*, Vol. 148. 1991, pp. 495-505. Journal of the Geological Society, 149: 473-478.

Kaneoka, I. and Haramura, H., 1973. K-Ar ages of successive lava flows from the Deccan Traps, India. Earth and Planetary Science Letters, 18(229-236).

Karmalkar, N.R., Soman, G.R., Duraiswami, R.A. and Phadke, A.V., 1998. Rare evidence of fissure type eruption; from the southern part of the Deccan Volcanic Province, India. Gondwana Geological Magazine, 13(1): 13-19.

Katz, M., G. and Cashman, K.V., 2003. Hawaiian lava flows in the third dimension: Identification and interpretation of pahoehoe and 'a'a distribution in the KP-1 and SOH-4 cores. Geochemistry Geophysics Geosystems, 4(2): doi:10.1029/2001GC000209.

Kauahikaua, J.P., Cashman, K.V., Mattox, T.N., Heliker, C., Hon, K., Mangan, M.T. and Thornber, C., R., 1998. Observations on basaltic lava streams in tubes from Kilauea Volcanic, Island of Hawai'i. Journal of Geophysical Research, B, Solid Earth and Planets, 103(11): 27,3003-27,323.

Kent, R.W., Storey, M. and Saunders, A.D., 1992. Large igneous provinces; sites of plume impact or plume incubation? Geology, 20(10): 891-894.

Kent, R.W., Thomson, B.A., Skelhorn, R.R., Kerr, A.C., Norry, M.J. and Walsh, J.N., 1996. Emplacement of Hebridean Tertiary flood basalts; evidence from an inflated pahoehoe lava flow on Mull, Scotland. Journal of the Geological Society of London, 155: 599-607.

Kerr, A.C., 1991. Cows and climate; sundry catastrophes. Science, 252: 1496-1497.

Kerr, A.C., 1995. Geoscientists contemplate a fatal belch and a living ocean. Science, 270(5241): 1441-1442.

Keszthelyi, L., 2000. Rubbly pahoehoe; a previously undescribed but widespread lava type transitional between aa and pahoehoe, Geological Society of America, 2000 annual meeting, 32, pp. 394.

Keszthelyi, L., 2002. Classification of the mafic lava flows from ODP Leg 183. In: Frey FA, Coffin MF, Wallace PJ and P.G. Quilty (Editors), Proceedings of the ODP, Scientific Results, pp. 1-28.

Keszthelyi, L. and Self, S., 1997. The standard way of emplacing large lavas; the SWELL hypothesis. Geological Society of America, 1997 annual meeting Abstracts with Programs - Geological Society of America, 29(6): 137.

Keszthelyi, L. and Self, S., 1998. Some physical requirements for the emplacement of long basaltic lava flows. Journal of Geophysical Research, 103(b11): 27447-27464.

Keszthelyi, L., Self, S. and Thordarson, T., 1999. Application of recent studies on the emplacement of basaltic lava flows to the Deccan Traps. In: K.V. Subbarao (Editor), Deccan volcanic province Memoir - Geological Society of India 43 (1999). Geological Society of India, Bangalore, India, pp. 485-520.

Khadkikar, A.S., Sant, D.A., Gogte, V. and Karanth, R.V., 1999. The influence of Deccan volcanism on climate: insights from lacustrine intertrappean deposits, Anjar, western India. Palaeogeography, Palaeoclimatology, Palaeoecology, 147: 141-149.

Khadri, S.F.R., Subbarao, K.V. and Bodas, M.S., 1988a. Magnetic Studies on a thick pile of Deccan Trap flows at Kalsubai. Deccan Flood Basalts Memoir, Geological Society of India., 10: 163-179.

Khadri, S.F.R., Subbarao, K.V., Hooper, P.R. and Walsh, J.N., 1988b. Stratigraphy of the Thakurvadi Formation, Western Deccan Volcanic Province. Deccan Flood Basalts Memoir, Geological Society of India., 10: 281-304.

Khadri, S.F.R., Subbarao, K.V. and Walsh, J.N., 1999a. Stratigraphy, form and structure of the east Pune basalts, western Deccan basalt province, India. In: K.V. Subbarao (Editor), Deccan Volcanic Province. Geological Survey of India, Bangalore, pp. 179-202.

Khadri, S.F.R., Walsh, J.N. and Subbarao, K.V., 1999b. Chemical and magnet-stratigraphy of Malwa Traps around Mograba region, Dhar District (M.P.). In: K.V. Subbarao (Editor), Memoir Geological Society of India. Geological Society of India, Bangalore, pp. 203-218.

Kilburn, C.R.J., 1996. Patterns and predictability in the emplacement of subaerial lava flows and flow fields. In: R. Scarpa and R.I. Tilling (Editors), Monitoring and mitigation of volcano hazards. Springer-Verlag.

Kilburn, C.R.J., 2000. Lava flows and flow fields. In: H. Sigurdsson (Editor), Encyclopedia of volcanoes. Academic Press, pp. 1417.

King, C.A.M., 1970. Feedback relationships in geomorphology. Geografiska Annaler, 52A: 147-159.

King, S.D. and Anderson, D.L., 1995. An alternative mechanism of flood basalt formation. Earth and Planetary Science Letters, 136(3-4): 269-279.

Kirschvink, J.L., 1980. The least squares line and plane and the analysis of palaeomagnetic data. Geophysical Journal of the Royal Astronomical Society, 62: 699-718.

Klootwijk, 1979. A review of palaeomagnetic data from the Indo-Pakistani fragment of Gondwanaland. In: A. Farah; and K.A. DeJong (Editors), Geodynamics of Pakistan. Geological Survey Pakistan,, Quetta, Pakistan.

Klootwijk, C.T. and Peirce, J.W., 1979. India's and Australia's pole path since the late Mesozoic and the India-Asia collision. Nature, 282: 605-607.

Knight, K.B., Renne, P.R., Halkett, A. and White, N., 2003. $^{40}Ar/^{39}Ar$ dating of the Rajahmundry traps, Eastern India and their relationship to the Deccan Traps. Earth and Planetary Science Letters, 208: 85-99.

Krishnan, M.S., 1956. Geology of India and Burma. Higginbothams, Madras.

Lange, R.A., 2002. Constraints on the preeruptive volatile concentrations in the Columbia River flood basalts. Geology, 30(2): 179-182.

Lassiter, J.C. and DePaolo, D.J., 1997. Plume/lithosphere interaction in the generation of continental and oceanic flood basalts: chemical and isotopic constraints. In: J.J. Mahoney and M.F. Coffin (Editors), Large igneous provinces; continental, oceanic, and planetary flood volcanism Geophysical Monograph 100 (1997). American Geophysical Union, Washington, DC, pp. 335-355.

Lightfoot, P.C., 1985. Isotope and trace element geochemistry of the South Deccan lavas, India., Open University, Milton Keynes.

Lightfoot, P.C. and Hawkesworth, C.J., 1988. Origin of the Deccan Trap lavas: evidence from combined trace element and Sr-, Nd- and Pb isotope studies. Earth and Planetary Science Letters, 91: 89-104.

Lightfoot, P.C., Hawkesworth, C.J., Devey, C.W., Rogers, N.W. and Van Calstren, P.W.C., 1990. Source of differentiation of Deccan Traps lavas: Implications of geochemical and mineral chemical variations. Journal of Petrology, 31: 1165-1200.

Lipman, P., W., Banks, N., G. and Rhodes, J.M., 1985. Degassing-induced crystallization of basaltic magma and effective on lava rheology. Nature, 317: 604-607.

Liu, Y.G. and Schmitt, R.A., 1996. Cretaceous Tertiary phenomena in the context of seafloor rearrangements and P(CO2) fluctuations over the past 100. Geochimica et Cosmochimica Acta, 60(6): 973-994.

Long, P.E. and Wood, B.J., 1986. Structures, textures and cooling histories of Columbia River basalt flows. Geological Society of America Bulletin, 97: 1144-1155.

Lyle, P., 2000. The eruption environment of multi-tiered columnar basalt lava flows. Journal of the Geological Society, London, 157(4): 715-722.

Macdonald, G., A., 1972. Volcanoes. Prentice Hall, New Jersey, 510 pp.

Mahoney, J.J., 1988. Deccan Traps. In: J.D. MacDougall (Editor), Continental Flood Basalts. Petrology and structural geology. Kluwer Academic Publishers, pp. 341.

Mahoney, J.J., MacDougall, J.D., Lugmair, G.W., Murali, A.V., Sankardas, M. and Gopalan, K., 1982. Origin of the Deccan Trap Flows at Mahabaleshwar inferred form Nd and Sr isotopic and chemical evidence. Earth and Planetary Science Letters, 60: 47-60.

Mahoney, J.J., Sheth, H.C., Chandrasekharam, D. and Peng, Z.X., 2000. Geochemistry of flood basalts on the Toranmal section, northern Deccan Traps, India: implications for regional Deccan stratigraphy. Journal of Petrology, 41: 1099-1120.

Manga, M., 1996. Waves of bubbles in basaltic magmas and lavas. Journal of Geophysical Research, 101(B8): 17,457-17,465.

McElhinny, M.W., 1968. Northward Drift of India-Examination of recent Palaeomagnetic Results. Nature, 217: 342-344.

McLean, D.M., 1985. Deccan traps mantle degassing in the terminal Cretaceous marine extinctions. Cretaceous Research, 6(3): 235-259.

McMillan, K., Long, P.E. and Cross, R.W., 1989. Vesiculation in Columbia River basalts. In: S.P. Reidel and P.R. Hooper (Editors), Volcanism and Tectonism in the Columbia River Flood-Basalt Province. Geological Society of America, Boulder, pp. 157-167.

Merrill, R.T., McElhinny, M.W. and McFadden, P.L., 1996. The magnetic field of the Earth: Palaeomagnetic, the core and the deep mantle. International Geophysics Series, 63. Academic Press, USA, New York, London, Toronto, 531 pp.

Misra, K.S., 2002. Arterial system of lava tubes and channels within Deccan volcanics of western India. Journal of the Geological Society of India, 59: 115-124.

Mitchell, C. and Widdowson, M., 1991. A geological map of the southern Deccan Traps, India and its structural implications. Journal of the Geological Society, 148: 495-505.

Moore, J.G., 2001. Density of basalt core from Hilo drill hole, Hawaii. Journal of Volcanology and Geothermal Research, 112: 221-230.

Morgan, J.W., Laul, J.C., Ganapathy, R. and Anders, E., 1971. Glazed lunar rocks; origin by impact. Science, 172(3983): 556-558.

Morgan, M.G., 1971a. Laboratory model for radio-star scintillation and other diffraction phenomena. Journal of Geophysical Research, 76(10): 2469-2486.

Morgan, W.J., 1971b. Convection plumes in the lower mantle. Nature (London), 230(5288): 42-43.

Morgan, W.J., 1971c. Island chains, aseismic ridges, and hot-spots. Eos, Transactions, American Geophysical Union, 52(4): 371.

Morgan, W.J., 1972. Plate Motions and Deep Mantle Convection, Studies in Earth and Space Sciences

Memoir - Geological Society of America. Geological Society of America, Boulder, pp. 7-22.

Morgan, W.J. and Loomis, T.P., 1969. Correlation coefficients and sea-floor spreading; an automated analysis of magnetic profiles. Marine Geophysical Researches, 1(3): 248-260.

Morris, W.A., 2002. The Sudbury Structure: A circular impact crater? Geophysical Research Letters, 29(20).

Murphy, M.T., Self, S. and Long, P.E., 1996. The morphology and chemical composition of distal Columbia River Basalt flows, Deschutes River canyon, Wasco & Sherman Co., Oregon. Geological Society of America, Cordilleran Section, 92nd annual meeting Abstracts with Programs - Geological Society of America, 28(5): 95.

Murphy, M.T., Self, S. and Long, P.E., 1997. The lava-flow-front morphology and textures of Columbia River Basalt. Geological Society of America, 1997 annual meeting Abstracts with Programs - Geological Society of America, 29(6): 137.

Nair, K.K.K. and Bhusari, B., 2001. Stratigraphy of the Deccan Traps : A Review, Recent Advances in the Field of Earth Sciences and their Implications in Nation. Geological Survey of India Special Publication, pp. 477-491.

Najafi, S.J., Cox, K.G. and Sukheswala, R.N., 1981. Geology and geochemistry of the basalt flows (Deccan Traps) of the Mahad-Mahabaleshwar section, India. In: K.V. Subbarao and R.N. Sukheswala (Editors), Deccan volcanism and related basalt provinces in other parts of the world. Geological Society of India, pp. 300-315.

Nichols, R.L., 1936. Flow units in basalt. Journal of Geology, 44(5): 617-630.

Nordt, L., Atchley, S. and Dworkin, S., 2003. Terrestrial evidence for two greenhouse events in the Late Cretaceous. GSA Today, 13(12): 4-9.

O' Keefe, J.D. and Ahrens, T.J., 1993. Planetary cratering mechanics. Journal of Geophysical Research, 98: 17011-17028.

Osawa, M. and Goles, G.G., 1970. Trace element abundances in Columbia River basalts. In: E. Gilmour and D. Stradling (Editors), Proceedings, 2nd Columbia River Basalt Symposium. Eastern Washington State College Press, Cheney, pp. 55-71.

Pal, P.C., 1969. Palaeomagnetic of the Deccan Flood Basalts. Nature, 223: 820-822.

Pal, P.C., Bindu Madhav, U. and Bhimasankaram, V.L.S., 1971. Early Tertiary geomagnetic polarity reversals in India. Nature, 230: 133-135.

Pande, K., 2002. Age and duration of the Deccan Traps, India: a review of radiometric and palaeomagnetic constraints. Proceedings of the Indian Academy of Science (Earth and Planetary Science), 111(2): 115-123.

Pandey, O.P. and Negi, J.G., 1987. A new theory of the origins and evolution of the Deccan Traps (India). Tectonophysics, 142: 329-335.

Pascoe, E.H., 1964. A manual of the geology of India and Burma. Government of India Press, Calcutta.

Pearce, N.J.G., Westgate, J.A., Preece, S.J., Eastwood, W.J. and Perkins, W.T., 2004. Identification of Aniakchak (Alaska) tephra in Greenland ice core challenges in the i645 BC date for Minoan eruption of Santorini. Geochemistry Geophysics Geosystems, 5(3): doi:10.1029/2003gc000672.

Peng, Z.X., Mahoney, J.J., Hooper, P.R., Harris, C. and Beane, J.E., 1994. A role for lower continental crust in flood basalt genesis? isotopic and incompatible element study of the lower six formations of the western Deccan Traps. Geochimica et Cosmochimica Acta, 58: 267-288.

Peng, Z.X. and Mahoney, J.J., 1995. Drillhole lavas from the northwestern Deccan Traps, and the evolution of the Reunion hotspot mantle. Earth and Planetary Science Letters, 134: 169-185.

Peng, Z.X., Mahoney, J.J., Hooper, P.R., MacDougall, J.D. and Krishnamurthy, P., 1998. Basalts of the northeastern Deccan Traps, India: Isotopic elemental geochemistry and relation to the southwestern Deccan stratigraphy. Journal of Geophysical Research, 103(12B): 23,843-29,865.

Perkins, M.E., Nash, W.P., Brown, F.H. and Fleck, R.J., 1995. Fallout tuffs of Trapper Creek, Idaho: record of Miocene explosive volcanism in the Snake River Plain volcanic province. Bulletin of the Geological Society of America, 110: 344-360.

Peterson, D.W. and Moore, R.B., 1987. Geologic history and evolution of geologic concepts, Island of Hawaii. In: R.W. Decker, T.L. Wright and P.H. Stauffer (Editors), Volcanism in Hawaii, (U.S. Geological survey Professional Paper 1350). U.S.G.S., Washington, pp. 149-189.

Peterson, D.W. and Swanson, D., 1974. Observed formation of lava tubes during 1970-1971 at Kilauea volcano, Hawaii. Studies in Speleology, 2(6): 209-222.

Philpotts, A., R. and Carroll, M., 1996. Physical properties of partly melted tholeiitic basalt. Geology, 24(11): 1029-1032.

Philpotts, A., R. , Shi, J. and Brustman, C., 1998. Role of plagioclase crystal chains in the differentiation of partly crystallized basaltic magma. Nature, 395: 343-346.

Phipps Morgan, J., Reston, T.J. and Ranero, C.R., 2004. Contemporaneous mass extinctions, continental flood basalts, and 'impact' signals': are mantle plume-induced lithospheric gas explosions the causal link? Earth and Planetary Science Letters, 217: 263-284.

Pilidou, S., Priestley, K., Gudmundsson, O. and Debayle, E., 2004. Upper mantle S-wave speed heterogeneity and anisotropy beneath the North Atlantic from regional surface wave tomography: the Iceland and Azores plumes. Geophysical Journal International, 159(3): 1057-1076.

Pinkerton, H., Herd, R.A., Kent, R.M. and Wilson, L., 1995. Field measurements of the rheological properties of basaltic lavas. Abstracts of papers submitted to the Twenty-sixth lunar and planetary science conference Abstracts of Papers Submitted to the Lunar and Planetary Science Conference, 26: 1127-1128.

Puchtel, I.S., Bruegmann, G.E. and Hofmann, A.W., 1999. Precise Re-Os mineral isochron and Pb-Nd-Os isotope systematics of a mafic-ultramafic sill in the 2.0 Ga Onega Plateau (Baltic Shield). Earth and Planetary Science Letters, 170(4): 447-461.

Raja Rao, C.S., Sahasrabudhe, S.S., Deshmukh, S.S. and Raman, R., 1999. Distribution, structure and petrography of the Deccan Traps, India. In: K.V. Subbarao (Editor), Deccan Volcanic Province. Geological Society of India, Bangalore, pp. 997.

Rampino, M.R., 1987. Impact cratering and flood basalt volcanism. Nature, 327: 468.

Rampino, M.R. and Haggerty, B.M., 1995. Episodes of flood basalt volcanism defined by (super 40) Ar/ (super 39) Ar age distributions; correlation with mass extinctions? International Union of Geodesy and Geophysics; XXI general assembly; abstracts International Union of Geodesy and Geophysics, General Assembly, 21: 466.

Rampino, M.R. and Stothers, R.B., 1988. Flood basalt volcanism during the past 250 million years. Science, 241: 663-668.

Rampino, M.R. and Stothers, R.B., 1989. Flood basalt volcanism in space and time. Bulletin - New Mexico Bureau of Mines & Mineral Resources, 131: 221.

Rao, A.T., Rao, K.S. and Vijayakumar, V., 2002. Basic Volcanism along the K-T boundary from Rajahmundry, East Coast of India. Journal of the Geological Society of India, 60(5): 583-586.

Rao, M.S., Reddy, N.R., Subbarao, K.V., Prasad, C.V.R.K. and Radhakrishnamurty, C., 1985. Chemical and Magnetic stratigraphy of parts of Narmada region, Deccan Basalt Province. Journal of the Geological Society of India, 26: 617-639.

Ray, J.S., Ramesh, R., Pande, K., Trivedi, J.R., Shukla, P.N. and Patel, P.P., 2000. Isotope and rare earth element chemistry of carbonatite-alkaline complexes of Deccan volcanic province: implications to magmatic and alteration processes. Journal of Asian Earth Sciences, 18: 177-194.

Reddy, C.D., El-Fiky, G., Kato, T., Seiichi, S. and Vijay Kumar, K., 2000. Crustal strain fields in the Deccan Trap region, western India, derived from GPS measurements. Earth and Planetary Sciences letters, 52: 965-969.

Reichow, M.K., Saunders, A.D., White, R.V., Pringle, M.S., Al-Mukhamedov, A.I. and Kirda, N.P., 2002. $^{40}Ar/^{39}Ar$ dates for the west Siberian basin: Siberian flood basalt province doubled. Science, 296: 1846-1849.

Reidel, S.P., 1998. Emplacement of Columbia River Flood Basalt. Journal of Geophysical Research, 103(B11): 27,393-27,410.

Reidel, S.P. and Hooper, P.R. (Editors), 1989. Volcanism and Tectonism in the Columbia River Flood-Basalt Province. GSA Special Paper, 239. The Geological Society of America, Boulder, 386 pp.

Reidel, S.P. and Tolan, T., 1992. Eruption and emplacement of flood basalt: An example from the large-volume Teepee Butte Member, Columbia River Basalt Group. Geological Society of America Bulletin, 104: 1650-1671.

Rhodes, J.M., 1996. Geochemical stratigraphy of lava flows sampled by the Hawaii Scientific Drilling Project. Journal of Geophysical Research, 101(B5): 11,729-11,746.

Richards, M.A. and Duncan, R.A., 1988. Flood basalts and hotspot tracks; plume heads and tails. AGU 1988 fall meeting Eos, Transactions, American Geophysical Union, 69(44): 1421.

Rogan, W., Blake, S. and Smith, I., 1996. In situ chemical fractionation in thin basaltic flows: examples from Auckland volcanic field, New Zealand, and a general physical model. Journal of Volcanology and geothermal research, 74: 89-99.

Rossi, M.J. and Gudmindsson, 1996. The morphology and formation of flow-lobe tumuli on Icelandic shield volcanoes. Journal of Volcanology and Geothermal Research, 72: 291-308.

Rowland, S.K. and Walker, G.P., 1990. Pahoehoe and 'a'a in Hawaii: volumetric flow rate controls the lava structure. Bulletin of Volcanology, 52: 615-628.

Sahasrabudhe, P.W., 1963. Palaeomagnetic and the Geology of the Deccan Traps, Proceedings from the Seminar on Geophysical Investigations in the Peninsular Shield, pp. 227-243.

Sahasrabudhe, Y.S. et al., 1977. Deccan basalt flows exposed along Poladpur-Mahabaleshwar and Amboli Ghat sections in Western Ghat, India-A geological study. Records of the Geological Survey of India, 108: 69-80.

Sano, T., Fujii, T. Deshmukh, S.S., Fukuoka, T. and Aramaki, S., 2001. Differentiation processes of the Deccan Trap basalts: Contribution from geochemistry and experimental petrology. Journal of Petrology, 42: 2175-2195.

Self, S., 2004b. Personal communication.

Self, S., Finnemore, S., Thordarson, T. and Walker, G.P.L., 1991. Importance of compound lava and lava-rise mechanisms in emplacement of flood basalts. Eos, Transactions, American Geophysical Union, 72: 566.

Self, S., Jay, A.E. and Widdowson, M., in prep. The worlds longest lava flow.

Self, S., Keszthelyi, L. and Thordarson, T., 1998. The importance of pahoehoe. Annual Review of Earth and Planetary Sciences, 26: 81-110.

Self, S., Keszthelyi, L.P., Thordarson, T., Anderson, S.W., Stofan, E.R., Smrekar, S.E., Guest, J.E. and Wood, B., 2000. Enriched: Pulsed inflation of pahoehoe lava flows; implications for flood basalt emplacement; discussion and reply. Earth and Planetary Science Letters, 179(2): 421-428.

Self, S., Thordarson, T., Keszthelyi, L., Walker, G.P.L., Hon, K., Murphy, M.T., Long, P. and Finnemore, S., 1996. A new model for the emplacement of Columbia River Basalts as large, inflated pahoehoe lava flow fields. Geophysical Research Letters, 23(19): 2689-2692.

Self, S., Thordarson, T. and Keszthelyi, L.P., 1997. Emplacement of Continental Flood Basalt Lava Flows. In: J.J. Mahoney and M.F. Coffin (Editors), Large igneous provinces; continental, oceanic, and planetary flood volcanism Geophysical Monograph 100 (1997). American Geophysical Union, Washington, DC, pp. 381-410.

Sen, G., 2001. Generation of Deccan Trap Magmas. Proceedings of the Indian academy of Science (Earth and Planetary Science), 110: 409-431.

Sen, G., 2002. Giant Plagioclase Basalts, eruption rate verses time. Response to Sheth's comments and some additional thoughts. Proceedings of the Indian Academy of Science (Earth and Planetary Science), 11(4): 487-488.

Sengör, A.M.C., 2001. Elevation as an indicator of mantle-plume activity. In: R.E. Ernst and K.L. Buchan (Editors), Mantle plumes: Their Identification Through Time. Geological Society of America Special Paper, pp. 183-225.

Sengupta, S.K. and Deshmukh, S.S., 1996. Petrology and geochemistry of the Deccan Basalt flows intersected in Salbardi drill hole, Eastern Deccan Trap Province. Gondwana Geological Magazine, 2: 69-80.

Sepkoski, J., J.J., 1996. Patterns of the Phanerozoic extinction: a perspective from global data bases. In: O.H. Walliser (Editor), Global events and event stratigraphy. Springer-Verlag, Berlin, pp. 35-52.

Sharma, K., 2001. Cooling and crystallization of pahoehoe lava flows from Kilauea volcano, Hawai'i. Masters Thesis, University of Hawai'i at Manoa, Honolulu, 85 pp.

Sharma, K., Blake, S., Self, S. and Krueger, A.J., 2004. SO_2 emissions from basaltic eruptions, and the excess sulfur issue. Geophysical Research Letters, 31(13).

Sharma, R.K. and Vaddadi, S., 1996. Report on lava tubes/ channels from Deccan Volcanic Province, Pune and Ahmednager Districts, Maharashtra. Gondwana Geological Magazine, 2: 457-460.

Shaw, H.R. and Swanson, D., 1970. Eruption and flow rates of flood basalts. In: E. Gilmour and D. Stradling (Editors), Proceedings of the Second Columbia River Basalt Symposium. East Washington State College Press, Cheney, pp. 271-299.

Sheth, H.C., 1999. Flood basalts and large Igneous provinces from deep mantle plumes: fact, fiction and fallacy. Tectonophysics, 311: 1-29.

Sheth, H.C., Mahoney, J.J. and Chandrasekharam, D., 2004a. Geochemical stratigraphy of Deccan flood basalts of the Bijasan Ghat section, Satpura Range, India. Journal of Asian Earth Sciences, 23: 127-139.

Sheth, H.C., Matthew, G., Pande, K., Mallick, S. and Jena, B., 2004b. Cones and craters on Mount Pavagadh, Deccan Traps: Rootless cones? Proceedings of the Indian Academy of Science (Earth and Planetary Science), 113(4): 831-838.

Shukla, A.D., Bhandari, N., Kusumgar, S., Shukla, P.N., Ghevariya, Z.G., Gopalan, K. and Balaram, V., 2002. Geochemistry and magnetostratigraphy of Deccan Flows at Anjar, Kutch. Proceedings of the Indian Academy of Science (Earth and Planetary Science), 110(2): 111-132.

Sigurdsson, H., Houghton, B., McNutt, S.R., Rymer, H. and Stix, J. (Editors), 2000. Encyclopedia of volcanoes. Academic Press, 1417 pp.

Stewart, C.A., Rampino, M.R. and Robinson, C., 1993. Impact shocks in the transition zone; enough energy to trigger a plume? Venus coronae linked to missing population of large Venus impact craters. AGU 1993 fall meeting Eos, Transactions, American Geophysical Union, 74(43): 80.

Storey, M., Mahoney, J.J., Saunders, A.D., Duncan, R.A., Kelley, S.P. and Coffin, M.F., 1995. Timing of hot spot-related volcanism and the break-up of Madagascar and India. Science, 267: 852-855.

Stothers, R.B., Rampino, M.R., Self, S. and Wolff, J.A., 1989. Volcanic winter? Climatic effects of the largest volcanic eruptions. In: J.H. Latter (Editor), Volcanic hazards; assessment and monitoring. Springer-Verlag, Berlin, Federal Republic of Germany, pp. 3-9.

Stott, L.D. and Kennet, J.P., 1990. The palaeoceanographic and palaeoclimatic signature of the Cretaceous/Palaeogene boundary in the Antarctic: stable isotope results from ODP Leg 113, Ocean Drilling program Scientific Results 113.

Subbarao, K.V. (Editor), 1999. Deccan Volcanic Province, 1. Geological Society of India, Bangalore, 947 pp.

Subbarao, K.V., Bodas, M.S., Khadri, S.F.R. and Beane, J.E., 2000. Penrose Deccan 2002, Field excursion guide to the western Deccan Basalt Province. Penrose Field Guides. Geological Society of India, Bangalore.

Subbarao, K.V., Chandrasekharam, D., Navaneethakrishnan, P. and Hooper, P.R., 1994. Stratigraphy and structure of parts of the central Deccan basalt province: Eruptive

models. In: K.V. Subbarao (Editor), Volcanism. Wiley Eastern Publishers, New Delhi, pp. 321-332.

Subbarao, K.V. and Hooper, P.R., 1988. Reconnaissance map of the Deccan Basalt Group in the Western Ghats, India., A workshop on Deccan Flood Basalts. Geological Society of India, Memoir.

Subbarao, K.V., Ramasubba Reddy, N. and Prasad, C.V.R.K., 1988. Geochemistry and palaeomagnetic of dykes from Mandaleswar region, Deccan Basalt Province., Workshop on Deccan flood basalts, December 3-10, 1988. Geological Society of India, Bangalore, pp. 225-233.

Swanson, D., 1972. Magma supply rate at Kilauea Volcano 1952-1971. Science, 175(4018): 169-170.

Swanson, D., Wright, T.L. and Hertz, R.T., 1975. Linear vent system and estimated rates of magma production and eruption for the Yakima basalt on the Columbia River Plateau. American Journal of Science, 275(8): 877-905.

Talusani, R., V. R., 2001. A newly reported alkali basalt flow near Bhir, Deccan Volcanic Province, India. Journal of Asian Earth Sciences, 19: 501-506.

Tandon, S.K., 2002. Records of the influence of Deccan volcanism on contemporary sedimentary environments in Central India. Sedimentary Geology, 147: 177-192.

Tatsumoto, M., Hegner, E. and Unruh, M., 1987. Origin of the west Maui volcanic rocks inferred from Pb, Sr and Nd isotopes and a multi component model for oceanic basalt. In: R.W. Decker, T.L. Wright and P.H. Stauffer (Editors), Volcanism in Hawaii, (U.S. Geological survey Professional Paper 1350). U.S.G.S., Washington, pp. 723-744.

Taylor, G.J., 1996. Lava flow dynamics. (19960114). Available From: National Technical Information Service, (703)605-6000, order number N19980008060NEG, Springfield, VA, 3 pp.

Teasdale, R., Geist, D.J., Kurz, M. and Harpp, K., 2005. 1998 Eruption at Volcan Cerro Azul, Galapagos Islands: I. Syn-Eruptive Petrogenesis. Bulletin of Volcanology, 67: 170-185.

Theilig, E. and Greeley, R., 1987. Emplacement mechanism for compound pahoehoe lava flows. Geological Society of America, 1987 annual meeting and exposition Abstracts with Programs - Geological Society of America, 19(7): 866.

Thompson, G., M., Ali, J., R., Song, X. and Jolley, D.W., 2001. Emeishan Basalts, SW China: reappraisal of the formation's type area stratigraphy and a discussion of its significance as a large igneous province. Journal of the Geological Society, 158: 593-599.

Thorat, P.K., 1996. Occurrence of lava channels and tubes in the western part of Deccan Volcanic Province. Gondwana Geological Magazine, 2: 449-456.

Thordarson, T., 1995. Volatile release and atmospheric effects of basaltic fissure eruptions, University of Hawaii at Manoa, Honolulu, 580 pp.

Thordarson, T. and Hoskuldsson, A., 2002. Iceland. Classic Geology in Europe 3. Terra publishing, Harpenden.

Thordarson, T. and Self, S., 1993. The Laki (Skaftar Fires) and Grimsvotn eruptions in 1783-85. Bulletin of Volcanology, 55: 233-263.

Thordarson, T. and Self, S., 1996. Sulfur, chlorine and fluorine degassing and atmospheric loading by the Roza eruption, Columbia River Basalt Group, Washington, USA. Journal of Volcanology and Geothermal Research, 74: 49-73.

Thordarson, T. and Self, S., 1998. The Roza Member, Columbia River Basalt Group; a gigantic pahoehoe lava flow field formed by endogenous processes? Journal of Geophysical Research, B, Solid Earth and Planets, 103(11): 27,411-27,445.

Todal, A. and Eldholm, O., 1999. Continental margin off western India and Deccan large igneous province. In: J. Erzinger, J.-C. Sibuet and M. Talwani (Editors), Volcanic

margins Marine Geophysical Researches 20, no. 4 (1998). Kluwer Academic Publishers, Dordrecht, Netherlands, pp. 273-291.

Tolan, T.L., Reidel, S.P., Beeson, M.H., Anderson, J.L., Fecht, K.R. and Swanson, D., 1989. Revisions to the estimates of the areal extent and volume of the Columbia River Flood Basalt Province. In: S.P. Reidel and P.R. Hooper (Editors), Special Paper of the Geological Society of America, pp. 1-20.

Tomkeieff, S.I., 1940. The basalt lavas of the Giant's Causeway district of Northern Ireland. Bulletin of Volcanology, 11(6): 89-143.

Turner, W., 2003. Palaeomagnetic constraints on the timing and duration of the Deccan Flood Basalt Province. M.Sci. Thesis, University of Oxford, Oxford.

Vandamme, D., Courtillot, V., Besse, J. and Montigny, R., 1991. Palaeomagnetic and age determinations of the Deccan Traps (India); results of a Nagpur-Bombay traverse and review of earlier work. Reviews of Geophysics, 29(2): 159-190.

Vandamme, D. and Courtillot, V., E., 1992. Palaeomagnetic constraints on the structure of the Deccan Traps. Physics of the Earth and Planetary Interiors, 74: 241-261.

Venkata Rao, K., Nair, K.K.K., Srirama, B.V. and Satyanarayana, K.V., 1996. Crustal configuration of Central Satpura and identification of eruptive zones for Deccan basalts. Gondwana Geological Magazine, 2: 417-426.

Viswanathan, S. and Misra, K.S., 2002. Discussion. Arterial system of lava tubes and channels within Deccan volcanics of Western India. Journal of the Geological Society of India, 60(5): 595-600.

Wadia, D.N., 1937. The Geology of India, London.

Walker, G.P.L., 1972. Compound and simple lava flows and flood basalts. Bulletin of Volcanology, 35: 579-590.

Walker, G.P.L., 1987. Pipe vesicles in Hawaiian basaltic lavas: their origin and potential as palaeoslope indicators. Geology, 15: 84-87.

Walker, G.P.L., 1989. Spongy pahoehoe in Hawaii: a study of vesicle-distribution patterns in basalt and their significance. Bulletin of Volcanology, 51: 199-209.

Walker, G.P.L., 1991. Structure, and origin by injection of lava under surface crust, of tumuli, "lava rises", "lava-rise pits", and "lava-inflation clefts" in Hawaii. Bulletin of Volcanology, 53(7): 546-558.

Walker, G.P.L., 1995. Flood basalts verses central volcanoes and the British Tertiary Volcanic Province. In: M.J. Le Bas (Editor), Milestones in Geology,. Geological Society of London, London, pp. 195-202.

Walker, G.P.L., 1999. Some observations and interpretations on the Deccan Traps. In: K.V. Subbarao (Editor), Deccan Volcanic Province. Geological Society of India, Bangalore.

Walker, G.P.L., 2000. Basaltic volcanoes and volcanic systems. In: H. Sigurdsson, Houghton, B., McNutt, S., Rymer, H. and Stix, J. (Editor), Encyclopedia of Volcanoes. Academic Press, San Diego, pp. 1417.

Walker, G.P.L., Canon-Tapia, E. and Herrero-Bervera, E., 1999. Origin of vesicle layering and double imbrication by endogenous growth in the Birkett basalt flow (Columbia river plateau). Journal of Volcanology and Geothermal Research, 88: 15-28.

Wensink, H., 1973. Newer palaeomagnetic results of the Deccan traps, India. Tectonophysics, 17: 41-49.

Wensink, H. and Klootwijk, C.T., 1971. Palaeomagnetic of the Deccan Traps in the Western Ghats near Poona (India). Tectonophysics, 17: 41-59.

Wentworth, C.K. and Macdonald, G.A., 1953. Structures and forms of basaltic rock in Hawaii. United States Geological Survey Bulletin, 994: 98.

West, W.D., 1985. The Deccan Trap and other flood eruptions- a comparative study. Proceedings of the Indian National Science Academy, 51(3): 456-495.

West, W.D., 1999. The petrography and petrogenesis of forty-eight flows of Deccan Trap penetrated by borings in western India. In: K.V. Subbarao (Editor), Deccan

volcanic province (geomorphology, mineralogy and petrology, geochemistry, Lonar Lake) Memoir - Geological Society of India 43 (1999). Geological Society of India, Bangalore, India, pp. 641-704.

West, W.D., The source of the Deccan Traps. Journal of the Geological Society of India, 1: 1-56.

White, R., S. and McKenzie, D., 1989. Magmatism at rift zones; the generation of volcanic continental margins and flood basalts. In: W.P. Leeman and J.G. Fitton (Editors), Enriched. American Geophysical Union, Washington, DC, pp. Special section on Magmatism associated with lithospheric extension Journal of Geophysical Research, B, Solid Earth and Planets 94, no. 6 (19890610) 7685-7729.

White, R.S. and McKenzie, D., 1995. Mantle plumes and flood basalts. Journal of Geophysical Research, 100(B9): 17,543-17,585.

Whittaker, A., Cope, J.C.W. and Cowie, J.W., 1991. A guide to stratigraphical procedure. Journal of the Geological Society, 148: 813-824.

Widdowson, M., 1990. The Uplift History of the Western Ghats, India. D. Phil. Thesis, University of Oxford, Oxford.

Widdowson, M., 1997. Tertiary palaeosurfaces of the SW Deccan, western India; implications for passive margin uplift. In: M. Widdowson (Editor), Palaeosurfaces; recognition, reconstruction and palaeoenvironmental interpretation Geological Society Special Publications 120 (1997). Geological Society of London, London, United Kingdom, pp. 221-248.

Widdowson, M., 2005. personal communication.

Widdowson, M. and Cox, K.G., 1996. Uplift and erosional history of the Deccan Traps, India; evidence from laterites and drainage patterns of the Western Ghats and Konkan coast. Earth and Planetary Science Letters, 137(1-4): 57-69.

Widdowson, M. and Kelley, S.P., in prep. $^{40}Ar/^{39}Ar$ dating of the Mahabaleshwar Plateau.

Widdowson, M. and Mitchell, C., 1992. Discussion on a geological map of the southern Deccan Traps, India and its structural implications, (Vol. 148, 1991), pp. 495-505. Journal of the Geological Society, 149: 473-478.

Widdowson, M., Pringle, M.S. and Fernandez, O.A., 2000. A post K-T Boundary (Early Palaeocene) age for Deccan-type feeder dykes, Goa, India. Journal of Petrology, 41(7): 1177-1194.

Widdowson, M., Walsh, J.N. and Subbarao, K.V., 1997. The geochemistry of Indian bole horizons: palaeoenvironmental implications of Deccan intravolcanic palaeosurfaces. In: M. Widdowson (Editor), palaeosurfaces: recognition, reconstruction and palaeoenvironmental interpretation. Geological Society Special Publications, London, pp. 269-281.

Wignall, P.B., 2001. Large igneous provinces and mass extinctions. Earth Science Reviews, 53: 1-33.

Wilmoth, R.A. and Walker, G.P.L., 1993. P-type and S-type pahoehoe; a study of vesicle distribution patterns in Hawaiian lava flows. Journal of Volcanology and Geothermal Research, 55(1-2): 129-142.

Windley, B.F., 1992. The Evolving Continents. John Wiley & Sons, 399 pp.

Witham, C.S. and Oppenheimer, C., 2004. Mortality in England during the 1783-4 Laki craters eruption. Bulletin of Volcanology.

Wolff, J.A., Self, S., Rampino, M.R. and Stothers, R.B., 1984. Basaltic fissure eruptions, fire fountains, and atmospheric aerosols. AGU 1984 fall meeting Eos, Transactions, American Geophysical Union, 65(45): 1148-1149.

Wright, T.L. and Doherty, P.C., 1970. A linear programming and least squares computer method for solving petrologic mixing problems. Geological Society of America Bulletin, 81(7).

Zijderveld, J.D.A., 1967. A. C. demagnetization of rocks-analysis of results, Methods in palaeomagnetism-nato advanced study inst. on palaeomagnetic methods, Univ. Newcastle upon Tyne, 1964, proc. Elsevier, New York.

C1 X-Ray Fluorescence analysis methodology

The geochemistry in this thesis is based upon compositional data from whole rock analysis. As the samples are fine grained approximately 200g of each rock is needed to give a representative geochemistry. The samples were divided up to approximately 3cm cubes using a manual hydraulic rock splitter. These pieces were then fed into jaw crushers set on the finest (~.05 cm) setting. The crushate was placed in an agate Tema and milled for 9 minutes until a fine powder ($\leq$ 60 μm) is formed. To reduce cross contamination, thorough cleaning was carried out at each stage. If the sample being crushed was very different material, the Tema was either precontaminated or cleaned with pure quartz.

Both major and trace element analyses were carried out using an ARL 8420+ dual goniometer wavelength dispersive XRF spectrometer equipped with 3kW rhodium anode end-window X-ray tube, flow proportional and scintillation counters-fully collimated, diffracting crystals:AX06 (multilayer), PET (penta-erythrytol), Ge111, LiF200, LiF220.

Major element analysis

These analyses were performed on fused glass beads composed of exactly 0.7g of rock powder (dried over night at 100° C) and flux (lithium metaborate/tetraborate, Johnson Matthey Spectroflux 100B, dried at 110° C over night) at a 1 to 5 ratio. The rock and flux are mixed in Pt-5% Au crucibles then fused at 1100°C for 15 minutes. The samples are swirled 3 times at 5, 10 and 13 minutes to ensure total homogenisation, dissolution and removal of gas bubbles. The melt is then poured into the centre of a heated brass mould and pressed with a plunger. The plunger is preheated to avoid thermal shock. The glass beads are stored under glass evaporating dishes until cool in case of shattering.

To calculate the loss of volatiles during fusion, loss on ignition is carried out on approximately 1.2-1.25g of each sample of rock powder (loss on ignition is carried out on each batch of flux at the start of each bottle and recorded for everyone's use). Alumina crucibles are pre-ignited at 1000°C for at least 15 minutes and allowed to cool for 10 minutes before the rock sample is weighed out, recorded and the total mass of the sample plus crucible is recorded. The samples are ignited in the furnace at 1000°C for 1 hour. After ignition the samples and crucibles are cooled and reweighed. The percentage loss on ignition is calculated to two decimal places.

$$\text{Percentage loss on ignition} = \frac{\text{Loss or gain in weight of rock powder}}{\text{Original weight of rock powder}} \times 100$$

To test the precision and accuracy of the analysis two glass beads are made from known standards, OUG94 and WS-E these are run with the samples. Two pre-prepared and pre-analysed beads of the same standards were also run to test the accuracy.

The classification of samples into formations during this work has been carried out using the criteria of Devey and Lightfoot (1986). In order to reduce the error occurring due to my samples being analysed in a different laboratory, my samples were analysed with some from the University of Oxford, this has ensured that the data are comparable to and consistent with, all previous DVP data sets (Devey, 1986; Widdowson, 1990).

Trace Element analysis

The concentration of 20 trace elements can be calculated using the XRF technique, the elements are Rb, Sr, Y, Nb, Ba, Pb, Th, U, Sc, V, Cr, Co, Ni, Cu, Zn, Ga, Mo, and S The analyses were carried out on pressed pellets of approximately 10g of rock powder bound together with 0.7-1.0 ml of polyvinylpyrollidone (PVP). The moist powder

is the pressed in a mould at 5 ton in^{-2} to a minimum thickness of 3.5mm and dried overnight at 110°C.

Determining geochemical errors and cross laboratory compatibility

In order to maintain geochemical consistency between samples analyzed at the University of Oxford, Department of Earth Sciences and the Open University, Department of Earth Sciences internal standards from Widdowson (1990) were run as unknowns with every analysis. These specific samples were chosen because they matched all the geochemical criteria for the key formations laid down by Devey and Lightfoot (1986). The samples used for trace element comparison were CG2, CG5 and CG7, (Poladpur Formation), CG10, CG11, KP4, PH6, Ph7 and Ph10 (Ambenali Formation), SF1 (Mahabaleshwar Formation) and KP13 (Panhala Formation) Appendix C9. The samples used for major element comparison are CG2, (Poladpur Formation), KP4, PH6 and PH7, (Ambenali Formation) and SF1 (Mahabaleshwar Formation). These samples were recast into beads and pellets from the original powders although occasionally Widdowson's (1990) pellets and beads were run and are named as 'sample name' (old; -old in tables indicates that the calculation was carried out without these old sample's data).

The mean of each sample's results returned from the analyses was compared to the results previously determined by Widdowson (1990) (Appendix 10). The standard deviation was taken in order to check that the data were similar. The standard deviation between the important element concentrations and ratios, Y, Zr, Nb and Sr were very small (i.e., less than 0.65), the Ba concentrations returned had a slightly larger spread (the greatest Standard deviation is 7.7, the average is 4.04), but Ba gives variable results as it has a relatively high detection limit, 12 ppm, compared to Y, Zr, Nb and Sr which have detection limits of between 1.5 and 2 ppm (Table C9). Some elements gave very different concentrations between the University of Oxford and the Open University XRF machines.

These were mostly transition metals, but this is to be expected due to the high concentration of iron in the samples compared to the other transition metals. This produces a large iron peak from which it can be difficult to extract the concentrations of many of the other transition metals.

The Widdowson (1990) CG5 pellet was run on five different occasions and gave an average Cr concentration of 222.2 ppm, but the newer pellet (made in case of degradation from homogenised powder) gave an average Cr concentration of 353 ppm with all other elements within the usual range of each other. The likely explanation is that a small piece of metal from a rock preparation machine broke of and became incorporated in the powder during milling and unfortunately this was sampled when the second pellet was made. The iron content of basalt is high enough for such a small amount not to change the percentage concentration, but chromium is found in only small amounts in the basaltic opaque minerals and in clinopyroxene and so the addition of even the smallest amount will greatly affect the concentration. If Cr had been an important element for this work the pellet would have been re-made and analysed to further investigate this.

The error on an elemental abundance measurement is dependent on the concentration of that element. The ideal way to calculate this instrumental precision is to undertake a number of repeat analyses of each bead and pellet. This however, is not feasible, so during this work instrumental precision was calculated using the results from the Widdowson (1990) standards (Table C9). For each formation one or more samples from Widdowson (1990) were analysed with each batch of samples analyzed using XRF. This gave elemental data for estimating instrumental precision for the element concentrations of an 'average' sample for each of the main formations (Poladpur, Ambenali, Mahabaleshwar and Panhala Formations). The instrumental precision for each element in each formation was then calculated by calculating the mean of each elemental

abundance in each sample from Widdowson (1990), e.g., the mean of each elemental abundance value in CG2, CG5 and CG7 provides the mean of each elemental abundance value in an 'average' Poladpur Formation sample (Appendix C11). The mean was then taken of all the Widdowson (1990) samples for each formation and the standard deviation and standard error on the mean (often just called the "standard error") was calculated. The mean was then taken of these standard errors of the elements from each formation to provide a standard error for the Poladpur, Ambenali, Mahabaleshwar and Panhala Formations. From this, the final percentage errors were calculated (Appendix C11) and then applied to each element in every analysis (Figure 4.4).

C2 Geochemical analyses of Ambenali Ghat samples

C2 Ambenali Ghat

Elev. M asl	24	61	81	103	120	151	180	201	253	283	302	311
wt. %	PMag03Pmh1	PMag03PMh2	PMag03PMh3	PMag03PMh4	PMag03PMh5	PMag03PMh6	PMag03PMh7	PMag03PMh8	PMag03PMh9	PMag03PMh10	PMag03PMh11	PMag03PMh14
SiO2	50.12	49.53	48.90	48.70	48.25	48.26	49.30	50.48	50.86	50.78	49.70	50.31
TiO2	0.996	1.990	2.089	2.134	2.032	2.878	2.829	1.752	1.766	1.815	1.910	2.018
Al2O3	14.82	14.06	14.00	14.02	13.84	13.03	13.17	13.90	13.98	14.30	14.08	13.84
Fe2O3	11.03	14.82	14.94	15.03	14.99	16.90	16.58	12.68	12.61	12.09	12.56	12.97
MnO	0.174	0.199	0.235	0.227	0.211	0.230	0.234	0.186	0.192	0.178	0.168	0.300
MgO	7.24	6.06	6.23	6.21	6.13	5.70	5.69	6.67	6.58	6.54	7.15	6.64
CaO	10.69	10.83	10.98	10.80	10.32	9.90	9.79	10.60	10.76	10.81	11.19	10.57
Na2O	1.84	2.50	2.42	2.19	2.13	2.32	2.31	2.20	2.31	2.57	2.27	2.29
K2O	0.52	0.28	0.20	0.20	0.39	0.29	0.52	0.23	0.25	0.35	0.26	0.47
P2O5	0.108	0.152	0.178	0.187	0.175	0.267	0.242	0.168	0.175	0.181	0.171	0.194
LOI	2.76	0.28	-0.15	0.93	1.59	0.29	0.11	0.90	0.75	0.31	0.50	0.60
Total	100.30	100.70	100.01	100.63	100.06	100.06	100.78	99.77	100.24	99.93	99.95	100.20
	PMag03PMh1	Mag03PMh2	PMag03PMh3	PMag03PMh4	PMag03PMh5	PMag03PMh6	PMag03PMh7	Mag03PMh8	PMag03Pmh9	PMag03Pmh10	PMag03PMh11	PMag03PMh14
Rb	17	2	2	5	14	7	14	9	9	12	2	13
Sr	168	218	230	225	213	231	214	197	194	212	211	207
Y	23.2	30.6	32.4	32.6	31.4	41.9	38.9	30.9	30.4	30.0	28.0	33.9
Zr	95	118	128	134	127	194	177	133	136	133	128	140
Nb	5.2	7.1	8.1	7.5	7.4	12.9	11.5	7.9	8.1	7.5	8.3	10.0
Ba	126	85	94	74	51	103	123	117	120	164	108	122
Pb	3	1	1	3	2	1	4	3	5	2	1	2
Th	3	2	1	0	3	3	4	3	4	1	3	1
U	1	1	0	0	0	0	0	0	0	0	0	1
Sc	32	40	41	41	36	34	38	37	37	36	38	37
V	262	358	403	412	381	410	463	333	333	341	347	380
Cr	350	78	102	53	123	78	93	228	227	287	312	246
Co	41	44	45	48	43	40	38	40	41	39	41	41
Ni	130	67	67	68	70	68	66	99	97	113	118	104
Cu	105	138	183	184	198	195	196	122	130	145	166	140
Zn	72	99	113	114	109	130	114	90	96	96	95	95
Ga	17	20	22	23	22	24	23	20	19	21	20	19
Mo	0	0	0	0	0	0	0	0	0	0	0	0
As	4	3	1	0	3	1	4	0	0	1	5	4
S	103	69	41	105	83	62	45	109	40	30	48	65
Fm. criteria												
Sr	168	218	230	225	213	231	214	197	194	212	211	207
Ba	126	85	94	74	51	103	123	117	120	164	108	122
Ba/Y	5.41	2.77	2.90	2.27	1.61	2.46	3.17	3.79	3.93	5.47	3.87	3.59
Zr/Nb	18.27	16.58	15.74	17.85	17.15	15.00	15.36	16.82	16.81	17.67	15.45	14.01
	Bushe Fm.*	Poladpur Fm.*	Poladpur Fm.*	Poladpur Fm.*	Poladpur Fm.*	Poladpur Fm.*	Poladpur Fm.*	Poladpur Fm.	Poladpur Fm.	Poladpur Fm.	Poladpur Fm.	Poladpur Fm.*

There are no Sr criteria for the Bushe and Poladpur Fms. There is no Ba/Y criteria available for the Bushe Fm.

* inferred formation from overall geochemical characteristics and stratigraphic height in Devey and Lightfoot (1986)

Bold indicates sample criteria fit with the Devey and Lightfoot (1986) criteria for assigned sample

Ambenali Ghat

Elev. M asl	311	372	467	538	634	634	641	682	695	720	750	777	785
wt. %	PMagPMh14	PMag03PMh15	PMag03PMh16	PMag03PMh17	AG13	AG13	PMag03PMh18	PMagPMh1	PMagPMh2	PMagPMh3	No disk	PMagPMh5	No disk
SiO2	50.06	48.47	47.13	48.95	49.33	49.23	48.77	49.38	48.17	48.53		47.69	
TiO2	2.129	1.899	2.495	3.594	2.053	2.046	2.728	2.215	2.411	2.537		2.609	
Al2O3	14.15	14.47	13.31	13.23	16.28	16.26	14.66	14.37	13.61	13.36		12.97	
Fe2O3	12.70	14.27	15.16	15.82	12.16	12.13	14.65	12.96	15.69	15.45		17.40	
MnO	0.311	0.216	0.223	0.210	0.146	0.149	0.215	0.220	0.204	0.217		0.211	
MgO	6.48	5.77	5.85	5.60	5.38	5.35	5.66	6.60	6.26	6.80		5.90	
CaO	10.27	11.10	11.74	10.08	10.31	10.32	10.75	11.44	10.50	10.36		10.09	
Na2O	2.32	2.45	2.26	2.42	2.43	2.45	2.44	2.23	2.21	2.21		2.18	
K2O	0.47	0.41	0.25	0.37	0.54	0.55	0.14	0.31	0.15	0.27		0.36	
P2O5	0.208	0.162	0.234	0.346	0.194	0.191	0.247	0.200	0.208	0.223		0.223	
LOI	0.57	0.61	1.25	-0.18	1.01	1.01	0.05	0.30	0.83	0.27		0.74	
Total	99.67	99.83	99.90	100.44	99.82	99.69	100.32	100.21	100.24	100.23		100.36	
	spare	PMag03PMh15	PMag03PMh16	PMag03PMh17	spare	AG13	no pellet	PMagPmh1	PMagPmh2	PMagPmh3	PMagPmh4	PMagPmh5	PMagPmh6
Rb		10	3	6		9		10	2	3	3	25	3
Sr		206	216	223		235		221	205	196	209	190	206
Y		28.2	35.0	48.4		37.4		29.0	37.7	34.7	36.7	38.4	32.5
Zr		117	153	232		166		124	137	145	149	147	140
Nb		8.2	11.2	14.3		11.3		11.4	9.8	10.5	11.1	10.9	11.0
Ba		75	77	95		54		79	75	77	80	101	80
Pb		0	6	2		3		4	1	1	3	4	4
Th		1	3	2		4		1	3	1	2	0	1
U		0	0	0		2		0	0	0	0	0	0
Sc		39	40	40		36		38	41	40	41	41	35
V		367	421	553		462		372	415	441	419	415	383
Cr		117	71	127		154		213	108	114	126	116	200
Co		44	44	38		38		46	49	47	47	42	46
Ni		72	67	83		84		119	80	86	82	80	108
Cu		165	228	345		222		147	237	200	221	204	189
Zn		109	115	138		105		96	107	113	114	112	101
Ga		20	22	26		25		22	22	23	22	22	21
Mo		0	0	0		0		0	0	0	0	0	0
As		8	0	0		4		0	1	2	3	1	1
S		54	35	35		47		54	83	61	47	51	58
Fm. criteria													
Sr		**206**	**216**	**223**		**235**		**221**	**205**	196	**209**	190	**206**
Ba		**75**	**77**	**95**		**54**		**79**	**75**	**77**	**80**	101	**80**
Ba/Y		**2.66**	**2.21**	**1.97**		**1.44**		**2.71**	**1.99**	**2.23**	**2.19**	**2.63**	**2.46**
Zr/Nb		**14.21**	**13.68**	16.24		**14.73**		**10.87**	**14.02**	**13.82**	**13.45**	**13.48**	12.75
	Poladpur	Ambenali Fm.	Ambenali Fm.	Ambenali Fm.		Ambenali Fm.		Ambenali Fm.	Ambenali Fm.	Ambenali Fm.	Ambenali Fm.	Ambenali Fm.	Ambenali Fm.

Ambenali Ghat

Elev. M asl	847	900	930	938	950	957	982	998	1022	1040 (vesic.structure)	1040	1055
wt. %	PMagPMh7	PMagPMh8	no disk	PMagPMh10		PMhx3	PMagPMh12	PMagPMh13	PMagPMh14	Mh2	Mh1	PMagPMh15
SiO2	48.95	48.34		47.68		47.43	49.87	49.88	48.92	47.76	48.42	49.10
TiO2	2.712	3.393		4.255		3.180	2.106	2.178	3.315	3.377	3.279	3.356
Al2O3	13.56	12.47		12.33		15.97	14.39	14.34	13.01	13.07	12.88	12.77
Fe2O3	15.69	16.75		17.63		15.19	13.39	12.89	16.85	16.59	16.23	16.54
MnO	0.208	0.233		0.213		0.156	0.179	0.175	0.222	0.244	0.222	0.228
MgO	5.98	5.79		5.26		4.70	5.44	6.24	4.91	4.79	5.28	4.89
CaO	10.68	9.42		9.25		6.91	10.12	10.49	9.46	8.73	9.07	9.69
Na2O	2.43	2.64		2.45		1.49	2.60	2.63	2.50	2.46	2.40	2.62
K2O	0.20	0.41		0.52		0.28	0.81	0.38	0.59	0.57	0.62	0.41
P2O5	0.244	0.281		0.418		0.303	0.225	0.237	0.342	0.352	0.331	0.343
LOI	0.35	0.05		0.13		4.56	1.03	0.89	0.46	1.81	2.12	0.59
Total	101.01	99.76		100.13		100.17	100.16	100.33	100.58	99.76	100.85	100.54
	PMagPmh7	PMagPMh8	PMagPMh9	PMagPMh10	PmagPMh11	PMhx3	PMagPMh12	PMagPMh13	PMagPMh14	Mh2	Mh1	PMagPMh15
Rb	2	7	11	7	Sample not analysed	16	31	13	23	13	11	18
Sr	232	212	225	264		218	292	296	251	252	238	246
Y	36.0	45.0	48.4	49.2		37.5	27.6	28.6	42.2	43.9	42.7	44.1
Zr	157	206	219	255		198	155	157	222	226	223	230
Nb	12.8	17.0	17.4	27.9		21.2	15.6	15.8	21.5	22.3	22.0	22.3
Ba	104	121	105	186		215	210	193	201	225	210	187
Pb	3	3	5	3		4	5	2	4	3	4	4
Th	2	1	2	3		5	3	3	3	2	4	5
U	1	1	0	2		2	0	2	0	1	2	1
Sc	39	39	41	40		34	35	30	40	39	38	35
V	414	492	480	463		338	296	286	417	387	407	434
Cr	64	95	85	46		152	263	242	78	70	80	85
Co	45	41	42	42		33	42	42	38	39	42	39
Ni	74	71	72	70		85	119	125	56	60	57	57
Cu	200	529	316	337		211	147	149	237	267	236	278
Zn	121	137	135	166		126	105	95	127	122	124	135
Ga	22	26	25	26		27	20	21	23	25	26	25
Mo	0	0	0	0		0	0	0	0	0	0	0
As	0	6	4	4		0	3	0	0	0	0	2
S	69	35	57	173		111	82	44	54	74	44	68
Fm. criteria												
Sr	232	212	225	264		218	292	296	251	252	238	246
Ba	104	121	105	186		215	210	193	201	225	210	187
Ba/Y	2.89	2.68	2.17	3.77		5.74	7.62	6.74	4.76	5.125	4.925	4.25
Zr/Nb	12.28	12.12	12.56	9.13		9.34	9.93	9.92	10.31	10.121	10.141	10.30
	Ambenali Fm.	Ambenali Fm.	Ambenali Fm.	M'war Fm.		M'war Fm.	M'war Fm.	M'war Fm.	M'war Fm.	M'war Fm.	M'war	M'war

Ambenali Ghat

Elev. M asl	1055	1058	1090	1090	1092	1185	1254
wt. %	spare	PMagPMh16	Mh4	Mh3	PMagPMh17	PMagPMh18	Mh5
SiO2		49.44	48.42	49.29	49.93	49.57	47.94
TiO2		3.128	3.037	3.133	3.182	2.438	2.205
Al2O3		13.92	13.22	13.49	13.49	14.37	15.21
Fe2O3		15.14	16.52	14.81	14.97	14.18	13.38
MnO		0.189	0.215	0.246	0.205	0.219	0.209
MgO		4.75	5.21	4.29	5.75	5.79	6.13
CaO		9.57	9.67	8.83	10.30	10.96	11.09
Na2O		2.58	2.38	2.34	2.53	2.39	2.14
K2O		0.55	0.60	1.04	0.41	0.26	0.13
P2O5		0.330	0.294	0.293	0.301	0.243	0.199
LOI		0.44	0.70	1.19	-0.13	0.32	1.55
Total		100.04	100.27	98.95	100.95	100.74	100.18
	PMagPMh15	PMagPMh16	Mh4	Mh3	PMagPMh17	PMagPMh18	Mh5
Rb	16	8	30	49	10	8	2
Sr	245	245	227	228	232	228	225
Y	44.8	42.6	41.8	42.5	41.3	33.7	41.9
Zr	229	217	191	198	194	161	128
Nb	22.4	19.6	17.4	17.5	17.3	13.6	10.8
Ba	190	190	188	170	155	122	89
Pb	4	3	3	1	5	4	3
Th	3	3	2	2	0	3	0
U	0	1	1	0	2	0	2
Sc	41	37	36	38	38	38	39
V	431	417	411	445	440	378	368
Cr	85	127	139	148	141	143	184
Co	40	38	35	32	38	41	42
Ni	57	67	73	69	75	79	95
Cu	278	255	246	350	241	194	180
Zn	134	123	116	120	120	107	97
Ga	23	26	22	24	24	22	22
Mo	0	0	0	0	0	0	0
As	2	1	4	1	0	0	0
S	67	58	37	66	54	85	41
Fm. criteria							
Sr	245	245	227	228	232	228	225
Ba	190	190	188	170	155	122	89
Ba/Y	4.23	4.47	4.490	4.00	3.75	3.61	2.11
Zr/Nb	10.24	11.06	10.966	11.31	11.24	11.85	11.83
	M'war	Mwar/Amb	M'war	M'war	Ambenali like	Ambenali like	Ambenali like

C3 Geochemical analyses of Tapola Road samples

C3 Tapola Road

Elev. M	703	745	760	830	830	830	832	856	896	945	962	977	977
Gbst section	Tapola road	Tapola road	Tapola road	Tapola road	Tapola road	Tapola road	Tapola road	Tapola road	Tapola road	Tapola road	Tapola road	Tapola road	Tapola road
Wt. %	**TMh1**	**PMagTMh11**	**TMh2**	**TMh5**	**TMh5a**	**TMh4**	**PMagTMh14**	**PMagTMh15**	**PMagTMh16**	**PMagTMh17**	**PMagTMh18**	**PMagTMh8**	**PMagTMh8**
SiO2	48.02	48.35	47.88	47.54	49.12	45.11	48.99	47.89	49.27	49.03	49.10	49.19	49.13
TiO2	2.583	2.625	2.821	3.749	2.374	3.087	2.602	3.901	2.184	2.783	3.282	3.215	3.190
Al2O3	13.37	13.52	13.36	13.01	14.47	12.65	13.88	12.99	14.33	13.55	13.22	13.14	13.20
Fe2O3	15.26	15.87	15.45	16.26	13.89	15.49	15.42	15.89	12.12	15.60	16.37	16.26	16.27
MnO	0.211	0.209	0.193	0.177	0.190	0.199	0.222	0.218	0.158	0.211	0.233	0.223	0.226
MgO	6.42	6.14	6.01	5.13	6.13	5.50	5.92	5.09	6.60	5.86	5.16	5.12	5.08
CaO	10.70	10.25	10.36	8.69	10.44	9.95	10.36	9.69	11.04	10.09	9.59	9.55	9.56
Na2O	2.29	2.40	2.37	2.03	2.37	2.14	2.41	2.61	2.26	2.40	2.50	2.61	2.58
K2O	0.16	0.29	0.31	0.86	0.47	0.13	0.21	0.38	0.22	0.30	0.50	0.64	0.64
P2O5	0.228	0.227	0.260	0.351	0.240	0.258	0.247	0.379	0.225	0.272	0.335	0.332	0.329
LOI	0.48	0.54	1.15	2.15	0.31	1.61	0.00	-0.26	1.41	0.39	-0.06	0.03	0.03
Total	99.71	100.42	100.14	99.95	100.00	96.13	100.26	98.77	99.82	100.49	100.23	100.32	100.21
	TMh1	**PMagTMw11**	**TMh2**	**TMh5**	**TMh5a**	**TMh4**	**PMagTMh14**	**PMag TMh15**	**PMag TMh16**	**PMagTMh17**	**PMagTMh18**	**PMagTMh8**	**PMagTMh8**
Rb	1	4	4	14	8	1	7	14	5	8	8	14	spare
Sr	216	229	238	217	234	230	227	278	318	275	258	250	
Y	37.2	33.7	37.5	51.4	34.4	42.8	36.8	46.5	25.3	37.3	43.6	43.7	
Zr	150	150	167	226	161	192	162	245	147	180	219	221	
Nb	11.2	12.8	14.3	18.6	14.0	14.4	10.8	25.2	15.5	16.0	21.7	22.3	
Ba	86	89	110	210	145	84	103	170	126	161	207	196	
Pb	5	2	2	1	5	6	4	5	1	3	4	5	
Th	2	3	3	3	5	3	0	4	1	2	4	0	
U	1	0	1	2	1	0	0	1	0	1	1	0	
Sc	40	33	37	43	38	40	36	36	33	39	37	37	
V	428	401	404	435	369	447	417	429	330	375	414	428	
Cr	120	59	99	90	141	202	75	106	499	148	79	87	
Co	50	48	40	39	43	42	43	36	38	40	39	38	
Ni	100	74	81	78	78	80	72	60	113	80	58	61	
Cu	234	210	255	238	196	233	253	314	154	239	268	306	
Zn	113	110	114	130	108	132	109	144	97	114	127	133	
Ga	23	22	23	26	22	24	24	25	23	23	23	24	
Mo	0	0	0	1	0	0	0	0	0	0	0	0	
As	1	0	0	5	3	1	1	0	2	0	6	2	
S	37	43	37	81	61	80	50	30	130	41	45	64	
Fm. Criteria													
Sr	**216**	**229**	**238**	**217**	**234**	**230**	**227**	**278**	**318**	**275**	**258**	**250**	
Ba	**86**	**89**	110	**210**	**145**	**84**	103	**170**	**126**	**161**	**207**	**196**	
Ba/Y	**2.3**	**2.63**	**2.92**	**4.09**	**4.21**	**1.96**	**2.79**	3.65	**4.98**	**4.32**	**4.75**	**4.48**	
Zr/Nb	**13.4**	**11.70**	**11.66**	**12.12**	**11.46**	**13.32**	**14.99**	**9.73**	**9.48**	11.24	**10.08**	9.92	
	Ambenali Fm.	**Ambenali Fm.**	**Ambenali Fm.**	**Ambenali Fm.***	**Ambenali Fm.***	**Ambenali Fm.**	**Ambenali Fm.**	**M'war Fm.**	**M'war Fm.**	**M'war Fm.**	**M'war Fm.**	**M'war Fm.**	

Tapola Road

Elev. M	1001	1004	1136	1136	1174	1215	1215
Tapola road	Tapola road	Tapola road	Tapola road	Tapola road	Tapola road	Tapola road	Tapola road
Wt. %	**PMagTMh6**	**PMagTMh5**	**PMagTMh4**	**PMagTMh4**	**PMagTMh2**	**PMagTMh1**	**TMh7**
SiO2	49.03	broke	49.48	49.09	49.50	49.05	48.54
TiO2	3.261		2.417	2.696	2.355	2.492	2.404
Al2O3	13.25		14.37	13.55	15.51	14.39	14.35
Fe2O3	15.83		14.17	15.84	12.73	14.15	13.82
MnO	0.224		0.242	0.204	0.193	0.232	0.241
MgO	5.06		5.81	6.28	5.51	5.89	5.96
CaO	9.72		10.53	10.68	11.08	10.89	11.03
Na2O	2.49		2.41	2.39	2.57	2.27	2.31
K2O	0.41		0.55	0.24	0.27	0.22	0.21
P2O5	0.325		0.253	0.232	0.231	0.234	0.228
LOI	0.39		0.35	0.09	0.34	0.43	0.52
Total	99.99		100.57	101.29	100.31	100.26	99.62
	PMagTMh6	**PMagTMh5**	**PMagTMh4**	**PMagTMh4**	**PMagTMh2**	**PMagTMh1**	**TMh7**
Rb	11	21	14	spare	9	1	3
Sr	257	228	229		237	225	232
Y	45.4	49.4	34.3		33.7	35.8	35.2
Zr	221	229	171		156	157	155
Nb	21.1	20.2	14.3		12.2	13.0	12.8
Ba	199	208	154		122	120	138
Pb	4	2	4		0	3	3
Th	2	2	2		1	0	3
U	1	0	2		1	0	0
Sc	39	39	38		37	40	41
V	436	429	353		381	386	366
Cr	86	122	137		185	130	142
Co	41	35	43		36	42	40
Ni	59	63	75		79	78	80
Cu	265	252	209		207	190	185
Zn	130	128	109		100	104	101
Ga	25	21	21		22	21	22
Mo	0	0	0		0	0	0
As	0	0	2		1	3	0
S	74	58	70		47	56	34
Fm. Criteria							
Sr	257	228	229		237	225	232
Ba	199	208	154		122	120	138
Ba/Y	4.39	4.21	4.50		3.61	3.35	3.92
Zr/Nb	10.46	11.33	11.99		12.82	12.05	12.07
	M'war Fm.	Amb/Mwar	Amb/Mwar		Ambenali like	Ambenali like	Ambenali like

C4 Geochemical analysis of the Kelgar Road samples

C4 Kelgar Road

Elev. M asl	772	789	803	834	861	908	919	935	935	936	945	953	967	951
Wt. %	PMagKmw1	PMagKmw2	PMagKmw3	PMagKmw4	PMagKmw5	PmagKMw6	KMh1	PMagKmw8	PMagKmw8	KMh2	03kMh2	PMagKmw9	PMagKmw7	03kMh1
SiO2	48.24	47.81		48.98			48.50	49.53	49.40	48.46	49.01	49.17	45.14	48.24
TiO2	2.403	2.776		3.210			2.443	2.062	2.065	2.079	3.127	2.501	2.502	2.724
Al2O3	13.35	13.37		12.98			15.12	13.39	13.35	13.02	14.52	13.55	14.04	14.58
Fe2O3	14.55	15.25		15.72			12.73	12.85	12.81	12.79	14.97	13.27	14.34	14.09
MnO	0.230	0.229		0.235			0.167	0.268	0.268	0.265	0.219	0.227	0.211	0.179
MgO	6.65	6.22		5.89			5.19	7.84	7.83	7.31	5.22	5.80	7.78	5.68
CaO	10.99	10.53		10.24			9.41	10.76	10.68	10.57	9.73	10.49	9.87	9.96
Na2O	2.51	2.63		2.60			2.43	2.26	2.28	2.24	2.48	2.53	1.95	2.36
K2O	0.20	0.31		0.30			0.31	0.48	0.48	0.42	0.36	0.40	0.33	0.20
P2O5	0.210	0.252		0.288			0.251	0.225	0.229	0.221	0.323	0.282	0.230	0.280
LOI	0.58	0.69		0.02			2.12	0.48	0.48	1.44	0.31	1.93	3.45	1.73
Total	99.92	100.06		100.47			98.67	100.14	99.88	98.81	100.26	100.15	99.86	100.02
	PMagKmw1	PMagKmw2	PMagKmw3	PMagKmw4	PMagKmw5	PmagKMw6	KMh1	PMagKmw8	PMagKmw8	KMh2	03kMh2	PMagKmw9	PMagKmw7	03kMh1
Rb	1	3	3	4	10	not made	3	5	Spare	7	11	17	7	2
Sr	221	237	231	233	252		320	309		306	250	297	235	310
Y	31.3	35.1	35.0	43.9	28.6		32.3	28.3		26.6	44.0	34.2	29.8	34.6
Zr	140	160	161	201	140		161	152		150	213	192	160	177
Nb	12.1	14.4	14.2	16.6	14.3		17.0	15.3		13.2	19.7	19.5	15.1	19.0
Ba	84	95	106	120	167		207	194		200	183	213	159	156
Pb	2	1	3	4	3		2	3		2	4	5	4	2
Th	1	4	1	2	0		2	0		4	4	4	2	3
U	0	0	2	1	0		1	0		2	1	0	0	0
Sc	38	39	37	38	31		28	34		32	34	34	36	31
V	399	410	416	449	326		306	333		327	413	328	267	375
Cr	201	103	99	104	498		306	390		439	144	183	438	384
Co	50	41	45	38	50		38	46		50	35	42	48	35
Ni	105	86	87	78	184		96	136		137	75	112	160	98
Cu	205	187	310	282	150		163	134		123	263	175	151	181
Zn	106	114	116	129	110		106	100		110	116	111	122	121
Ga	22	23	23	24	19		25	20		21	24	21	24	25
Mo	0	0	0	0	0		0	0		0	0	0	0	0
As	1	1	0	0	0		2	0		0	1	6	2	4
S	58	44	73	54	57		61	52		41	33	78	135	87
Fm. criteria														
Sr	221	237	231	233	252		320	309		306	250	297	235	310
Ba	84	95	106	120	167		207	194		200	183	213	159	156
Ba/Y	2.69	2.72	3.04	2.74	5.83		6.396	6.84		7.504	4.17	6.22	5.32	4.51
Zr/Nb	11.53	11.14	11.35	12.08	9.80		9.471	9.95		11.326	10.82	9.84	10.58	9.32
	Ambonali Fm.	Ambonali Fm.	Ambonali Fm.*	Ambonali Fm.*	M'war Fm.		M'war Fm.	M'war Fm.		M'war Fm.	M'war Fm.	M'war Fm.	M'war Fm.*	M'war Fm.

Kelgar Road

Elev. M asl	984	1017	1045	1061	1092	1150	1175	1202	1211	1215	1215
Wt. %	PMagKmw10	PMagKmw11	PMagKmw12	PMagKmw13	PMagKmw14	PMagKmw15	PMagKmw16	PMagKMW17	PMagKmw18	PMagKMW19	KMh3
SiO2	49.53	48.54	49.43	49.87	49.74	49.55	49.29	47.57	49.05	49.76	48.67
TiO2	3.268	3.280	3.105	3.072	3.162	2.225	2.370	2.569	2.740	2.626	2.527
Al2O3	13.18	13.11	13.85	13.94	13.34	14.33	14.69	14.06	14.46	14.50	14.52
Fe2O3	16.16	16.23	15.24	14.71	15.06	13.60	13.98	15.31	14.12	14.51	13.93
MnO	0.237	0.225	0.203	0.216	0.205	0.203	0.196	0.204	0.199	0.208	0.204
MgO	4.92	5.11	5.02	5.24	5.83	6.01	5.77	5.51	5.20	5.50	5.49
CaO	9.12	9.59	9.60	9.77	10.17	11.25	11.04	9.93	10.69	10.44	10.67
Na2O	2.48	2.96	2.70	2.58	2.50	2.33	2.55	2.10	2.36	2.33	2.46
K2O	0.72	0.54	0.49	0.49	0.30	0.27	0.27	0.23	0.30	0.38	0.34
P2O5	0.352	0.328	0.333	0.333	0.305	0.209	0.234	0.270	0.271	0.275	0.253
LOI	1.06	0.29	0.30	0.34	0.44	0.32	0.15	2.56	0.75	0.93	0.41
Total	101.05	100.20	100.28	100.57	101.06	100.30	100.56	100.32	100.13	101.46	99.50
	PMagKmw10	PMagKmw11	PMagKmw12	PMagKmw13	PMagKmw14	PMagKmw15	PMagKmw16	PMagKMW17	PMagKmw18	PMagKMW19	KMh3
Rb	4	14	6	16	10	11	5	9	11	16	11
Sr	258	256	243	244	230	226	225	219	222	233	234
Y	32.5	44.6	45.1	42.1	40.3	30.4	32.8	34.8	39.2	37.6	37.3
Zr	163	222	217	216	198	136	150	158	183	177	172
Nb	16.4	21.6	19.0	19.6	16.5	12.5	13.0	12.7	14.8	14.2	14.0
Ba	165	208	181	166	139	80	140	97	124	166	120
Pb	4	4	5	4	4	0	2	2	3	4	4
Th	5	4	1	2	2	2	3	2	2	2	2
U	1	1	0	2	0	2	2	0	1	1	0
Sc	35	37	37	34	37	38	35	38	38	39	35
V	391	409	417	412	454	396	362	381	417	399	383
Cr	149	80	133	148	141	139	141	285	121	126	139
Co	41	38	40	35	41	43	42	44	40	37	41
Ni	72	57	70	71	76	91	77	98	73	77	84
Cu	199	322	267	245	237	160	196	178	251	220	215
Zn	100	134	122	117	121	102	103	110	119	117	109
Ga	21	23	24	25	24	21	21	21	21	22	23
Mo	0	0	0	0	0	0	0	0	0	0	0
As	1	0	3	0	0	2	3	0	0	0	0
S	53	49	49	46	47	48	59	55	74	32	38
Fm. criteria											
Sr	258	256	243	244	230	226	225	219	222	233	234
Ba	165	208	181	166	139	80	140	97	124	166	120
Ba/Y	5.09	4.66	4.00	3.94	3.46	2.63	4.25	2.78	3.16	4.43	3.225
Zr/Nb	9.95	10.28	11.44	11.02	11.99	10.84	11.56	12.46	12.37	12.44	12.300
	M'war Fm.	M'war Fm.	Amb/Mwar	Amb/Mwar	Amb like	Amb like	Amb/Mwar	Amb like	Amb like	Amb/Mwar	Amb like

C5 Geochemical analysis of the Wai Panchgani Road samples

C5 Wai-Panchgani

Elev. M	818	824	824	841	864	877	905	918	851	970	980	996	1036	1072
Wt. %	PMagWP1	PMagWP2	PmagWP2	PMagWP3	PMagWP4	PMagWP5	PmagWP6	PMagWP7	PMagWP8	PMagWP9	PMagWP10	PMagWP11	PMagWP12	PMagWP13
SiO2	48.42	48.43	48.38	48.11	47.53	47.79	48.84	49.39	50.13	49.28	48.14	50.58	48.07	48.61
TiO2	2.820	2.351	2.337	2.879	2.788	2.875	3.178	2.471	2.451	2.538	2.514	2.043	2.672	3.248
Al2O3	13.23	13.99	13.96	13.19	13.08	13.28	13.08	14.73	14.31	13.66	13.35	13.15	15.32	13.07
Fe2O3	16.36	14.34	14.31	16.61	15.52	15.75	15.82	13.28	13.06	13.20	13.68	12.60	14.21	16.56
MnO	0.203	0.215	0.215	0.217	0.226	0.200	0.234	0.196	0.198	0.202	0.165	0.189	0.149	0.224
MgO	5.87	6.85	6.82	6.04	6.30	6.30	5.88	6.25	6.12	6.49	6.20	7.82	4.74	5.03
CaO	10.06	11.00	10.90	10.47	10.79	10.60	10.22	10.81	10.53	9.89	10.06	10.67	9.73	9.61
Na2O	2.38	2.29	2.26	2.87	2.27	2.34	2.41	2.39	2.55	2.54	2.49	2.27	2.40	2.55
K2O	0.31	0.23	0.24	0.28	0.21	0.24	0.32	0.34	0.37	0.59	0.68	0.56	0.21	0.40
P2O5	0.237	0.207	0.202	0.246	0.249	0.251	0.286	0.223	0.254	0.293	0.295	0.225	0.251	0.328
LOI	0.61	0.40	0.40	0.10	1.69	0.89	-0.05	0.38	0.69	0.68	2.50	0.44	2.43	0.28
Total	100.50	100.32	100.01	101.01	100.66	100.51	100.22	100.45	100.66	99.37	100.06	100.56	100.20	99.91
	PMagWp1	PMagWP2	spare	PMagWP3	PMagWP4	PMagWP5	PMagWP6	PMagWP7	PMagWP8	PMagWP9	PMagWP10	PMagWP11	PmagWP12	PmagWP13
Rb	4	2		2	3	2	5	6	8	12	11	12	5	12
Sr	217	222		224	237	240	232	266	288	318	327	284	306	254
Y	38.1	31.0		37.5	35.3	34.7	42.3	28.6	30.8	30.5	30.4	24.6	33.5	41.8
Zr	160	137		165	162	165	195	138	156	180	176	147	176	220
Nb	12.1	11.0		13.5	13.8	15.2	15.3	15.1	16.0	17.3	16.9	14.4	16.2	20.4
Ba	88	86		96	85	89	109	113	164	190	205	178	117	193
Pb	2	1		5	4	3	4	1	4	4	2	3	2	5
Th	2	0		1	4	3	4	3	5	2	2	2	2	3
U	1	0		1	0	0	1	1	2	2	0	1	1	0
Sc	42	37		41	33	36	42	36	36	31	35	30	35	35
V	416	395		432	388	395	445	366	326	337	316	306	347	429
Cr	81	186		55	101	148	102	159	246	284	387	410	218	83
Co	47	46		46	42	44	41	44	40	47	40	47	38	41
Ni	74	104		80	88	93	76	101	107	128	117	137	69	57
Cu	210	179		246	183	239	202	167	175	172	145	141	230	296
Zn	125	102		119	103	115	123	99	101	109	108	96	121	139
Ga	24	22		23	22	23	22	23	23	22	23	19	25	24
Mo	0	0		0	0	0	0	0	0	0	0	0	0	0
As	0	4		0	7	0	0	3	0	0	1	0	0	0
S	54	51		42	47	48	49	63	68	63	233	52	109	26
Fm. criteria														
Sr	217	222		224	237	240	232	266	288	318	327	284	306	254
Ba	88	86		96	85	89	109	113	164	190	205	178	117	193
Ba/Y	2.31	2.76		2.55	2.41	2.57	2.58	3.93	5.33	6.22	6.75	7.22	3.48	4.62
Zr/Nb	13.22	12.41		12.21	11.76	10.87	12.76	9.15	9.74	10.41	10.40	10.22	10.85	10.77
Fm.	Ambenali Fm.	Ambenali Fm.		Ambenali Fm.	Ambenali Fm.	Ambenali Fm.	Ambenali Fm.	M'war Fm.	M'war Fm.	M'war Fm.	M'war Fm.	M'war Fm.	M'war Fm.*	M'war Fm.

Wai-Panchgani

Elev. M	1098	1152	1181	1198
Sample	PMagWP14		PMagWP16	PMagWP17
SiO2	48.62		49.50	48.06
TiO2	3.369		2.201	2.289
Al2O3	13.83		14.44	14.46
Fe2O3	15.84		13.67	14.43
MnO	0.206		0.184	0.204
MgO	5.23		6.50	6.13
CaO	9.84		11.19	11.33
Na2O	2.47		2.35	2.13
K2O	0.46		0.27	0.18
P2O5	0.349		0.207	0.217
LOI	0.00		0.15	0.89
Total	100.21		100.67	100.32

	PMagWP14	PMagWP15	PMag WP16	PMagWP17
Rb	6	12	2	8
Sr	246	227	217	225
Y	45.6	36.4	29.1	31.6
Zr	230	169	130	138
Nb	20.8	14.4	11.7	11.9
Ba	173	158	92	73
Pb	5	3	0	2
Th	2	1	2	3
U	1	0	0	0
Sc	38	41	35	39
V	438	393	360	378
Cr	121	132	144	134
Co	35	38	42	40
Ni	60	72	95	85
Cu	296	211	172	194
Zn	122	119	99	107
Ga	26	23	22	22
Mo	0	0	0	0
As	3	1	2	0
S	49	34	63	52
Fm. criteria				
Sr	246	227	217	225
Ba	173	158	92	73
Ba/Y	3.79	4.34	3.17	2.31
Zr/Nb	11.06	11.73	11.13	11.63
Fm.	Amb/M'war	Amb/M'war	Amb like	Amb like

C6 Geochemical analysis of Varandah Ghat samples

C6 Varandah Ghat

Elev. M	16	62	92	115	119	129	133	157	181	205	218	236	278
	PMag03VG1	PMag03VG2	PMag03VG3	PMag03VG4	PMag03VG5	PMag03VG6	PMag03VG7	PMag03VG8	PMag03VG17	PMag03VG16	PMag03VG15	PMag03VG14	PMag03VG13
SiO2	49.28	51.55	51.08	46.89	49.41	48.89	50.33	49.88	51.28	50.73	50.77	50.70	48.35
TiO2	2.520	1.396	1.325	1.205	1.178	1.217	1.317	1.337	1.103	1.117	1.089	2.056	2.136
Al2O3	13.86	14.59	15.15	14.41	15.54	14.64	15.04	15.07	14.69	15.09	15.33	13.89	13.90
Fe2O3	14.87	10.92	11.47	11.13	11.05	11.70	11.39	11.48	11.30	11.30	10.99	14.39	15.85
MnO	0.207	0.138	0.166	0.190	0.154	0.186	0.141	0.172	0.159	0.193	0.149	0.206	0.202
MgO	5.09	6.75	6.27	5.85	6.16	7.19	6.72	6.65	7.07	7.03	6.42	5.76	5.91
CaO	9.77	10.52	10.36	13.58	9.88	10.66	10.10	11.03	11.23	10.64	9.57	10.16	10.54
Na2O	2.60	2.21	2.37	2.63	2.06	2.25	2.43	2.44	2.06	2.25	2.21	2.45	2.26
K2O	0.28	0.54	0.55	0.82	0.93	0.43	0.83	0.28	0.42	0.50	1.80	0.40	0.36
P2O5	0.246	0.130	0.135	0.125	0.122	0.129	0.134	0.127	0.106	0.116	0.114	0.186	0.183
LOI	0.75	1.26	1.22	0.11	1.83	4.57	1.79	1.41	0.86	1.28	1.89	0.03	0.56
Total	99.47	100.01	100.09	96.95	98.31	101.88	100.21	99.88	100.28	100.24	100.31	100.23	100.25
	PMag03VG1	PMag03VG2	PMag03VG3	PMag03VG4	PMag03VG5	PMag03VG6	PMag03VG7	PMag03VG8	PMag03VG17	PMag03VG16	PMag03VG15	PMag03VG14	PMag03VG13
Rb	2	14	11	21	10	48	21	4	9	9	66	11	16
Sr	284	179	161	141	160	104	153	173	160	160	154	213	219
Y	37.4	27.1	27.9	25.7	26.0	23.6	26.4	27.0	30.7	25.5	24.1	33.5	31.1
Zr	186	107	114	105	106	103	115	113	82	98	95	145	130
Nb	11.0	6.4	6.4	5.3	5.2	5.3	5.5	7.1	5.9	5.5	5.8	9.9	8.0
Ba	227	106	148	168	118	158	170	121	129	137	451	144	67
Pb	3	4	5	3	5	3	3	4	2	3	2	5	2
Th	0	5	1	3	2	3	5	3	0	2	3	2	1
U	0	1	0	1	0	0	1	0	0	2	0	0	0
Sc	36	39	32	33	30	27	33	32	43	34	35	38	40
V	354	296	277	259	246	248	271	283	289	273	270	393	397
Cr	173	646	188	329	396	330	269	317	323	354	308	137	54
Co	39	38	42	42	46	43	40	45	42	42	39	38	46
Ni	51	94	93	109	148	123	113	111	83	117	104	64	60
Cu	175	114	116	104	111	102	124	127	126	125	122	196	168
Zn	110	81	76	81	78	82	87	83	79	76	78	110	110
Ga	23	19	18	16	19	18	21	21	18	20	18	22	21
Mo	0	0	0	0	0	0	0	0	0	0	0	0	0
As	1	5	4	5	2	6	2	1	6	1	3	3	4
S	55	248	57	104	86	126	86	93	101	86	84	41	61
Fm. criteria													
Sr	284	179	161	141	160	104	153	173	160	160	154	213	219
Ba	227	106	148	168	118	158	170	121	129	137	451	144	67
Ba/Y	6.07	3.89	5.32	6.54	4.53	6.68	6.45	4.48	4.21	5.36	18.69	4.30	2.14
Zr/Nb	16.86	16.64	17.80	19.74	20.38	19.36	20.89	15.87	13.95	17.85	16.34	14.61	16.26
Formation	Bushe Fm.*	Bushe Fm.*	Bushe Fm.*	Bushe Fm.*	Bushe Fm.*	Bushe Fm.*	Bushe Fm.*	Bushe Fm.*	Bushe Fm.*	Bushe Fm.*	unique	Poladpur Fm.*	Poladpur Fm.*

	PMagVG12	VG12C	BhG9	PMag03VG11	02BhG8	02BhG8	02BhG7	02BhG6	02BhG5	02BhG4	02BhG3	02BhG2	PMagVG10
SiO2	47.96	50.48	50.96	50.75	49.41	49.49	49.63	50.15	49.51	48.98	48.14	48.44	48.02
TiO2	2.750	1.465	1.759	1.831	1.844	1.819	2.091	2.300	2.283	2.452	3.054	2.580	2.439
Al2O3	12.93	14.49	14.40	14.52	14.36	14.38	13.96	14.20	14.28	12.50	11.65	13.29	13.27
Fe2O3	16.52	12.21	11.96	12.43	12.00	11.95	12.47	12.41	12.35	16.47	18.76	16.41	16.22
MnO	0.195	0.163	0.177	0.168	0.191	0.191	0.192	0.172	0.168	0.238	0.237	0.240	0.264
MgO	5.94	6.74	6.58	6.75	6.30	7.25	7.10	6.49	6.42	5.39	4.71	5.60	6.09
CaO	10.11	9.62	10.65	10.86	11.52	11.50	11.10	10.77	10.83	10.12	9.17	10.45	10.37
Na2O	2.50	2.13	2.50	2.35	2.19	2.20	2.34	2.49	2.51	2.37	2.22	2.30	2.14
K2O	0.35	0.41	0.36	0.44	0.20	0.20	0.17	0.36	0.38	0.26	0.38	0.22	0.35
P2O5	0.244	0.170	0.192	0.185	0.179	0.179	0.193	0.222	0.216	0.222	0.255	0.249	0.231
LOI	0.45	1.96	1.20	0.21	0.64	0.64	0.51	1.04	0.56	0.57	1.26	0.07	0.59
Total	99.96	99.82	100.73	100.49	98.84	99.81	99.73	100.60	99.50	99.57	99.83	99.84	99.98

	PMagVG12	VG12C	BhG9	Pmag03VG11	02BhG8	02BhG8	02BhG7	02BhG6	02BhG5	02BhG4	02BhG3	02BhG2	PMagVG10
Rb	3	9	15	6		2	1	5	6	9	18	3	9
Sr	224	271	207	211		223	220	225	224	203	202	195	185
Y	38.7	26.1	31.8	32.0		31.1	33.3	35.1	33.7	39.9	43.7	41.0	36.1
Zr	177	119	136	132		131	138	152	151	164	195	167	156
Nb	11.8	8.1	9.1	8.8		8.5	10.6	11.7	11.3	11.2	12.8	11.4	9.9
Ba	110	148	169	155		114	114	135	133	107	127	101	101
Pb	4	6	5	3		2	2	2	4	3	3	1	3
Th	4	4	2	1		4	1	4	3	4	5	6	2
U	0	2	2	0		1	1	-2	1	0	3	1	0
Sc	37	37	35	33		34	36	38	40	39	36	47	41
V	396	306	335	332		357	377	382	380	427	482	416	413
Cr	112	501	275	275		294	311	269	264	45	28	74	91
Co	43	40	38	40		40	40	36	35	37	41	41	45
Ni	83	105	107	111		108	120	104	102	60	33	68	68
Cu	235	122	135	110		120	169	183	178	243	246	210	234
Zn	131	85	87	91		80	85	96	92	116	125	115	125
Ga	24	19	19	20		20	20	22	22	21	22	23	21
Mo	0	0	0	0		0	0	0	0	0	0	0	0
As	2	0	0	0		0	6	1	2	1	3	7	4
S	45	127	30	50		50	37	46	41	75	70	56	309
Fm. criteria													
Sr	224	271	207	211		223	220	225	224	203	202	195	185
Ba	110	148	169	155		114	114	135	133	107	127	101	101
Ba/Y	2.84	5.66	5.30	4.85		3.66	3.42	3.85	3.96	2.68	2.92	2.47	2.80
Zr/Nb	14.96	14.74	14.98	15.02		15.46	13.00	12.97	13.35	14.66	15.20	14.65	15.74
Formation	Poladpur Fm.*	Poladpur Fm.*	Poladpur Fm.*	Poladpur Fm.		Poladpur Fm.	Ambenali Fm.*	Ambenali Fm.*	Ambenali Fm.*	Ambenali Fm.	Ambenali Fm.*	Ambenali Fm.*	Ambenali Fm.*

Varandah Ghat

Elev. M	561	562	582	582
	02BhG1	PMagVG9	02BhG10	02BhG10
SiO2	48.48	51.35	48.77	48.66
TiO2	1.953	1.236	1.951	1.960
Al2O3	14.11	15.43	14.52	14.39
Fe2O3	13.45	11.02	13.68	13.59
MnO	0.208	0.144	0.235	0.237
MgO	6.59	6.45	5.61	5.63
CaO	11.64	9.95	10.40	10.39
Na2O	2.24	2.43	2.13	2.13
K2O	0.15	0.93	1.14	1.15
P2O5	0.177	0.133	0.187	0.183
LOI	0.40	1.56	1.19	2.11
Total	99.39	100.64	99.81	100.43
	02BhG1	PMagVG9	O2BhG10	02BhG10
Rb	3	28	37	
Sr	216	150	193	
Y	30.2	25.3	38.0	
Zr	121	109	124	
Nb	7.8	5.4	7.8	
Ba	89	179	103	
Pb	3	4	2	
Th	2	3	4	
U	0	1	1	
Sc	40	36	40	
V	385	260	378	
Cr	103	430	101	
Co	44	41	42	
Ni	86	109	89	
Cu	183	109	241	
Zn	93	76	125	
Ga	21	18	22	
Mo	0	0	0	
As	4	1	3	
S	48	152	72	
Fm. criteria				
Sr	216	150	193	
Ba	89	179	103	
Ba/Y	2.94	7.06	2.70	
Zr/Nb	15.51	20.17	15.92	
Formation	Ambenali Fm.	Unique	Ambenali Fm.	

C7 Geochemical analysis of the Khumbarli Ghat samples

C7 Khumbarli Ghat

Elev. M	129	148	182	221	237	270	280	291	325	364	403	478	570
	PMagKG1	PMagKG2	PMagKG3	PMagKG4	PMagKG5	PMagKG6	KG6D	PMagKG7	PMagKG8	PMagKG10	PMagKG11	PMagKG17	PMagKG21
SiO2	48.96	49.32	49.19	48.79	48.67	47.68	49.35	48.99	48.95	49.17	48.45	49.11	48.39
TiO2	2.212	2.470	2.107	2.364	2.581	2.565	2.430	2.252	2.369	2.474	2.354	2.602	2.850
Al2O3	13.74	13.67	14.09	13.96	13.38	13.55	14.47	14.35	14.62	13.64	13.67	13.37	13.08
Fe2O3	14.78	15.23	14.45	14.88	15.96	15.66	14.22	13.61	14.43	14.97	15.33	15.75	16.95
MnO	0.219	0.229	0.203	0.199	0.205	0.209	0.194	0.190	0.196	0.216	0.211	0.195	0.269
MgO	6.30	6.08	6.70	6.32	6.16	6.45	6.09	6.56	6.26	6.16	6.50	5.80	5.55
CaO	10.42	10.68	10.49	11.00	10.24	10.59	10.93	10.99	11.33	10.05	10.18	10.40	9.81
Na2O	2.28	2.35	2.22	2.26	2.25	2.13	2.29	2.28	2.30	2.35	2.26	2.30	2.47
K2O	0.29	0.30	0.35	0.15	0.28	0.10	0.26	0.23	0.11	0.42	0.31	0.47	0.46
P2O5	0.203	0.217	0.188	0.207	0.227	0.209	0.219	0.201	0.199	0.224	0.201	0.242	0.276
LOI	1.15	0.18	0.22	0.13	0.65	0.84	-0.10	2.26	0.43	0.40	0.35	0.66	0.32
Total	100.56	100.73	100.20	100.26	100.60	99.99	100.36	101.90	101.18	100.07	99.82	100.91	100.42
	PMagKG1	PMagKG2	PMagKG3	PMagKG4	PMagKG5	PMagKG6	KG6D	PMagKG7	PMagKG8	PMagKG10	PMagKG11	PMagKG17	PMagKG21
Rb	4	8	7	2	4	1	4	3	2	9	7	24	19
Sr	209	220	200	224	212	220	220	218	222	212	199	200	214
Y	33.2	34.1	31.4	36.2	36.3	44.2	32.8	31.6	30.2	36.5	32.9	34	38
Zr	135	140	128	141	147	144	142	132	126	152	137	150	173
Nb	8.7	10.4	9.0	11.0	10.0	10.1	9.0	9.7	8.2	8.5	8.6	10	13
Ba	94	78	74	72	76	63	78	54	51	116	81	92	110
Pb	3	3	3	2	3	3	0	0	3	3	3	5	5
Th	4	3	0	0	1	1	2	0	2	4	0	2	0
U	0	2	1	0	1	0	1	0	1	1	2	0	0
Sc	43	40	36	38	44	43	37	36	35	38	40	40	41
V	405	448	376	398	439	442	418	397	408	421	436	438	448
Cr	94	72	97	102	67	195	128	177	109	158	70	118	163
Co	45	44	44	43	42	43	38	41	39	46	47	45	38
Ni	74	76	79	76	73	78	80	88	86	74	79	87	69
Cu	195	191	190	215	218	205	207	209	183	214	229	253	228
Zn	108	115	106	112	121	119	93	100	94	118	119	122	124
Ga	23	23	22	18	22	23	23	24	21	24	22	22	24
Mo	0	0	0	0	0	0	0	0	0	0	0	0	0
As	0	2	1	5	5	3	3	3	0	1	0	1	0
S	24	22	39	50	27	93	37	36	56	27	27	31	34
Fm. criteria													
Sr	209	220	200	224	212	220	220	218	222	212	199	200	214
Ba	94	78	74	72	76	63	78	54	51	116	81	92	110
Ba/Y	2.84	2.30	2.34	1.99	2.10	1.43	2.38	1.70	1.69	3.17	2.46	2.71	2.86
Zr/Nb	15.54	13.48	14.17	12.81	14.65	14.23	15.82	13.57	15.37	17.92	15.95	14.45	13.55
Fm.	Ambenali Fm.	Ambenali Fm.	Ambenali Fm.	Ambenali Fm.	Ambenali Fm.	Ambenali Fm.	Ambenali Fm.	Ambenali Fm.	Ambenali Fm.	Ambenali Fm.	Ambenali Fm.*	Ambenali Fm.	Ambenali Fm.

Khumbarli Ghat

Elev. M	573	652	675	684	695	~750 cliff above road
	PMagKG20	PMagKG15	PMagKG14	PMagKG13	PMagKG12	KG13C
SiO2	49.13	48.17	49.41	49.35	47.78	49.01
TiO2	3.195	3.319	1.928	1.995	3.273	3.173
Al2O3	12.98	13.78	13.92	14.36	13.78	13.86
Fe2O3	15.87	16.02	12.47	12.76	15.34	15.37
MnO	0.192	0.301	0.197	0.205	0.185	0.210
MgO	5.84	5.69	6.78	6.44	5.64	5.44
CaO	9.74	10.02	10.67	10.83	9.83	10.09
Na2O	2.48	2.48	2.45	2.43	2.34	2.48
K2O	0.43	0.26	0.25	0.19	0.26	0.36
P2O5	0.293	0.324	0.206	0.220	0.304	0.330
LOI	1.21	0.06	1.90	1.58	1.01	-0.18
Total	101.36	100.43	100.18	100.36	99.73	100.13
	PMagKG20	PMagKG15	PMagKG14	PMagKG13	PMagKG12	KG13C
Rb	10	4	8	4	4	10
Sr	225	284	336	330	242	236
Y	40.2	37.7	24.1	24.1	43.6	40.0
Zr	188	189	141	146	202	203
Nb	13.9	18.8	13.7	13.1	17.5	18.5
Ba	124	124	150	130	154	148
Pb	7	3	5	3	3	4
Th	3	2	0	0	4	6
U	1	1	0	0	0	2
Sc	40	40	29	34	41	41
V	377	421	293	316	443	425
Cr	154	104	173	171	170	122
Co	40	40	47	52	38	38
Ni	72	79	121	115	81	69
Cu	249	250	174	143	366	280
Zn	134	149	100	115	118	114
Ga	25	23	20	19	24	25
Mo	0	0	0	0	0	0
As	0	0	7	0	0	6
S	29	31	50	190	31	44
Sr	225	284	336	330	242	236
Ba	124	124	150	130	154	148
Ba/Y	3.07	3.30	6.20	5.41	3.52	3.70
Zr/Nb	13.54	10.03	10.27	11.12	11.57	10.95
Fm.	Ambonali Fm.	M'war Fm.	M'war Fm.	M'war Fm.	M'war Fm.	M'war Fm.

C8 Geochemical analysis of the Matheran Ghat samples

C8 Matheran Ghat

Elev. M	53	53	65	88	117	135	153	170	170	170	191	224	224	262
Wt. %	PMagMG1	MG1D	PMagMG2	PMagMG3	PMagMG4	PMagMG5	PMagMG6	PMagMG7	MG7C	MG7D	PMagMG8	PMagMG9	MG9C	PMagMG10
SiO2	51.00	49.10	50.69	50.84	50.57	49.39	50.64	48.53	49.03	47.86	51.05	52.59	52.29	49.54
TiO2	1.581	1.578	1.608	1.528	1.551	1.249	1.524	3.286	3.246	3.466	2.149	2.738	2.732	1.845
Al2O3	12.29	12.98	13.81	12.23	12.79	11.83	11.76	13.01	13.27	12.94	13.88	13.15	13.15	12.21
Fe2O3	11.44	12.51	10.94	11.46	12.22	11.77	11.87	16.80	16.70	17.71	13.19	14.78	14.68	12.39
MnO	0.173	0.246	0.153	0.162	0.173	0.159	0.169	0.207	0.207	0.257	0.180	0.181	0.171	0.165
MgO	6.13	7.94	7.09	7.12	9.94	10.94	9.42	3.91	4.27	4.46	5.25	3.68	3.55	7.97
CaO	9.62	10.14	10.31	8.53	10.76	10.07	10.72	9.24	9.07	9.42	9.80	7.68	7.45	10.43
Na2O	2.86	2.29	2.76	2.81	1.87	1.88	2.02	2.68	2.70	2.39	2.51	2.88	2.84	2.17
K2O	1.74	0.97	0.38	1.00	0.53	0.33	0.38	0.79	0.67	0.59	1.14	1.76	1.80	0.54
P2O5	0.229	0.229	0.233	0.230	0.239	0.179	0.182	0.343	0.343	0.366	0.252	0.345	0.347	0.192
LOI	2.61	1.23	1.93	3.84	0.69	2.26	1.03	1.23	0.60	0.84	0.85	0.82	0.76	3.15
Total	99.66	99.22	99.90	99.75	101.33	100.05	99.71	100.01	100.11	100.30	100.26	100.61	99.77	100.60
	PMagMG1	MG1D	PMagMG2	PMagMG3	PMagMG4	PMagMG5	PMagMG6	PMagMG7	MG7C	MG7D	PMagMG8	PMagMG9	MG9C	PMagMG10
Rb	52	27	12	22	7	3	5	43	31	24	33	52	57	23
Sr	275	293	682	900	308	305	277	298	303	297	318	285	286	330
Y	20.2	21.1	21.2	23.0	19.7	16.6	21.6	41.9	43.7	45.6	29.7	41.1	42.4	23.3
Zr	113	114	118	118	108	92	110	242	243	261	174	259	270	124
Nb	6.8	9.6	7.2	7.0	6.4	6.0	8.1	17.0	18.7	20.0	17.0	19.6	22.3	9.5
Ba	344	257	168	403	285	225	169	298	284	266	288	423	456	138
Pb	2	2	2	3	3	3	2	6	3	6	5	9	7	2
Th	2	1	2	1	0	1	2	8	8	6	3	8	8	3
U	2	0	0	0	0	2	1	1	2	1	0	3	3	1
Sc	34	39	33	34	31	29	31	32	33	35	33	31	26	35
V	293	314	315	275	268	226	267	369	358	380	309	362	356	315
Cr	319	683	339	353	595	636	606	47	43	89	91	23	18	385
Co	39	50	43	47	46	58	49	37	35	35	37	34	30	45
Ni	66	132	67	93	143	162	128	41	42	39	38	21	22	103
Cu	82	83	89	85	94	59	68	242	239	266	101	109	102	136
Zn	85	95	87	91	76	84	90	127	116	128	88	120	111	99
Ga	15	19	18	15	18	16	18	26	27	25	21	23	26	17
Mo	0	0	0	0	0	0	0	0	0	0	0	0	0	0
As	1	0	1	4	0	0	2	2	0	0	0	0	2	0
S	207	112	410	116	240	32	41	117	88	156	35	53	58	196
Fm. criteria														
Sr	275	293	682	900	308	305	277	298	303	297	318	285	286	330
Ba	344	257	168	403	285	225	169	298	284	266	288	423	456	138
Ba/Y	17.03	12.17	7.94	17.50	14.47	13.55	7.82	7.11	6.49	5.82	9.68	10.29	10.76	5.91
Zr/Nb	16.54	11.85	16.40	16.83	16.84	15.30	13.63	14.24	12.97	13.03	10.25	13.23	12.11	13.05
Fm.	Neral Fm.	Neral Fm.	Neral Fm.	Neral Fm.	Neral Fm.	Neral Fm.	Neral Fm.	Neral Fm.	Neral Fm.	Neral Fm.	Th'vadi Fm.	Th'vadi Fm.	Th'vadi Fm.	Th'vadi Fm.

Th'vadi is Thakurvadi Fm.

Matheran Ghat

Elev. M	259	338	364	524	546	558	562	576	606	648	665	666
Wt. %	PMagMG11	PMagMG12	PMagMG13	PMagMG19	PMagMG18	MG17E	MG17C	PMagMG17	PMagMG16	PMagMG15	PMagMG14	MG14B
SiO2	48.39	51.72	52.78	49.17	50.35	49.18	49.28	49.62	46.73	48.05	51.37	45.45
TiO2	1.779	1.402	1.489	1.964	1.824	2.323	2.026	3.108	1.358	1.011	2.595	0.986
Al2O3	12.37	13.05	13.38	13.47	12.90	14.70	16.16	12.43	16.90	13.45	13.44	13.56
Fe2O3	12.71	11.47	11.47	12.98	12.69	13.63	12.09	15.65	13.10	11.80	15.30	11.78
MnO	0.181	0.170	0.165	0.224	0.169	0.186	0.146	0.189	0.156	0.177	0.207	0.183
MgO	8.38	8.34	6.91	8.01	8.35	5.56	5.33	5.43	5.86	9.14	4.64	9.25
CaO	10.83	9.55	9.09	10.63	10.56	10.50	10.25	7.15	10.92	9.91	9.54	9.31
Na2O	2.30	2.27	2.38	2.33	2.23	2.37	2.44	2.35	2.41	2.09	2.76	1.18
K2O	0.50	0.61	0.83	0.43	0.27	0.51	0.54	1.69	0.25	0.58	0.39	1.80
P2O5	0.179	0.164	0.185	0.173	0.201	0.233	0.189	0.329	0.144	0.121	0.276	0.118
LOI	1.62	1.35	2.30	1.00	1.94	0.98	1.06	1.94	1.94	2.74	0.31	6.13
Total	99.24	100.09	100.98	100.39	101.49	100.16	99.51	99.88	99.77	99.06	100.83	99.76
	PMagMG11	PMagMG12	PMagMG13	PMagMG19	PMagMG18	MG17E	MG17C	PMagMG17	PMagMG16	PMagMG15	PMagMG14	MG14B
Rb	20	13	34	10	4	19	14	49	4	8	19	79
Sr	239	320	495	243	267	287	383	223	209	369	268	181
Y	26.2	18.3	18.7	26.8	24.5	31.7	30.9	39.2	25.4	20.9	39.2	19.6
Zr	119	117	127	124	127	162	131	220	95	80	201	74
Nb	9.2	7.2	8.4	9.0	8.5	13.9	11.0	15.3	3.0	2.8	11.9	4.6
Ba	134	175	247	103	129	119	147	250	143	231	255	749
Pb	1	4	4	3	1	5	0	5	0	2	3	0
Th	2	3	2	5	2	4	2	6	0	2	4	1
U	2	1	0	1	3	1	1	0	1	1	1	1
Sc	36	28	26	37	34	31	32	34	28	34	37	37
V	308	257	291	330	292	341	322	390	224	250	396	263
Cr	465	305	307	492	467	291	208	117	78	736	52	687
Co	51	51	41	46	52	34	34	40	53	53	36	55
Ni	128	141	93	188	185	61	87	68	147	217	44	232
Cu	129	94	108	162	116	153	139	264	133	90	227	67
Zn	96	74	80	96	98	89	86	132	95	83	121	74
Ga	20	21	18	21	20	23	25	24	20	14	22	16
Mo	0	0	0	0	0	0	0	0	0	0	0	0
As	2	4	0	0	0	0	2	1	4	0	6	0
S	52	169	209	31	43	109	90	549	72	188	52	93
Fm. criteria												
Sr	239	320	495	243	267	287	383	223	209	369	268	181
Ba	134	175	247	103	129	119	147	250	143	231	255	749
Ba/Y	5.12	9.54	13.20	3.82	5.27	3.76	4.77	6.37	5.63	11.04	6.51	38.21
Zr/Nb	12.95	16.31	15.13	13.77	14.99	11.68	11.87	14.36	31.67	28.68	16.87	16.13
Fm.	Th'vadi Fm.	Th'vadi Fm.	Th'vadi Fm.	Th'vadi Fm.	Th'vadi Fm.	Th'vadi Fm.	B'shanka Fm.	B'shanka Fm.	Khandala Fm.	Khandala Fm.	Khandala Fm.	Khandala Fm.

C9 Internal standards, their mean and standard deviation

	Approx. Det.Lt.	CG5	CG5	CG5	CG5	CG5	CG5	CG5	CG5	CG5	CG5(OLD)	CG5(OLD)	CG5(OLD)	CG5(OLD)	CG5(OLD)	Mean CG5 - old	CG5 St. Dev. -old
Rb	2	15	15	15	15	14	15	15	14	15	15	15	15	15	16	15	0.34
Sr	2	224	227	222	223	223	227	223	226	227	233	232	234	232	232	225	1.89
Y	2.0	31.3	30.4	30.6	32.7	32.6	32.3	31.4	32.3	31.5	32.0	32.8	32.2	32.8	32.2	32	0.80
Zr	2	137	135	136	136	135	137	137	137	136	138	139	139	138	139	136	0.82
Nb	1.5	8.8	8.7	9.7	8.7	9.1	8.7	9.0	9.4	9.0	9.6	9.7	8.5	9.7	8.8	9	0.33
Ba	12	168	178	176	176	170	180	176	185	186	192	187	197	188	183	177	5.63
Pb	5	3	4	2	6	4	2	4	4	3	4	6	4	1	3	4	1.06
Th	4	4	2	5	1	4	3	2	3	2	1	3	4	2	4	3	1.06
U	3	0	0	3	0	0	0	0	1	1	0	1	2	1	1	0	0.89
Sc	5	36	34	35	33	33	34	36	34	37	36	36	37	36	34	35	1.32
V	5	335	333	326	334	338	332	332	334	333	332	338	340	343	341	333	2.92
Cr	4	348	351	350	350	353	350	355	356	360	223	223	220	221	224	353	3.47
Co	2	35	34	37	37	39	38	36	37	37	40	36	37	38	38	36	1.25
Ni	3	98	96	92	97	96	99	98	101	101	101	98	99	100	100	98	2.81
Cu	3	117	120	121	117	120	117	117	117	118	112	115	114	110	111	118	1.69
Zn	3	88	88	87	89	86	88	90	88	88	88	89	89	89	89	88	0.94
Ga	3	22	20	19	20	20	20	21	20	20	20	21	20	21	21	20	0.65
Mo	2	0	0	0	0	0	0	0	0	0	0	0	0	0	0	0	0.00
As	5	0	3	2	0	0	3	3	5	2	3	0	9	1	0	2	1.59
S	50	104	95	95	68	81	87	86	63	71	101	107	103	104	92	83	12.90

(old = original beads from Widdowson (1990), - old = calculation carried out without the data from the old beads)

	CG5 St. Er. - old	CG5 St. Dev. All	CG5 St. Er. All	Mean CG5 All
Rb	0.11	0.42	0.11	14.95
Sr	0.63	4.01	1.07	227.38
Y	0.27	0.75	0.20	31.94
Zr	0.27	1.33	0.36	137.10
Nb	0.11	0.42	0.11	9.10
Ba	1.88	7.84	2.10	181.57
Pb	0.35	1.23	0.33	3.56
Th	0.35	1.14	0.31	2.76
U	0.30	0.84	0.23	0.54
Sc	0.44	1.30	0.35	34.94
V	0.97	4.31	1.15	335.03
Cr	1.16	62.55	16.72	305.99
Co	0.42	1.51	0.40	37.01
Ni	0.94	2.55	0.68	98.33
Cu	0.56	3.27	0.87	116.07
Zn	0.31	0.91	0.24	88.27
Ga	0.22	0.61	0.16	20.38
Mo	0.00	0.00	0.00	0.00
As	0.53	2.46	0.66	2.09
S	4.30	13.88	3.71	89.69

	Approx. Det.Lt.	CG7	CG7	CG7	CG7	CG7	CG7	CG7	Mean	St. Dev.	St. Er.
Rb	2	16	15	16	15	16	16	15	15.56	0.30	0.11
Sr	2	244	244	242	242	243	245	241	242.97	1.26	0.47
Y	2.0	37.5	38.2	37.7	38.0	38.7	38.8	37.9	38.11	0.45	0.17
Zr	2	178	177	175	176	176	178	174	176.31	1.08	0.41
Nb	1.5	12.9	13.4	12.5	12.0	12.6	12.8	13.4	12.80	0.46	0.17
Ba	12	156	147	143	153	157	159	155	152.93	5.30	2.00
Pb	5	2	5	4	5	1	4	5	3.57	1.41	0.53
Th	4	2	2	4	3	5	2	4	3.00	1.09	0.41
U	3	1	0	1	2	1	1	2	1.24	0.80	0.30
Sc	5	32	32	32	33	36	29	36	32.83	2.27	0.86
V	5	410	420	403	417	421	416	409	413.64	6.14	2.32
Cr	4	110	110	113	112	110	112	112	111.24	1.17	0.44
Co	2	32	35	35	38	36	37	37	35.81	1.85	0.70
Ni	3	72	72	72	69	74	73	70	71.61	1.30	0.49
Cu	3	216	217	214	215	217	217	213	215.61	1.48	0.56
Zn	3	86	85	87	87	88	86	86	86.47	0.77	0.29
Ga	3	23	23	23	24	22	22	24	23.00	0.71	0.27
Mo	2	0	0	0	0	0	0	0	0.00	0.00	0.00
As	5	3	0	2	2	2	5	2	2.44	1.33	0.50
S	50	30	30	32	26	31	26	32	29.47	2.42	0.91

	CG2	CG2	CG2	CG2	CG2	CG2	CG2	CG2	CG2	CG2	CG2	CG2	CG2	CG2	CG2	CG2	CG2	CG2
SiO2	50.55	50.47	50.91	50.84	50.82	50.80	50.79	50.74	50.91	50.88	50.87	50.77	50.87	50.70	50.52	50.42	50.56	50.42
TiO2	1.820	1.833	1.825	1.836	1.826	1.842	1.825	1.820	1.830	1.841	1.849	1.832	1.842	1.837	1.839	1.829	1.823	1.825
Al2O3	13.92	13.93	14.00	14.01	13.99	13.96	13.98	14.00	14.07	14.08	14.07	14.00	14.07	13.94	13.91	13.92	13.87	13.86
Fe2O3	12.37	12.36	12.42	12.39	12.39	12.39	12.37	12.37	12.37	12.37	12.41	12.40	12.37	12.38	12.45	12.42	12.43	12.41
MnO	0.188	0.190	0.188	0.189	0.191	0.189	0.188	0.191	0.188	0.188	0.190	0.188	0.188	0.191	0.188	0.187	0.189	0.188
MgO	7.02	7.03	6.95	6.92	6.98	6.94	6.95	6.92	7.02	6.99	7.02	7.01	7.02	7.01	6.99	6.93	6.98	6.96
CaO	10.67	10.74	10.64	10.64	10.65	10.64	10.63	10.64	10.75	10.80	10.71	10.69	10.68	10.63	10.66	10.66	10.68	10.69
Na2O	2.39	2.45	2.50	2.48	2.48	2.50	2.48	2.51	2.42	2.42	2.36	2.31	2.31	2.33	2.19	2.20	2.26	2.21
K2O	0.26	0.26	0.26	0.26	0.26	0.26	0.26	0.26	0.25	0.25	0.25	0.25	0.25	0.25	0.25	0.25	0.24	0.24
P2O5	0.196	0.195	0.189	0.193	0.190	0.187	0.193	0.194	0.195	0.192	0.193	0.191	0.188	0.187	0.185	0.192	0.185	0.183
Total	99.39	99.45	99.87	99.76	99.78	99.70	99.66	99.64	100.00	100.02	99.91	99.64	99.78	99.43	99.19	99.00	99.22	98.99

	CG2	CG2	CG2	CG2	CG2	CG2	CG2	CG2	CG2	CG2	St. Dev.	St. Er.
SiO2	50.28	50.30	50.18	50.62	50.62	50.66	50.70	50.69	50.63	50.57	0.20	0.04
TiO2	1.822	1.833	1.826	1.849	1.849	1.843	1.841	1.849	1.847	1.846	0.01	0.00
Al2O3	13.77	13.81	13.79	13.86	13.87	13.89	13.82	13.89	13.86	13.94	0.09	0.02
Fe2O3	12.40	12.41	12.42	12.42	12.44	12.43	12.39	12.39	12.42	12.39	0.02	0.00
MnO	0.189	0.188	0.191	0.187	0.186	0.188	0.187	0.186	0.188	0.188	0.00	0.00
MgO	6.89	6.87	6.88	7.00	7.02	7.00	7.01	7.07	7.06	6.99	0.05	0.01
CaO	10.61	10.60	10.58	10.64	10.65	10.68	10.69	10.65	10.64	10.70	0.05	0.01
Na2O	2.22	2.18	2.20	2.29	2.25	2.26	2.22	2.26	2.25	2.28	0.11	0.02
K2O	0.25	0.25	0.24	0.25	0.25	0.25	0.25	0.25	0.24	0.25	0.01	0.00
P2O5	0.182	0.190	0.179	0.188	0.193	0.191	0.192	0.191	0.188	0.186	0.00	0.00
Total	98.61	98.63	98.49	99.31	99.33	99.39	99.30	99.42	99.33	99.34		

	Approx. Det.Lt.	CG2	CG2	CG2	CG2	CG2	CG2	CG2	CG2	CG2	CG2	CG2	CG2	CG2	CG2
Rb	**2**	11	11	11	11	11	12	12	11	11	11	11	11	11	12
Sr	**2**	215	214	217	217	217	218	216	218	218	216	216	219	217	218
Y	**2.0**	31.1	30	31.2	31.2	31.3	30.6	29.9	29.8	30.5	30.3	30.2	30.6	30.4	31.0
Zr	**2**	137	137	137	140	140	138	137	138	137	137	136	136	138	136
Nb	**1.5**	8.3	8	7.9	7.7	8.1	7.6	8.1	9	8.1	7.1	7.4	7.8	8.1	7.1
Ba	**12**	134	136	143	129	139	133	147	145	141	142	133	130	137	136
Pb	**5**	5	4	2	2	3	3	2	0	3	3	0	3	2	4
Th	**4**	0	2	1	2	3	4	0	2	2	1	1	2	1	2
U	**3**	0	1	1	1	1	1	2	0	1	1	2	1	1	0
Sc	**5**	32	32	29	29	33	34	33	33	32	29	32	30	34	29
V	**5**	291	303	289	293	299	298	301	299	295	290	298	284	296	286
Cr	**4**	253	255	249	251	251	253	253	253	250	251	255	254	253	252
Co	**2**	40	41	41	41	40	41	45	43	43	43	42	42	41	41
Ni	**3**	122	122	123	125	119	120	120	124	123	121	121	120	123	124
Cu	**3**	131	133	134	131	131	131	130	132	134	132	130	129	129	132
Zn	**3**	81	79	82	83	80	80	80	77	80	79	77	79	79	81
Ga	**3**	21	20	21	20	20	21	21	19	21	19	20	21	21	20
Mo	**2**	0	0	0	0	0	0	0	0	0	0	0	0	0	0
As	**5**	1	3	1	0	0	0	0	0	0	5	4	3	3	0
S	**50**	41	45	39	39	43	40	38	41	41	38	43	38	37	41

	CG2	CG2	CG2	CG2	CG2	CG2	CG2	CG2	CG2	CG2	CG2	CG2	CG2	CG2	Mean	St. Dev.	St. Er.
Rb	10	11	11	12	11	12	11	12	10	11	12	12	11	11	11.14	0.50	0.09
Sr	214	215	214	212	216	216	219	222	215	212	219	221	213	219	216.53	2.51	0.47
Y	30.7	31.3	30.4	31.4	31.3	32.2	31.7	32.5	32.6	31.5	31.7	33.0	31.5	31.9	31.15	0.80	0.15
Zr	138	139	137	140	138	140	140	140	138	138	142	143	137	140	138.23	1.70	0.32
Nb	7.9	8.8	8.5	8.9	8.5	9.0	9.4	8.9	8.6	8.8	9.2	10.5	8.7	7.7	8.34	0.74	0.14
Ba	131	126	121	135	137	140	143	144	137	132	151	148	138	153	137.83	7.31	1.38
Pb	6	4	3	3	5	5	4	5	4	1	4	5	5	3	3.31	1.46	0.28
Th	4	3	2	0	3	2	3	3	3	5	3	4	2	2	2.20	1.20	0.23
U	0	1	0	1	1	0	0	1	1	1	0	0	1	1	0.64	0.51	0.10
Sc	33	30	36	30	29	30	31	36	29	29	30	30	34	32	31.41	2.14	0.40
V	290	294	280	291	293	287	297	299	293	299	291	300	289	292	293.39	5.46	1.03
Cr	252	248	249	254	253	251	260	257	250	248	256	255	255	257	252.68	2.83	0.53
Co	40	39	37	43	38	37	44	43	41	39	42	42	39	41	41.04	1.88	0.36
Ni	119	119	117	121	124	122	127	124	121	123	124	126	121	125	122.08	2.38	0.45
Cu	127	127	125	128	130	131	132	133	126	123	129	133	128	132	130.01	2.61	0.49
Zn	72	73	72	73	72	72	76	75	73	73	76	78	73	75	76.75	3.44	0.65
Ga	21	21	20	22	20	22	21	21	20	22	21	22	21	19	20.56	0.86	0.16
Mo	0	0	0	0	0	0	0	0	0	0	0	0	0	0	0.00	0.02	0.00
As	4	4	0	0	5	5	2	3	7	1	0	5	2	4	2.16	2.05	0.39
S	37	34	33	26	22	25	84	90	31	29	90	86	31	80	45.06	19.89	3.76

	CG11	CG11	CG11	CG11	CG11	CG11	CG11	CG11	CG11	CG11	CG11	CG11	CG11	St. Dev.	St. Er.
SiO2	47.18	47.71	47.76	47.38	47.41	47.26	47.60	47.61	47.77	47.66	47.74	47.57	47.47	0.19	0.67
TiO2	2.420	2.426	2.434	2.423	2.401	2.403	2.449	2.430	2.446	2.439	2.447	2.442	2.413	0.02	0.06
Al2O3	13.58	13.82	13.78	13.78	13.72	13.67	13.73	13.78	13.75	13.72	13.70	13.73	13.78	0.06	0.22
Fe2O3	14.58	14.64	14.60	14.55	14.57	14.52	14.58	14.55	14.56	14.56	14.55	14.59	14.50	0.03	0.12
MnO	0.224	0.231	0.225	0.223	0.224	0.229	0.226	0.224	0.222	0.224	0.223	0.225	0.225	0.00	0.01
MgO	6.72	6.91	6.95	6.89	6.87	6.82	6.96	6.98	6.98	6.96	6.98	6.96	6.88	0.07	0.27
CaO	10.80	10.88	10.83	10.79	10.76	10.73	10.80	10.79	10.78	10.79	10.76	10.79	10.79	0.03	0.12
Na2O	2.08	2.13	2.14	2.12	2.12	2.16	2.17	2.18	2.18	2.17	2.19	2.18	2.17	0.03	0.11
K2O	0.18	0.17	0.17	0.17	0.17	0.17	0.17	0.17	0.17	0.17	0.17	0.17	0.17	0.00	0.01
P2O5	0.207	0.210	0.211	0.211	0.212	0.207	0.216	0.213	0.215	0.209	0.212	0.213	0.212	0.00	0.01
Total	97.97	99.12	99.10	98.54	98.47	98.17	98.90	98.94	99.07	98.91	98.97	98.86	98.61		

	CG11	CG11	CG11	CG11	CG11	CG11	CG11	CG11	CG11	CG11	CG11	CG11	CG11	CG11	CG11	CG11
Rb	2	2	2	1	2	2	2	1	2	2	2	1	3	1	1	2
Sr	222	221	227	225	226	226	226	228	227	226	225	226	227	225	225	226
Y	31.6	32	32.9	33.2	32.3	32.1	32.7	32.3	32.1	32.4	31.7	33.7	33.0	32.4	33.2	33.4
Zr	139	138	138	138	140	140	139	140	140	139	138	140	139	137	140	137
Nb	8.1	11	9.5	8.8	9.6	10.0	9.7	9.7	9.8	10.3	10.6	9.5	9.2	9.5	9.5	11.2
Ba	90	86	84	82	85	88	92	91	88	85	87	81	79	80	79	71
Pb	4	4	3	2	2	2	2	3	2	4	3	0	2	0	3	1
Th	0	0	2	3	3	4	0	2	1	0	2	2	2	0	1	2
U	-2	1	3	1	1	0	0	0	3	0	1	0	3	0	0	0
Sc	35	35	34	33	35	35	36	35	37	32	35	34	34	35	32	35
V	363	371	359	366	359	369	366	379	373	359	365	360	358	354	358	356
Cr	185	184	183	183	182	183	181	180	186	181	180	182	185	185	182	181
Co	47	46	51	44	47	45	48	48	45	47	48	43	48	45	45	44
Ni	102	104	104	105	102	102	104	103	108	105	105	108	102	103	102	103
Cu	183	179	184	184	187	184	185	187	184	186	184	184	184	181	180	177
Zn	116	117	117	118	120	119	118	118	119	120	117	118	118	119	107	106
Ga	22	22	22	24	23	22	24	23	25	23	22	23	23	23	23	22
Mo	0	0	0	0	0	0	0	0	0	0	0	0	0	0	0	0
As	1	3	0	2	0	0	0	0	2	4	2	2	4	3	2	5
S	55	48	46	49	48	49	47	52	45	45	48	44	46	46	42	45

	CG11	CG11	CG11	CG11	CG11	CG11	Mean	St. Dev.	St Er.
Rb	2	2	1	1	1	1	2	0.44	0.09
Sr	222	225	224	221	226	226	225	1.94	0.41
Y	32.6	33.1	32.4	33.7	33.5	34.2	33	0.66	0.14
Zr	138	140	138	140	138	138	139	0.94	0.20
Nb	9.5	10.5	12.0	11.0	10.0	11.0	10	0.84	0.18
Ba	80	86	76	85	78	83	83	5.03	1.07
Pb	3	2	1	3	0	3	2	1.23	0.26
Th	4	3	3	3	3	0	2	1.31	0.28
U	0	0	1	0	0	1	1	1.13	0.24
Sc	35	34	33	37	33	34	35	1.31	0.28
V	361	362	348	369	357	358	362	6.83	1.46
Cr	183	181	182	184	183	182	183	1.65	0.35
Co	46	46	41	41	45	45	46	2.23	0.48
Ni	102	102	103	101	106	106	104	1.89	0.40
Cu	177	179	181	175	180	178	182	3.38	0.72
Zn	107	106	108	108	109	107	114	5.34	1.14
Ga	22	22	24	21	24	24	23	0.99	0.21
Mo	0	0	0	0	0	0	0	0.00	0.00
As	0	2	2	1	0	1	2	1.34	0.29
S	38	32	44	36	40	31	44	5.69	1.21

	KP4	KP4	KP4	KP4	KP4	KP4	KP4	KP4	KP4	KP4	KP4	KP4	KP4	KP4	KP4	KP4	KP4
SiO2	48.06	48.08	48.42	48.43	48.46	48.42	48.38	48.46	48.56	48.53	48.65	48.54	48.61	48.61	48.19	48.32	48.30
TiO2	3.535	3.547	3.545	3.560	3.540	3.551	3.556	3.547	3.590	3.601	3.586	3.576	3.592	3.580	3.587	3.569	3.546
Al2O3	12.18	12.22	12.29	12.28	12.29	12.30	12.27	12.33	12.44	12.40	12.41	12.34	12.41	12.38	12.29	12.30	12.33
Fe2O3	17.45	17.41	17.47	17.50	17.46	17.47	17.47	17.45	17.49	17.48	17.50	17.47	17.47	17.46	17.56	17.51	17.52
MnO	0.242	0.241	0.242	0.243	0.243	0.242	0.239	0.241	0.241	0.241	0.244	0.239	0.240	0.239	0.244	0.247	0.242
MgO	5.28	5.29	5.29	5.28	5.27	5.27	5.28	5.25	5.27	5.32	5.35	5.33	5.34	5.30	5.28	5.30	5.33
CaO	9.31	9.32	9.28	9.26	9.29	9.31	9.33	9.27	9.40	9.41	9.34	9.33	9.31	9.27	9.33	9.32	9.31
Na2O	2.57	2.58	2.65	2.65	2.68	2.66	2.67	2.68	2.58	2.57	2.55	2.48	2.50	2.50	2.40	2.39	2.38
K2O	0.46	0.47	0.47	0.47	0.47	0.46	0.47	0.47	0.46	0.46	0.46	0.46	0.46	0.46	0.45	0.46	0.46
P2O5	0.329	0.326	0.320	0.326	0.321	0.322	0.326	0.324	0.319	0.328	0.323	0.326	0.323	0.317	0.319	0.323	0.321
Total	99.43	99.48	99.98	99.99	100.03	100.00	100.00	100.01	100.36	100.34	100.41	100.09	100.24	100.11	99.65	99.74	99.74

	KP4	KP4	KP4	KP4	KP4	KP4	KP4	KP4	KP4	KP4	KP4	KP4	KP4	St. Dev	St. Er.
SiO2	48.27	48.14	48.13	48.49	48.44	48.06	48.21	48.40	48.41	48.49	48.49	48.14	48.25	0.17	0.03
TiO2	3.568	3.558	3.561	3.602	3.613	3.547	3.586	3.619	3.622	3.611	3.609	3.590	3.563	0.03	0.00
Al2O3	12.30	12.25	12.21	12.25	12.26	12.24	12.20	12.24	12.22	12.26	12.27	12.24	12.27	0.07	0.01
Fe2O3	17.54	17.51	17.51	17.51	17.55	17.50	17.49	17.51	17.49	17.54	17.50	17.46	17.46	0.03	0.01
MnO	0.243	0.239	0.242	0.241	0.241	0.244	0.240	0.240	0.240	0.243	0.240	0.240	0.245	0.00	0.00
MgO	5.36	5.28	5.28	5.35	5.36	5.28	5.27	5.35	5.31	5.36	5.37	5.32	5.36	0.03	0.01
CaO	9.30	9.26	9.26	9.31	9.30	9.24	9.29	9.33	9.29	9.32	9.30	9.30	9.29	0.04	0.01
Na2O	2.38	2.37	2.39	2.44	2.41	2.38	2.39	2.42	2.38	2.43	2.43	2.42	2.41	0.11	0.02
K2O	0.45	0.46	0.45	0.46	0.45	0.46	0.45	0.46	0.46	0.46	0.46	0.46	0.46	0.01	0.00
P2O5	0.323	0.313	0.311	0.325	0.325	0.317	0.319	0.331	0.324	0.321	0.326	0.317	0.326	0.00	0.00
Total	99.72	99.38	99.35	99.96	99.96	99.26	99.44	99.91	99.73	100.04	99.98	99.48	99.63	0.31	0.06

	Approx. Det.Lt.	KP4	KP4	KP4	KP4	KP4	KP4	KP4	KP4	KP4	KP4	KP4	KP4	KP4	KP4	KP4	KP4	KP4	KP4
Rb	2	12	12	11	12	11	11	12	12	11	12	12	10	11	11	12	11	12	11
Sr	2	221	224	224	223	224	224	222	225	227	225	225	225	223	224	221	222	223	221
Y	2.0	47.6	48	46.7	47.1	47.0	47.7	48.1	48.2	47.7	47.2	47.3	48.3	47.4	47.7	46.6	47.6	48.3	48.6
Zr	2	218	218	218	216	216	217	214	218	220	217	217	216	216	215	218	219	218	218
Nb	1.5	17.8	20	16.6	16.8	18.0	19.0	18.3	18	18.1	17.8	18.2	18.8	18.9	18.9	17.8	18.3	18.0	18.1
Ba	12	148	132	138	139	140	137	139	153	138	129	125	120	123	131	125	119	124	127
Pb	5	7	7	5	4	2	1	4	5	4	3	3	3	2	1	4	4	5	2
Th	4	3	1	2	5	0	1	3	2	4	2	2	1	2	4	3	5	2	3
U	3	0	0	1	0	1	3	2	0	0	3	0	0	0	0	0	1	3	0
Sc	5	39	38	37	40	44	42	43	41	40	41	36	43	44	40	40	41	41	41
V	5	474	488	481	483	477	476	486	484	480	472	470	462	478	474	483	475	473	467
Cr	4	55	57	57	58	58	59	57	57	57	58	57	58	55	55	52	54	56	56
Co	2	47	48	47	47	48	47	46	47	50	49	45	47	48	47	41	40	41	43
Ni	3	62	61	57	60	62	60	61	60	61	58	61	60	58	59	58	62	59	59
Cu	3	334	335	337	329	330	332	337	341	336	332	338	334	333	332	320	322	322	326
Zn	3	158	160	157	156	156	157	157	158	158	158	157	158	159	158	141	143	145	144
Ga	3	24	24	25	25	26	26	26	26	24	25	25	24	26	24	25	24	26	25
Mo	2	0	0	0	0	0	0	0	0	0	0	0	0	0	0	0	0	0	0
As	5	3	0	0	2	0	0	0	2	1	2	8	3	0	3	3	0	0	4
S	50	85	84	81	79	85	80	82	84	81	82	78	78	83	80	79	74	75	64

	KP4	KP4	KP4	KP4	Mean	Stan. Dev.	St. Er.
Rb	11.30	10	11	9	11.22	0.71	0.15
Sr	219.60	223	222	223	223.12	1.55	0.33
Y	47.80	49.2	49.1	49.3	47.84	0.74	0.16
Zr	216.10	220	219	219	217.35	1.44	0.31
Nb	18.10	19.0	17.7	18.9	18.22	0.71	0.15
Ba	131.60	118	139	132	132.16	9.01	1.92
Pb	5.40	4	4	6	3.85	1.68	0.36
Th	4.50	3	2	1	2.51	1.23	0.26
U	1.20	0	1	1	0.73	0.99	0.21
Sc	40.10	43	40	40	40.61	2.00	0.43
V	477.20	474	478	473	476.68	6.12	1.30
Cr	55.90	57	59	57	56.61	1.59	0.34
Co	45.00	45	45	41	45.75	2.79	0.59
Ni	59.50	60	56	61	59.69	1.56	0.33
Cu	321.70	325	326	327	330.41	5.85	1.25
Zn	144.10	144	145	146	152.62	6.69	1.43
Ga	24.50	24	25	25	24.90	0.79	0.17
Mo	0.00	0	0	0	-0.01	0.04	0.01
As	0.00	3	3	0	1.65	2.00	0.43
S	68.80	68	69	67	77.52	6.24	1.33

	PH6	PH6	PH6	PH6	PH6	PH6	PH6	PH6	PH6	PH6	PH6	PH6	PH6	PH6	PH6	PH6
SiO2	48.07	47.85	48.08	48.14	48.14	48.04	48.04	48.09	48.26	48.27	48.51	48.43	48.58	48.48	48.31	48.25	48.29
TiO2	2.309	2.328	2.328	2.326	2.328	2.321	2.323	2.308	2.337	2.339	2.350	2.341	2.334	2.335	2.331	2.319	2.330
Al2O3	13.53	13.57	13.63	13.63	13.63	13.60	13.59	13.65	13.78	13.75	13.78	13.74	13.78	13.77	13.69	13.72	13.68
Fe2O3	13.67	13.69	13.73	13.73	13.71	13.72	13.71	13.72	13.68	13.68	13.72	13.71	13.70	13.68	13.74	13.73	13.73
MnO	0.212	0.211	0.212	0.213	0.212	0.212	0.212	0.216	0.215	0.210	0.212	0.209	0.207	0.212	0.214	0.214	0.212
MgO	6.49	6.46	6.46	6.46	6.47	6.42	6.45	6.48	6.50	6.51	6.61	6.56	6.56	6.60	6.53	6.51	6.52
CaO	11.40	11.36	11.31	11.36	11.28	11.34	11.35	11.33	11.47	11.47	11.43	11.38	11.37	11.34	11.38	11.31	11.34
Na2O	2.25	2.26	2.26	2.25	2.27	2.29	2.27	2.25	2.28	2.28	2.21	2.19	2.20	2.18	2.08	2.05	2.08
K2O	0.16	0.16	0.15	0.15	0.16	0.16	0.16	0.15	0.15	0.15	0.15	0.14	0.15	0.14	0.14	0.14	0.14
P2O5	0.216	0.209	0.207	0.202	0.209	0.202	0.206	0.207	0.207	0.212	0.210	0.204	0.208	0.203	0.209	0.203	0.198
Total	98.30	98.09	98.36	98.46	98.41	98.30	98.31	98.40	98.87	98.88	99.19	98.90	99.08	98.95	98.62	98.44	98.53

	PH6	PH6	PH6	PH6	PH6	PH6	PH6	PH6	PH6	PH6	PH6	PH6	PH6	Stan. Dev.	St. Er.
SiO2	48.27	48.03	48.01	48.12	48.05	48.41	48.33	48.42	48.45	48.50	48.47	48.30	48.22	0.18	0.04
TiO2	2.334	2.317	2.326	2.322	2.327	2.350	2.350	2.353	2.353	2.355	2.356	2.332	2.332	0.01	0.00
Al2O3	13.75	13.59	13.57	13.59	13.61	13.71	13.68	13.64	13.64	13.71	13.68	13.71	13.70	0.07	0.02
Fe2O3	13.72	13.72	13.74	13.73	13.74	13.74	13.71	13.74	13.73	13.71	13.73	13.66	13.68	0.02	0.00
MnO	0.212	0.213	0.212	0.215	0.212	0.211	0.208	0.209	0.209	0.209	0.212	0.210	0.212	0.00	0.00
MgO	6.52	6.47	6.44	6.48	6.47	6.60	6.55	6.59	6.60	6.63	6.60	6.53	6.51	0.06	0.01
CaO	11.32	11.32	11.31	11.31	11.3	11.38	11.32	11.36	11.39	11.34	11.35	11.38	11.40	0.05	0.01
Na2O	2.06	2.05	2.03	2.06	2.06	2.08	2.10	2.09	2.07	2.11	2.10	2.11	2.11	0.09	0.02
K2O	0.14	0.14	0.14	0.14	0.14	0.14	0.14	0.14	0.14	0.14	0.14	0.14	0.14	0.01	0.00
P2O5	0.201	0.203	0.204	0.204	0.204	0.204	0.204	0.208	0.207	0.214	0.212	0.212	0.213		
Total	98.54	98.06	97.98	98.77	98.72	98.83	98.60	98.75	98.80	98.92	98.85	98.58	98.52		

	PH7	PH7	PH7	PH7	PH7	PH7	PH7	PH7	PH7	PH7	PH7	PH7	PH7	PH7	PH7	PH7	PH7	St. Dev.	St. Er.
SiO2	48.54	48.52	48.57	48.61	48.55	48.51	48.57	48.51	48.43	48.40	48.59	48.57	48.65	48.56	47.45	48.19	48.24	0.27	0.07
TiO2	2.747	2.758	2.766	2.773	2.748	2.749	2.783	2.777	2.800	2.786	2.801	2.782	2.796	2.782	2.756	2.757	2.774	0.02	0.00
Al2O3	13.40	13.42	13.45	13.44	13.45	13.40	13.41	13.43	13.46	13.48	13.53	13.48	13.51	13.46	13.07	13.32	13.35	0.10	0.02
Fe2O3	16.11	16.11	16.18	16.15	16.13	16.14	16.16	16.15	16.17	16.16	16.20	16.17	16.13	16.17	16.09	16.23	16.25	0.04	0.01
MnO	0.208	0.206	0.208	0.209	0.208	0.207	0.209	0.209	0.207	0.205	0.210	0.206	0.207	0.208	0.207	0.208	0.208	0.00	0.00
MgO	6.14	6.12	6.05	6.06	6.09	6.09	6.08	6.08	6.08	6.07	6.09	6.13	6.15	6.08	5.93	6.07	6.08	0.05	0.01
CaO	10.40	10.43	10.38	10.36	10.38	10.34	10.41	10.40	10.52	10.45	10.43	10.40	10.36	10.36	10.19	10.38	10.40	0.06	0.02
Na2O	2.53	2.56	2.54	2.58	2.57	2.55	2.57	2.57	2.51	2.51	2.44	2.41	2.44	2.41	2.28	2.31	2.29	0.10	0.02
K2O	0.37	0.37	0.36	0.36	0.36	0.36	0.36	0.36	0.36	0.36	0.36	0.36	0.35	0.35	0.36	0.35	0.35	0.01	0.00
P2O5	0.253	0.251	0.243	0.241	0.243	0.243	0.241	0.245	0.243	0.234	0.243	0.237	0.246	0.240	0.228	0.239	0.234	0.01	0.00
Total	100.69	100.75	100.74	100.77	100.73	100.59	100.79	100.74	100.78	100.65	100.90	100.75	100.84	100.62	98.57	100.05	100.17		

	Approx. Det.Lt.	PH7	PH7	PH7	PH7	PH7	PH7	PH7	PH7	PH7	PH7	PH7	PH7	PH7	PH7	PH7	PH7	PH7	PH7	PH7
Rb	2	8	8	8	8	8	7	8	9	8	8	8	9	8	9	8	9	8	8	9
Sr	2	231	230	234	232	232	229	234	231	234	231	232	232	229	235	231	228	228	228	227
Y	2.0	35.2	36	35.2	35.8	34.6	36.1	36.2	34.2	36.4	35.5	34.9	34.0	35.5	35.5	35.7	34.4	35.3	36.4	35.3
Zr	2	153	155	152	153	151	152	153	155	156	154	153	155	153	153	153	153	151	154	152
Nb	1.5	11.6	13	12.1	11.1	11.4	11.1	12.1	11.9	11.7	12.2	12.0	11.3	13.2	10.7	11.9	12.5	13.5	13.5	11.8
Ba	12	101	100	105	107	94	91	106	100	105	95	90	89	99	90	82	96	84	88	92
Pb	5	4	4	2	4	4	5	3	1	4	1	1	1	3	0	1	1	2	3	1
Th	4	3	0	2	0	2	2	3	3	3	2	0	0	2	1	1	2	4	4	3
U	3	0	0	2	1	0	0	1	0	0	0	0	1	0	0	1	0	0	2	0
Sc	5	34	35	36	37	38	35	37	41	35	37	38	37	37	38	37	32	34	38	35
V	5	370	372	365	373	372	368	368	374	375	367	368	362	367	366	364	373	363	366	368
Cr	4	49	51	50	51	52	51	52	53	49	49	49	50	50	49	49	48	48	49	50
Co	2	49	47	47	47	44	48	45	48	45	45	46	46	46	45	43	43	43	47	47
Ni	3	80	77	78	75	75	79	76	80	78	77	80	77	78	80	75	76	75	75	76
Cu	3	230	229	226	228	227	229	232	233	230	229	224	231	228	231	220	221	218	220	219
Zn	3	115	115	120	114	117	113	114	115	116	116	114	115	116	117	108	105	103	109	107
Ga	3	22	24	24	24	23	23	24	24	23	24	24	25	24	25	23	24	23	25	25
Mo	2	0	0	0	0	0	0	0	0	0	0	0	0	0	0	0	0	0	0	0
As	5	3	3	0	1	1	0	0	1	0	5	4	2	0	0	0	3	0	7	1
S	50	47	50	43	46	48	44	47	47	46	43	46	43	44	47	35	39	42	29	34

	PH7	PH7	PH7	Mean	St. Dev.	St. Er.
Rb	8	8	8	8	0.41	0.09
Sr	227	229	232	231	2.20	0.47
Y	36.3	37.1	35.7	35	0.75	0.16
Zr	153	155	154	153	1.19	0.25
Nb	12.2	12.6	12.1	12	0.72	0.15
Ba	93	92	98	95	6.87	1.46
Pb	1	3	1	2	1.47	0.31
Th	2	2	1	2	1.16	0.25
U	0	2	0	0	0.71	0.15
Sc	35	35	36	36	1.89	0.40
V	365	368	370	368	3.52	0.75
Cr	51	50	48	50	1.28	0.27
Co	45	47	46	46	1.60	0.34
Ni	77	74	79	77	1.79	0.38
Cu	219	221	228	226	4.75	1.01
Zn	107	109	107	112	4.54	0.97
Ga	24	25	25	24	0.81	0.17
Mo	0	0	0	0	0.04	0.01
As	1	0	6	2	2.08	0.44
S	37	36	32	42	5.64	1.20

	CG10	CG10	CG10	CG10	CG10	CG10	CG10	CG10	CG10	CG10	CG10	CG10	CG10	St. Dev.	St. Er.
SiO2	47.39	47.40	47.40	47.43	47.19	47.17	47.11	47.09	47.55	47.61	47.64	47.61	47.40	0.18	0.05
TiO2	2.390	2.388	2.395	2.400	2.402	2.410	2.387	2.394	2.425	2.422	2.442	2.437	2.418	0.02	0.00
Al2O3	13.38	13.40	13.41	13.39	13.23	13.27	13.29	13.25	13.37	13.35	13.34	13.34	13.36	0.06	0.02
Fe2O3	14.69	14.68	14.66	14.68	14.69	14.69	14.67	14.66	14.72	14.68	14.69	14.70	14.66	0.02	0.00
MnO	0.221	0.220	0.218	0.216	0.221	0.217	0.219	0.217	0.214	0.214	0.217	0.215	0.217	0.00	0.00
MgO	5.95	5.95	5.99	5.96	5.89	5.88	5.91	5.87	6.00	5.99	6.03	5.98	6.00	0.05	0.01
CaO	9.74	9.73	9.72	9.72	9.72	9.67	9.68	9.71	9.77	9.76	9.77	9.76	9.78	0.03	0.01
Na2O	2.19	2.21	2.23	2.22	2.21	2.19	2.18	2.18	2.22	2.25	2.22	2.22	2.23	0.02	0.01
K2O	0.35	0.35	0.34	0.35	0.35	0.34	0.35	0.35	0.35	0.35	0.35	0.35	0.35	0.00	0.00
P2O5	0.207	0.211	0.206	0.210	0.209	0.207	0.212	0.208	0.214	0.216	0.215	0.215	0.215	0.00	0.00
Total	96.49	96.53	96.57	96.58	96.12	96.06	96.00	95.92	96.84	96.84	96.91	96.83	96.64	0.34	0.09

	Approx. det. limit	CG10	CG10	CG10	CG10	CG10	CG10	CG10	CG10	CG10	CG10(OLD)	CG10(OLD)	CG10(OLD)	CG10(OLD)	CG10(OLD)
Rb	2	8	9	7	8	8	10	9	8	8	8	8	8	8	8
Sr	2	236	237	238	237	237	238	239	241	239	246	247	244	246	244
Y	2.0	35.9	35.0	35.7	36.3	36.0	36.3	36.2	37.2	36.1	36.7	37.4	37.4	37.7	37.4
Zr	2	151	152	152	154	152	152	152	152	152	156	156	157	157	155
Nb	1.5	10.6	12.2	12.3	10.4	11.4	11.8	12.4	11.6	11.2	11.9	11.6	12.3	10.9	11.4
Ba	12	124	135	126	123	131	131	135	125	135	131	137	139	143	147
Pb	5	2	3	3	4	4	3	5	3	2	4	5	3	5	2
Th	4	1	1	1	4	3	1	2	0	1	3	1	5	3	4
U	3	1	0	2	2	1	0	0	0	1	0	3	1	0	0
Sc	5	33	33	35	31	33	35	36	34	32	33	37	33	37	35
V	5	349	354	347	357	347	352	354	351	349	357	364	353	364	362
Cr	4	154	152	154	153	153	154	154	152	152	153	156	154	153	152
Co	2	45	44	42	48	45	45	44	45	46	49	46	45	46	49
Ni	3	88	85	88	88	90	88	92	90	90	97	95	91	93	92
Cu	3	213	214	220	217	218	218	220	221	219	231	228	227	224	225
Zn	3	95	96	96	95	97	95	98	98	97	101	101	103	102	101
Ga	3	23	22	23	24	24	23	25	23	23	24	24	24	24	24
Mo	2	0	0	0	0	0	0	0	0	0	0	0	0	0	0
As	5	0	4	0	2	1	1	2	0	0	0	3	1	0	0
S	50	40	44	42	35	40	38	38	32	35	251	251	257	254	242

	Mean CG10 -old	CG10 St. Dev. -old	CG10 -Old St. Er.	Mean CG10 All	CG10 St. Dev. All	CG10 St. Er. All
Rb	8	0.74	0.25	8.11	0.64	0.17
Sr	238	1.43	0.48	240.66	3.87	1.03
Y	36	0.55	0.18	36.52	0.77	0.20
Zr	152	0.84	0.28	153.39	2.10	0.56
Nb	12	0.68	0.23	11.57	0.61	0.16
Ba	129	4.58	1.53	132.96	6.87	1.84
Pb	3	0.75	0.25	3.34	0.91	0.24
Th	1	1.01	0.34	2.03	1.47	0.39
U	1	0.72	0.24	0.82	0.93	0.25
Sc	33	1.56	0.52	33.99	1.77	0.47
V	351	3.22	1.07	354.16	5.66	1.51
Cr	153	0.79	0.26	153.37	0.98	0.26
Co	45	1.49	0.50	45.63	1.81	0.48
Ni	89	1.82	0.61	90.51	3.07	0.82
Cu	218	2.64	0.88	221.03	5.25	1.40
Zn	96	1.27	0.42	98.16	2.58	0.69
Ga	23	0.86	0.29	23.46	0.77	0.21
Mo	0	0.09	0.03	0.01	0.10	0.03
As	1	1.42	0.47	1.07	1.40	0.37
S	38	3.62	1.21	114.29	101.92	27.24

	Approx. Det.Lt.	PH10	PH10	PH10	PH10	PH10	PH10	PH10	PH10	PH10	Ph10(OLD)	Ph10(OLD)	PH10	PH10	PH10	Mean	St. Dev.	St. Er.
Rb	2	3	2	2	1	1	2	1	2	2	1	2	2	2	2	1.82	0.46	0.12
Sr	2	226	224	226	224	222	224	225	228	225	232	233	232	230	232	227.21	3.55	0.95
Y	2.0	31.1	30.6	31.3	31.8	30.7	31.9	32.1	32.7	31.2	34.0	33.6	31.8	31.8	32.1	31.91	0.95	0.25
Zr	2	130	130	131	129	129	130	131	130	131	133	134	133	133	132	131.23	1.57	0.42
Nb	1.5	8.8	9.6	9.4	9.8	7.9	9.1	9.1	9.9	9.4	9.6	9.5	9.9	9.9	9.0	9.35	0.53	0.14
Ba	12	62	59	61	69	69	63	61	59	61	69	67	78	77	76	66.46	6.47	1.73
Pb	5	0	0	2	2	1	2	2	4	5	2	2	4	1	2	2.13	1.27	0.34
Th	4	0	0	2	2	2	1	2	0	0	0	0	1	2	2	0.95	0.94	0.25
U	3	0	1	1	0	0	1	1	0	1	1	0	1	3	0	0.76	0.86	0.23
Sc	5	37	36	35	35	36	40	35	34	36	37	37	35	38	34	36.01	1.54	0.41
V	5	411	406	409	411	422	420	411	405	410	419	417	427	411	417	414.13	6.25	1.67
Cr	4	89	92	91	90	92	93	95	91	93	92	90	88	91	94	91.51	1.88	0.50
Co	2	42	40	40	47	45	43	41	42	43	43	44	42	44	43	42.66	1.68	0.45
Ni	3	79	77	76	79	78	78	79	82	79	84	82	84	84	82	80.16	2.83	0.76
Cu	3	197	194	193	190	194	194	194	201	198	204	203	198	197	203	197.16	4.16	1.11
Zn	3	92	90	92	92	92	91	91	92	92	94	94	96	96	98	93.01	2.23	0.60
Ga	3	23	23	22	24	21	22	22	21	23	24	22	23	23	24	22.74	0.90	0.24
Mo	2	0	0	0	0	0	0	0	0	0	0	0	0	0	0	0.00	0.00	0.00
As	5	3	2	1	0	5	1	0	2	1	5	5	3	3	1	2.30	1.60	0.43
S	50	29	30	29	25	28	28	30	25	21	53	57	51	53	51	36.44	12.59	3.37

	SF1	SF1	SF1	SF1	SF1	SF1	SF1	SF1	SF1	SF1	SF1	SF1	SF1	SF1 St. Dev.	SF1 St. Er.
SiO2	49.42	49.60	49.62	49.62	49.58	49.38	49.87	49.88	49.90	49.81	49.83	49.85	49.72	0.17	0.05
TiO2	3.046	3.054	3.055	3.057	3.040	3.038	3.100	3.086	3.101	3.092	3.087	3.099	3.058	0.02	0.01
Al2O3	13.99	14.06	14.06	14.02	14.06	13.92	14.07	14.05	14.06	14.03	14.01	14.02	14.11	0.04	0.01
Fe2O3	14.93	14.91	14.87	14.90	14.89	14.91	14.90	14.88	14.89	14.90	14.91	14.90	14.85	0.02	0.01
MnO	0.210	0.211	0.208	0.208	0.206	0.211	0.213	0.207	0.208	0.208	0.209	0.209	0.207	0.00	0.00
MgO	5.05	5.09	5.11	5.10	5.11	5.03	5.13	5.14	5.20	5.18	5.16	5.16	5.09	0.05	0.01
CaO	9.78	9.80	9.75	9.78	9.74	9.73	9.77	9.75	9.78	9.76	9.81	9.74	9.79	0.02	0.01
Na2O	2.56	2.63	2.62	2.62	2.60	2.57	2.63	2.61	2.64	2.64	2.64	2.64	2.66	0.03	0.01
K2O	0.46	0.46	0.46	0.46	0.46	0.47	0.47	0.46	0.46	0.46	0.46	0.47	0.45	0.00	0.00
P2O5	0.323	0.328	0.325	0.325	0.332	0.325	0.336	0.335	0.333	0.335	0.340	0.337	0.331	0.01	0.00
Total	99.76	100.14	100.08	100.09	100.02	99.59	100.48	100.39	100.58	100.41	100.46	100.43	100.27		

	Approx. Det.Lt.	SF1	SF1	SF1	SF1	SF1	SF1	SF1	SF1	SF1	SF1	SF1	SF1	SF1	SF1	SF1	SF1	SF1	SF1	SF1	SF1	SF1
Rb	**2**	17	15	17	16	15	16	15	15	15	16	15	16	16	16	16	16	15	16	16	15	15
Sr	**2**	253	252	253	253	253	253	252	253	255	255	254	255	255	251	252	249	250	250	250	252	253
Y	**2.0**	40.9	42	41.4	40.0	41.5	41.6	42.8	41.3	41.6	41.7	41.7	40.9	41.4	41.1	41.6	39.9	43.0	42.5	42.1	42.4	42.8
Zr	**2**	213	209	211	212	209	210	212	210	213	212	210	211	209	209	211	212	212	213	211	211	212
Nb	**1.5**	17.6	19	18.4	18.0	17.9	17.5	18.4	18.8	17.1	18.3	17.6	17.8	17.4	18.1	17.5	18.7	18.5	18.4	18.0	18.9	18.4
Ba	**12**	188	177	199	180	195	177	195	180	179	186	164	174	182	170	165	163	178	172	172	175	180
Pb	**5**	8	6	4	4	2	5	4	2	3	5	5	3	3	3	3	5	5	4	5	5	5
Th	**4**	0	4	2	6	2	2	5	5	2	4	0	3	3	4	4	3	3	4	1	5	3
U	**3**	2	0	2	1	0	1	0	1	1	2	1	0	0	1	0	0	1	0	2	0	2
Sc	**5**	32	35	38	32	36	35	32	34	36	35	36	35	36	37	32	33	35	37	34	33	38
V	**5**	373	378	375	372	378	377	392	384	373	376	366	379	379	374	383	367	377	383	379	379	371
Cr	**4**	123	118	119	122	124	124	120	119	122	122	121	120	121	120	121	119	117	122	121	124	119
Co	**2**	39	36	35	36	38	36	36	38	37	38	38	36	38	35	33	35	36	38	35	34	39
Ni	**3**	68	65	66	64	65	63	68	68	67	68	66	68	65	66	64	66	69	70	67	67	69
Cu	**3**	302	300	298	297	299	298	299	301	303	304	299	302	301	290	289	289	289	292	289	290	296
Zn	**3**	121	122	121	121	123	123	120	122	121	123	120	120	120	109	114	111	111	113	110	111	113
Ga	**3**	23	24	24	24	25	24	23	24	24	25	23	23	24	25	26	25	25	24	25	25	25
Mo	**2**	0	0	0	0	0	0	0	0	0	0	0	0	0	0	0	0	0	0	0	0	0
As	**5**	1	0	4	6	0	3	0	0	0	4	0	0	5	3	0	0	0	0	1	0	0
S	**50**	75	73	67	73	71	66	71	69	72	71	71	73	70	63	67	65	66	63	66	63	57

	SF1	SF1(OLD)	SF1(OLD)	SF1(OLD)	SF1(OLD)	SF1(OLD)	Mean SF1 -old	SF1 St. Dev. -old	SF1 St. Er.-old	Mean SF1 all	SF1 St. Dev. all	SF1 St. Er. All
Rb	17	15	16	16	16	16	15.60	0.51	0.11	15.60	0.54	0.10
Sr	253	259	258	259	261	257	252.48	1.63	0.35	253.65	2.90	0.55
Y	42.5	42.2	43.3	43.3	43.3	43.5	41.66	0.80	0.17	41.93	0.94	0.18
Zr	213	215	217	217	219	217	211.10	1.17	0.25	212.20	2.61	0.49
Nb	17.9	19.3	19.6	19.0	18.1	19.0	18.09	0.51	0.11	18.26	0.61	0.12
Ba	178	181	170	190	194	190	178.52	9.64	2.06	179.74	9.68	1.83
Pb	7	5	4	3	5	3	4.36	1.42	0.30	4.29	1.43	0.27
Th	5	2	3	4	4	3	3.10	1.54	0.33	3.12	1.43	0.27
U	2	0	0	3	0	1	0.79	0.74	0.16	0.79	0.83	0.16
Sc	35	36	37	35	35	36	34.85	1.76	0.38	34.98	1.61	0.30
V	371	377	383	383	384	374	376.58	5.70	1.21	377.27	5.60	1.06
Cr	121	122	123	117	123	123	120.80	1.89	0.40	120.92	1.96	0.37
Co	36	31	37	34	36	37	36.40	1.58	0.34	36.13	1.77	0.33
Ni	67	69	68	67	70	70	66.63	1.76	0.37	67.06	1.88	0.36
Cu	295	306	303	301	308	302	296.45	5.23	1.12	297.88	5.63	1.06
Zn	111	112	116	116	118	115	117.23	5.00	1.07	116.89	4.69	0.89
Ga	25	25	25	25	25	25	24.28	0.88	0.19	24.42	0.84	0.16
Mo	0	0	0	0	0	0	0.00	0.00	0.00	-0.02	0.08	0.01
As	1	0	2	2	2	2	1.35	1.93	0.41	1.39	1.75	0.33
S	61	97	98	95	96	89	67.90	4.28	0.91	72.93	11.36	2.15

	Apprax. Det.Lt.	KP13	KP13	KP13	KP13	KP13	KP13	KP13	Mean	St. Dev.	St. Er.
Rb	2	2	1	2	2	2	2	3	2.00	0.42	0.16
Sr	2	160	160	159	161	160	158	159	159.54	0.90	0.34
Y	2.8	91.6	90.8	90.2	94.3	92.7	91.4	91.5	91.79	1.25	0.47
Zr	2	112	111	113	112	111	110	112	111.39	0.80	0.30
Nb	1.5	8.0	8.0	8.0	7.5	7.1	8.2	8.2	7.86	0.38	0.14
Ba	12	72	73	68	73	70	73	67	70.87	2.45	0.92
Pb	5	1	5	1	3	1	3	3	2.50	1.34	0.50
Th	4	0	1	2	1	2	1	2	1.30	0.85	0.32
U	3	1	1	1	0	0	1	0	0.59	0.61	0.23
Sc	5	35	37	38	37	34	38	38	36.49	1.53	0.58
V	5	345	344	341	349	341	354	353	346.61	4.94	1.87
Cr	4	69	70	66	69	67	69	69	68.50	1.09	0.41
Co	2	57	56	58	55	58	60	58	57.24	1.55	0.59
Ni	3	78	75	74	80	76	75	79	76.66	1.95	0.74
Cu	3	229	228	220	230	226	225	224	226.11	3.19	1.21
Zn	3	87	89	88	88	86	86	88	87.30	1.00	0.38
Ga	3	20	20	22	21	22	20	20	20.56	0.74	0.28
Mo	2	0	0	0	0	0	0	0	0.00	0.00	0.00
As	5	1	0	1	2	0	2	4	1.36	1.09	0.41
S	50	34	32	33	30	30	32	33	31.93	1.33	0.50

C10 Mean of error data compared with Widdowson (1990) values

	Mean CG5	Widd. CG5	CG5 St. Dev.	Mean CG7	Widd. CG7	CG7 St. Dev.	Mean CG2	Widd. CG2	CG2 St. Dev.	Mean CG11	Widd. CG11	CG11 st. dev.	Mean KP4	Widd. KP4	KP4 Stan. Dev.
Rb	14.95	19.10	0.42	15.56	21.10	0.30	11.14	14.80	0.50	1.53	7.40	0.44	11.22	17.20	0.71
Sr	227.38	227.50	4.01	242.97	244.50	1.26	216.53	212.50	2.51	225.08	225.10	1.94	223.12	220.50	1.55
Y	31.94	31.70	0.75	38.11	38.00	0.45	31.15	30.50	0.80	32.77	33.10	0.66	47.84	46.70	0.74
Zr	137.10	137.20	1.33	176.31	173.70	1.08	138.23	137.30	1.70	138.76	140.50	0.94	217.35	211.80	1.44
Nb	9.10	7.80	0.42	12.80	11.70	0.46	8.34	8.00	0.74	9.98	9.90	0.84	18.22	18.20	0.71
Ba	181.57	177.30	7.84	152.93	146.10	5.30	137.83	132.10	7.31	83.47	71.00	5.03	132.16	129.40	9.01
Pb	3.56	3.80	1.23	3.57	2.80	1.41	3.31	2.30	1.46	2.27	2.00	1.23	3.85	3.60	1.68
Th	2.76	*	1.14	3.00	*	1.09	2.20	*	1.20	1.69	*	1.31	2.51	2.70	1.23
U	0.54	*	0.84	1.24	*	0.80	0.64	*	0.51	0.58	*	1.13	0.73	*	0.99
Sc	34.94	*	1.30	32.83	*	2.27	31.41	*	2.14	34.56	*	1.31	40.61	*	2.00
V	335.03	308.40	4.31	413.64	395.00	6.14	293.39	277.70	5.46	362.20	345.00	6.83	476.68	477.20	6.12
Cr	305.99	211.90	62.55	111.24	101.20	1.17	252.68	242.00	2.83	182.55	182.30	1.65	56.61	67.80	1.59
Co	37.01	41.80	1.51	35.81	39.50	1.85	41.04	43.60	1.88	45.74	45.60	2.23	45.75	58.50	2.79
Ni	98.33	99.40	2.55	71.61	74.30	1.30	122.08	124.00	2.38	103.59	107.00	1.89	59.69	61.00	1.56
Cu	116.07	125.30	3.27	215.61	255.00	1.48	130.01	146.00	2.61	181.86	208.50	3.38	330.41	331.20	5.85
Zn	88.27	93.10	0.91	86.47	93.30	0.77	76.75	79.60	3.44	114.21	115.10	5.34	152.62	156.60	6.69
Ga	20.38	*	0.61	23.00	*	0.71	20.56	*	0.86	22.77	*	0.99	24.90	26.10	0.79
Mo	0.00	*	0.00	0.00	*	0.00	0.00	*	0.02	0.00	*	0.00	-0.01	*	0.04
As	2.09	*	2.46	2.44	*	1.33	2.16	*	2.05	1.62	*	1.34	1.65	*	2.00
S	89.69	*	13.88	29.47	*	2.42	45.06	*	19.89	44.27	*	5.69	77.52	*	6.24
	Pol. Fm.	*		Pol. Fm.			Pol. Fm.			Amb. Fm			Amb. Fm		

Comparison of the mean of the samples from Widdowson (1990) run at The Open University, compared with the values stated in Widdowson (1990) and the standard deviation of the samples run at the OU.

	Mean PH6	Widd. PH6	Ph6 St. Dev.	Mean PH7	Widd. PH7	PH7 St. Dev.	Mean CG10	Widd. CG10	CG10 St. Dev.	Mean PH10	Widd. PH10	PH10 St. Dev.	Mean SF1	Widd. SF1	SF1 St. Dev.
Rb	5.44	10.70	0.53	8.29	14.30	0.41	8.11	14.00	0.64	1.82	8.10	0.46	15.60	20.00	0.54
Sr	215.89	215.30	1.49	230.66	231.00	2.20	240.66	238.50	3.87	227.21	226.70	3.55	253.65	250.90	2.90
Y	33.12	33.90	0.64	35.50	36.10	0.75	36.52	36.10	0.77	31.91	30.60	0.95	41.93	41.40	0.94
Zr	144.64	146.20	0.79	153.20	153.00	1.19	153.39	153.50	2.10	131.23	131.80	1.57	212.20	207.40	2.61
Nb	11.35	11.20	0.46	12.05	11.40	0.72	11.57	10.60	0.61	9.35	8.60	0.53	18.26	16.90	0.61
Ba	67.16	53.10	6.00	95.32	88.50	6.87	132.96	117.80	6.87	66.46	51.00	6.47	179.74	176.80	9.68
Pb	2.13	2.70	1.38	2.21	3.60	1.47	3.34	2.40	0.91	2.13	3.10	1.27	4.29	4.60	1.43
Th	1.21	*	1.26	1.79	*	1.16	2.03	*	1.47	0.95	*	0.94	3.12	*	1.43
U	0.67	*	1.00	0.47	*	0.71	0.82	*	0.93	0.76	*	0.86	0.79	*	0.83
Sc	37.45	*	2.01	36.15	*	1.89	33.99	*	1.77	36.01	*	1.54	34.98	*	1.61
V	369.94	339.80	5.42	368.27	367.20	3.52	354.16	345.20	5.66	414.13	403.30	6.25	377.27	359.60	5.60
Cr	179.35	175.10	1.92	49.87	47.20	1.28	153.37	144.70	0.98	91.51	84.70	1.88	120.92	116.70	1.96
Co	44.75	48.30	2.13	45.85	54.20	1.60	45.63	53.00	1.81	42.66	51.40	1.68	36.13	43.20	1.77
Ni	95.90	98.70	2.19	77.00	81.70	1.79	90.51	93.30	3.07	80.16	83.30	2.83	67.06	68.60	1.88
Cu	182.69	208.20	3.26	225.87	261.70	4.75	221.03	258.30	5.25	197.16	226.30	4.16	297.88	346.90	5.63
Zn	103.50	104.50	4.70	112.38	113.10	4.54	98.16	103.60	2.58	93.01	98.00	2.23	116.89	119.10	4.69
Ga	21.25	*	0.56	23.94	*	0.81	23.46	*	0.77	22.74	*	0.90	24.42	*	0.84
Mo	-0.16	*	0.73	0.01	*	0.04	0.01	*	0.10	0.00	*	0.00	-0.02	*	0.08
As	1.45	*	1.56	1.70	*	2.08	1.07	*	1.40	2.30	*	1.60	1.39	*	1.75
S	47.05	*	5.70	42.09	*	5.64	114.29	*	101.92	36.44	*	12.59	72.93	*	11.36
	Amb. Fm			Amb. Fm.			Amb. Fm.			Amb. Fm.			Mahabaleshwar Fm.		

	Mean KP13	Widd. KP13	KP13 St. Dev.
Rb	2.00	8.20	0.12
Sr	159.54	161.90	1.01
Y	91.79	94.80	0.04
Zr	111.39	114.10	0.47
Nb	7.86	6.30	
Ba	70.87	68.60	1.63
Pb	2.50	2.70	0.32
Th	1.30	*	0.10
U	0.59	*	0.09
Sc	36.49	*	0.29
V	346.61	346.10	0.48
Cr	68.50	60.50	0.30
Co	57.24	62.80	0.40
Ni	76.66	79.50	0.65
Cu	226.11	265.50	1.05
Zn	87.30	95.20	1.71
Ga	20.56	*	0.10
Mo	0.00	*	0.04
As	1.36	*	0.30
S	31.93	*	45.24

Pan. Fm.

C11 Percentage error for each formation

	Mean of Pol Fm. Standards	Standard Error of Pol. Fm. Standards	% Error of Pol. Fm. Standards	Mean of Amb. Fm. Standards	Standard Error of Amb. Fm. Standards	% Error of Amb Fm. Standards	Mean of Mahabaleshwar Fm. Standards	Standard Error of Mahabaleshwar Fm. Standards	% Error of Mahabaleshwar Fm. Standards	Mean of Pan. Fm. Standards	Standard Error of Pan. Fm. Standards	% Error of Pan Fm. Standards
Rb	13.88	0.11	0.77	6.07	0.12	2.02	15.60	0.10	0.66	2.00	0.16	7.89
Sr	228.96	0.67	0.29	227.10	0.55	0.24	253.65	0.55	0.22	159.54	0.34	0.21
Y	33.73	0.17	0.52	36.28	0.17	0.46	41.93	0.18	0.42	91.79	0.47	0.51
Zr	150.55	0.36	0.24	156.43	0.32	0.20	212.20	0.49	0.23	111.39	0.30	0.27
Nb	10.08	0.14	1.41	12.09	0.15	1.26	18.26	0.12	0.63	7.86	0.14	1.82
Ba	157.44	1.83	1.16	96.26	1.61	1.67	179.74	1.83	1.02	70.87	0.92	1.30
Pb	3.48	0.38	10.90	2.65	0.32	11.89	4.29	0.27	6.29	2.50	0.50	20.19
Th	2.65	0.31	11.86	1.70	0.28	16.48	3.12	0.27	8.69	1.30	0.32	24.77
U	0.81	0.21	25.67	0.67	0.22	32.07	0.79	0.16	19.81	0.59	0.23	39.09
Sc	33.06	0.54	1.63	36.46	0.42	1.15	34.98	0.30	0.87	36.49	0.58	1.58
V	347.35	1.50	0.43	390.90	1.33	0.34	377.27	1.06	0.28	346.61	1.87	0.54
Cr	223.31	5.90	2.64	118.88	0.36	0.30	120.92	0.37	0.31	68.50	0.41	0.60
Co	37.95	0.49	1.28	45.06	0.46	1.02	36.13	0.33	0.93	57.24	0.59	1.03
Ni	97.34	0.54	0.56	84.48	0.50	0.59	67.06	0.36	0.53	76.66	0.74	0.96
Cu	153.90	0.64	0.42	223.17	1.03	0.46	297.88	1.06	0.36	226.11	1.21	0.53
Zn	83.83	0.39	0.47	112.32	0.96	0.86	116.89	0.89	0.76	87.30	0.38	0.43
Ga	21.31	0.20	0.92	23.17	0.18	0.80	24.42	0.16	0.65	20.56	0.28	1.36
Mo	0.00	0.00	-98.20	-0.03	0.03	-118.33	-0.02	0.01	-66.82	0.00	0.00	
As	2.23	0.52	23.10	1.63	0.39	24.14	1.39	0.33	23.88	1.36	0.41	30.43
S	54.74	2.79	5.10	60.28	5.15	8.55	72.93	2.15	2.94	31.93	0.50	1.58

The percentage error for each element in each formation, with the applicable mean and standard error values

D1 GPS Methodology

A static GPS Survey was carried out along the four traverses of the Mahabaleshwar Plateau in order to acquire accurate and precise elevations of key locations to aid the correlations of the logs.

Leica 530 Real time GPS equipment (during this study however, the real time capability was disabled) from the NERC Geophysical Equipment Facility, Edinburgh was used to carry out the survey.

A GPS reference receiver was placed, and set to record satellite data, in the garden of the Dina Hotel, Mahabaleshwar in the same position every day, marked by a nail. Ideally, the reference receiver should be placed on a point whose coordinates are known exactly in WGS84, but the local trig point was isolated, and next to a number of aerials and satellite dishes which can affect the GPS equipment, so for accuracy and a safety of the equipment it was placed in the garden of the Dina hotel.

A rover receiver was placed at the required location on one of the logged sections. The rover receiver was set to record satellite data. The length of time the rover receiver recorded satellite data was dependent on the distance from the reference receiver, an approximation is, a minimum of one hour for a distance of 20 km from the reference receiver to the rover with five satellites and a prevailing geometric dilution of precision (GDOP) of eight, longer lines need longer observation times, the maximum time used during my survey was three hours for gps-AG1 near Poladpur. Once enough time had elapsed, the rover receiver was switched off and moved to the next location.

The data from both the rover and the reference receiver were stored on a memory card and the data were processed each evening using Ski-Pro software. The final data are in Appendix D2

D2 GPS Data

GPS point	Section	Type	Latitude	Longitude	ellipsoidal height/m	geoid separation/m	orthometric height/m	error/m
gpsAG1	Ambenali Ghat	Measured	17° 58' 41.43620" N	73° 28' 14.14332" E	-50.0227	-75.4489	25.4262	0.0009
gpsAG2	Ambenali Ghat	Control	17° 55' 59.81087" N	73° 33' 32.59313" E	454.4708	-75.4811	529.9519	0.00
gpsAG3	Ambenali Ghat	Measured	17° 57' 03.07134" N	73° 35' 00.19094" E	617.6686	-75.3374	693.006	0.0015
gpsAG4	Ambenali Ghat	Measured	17° 55' 41.64025" N	73° 37' 49.97140" E	889.6803	-75.2449	964.9252	0.0008
gpsAG5	Ambenali Ghat	Measured	17° 54' 58.39336" N	73° 37' 30.53488" E	1015.3919	-75.318	1090.7099	0.0007
gpsKG1	Kelgar Road	Measured	17° 51' 45.66597" N	73° 45' 32.46790" E	696.6534	-75.226	771.8794	0.0018
gpsKG2	Kelgar Road	Measured	17° 52' 09.50154" N	73° 44' 13.12742" E	878.7958	-75.2537	954.0495	0.0013
gpsKG3	Kelgar Road	Measured	17° 52' 47.28099" N	73° 44' 28.93020" E	968.4576	-75.1725	1043.6301	0.0015
gpsKG4	Kelgar Road	Measured	17° 53' 21.80688" N	73° 43' 31.90734" E	1142.1614	-75.169	1217.3304	0.0011
gpsTP1	Tapola Road	Measured	17° 46' 06.55917" N	73° 44' 20.42380" E	632.5237	-75.7241	708.2478	0.0021
gpsTP2	Tapola Road	Measured	17° 51' 55.03995" N	73° 40' 24.70911" E	1087.8605	-75.4469	1163.3074	0.1863
gpsTP3	Tapola Road	Measured	17° 51' 56.71325" N	73° 40' 27.22243" E	1091.473	-75.4428	1166.9158	0.002
gpsWP1	Wai-Panchgani	Measured	17° 56' 29.33913" N	73° 51' 44.02061" E	747.3781	-74.575	821.9531	0.0015
gpsWP2	Wai-Panchgani	Measured	17° 56' 09.89623" N	73° 49' 57.31402" E	1014.4461	-74.6717	1089.1178	0.0011
Elephant Head		Measured	17° 56' 25.97785" N	73° 37' 53.86072" E	1165.4655	-75.1826	1240.6481	0.0009
Dina Hotel	Reference stn	Reference	17° 55' 36.92764" N	73° 39' 48.92373" E	1267.5964	-75.1582	1342.7546	0.0666
24.1.03 ref	Reference stn	Reference	17° 55' 36.92792" N	73° 39' 48.81927" E	1265.6008	-75.1583	1340.7591	0.0517
26.1.03 ref	Reference stn	Reference	17° 55' 36.95740" N	73° 39' 48.86416" E	1267.0087	-75.1582	1342.1669	0.0472
28.1.03 ref	Reference stn	Reference	17° 55' 36.92053" N	73° 39' 48.87508" E	1264.3008	-75.1582	1339.459	0.0504
29.1.03 ref	Reference stn	Reference	17° 55' 36.93178" N	73° 39' 48.84267" E	1265.9074	-75.1582	1341.0656	0.0486
30.1.03 ref	Reference stn	Reference	17° 55' 36.95651" N	73° 39' 48.85699" E	1266.2957	-75.1582	1341.4539	0.0407

Endpiece

Sunrise over the Western Ghats on my final day in India, looking east from the Bombay-Agra Road on the northern Konkan Plain